KU Leuven
Biomedical Sciences Group
Faculty of Medicine
Department of Oncology
Doctoral School of Cognitive and Molecular Neurosciences

Neurotoxicity and potential risk factors in childhood solid tumor patients

Charlotte SLEURS

Jury

Promotor :   Prof. Dr. Anne Uyttebroeck
Co-promotors :   Dr. Sabine Deprez
                        Dr. Jurgen Lemiere
Chair :   Prof. Dr. Johan Swinnen
Jury members :   Prof. Dr. Nele Demeyere
                        Prof. Dr. Lieven Lagae
                        Prof. Dr. Hans Op de Beeck
                        Prof. Dr. Andrew Peet
Delegate examining committee : Prof. Dr. Michel Delforge

Dissertation presented in partial fulfillment
of the requirements for the degree
of Doctor in Biomedical Sciences

October 2018

There is in every child,
at every stage,
a new miracle
of vigorous unfolding.

Erik Erikson

de helden
voor charlotte

Table of Contents

List of figures

List of tables

Abbreviations

A	Arithmetic (subtask WAIS)
AaD	Age at Diagnosis
ADC	Apparent Diffusion Coefficient
AFD	Apparent Fiber Density
ApoE	Apolipoprotein E
ALL	Acute Lymphoblastic Leukemia
ANT	Amsterdam Neuropsychological Tasks
AVLT	Auditory Verbal Learning Test
BBB	Blood-brain-barrier
BCT	Brain Connectivity Toolbox
BDI	Beck Depression Inventory
BDNF	Brain-Derived-Neurotrophic-Factor
BOLD	Blood-oxygenation-level dependent signal
BRIEF	Behavior Rating Inventory of Executive Function
BS	Baseline Speed (subtask ANT)
C	Coding (subtask WAIS)
CAT12	Computational Anatomy Toolbox v.12
CC	Corpus Callosum
CFQ	Cognitive Failures Questionnaire
CNS	Central Nervous System
CMS	Children Memory Scale
COWAT	Controlled Oral Word Association Test
CSD	Constrained Spherical Deconvolution
CSF	Cerebrospinal Fluid
DMN	Default-Mode-Network
DS	Digit Span (subtask WAIS)
DTI	Diffusion Tensor Imaging
DWI	Diffusion-Weighted Imaging
EEG	Electro-encephalography
EPI	Echo-Planar Imaging
FA	Fractional Anisotropy
FA4O/FA4L	Focused Attention for Objects/Letters (subtask ANT)
FBA	Fixel-based Analysis
FC	Fiber Cross-section
FLAIR	Fluid Attenuation Inversion Recovery
FOD	Fiber Orientation Distribution
FSIQ	Full Scale Intelligence Quotient
FSL	FMRIB Software Library

GM	Grey Matter
GMD	Grey Matter Density
GRASE	Gradient Spin Echo
GST	Glutathione S-transferases
HD-MTX	High-dose methotrexate
HRQoL	Health-Related Quality of Life Inventory
HPA-axis	Hypothalamic-Pituitary-Adrenal axis
I	Information (subtask WAIS)
IEWF	Intra-Extra cellular Water Fraction
IT-MTX	Intrathecal methotrexate
IV-MTX	Intravenous methotrexate
IQ	Intelligence Quotient
IQR	Interquartile range
LR	Likelihood Ratio
MAO-A	Monoamine-Oxidase-A
MET2	Multi-exponential T2 relaxation
MR	Matrix Reasoning (subtask WAIS)
MRI	Magnetic Resonance Imaging
MRS	Magnetic Resonance Spectroscopy
MS	Methionine Synthase
MSO2/MSL	Memory Search for Objects/Letters (subtask ANT)
MTHFR	Methylene tetrahydrofolate reductase
MTX	Methotrexate
MWF	Myelin Water Fraction
MWI	Myelin-Water-Imaging
NDI	Neurite Density Index
NODDI	Neurite Orientation and Dispersion and Density Imaging
ODI	Orientation Dispersion Index
PET	Positron Emission Tomography
PIQ	Performance Intelligence Quotient
PPVT	Peabody Picture Vocabulary Test
PRI	Perceptual Reasoning Index
PS	Processing Speed
rsfMRI	Resting-state Functional Magnetic Resonance Imaging
ROO	Response Organization Objects (subtask ANT)
RT	Radiotherapy
RVDLT	Rey Visual Design Learning Test
S	Similarities (subtask WAIS)
SAO2	Sustained Attention for Objects (subtask ANT)
SBM	Surface-based Morphometry
SES	Socio-economic status
SPM	Statistical Parametric Mapping toolbox
SS	Symbol Search (subtask WAIS)
SSV	Shifting Attentional Set-Visual (subtask ANT)

STAI	State-Trait Anxiety Inventory
TE	Echo Time
TP	Tapping
TR	Repetition Time
V	Vocabulary (subtask WAIS)
VBM	Voxel-based Morphometry
VCI	Verbal Comprehension Index
VISO	Isotropic Volume Fraction
VIQ	Verbal Intelligence Quotient
VMI	Visual-Motor Integration
VP	Visual Puzzles
WAIS	Wechsler Adult Intelligence Scale
WISC	Wechsler Intelligence Scale for Children
WPPSI	Wechsler Preschool and Primary Scale of Intelligence
WM	White Matter/Working Memory

Abstract

As survival rates of childhood cancer patients improved throughout the last decades, long-term sequelae after treatment became an important area of research. Given that childhood cancer treatments differ according to the specific diagnosis, age at diagnosis, response to treatment, etc., they can result in very different long-term outcomes and symptoms. One of the potential side effects includes neurocognitive impairment. Neurosurgery, cranial radiotherapy (RT) and central nervous system-(CNS-)directed chemotherapy are known to lead to neurocognitive alterations in childhood brain tumor and leukemia patients. By contrast, in solid non-CNS tumor patients, findings about potential neurotoxicity due to intravenous chemotherapy only, remain limited. Nevertheless, case reports showed that even (high-dose) intravenous chemotherapy can induce acute (leuko-)encephalopathy. However, underlying neurotoxic mechanisms and neurocognitive outcomes are still to be unraveled.

Given that neurocognitive research in childhood cancer remained restricted to patients who were treated with CNS prophylaxis only, the main goal of this PhD project was to explore potential neurotoxicity due to high-dose intravenous chemotherapy in pediatric oncology. By combining neurocognitive assessments, genetic analyses, clinical (treatment and symptom) features and advanced neuroimaging techniques in both current pediatric oncology patients and (adult) survivors, we aimed to discover new insights into neurodevelopmental patterns and related biomarkers during childhood cancer.

To address neurocognitive outcomes, behavioral tests included intelligence assessments, verbal and visual memory, attentional functioning, visuomotor functioning, word fluency and object naming. Combined with behavioral assessments, MRI imaging covered state-of-the-art advanced MRI sequences including diffusion-weighted (DWI), myelin-water imaging (MWI), FLAIR, T1-weighted imaging, resting state functional MRI (RsfMRI). Based on these images, we aimed to investigate anatomical and functional information of the developing brain after high-dose chemotherapeutic treatments.

First, we performed an extensive literature review which summarized the existing evidence on potential neurotoxicity of non-CNS directed (i.e. intravenous) chemotherapy in solid non-CNS tumor patients. This review demonstrated that current research in pediatrics is very limited so far, with a lack of research in solid tumor patients.

Second, in order to explore neurocognitive developmental patterns in current childhood cancer patients, a longitudinal follow-up study of intelligence scores was performed in childhood leukemia patients, who were treated with intrathecal chemotherapy. This study demonstrated increases in verbal and performance IQ scores (which were within the normal range), and the negative impact of younger age at diagnosis and lower educational status of parents.

Third, a cross-sectional survivor cohort study was performed in adult survivors of childhood non-CNS tumors, treated with high dose intravenous chemotherapy only. To investigate chemotherapy-induced neuro-anatomical and physiological changes in these patients, different MRI sequences were investigated. More specifically, white matter microstructure was investigated using FLAIR, DWI and MWI, while grey matter anatomical and functional information was derived from T1-weighted MRI and rsfMRI, respectively. FLAIR images were first visually inspected for white matter lesions (i.e. observable leukoencephalopathy), which were further investigated using additional parameters estimating white matter integrity (derived from DWI and MWI). In this study, a substantial group of 27% of the childhood cancer survivors demonstrated leukoencephalopathy, which was associated with DWI, but not MWI. Given that the latter imaging type is more closely associated with the level of myelination, this study suggests long-term neurotoxicity but with possibly midterm remyelination and other underlying long-term neural damage. Leukoencephalopathy was mainly associated with delayed reaction times on focused and divided attention tasks. In addition to the observable lesions, DWI images provide more information about white matter directionality (e.g. tractography) and microstructure. Hence, we aimed to clarify white matter microstructure in long-term survivors using multiple recent diffusion models. These analyses provided evidence for central white matter tracts to be more affected (i.e. showing lower fiber density) compared to other tracts. Complementing these white matter investigations, we analyzed the grey matter structure and functioning using T1 and RsfMRI. Based on T1-weighted images, we encountered lower grey matter density and cortical thickness, while RsfMRI demonstrated differences in functional co-activation of brain regions in patients compared to controls. This mainly appeared in frontal and parahippocampal areas, of which the latter also showed decreased functional coherence.

Fourth, although evidence for chemotherapy-induced neurotoxicity is increasing based on cross-sectional studies, longitudinal studies are non-existing in children. Therefore, a preliminary neuroimaging and neurocognitive follow-up study was conducted of current non-CNS tumor patients who received high doses of chemotherapy. This study demonstrates acute leukoencephalopathy but rather stable cognitive scores. In addition to the survivor study, this suggests that behavioral effects of neurotoxicity would possibly only occur in a delayed stage.

Finally, as secondary brain damage can be hypothesized in case of extensive neural damage, recent applicable techniques are discussed to investigate the affected underlying brain network, or so-called "structural human connectome". Multi-modal analyses were applied in patients who suffer from long-term clearly visible brain damage located in the cerebellum, in childhood posterior fossa tumor survivors. This study suggested not only global decline in neural integrity, but also possible topological reorganization of the network. To investigate structural connectivity, pros and cons of these methods are summarized for future directions.

In summary, our current research suggests widespread acute and long-term neural damage due to high-dose intravenous chemotherapy, which can highly affect neurodevelopment throughout childhood. Multiple associated neural changes (e.g. altered white matter fiber density, decreased grey matter density and cortical thickness) were concluded. Furthermore, age at diagnosis and recovery patterns were explored using correlation analyses with imaging parameters. Still, to address subject-specific vulnerability, future studies are required including (pre-)clinical biochemical biomarkers (i.e. CSF toxicity values, (stress-related) hormonal fluctuations, GWAS, …) and state-of-the art imaging techniques (i.e. PET-MRI, EEG, MRS, Glu-CEST, ASL, SWI, …) in order to clarify altered synaptogenesis, neurotransmission and/or metabolite changes. Furthermore, longitudinal designs are recommended to investigate developmental and degeneration patterns throughout time. Finally, given that patients mainly complain about long-term emotional rather than cognitive problems, alterations in neurodevelopment might not necessarily be related with cognitive difficulties only. By contrast, the measured brain alterations could potentially yield other (e.g. emotional) psychological difficulties in daily life as well. This highly suggests to expand the existing research with *neuro-emotional* assessments. At the prospect of advanced treatment techniques, the long-term goal within this research domain is to reduce neurotoxicity, e.g. by modifying doses of toxic chemotherapy, focusing cranial radiotherapy doses, adding neuroprotective medication and neurorehabilitation, providing subject-specific psychosocial support; in order to improve the long-term quality of life in survivors of childhood cancer.

Dankzij de medische vooruitgang zijn overlevingskansen na kinderkanker enorm toegenomen doorheen de afgelopen decennia. Om die reden worden mogelijke neveneffecten van de therapie in toenemende mate onderzocht. De vorm en duur van de therapie is afhankelijk van de leeftijd van het kind, het type diagnose, de lichamelijke reactie op de therapie, enzovoort. Iedere vorm van therapie (bv. chemotherapie, radiotherapie, chirurgie, …) kan verschillende onmiddellijke bijwerkingen teweegbrengen. Een van de mogelijke acute bijwerkingen kan cognitieve symptomatologie zijn, bv. moeite met aandacht of concentratie, geheugenklachten, planningsproblemen, … Vroeger onderzoek toonde aan dat neurochirurgie en bestraling van het brein dergelijke (korte-, maar ook langetermijn) symptomen kan veroorzaken bij kinderen met hersentumoren. Bovendien neemt evidentie toe voor neurologische schade na chemotherapie die via het ruggenmergvocht wordt toegediend, dit bij patiënten met leukemie. Echter, voor kinderen die gediagnosticeerd worden met een vaste tumor (in het lichaam), die chemotherapie ontvangen via de bloedbaan (intraveneus), zijn dergelijke studies beperkt. Nochtans bestaan er casussen bij wie acute symptomen (bv. hoofdpijn, vermoeidheid, …) en neurologische schade werd vastgesteld. De onderliggende mechanismen van de chemotherapie zijn echter nog onduidelijk.

    In dit project onderzochten we daarom mogelijke neurologische schade en de neuropsychologische impact ervan na chemotherapie bij kinderen die werden behandeld voor kanker. We verzamelden neuropsychologische tests, genetisch materiaal, klinische gegevens i.v.m. therapie en symptomatologie, en MRI hersenbeeldvorming van zowel kinderen als volwassenen die behandeld werden op kinderleeftijd. Op die manier poogden we meer inzicht te verkrijgen in hun breinontwikkeling en geassocieerde biologische parameters.

    In een eerste studie bij kinderen die behandeld werden voor leukemie, toonden we aan dat jongere leeftijd bij diagnose en lagere opleiding van de ouders mogelijke risicofactoren kunnen zijn voor lagere cognitieve scores. Bovendien zagen we in een studie bij volwassenen die (op kinderleeftijd) behandeld werden voor vaste tumoren, dat intraveneuze chemotherapie zowel anatomische als functionele veranderingen in het brein op langetermijn kon teweegbrengen. Zo werden er op basis van klinische MRI scans (enkele jaren na therapie) letsels vastgesteld in de zogenaamde 'witte stof' (de langere verbindingsbanen van het brein) in 27% van de patiënten. Deze gedetecteerde letsels bleken geassocieerd te zijn met langere reactietijden op aandachtstaken. In diezelfde studie werden er echter ook meer subtiele neurologische veranderingen ontdekt, dit dankzij innovatieve beeldvorming analyses. Zulke veranderingen werden niet enkel in de witte stof, maar ook in de 'grijze stof' (voornamelijk cellichamen, en kortere verbindingsbanen) vastgesteld. Deze subtiele veranderingen konden ook aanwezig zijn indien er geen letsels te onderscheiden waren. Nadien toonden we in een opvolgingsstudie van huidige patiënten aan dat de observeerbare letsels reeds op het einde

van de therapie detecteerbaar zijn. Deze patiënten toonden echter relatief stabiele cognitieve scores, waardoor we vermoeden dat subtiele veranderingen in cognitief functioneren voornamelijk op latere leeftijd kunnen optreden. Tot slot toonden we in een studie met volwassenen die op kinderleeftijd behandeld werden voor een hersentumor, aan dat in geval van opvallende neurologische schade, de onderliggende hersennetwerken structureel kunnen wijzigen, hetgeen tot meer opmerkelijke cognitieve problemen kan leiden.

Concluderend stellen we dus dat intraveneuze chemotherapie in hoge dosissen neurologische schade kan veroorzaken, zowel acuut als op lange termijn. Dit kan breinontwikkeling structureel en functioneel beïnvloeden. Toekomstig onderzoek zal idealiter ook biologische parameters onderzoeken, om de validiteit van de beeldvorming na te gaan, en (in-)directe mechanismen van chemotherapie beter in kaart te brengen. Tot slot worden ook onderzoeksvragen naar emotie-gerelateerde klachten aanbevolen, om psychologische symptomen te reduceren en de kwaliteit van het leven op langetermijn te verhogen.

<div style="border:1px solid #ccc; padding:1em;">

1

<div align="right">

Introduction

</div>
</div>

Abstract

Neurocognitive sequelae are known to be induced by cranial radiotherapy and central-nervous-system-directed chemotherapy in childhood Acute Lymphoblastic Leukemia (ALL) and brain tumor patients. However, less evidence exists for solid non-CNS-tumor patients. To get a better understanding of the potential neurotoxic mechanisms of non-CNS-directed chemotherapy during childhood, we performed a comprehensive literature review of this topic. Here, we provide an overview of preclinical and clinical studies investigating neurotoxicity associated with chemotherapy in the treatment of pediatric solid non-CNS tumors. Research to date suggests that chemotherapy has deleterious biological and psychological effects, with animal studies demonstrating histological evidence for neurotoxic effects of specific agents and human studies demonstrating acute neurotoxicity. Although the existing literature suggests potential neurotoxicity throughout neurodevelopment, research into the long-term neurocognitive sequelae in survivors of non-CNS cancers remains limited. Therefore, we stress the critical need for neurodevelopmental focused research in children who are treated for solid non-CNS tumors, since they are at risk for potential neurocognitive impairment.

Keywords: *pediatric oncology, solid non-CNS tumors, brain maturation, neurotoxicity, chemotherapy*

1.1   Introduction

Overall survival rates of children and adolescents diagnosed with cancer may reach 80% [1]. However, childhood cancer survivors often face residual physical [2] and psychological difficulties [3] which can have a significant impact on their daily lives. The cognitive deficits which limit daily life functioning in these patients are therefore receiving increased attention [4,5]. To date, evidence of late cognitive sequelae in childhood cancer survivors has been found in brain tumor and Acute Lymphoblastic Leukemia (ALL) patients [6,7]. These difficulties may arise due to the impact of both the disease and its treatment on the brain. For these patient groups, the tumor itself, neurosurgery, brain irradiation and/or CNS-directed chemotherapy can cause serious neurocognitive impairment [5,8–18].

By contrast, non-CNS solid tumors, which have a lower risk to metastasize to the CNS system, are treated with non-CNS-directed cancer treatment. Such treatment can include local surgery of the tumor, local radiotherapy, and/or intravenous chemotherapy. Intravenous chemotherapy [19] is administered through the blood vessel into the vascular system, which is assumed not to affect the CNS system directly, due to the blood-brain-barrier. However, non-CNS directed chemotherapy could also cause neurological damage by a variety of neurobiological mechanisms, including damage to the blood brain barrier and by stimulating neuroinflammatory responses [20]. In this context, non-CNS chemotherapy is known to cause acute neurological damage, which manifests clinically as a range of neurological conditions ranging from headaches to paralysis [21,22]. In addition, recent studies have suggested longer term neurotoxic effects, which could give rise to impaired cognition. These studies have mainly been conducted in non-CNS cancers in adult patients including breast cancer [23,24], ovarian cancer [25] and testicular cancer patients [26,27], and have found chemotherapy to be associated with attentional and executive dysfunction.

Unfortunately, neurocognitive research involving childhood survivors of solid non-CNS tumors is still rare, and therefore the neurotoxic effects of non-CNS-directed chemotherapy on cognition in this population are not well understood. With regard to this specific group, there have been only two studies to date: Mohrmann and colleagues (2015) recently reported that one in three solid non-CNS tumor patients experiences at least one subjective cognitive difficulty [9], whilst Bornstein and colleagues (2012) demonstrated significantly lower cognitive scores for current pediatric solid non-CNS tumor patients compared to controls [28]. The lack of research in pediatrics is problematic since the brain is most vulnerable during development and the consequences may be more severe than in adults. Given the increasing survival rates of childhood cancers, summarizing the present knowledge in the field is therefore both timely and important.

This review aims to highlight the role of chemotherapy-induced neurotoxicity on childhood brain development, and how this can be linked to impaired cognition and psychosocial function in later life. Animal studies demonstrate histological evidence for deleterious biological effects [29], and human studies demonstrate acute neurological symptoms when intravenous chemotherapy is administered. Such symptoms can include

headaches, diplopia, convulsions, hemiparesis, which suggests chemotherapy to induce biochemical neural changes.

From the Pubmed database, we extracted studies since 1990 which investigated neurotoxicity due to specific chemotherapeutic agents that are currently administered for childhood solid non-CNS tumor patients in frontline therapy.

In the first part of the review, non-CNS directed chemotherapeutic agents are discussed with regard to their acute symptoms in clinical and preclinical studies. For these sections we focus on three chemotherapeutic agents: methotrexate, alkylating agents (i.e. ifosfamide, cyclophosphamide, cisplatin) and vincristine. Search criteria such as vincristine [or] methotrexate [or] alkylating agents [and] neurotoxicity were used. We then describe potential neurotoxic mechanisms that could interact with neural development and discuss the current scientific literature on neurotoxicity in pediatric solid non-CNS tumors, covering both neuropsychological evaluation and neuroimaging research. Search criteria cognitive [or] neurocognitive [and] cancer [and] childhood were used. Finally, in our conclusion, we underline the importance of investigating the neurocognitive sequelae of chemotherapy in childhood cancers and provide recommendations for future studies in order to stimulate much needed research in this field.

1.2   Evidence for direct chemotherapy-induced neurotoxicity

For the purpose of this review, we have focused on three types of chemotherapy that are currently administered for childhood solid non-CNS tumor patients in frontline therapy: methotrexate, alkylating agents (i.e. ifosfamide, cyclophosphamide, cisplatin) and vincristine. These chemotherapeutic agents act through different toxic mechanisms on the cell during DNA replication. For example, methotrexate inhibits metabolism of folate acid; alkylating agents (e.g. cyclophosphamide, ifosfamide, cisplatin) inhibit cell proliferation by binding with an alkyl group to the DNA strand, and vinca alkaloids (e.g. vincristine) prevent the formation of microtubules in the new cell, which inhibits mitosis [30]. These mechanisms are summarized in Figure 1.1. For each type of chemotherapy, we provide an overview of existing studies since 1990 for methotrexate, alkylating agents (i.e. ifosfamide, cyclophosphamide, cisplatin) and vincristine. We will discuss acute symptoms in patients (section 1.2.1) and histological changes which are induced in animal models (section 1.2.2).
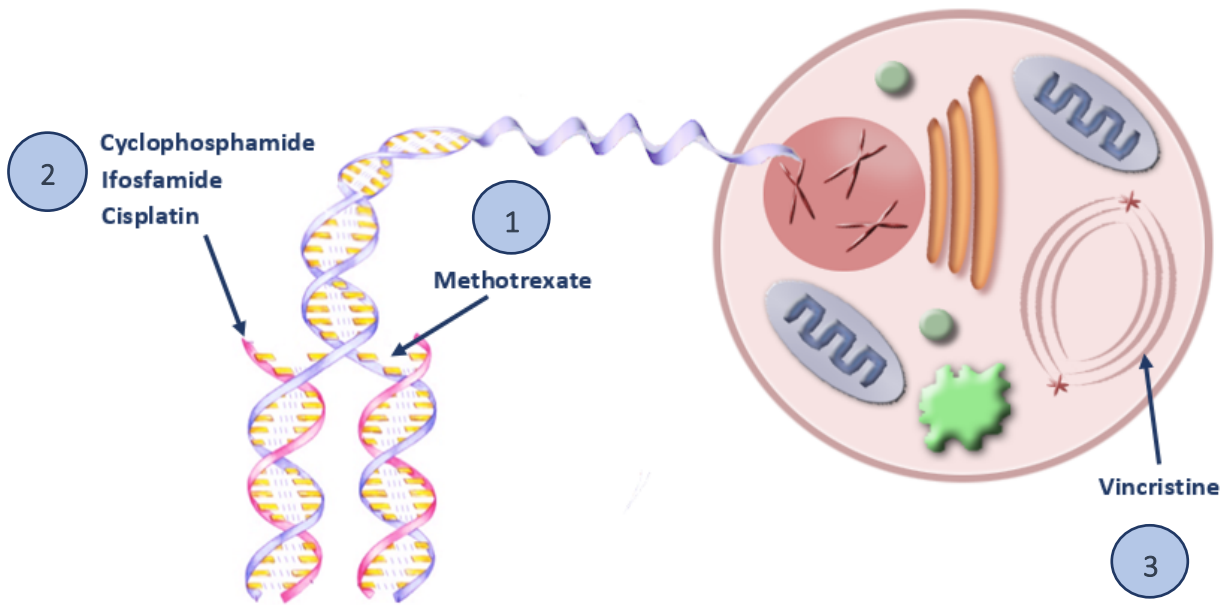
Figure 1.1 Mechanisms of chemotherapeutic agents on cell division

Legend: The chemotherapeutic agents currently used in solid non-CNS tumors, can be subdivided in the following groups: (1) Methotrexate inhibits metabolism of folate acid, which is necessary for the synthesis of the nucleoside thymidine in DNA synthesis (2) alkylating agents (e.g. cyclophosphamide, ifosfamide, cisplatin) inhibit cell proliferation by binding with an alkyl group to the DNA strand, crosslinks are formed in DNA strands, which cause apoptosis of the cell in its attempt to duplicate. (3) vinca alkaloids (e.g. vincristine) prevent the formation of microtubuli in the new cell, which inhibits mitosis.

Table 1.1 Overview of clinical case studies with acute symptoms of the central and peripheral nervous system

Chemotherapeutic agent	Acute central symptoms	Acute peripheral symptoms	References
Methotrexate (antimetabolite)	Epilepsy after treatment		Kasper et al. (2004)
	Transient aphasia 12 days after receiving intravenous high-dose MTX chemotherapy	Right hemiparesis	Eichler al. (2007)
	Stroke like events temporally related to intrathecal MTX, nonfluent aphasia	Bilateral upper-extremity weakness, right-sided or left-sided hemiparesis	Rollins et al. (2004)
		Right-sided hemiplegia, with brisk reflexes in limbs; left facial nerve and upper motor neuron palsy, dysarthria and dysphagia	Tsang & Khong (2005)
Ifosfamide (alkylating)	Encephalopathic symptoms: mostly confusion, associated with lowered albumin levels, not with creatinine or age		David & Picus (2005)
	Risk of encephalopathy in case of concomitant cisplatin		Pratt et al. (1990); Tajino et al. (2010)
	Headaches and seizures		Antunes & De Angelis (1999)
	Acute hallucinations, agitation, and delirium		Bernard et al. (2010)
	Visual and auditory hallucinations		DiMaggio et al. (1994)
	Seizures, irritability, somnolence, dizziness, headaches, with increased risk due to concomitant medication		Di Cataldo et al.(2009)
		Hemiballismic limb movements	Ames et al. (2010)
	Confusion/emotionality, headache and seizures	Hemiparesis, dysphasia, choreoathetosis	Inaba et al. (2008)
Cyclophosphamide (alkylating)	Acute confusion and cortical blindness, hemispatial neglect during treatment with high-dose methotrexate, cyclophosphamide, and dactinomycin	Apraxia	Sanchez-Carpintero et al. (2001)
Cisplatin (alkylating)	Progressive encephalopathy and partial loss of vision		Verschraegen et al. (1995)
	Elevated risk of encephalopathy after ifosfamide in case of concomitant cisplatin administration		Pratt et al. (1990) Tajino et al. (2010)
	Visual disturbance and unconsciousness	Hypertension, convulsions	Ito et al. (1998)
		Hearing loss	Hagleitner et al. (2012)
Vincristine (anti-mitotic)		Isolated abducens nerve palsy	Toker et al. (2004)
		Vocal fold palsy	Burns & Shotton (1998)
		Sensorineural hearing loss	Lugassy & Shapira (1990)
		Altered cochlear functioning	Riga et al. (2007)

1.2.1 Acute neurotoxicity reports

As shown in Table 1.1 , acute neurological events during treatment demonstrate the immediate impact of specific chemotherapeutic agents on the brain [31–33]. For all three agents, encephalopathic symptoms were reported. Nevertheless, a few differences should be discussed.

1.2.1.1   Methotrexate

Intrathecal MTX can lead to a wide range of acute encephalopathic symptoms [34]. Intravenous high-dose MTX can also lead to such symptoms, including hemiparesis or altered consciousness [35,36]. Stroke-like events associated with MTX, (e.g. aphasia and hemiplegia) have been related to acute white matter (WM) changes [34,37–39], most often after intrathecal administration in ALL patients [34,37], but also after high dose intravenous administration in osteosarcoma patients [38,39] (see Figure 1.2).
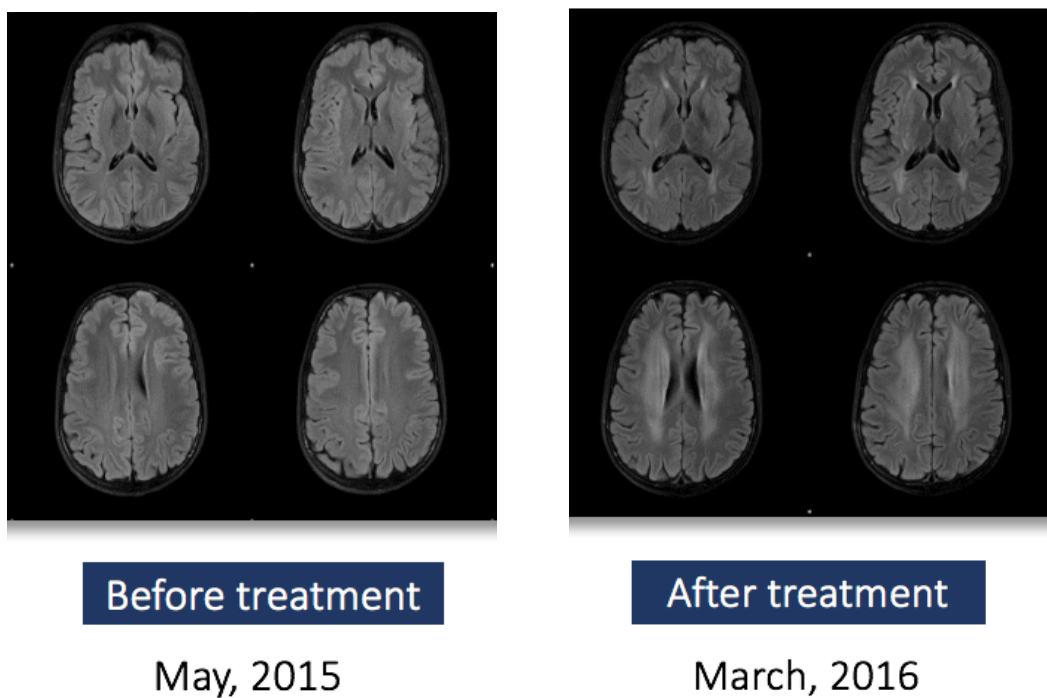
Figure 1.2 Case showing leukoencephalopathy at the end of chemotherapy treatment
Note. This image shows a 14-year old patient who was treated with high dose methotrexate for an osteosarcoma. The FLAIR MRI scan at diagnosis is presented on the left. The image at the end of treatment is shown on the right.

According to Saykin and colleagues [20,40], chemotherapy can induce such neurotoxicity via multiple main pathways, including direct neurotoxic effects, immunological responses, hormonal changes, genetic factors and DNA damage. These potential pathways will be discussed in more detail in Section 1.3.

1.2.1.2   Alkylating agents (ifosfamide, cyclophosphamide, cisplatin)

With regard to alkylating agents, most evidence for acute neurotoxicity has been found for ifosfamide [33,41]. Headaches and seizures [22,42,43], hallucinations [44], agitation, and delirium [45] as well as motor symptoms [46] have been reported.

Despite its similar mechanism on cell duplication, cyclophosphamide is less frequently associated with neurotoxic symptoms [47]. This could be because it crosses the BBB less easily than ifosfamide. Yule and colleagues (1997) demonstrated that cyclophosphamide was less apparent in the cerebrospinal fluid of pediatric oncology patients compared to ifosfamide[48]. Notably, sudden confusion and cortical blindness have been reported for cyclophosphamide used in combination with high dose methotrexate [36].

Neurological symptoms associated with cisplatin, are mostly limited to sensory hearing [49] and vision loss [50,51] and peripheral neuropathy, including pain and paresthesias [33]. Nevertheless, white matter alterations in the CNS have been reported [50]. A combination of cisplatin and ifosfamide may increase the risk of neurological side effects [52,53].

1.2.1.3 Vinca alkaloids (vincristine)

Central neurotoxicity due to vincristine is well known. Vincristine-related seizures and peripheral toxicity such as diplopia [54], nerve paralysis [55,56], sensory neuropathy [57,58], absence of peripheral of reflexes and hearing loss [59–61] have all been reported. Intrathecal administration leads immediately to death [62,63].

Although all of these studies demonstrated acute neurological symptoms according to the CTCAE criteria, none included neurocognitive assessments. Still, it is assumable that sudden symptoms such as confusion, hallucinations, but also peripheral pain and paresthesias interact with cognitive processes at central nervous system level. Hence, acute medical assessments of neurotoxicity would ideally be combined with cognitive screenings in the future.

1.2.2 Animal studies

In addition to the existing evidence for acute neurotoxicity, histological evidence has been demonstrated in rodent studies as shown in Table 1.2. We focused on ex vivo rodent studies. For interested readers, we also refer to a comprehensive review by Seigers et al. [29].

Dose-dependent apoptosis was found for all of the specified agents [64–66]. Notably, Briones & Woods (2013) also found evidence of myelination changes in white matter [67] when methotrexate was used in combination with cyclophosphamide. Overall, these studies demonstrated decreased neurogenesis at young age [64,66,68–75], as well as brain necrosis in adult rodents [65,67,76–81]. Most changes were found in the hippocampus [65,68,71,73,75,76,78,79,82], which is mainly associated with (episodic) memory functioning. Note that, in general, the hippocampus is mostly investigated in animal studies. For cisplatin in particular, deeper structures (e.g., the thalamus, hypothalamus and dorsal striatum) as well as higher order regions were affected [64,66,68–70,72,73,77,80,81,83]. To date, only a few studies in rodents have investigated effects of vincristine [66,84]. Note that acute vincristine-induced neurotoxicity in patients was also mainly limited to sensory hearing loss. Less evidence exists for central neurological symptoms.

Table 1.2 Overview of animal studies for neurotoxic effects of chemotherapeutic agents (used in pediatric solid non-CNS tumor patients)

Chemotherapeutic agent	Evidence for neurotoxicity	Age	Affected brain regions	References	Indication of potential neurotoxic mechanism
Methotrexate (antimetabolite)	Dose-dependent apoptosis	7 days	Cortex, thalamus, hippocampus, caudate nucleus	Rzeski et al. (2004)	All mechanisms
	Dose-dependent decline in neurogenesis	3 months	Hippocampus	Seigers et al. (2008)	All mechanisms
	Decline in neurogenesis	adult	Hippocampus	Briones & Woods (2011)*	All mechanisms
	Reduced blood vessel density and microglia, but no elevated cytokine levels	3 months	Hippocampus	Seigers et al. (2009)	Immune dysregulation
	Increased levels of IL-1β, TNF-α, and COX-2, decrease in cytokine IL-10	12 months	Corpus callosum	Briones et al. (2013)*	Immune dysregulation
	Decreased myelination Increased levels of free radicals as marker for oxidative stress	Not specified	Cerebrum, cerebellum, midbrain, pons medulla, hippocampus and hypothalamus	Rajamani et al. (2006)	Oxidative stress
	Increased levels of MDA (an important marker of lipid peroxidation)	Adult	Cerebellum	Uzar et al. (2006)	Oxidative stress
Ifosfamide (alkylating)	Dose-dependent apoptosis	7 days	Cortex, thalamus, hippocampus, caudate nucleus	Rzeski et al. (2004)	All mechanisms
Cyclophosphamide (alkylating)	Dose-dependent apoptosis	7 days	Cortex, thalamus, hippocampus, caudate nucleus	Rzeski et al. (2004)	All mechanisms
	Decline in neurogenesis	8-10 weeks 2 months	Hippocampal regions	Yang et al. (2010); Christie et al. (2012)	All mechanisms
	Decline in neurogenesis	adult	Hippocampal regions	Briones & Woods (2011)*	All mechanisms
	Decreased survival of cells dividing at the beginning of treatment, but no long-term effects	Not specified	Hippocampal regions	Lyons et al. (2011)	All mechanisms

	LTP was impaired during cyclophosphamide treatment, but was enhanced after recovery from chemotherapy	7 months	Hippocampal regions	Lee et al. (2006)	All mechanisms
	Increased levels of IL-1β, TNF-α, and COX-2, decrease in cytokine IL-10 Decreased myelination	12 months	Corpus callosum	Briones et al. (2013)*	Immune dysregulation
	Decreased growth and viability of neurons, damaged nuclear DNA and early apoptotic morphological changes	embryo	Neural tube in embryonal brains	Xiao et al. (2007)	DNA damage
	Decline in the levels of reduced glutathione, glutathione peroxidase, and alkaline phosphatase	6-8 weeks	Not specified	Bathia et al. (2006)	Oxidative stress
Cisplatin (alkylating)	Dose-dependent apoptosis	7 days	Cortex, thalamus, hippocampus, caudate nucleus	Rzeski et al. (2004)	All mechanisms
	Remodeling of excitatory afferents and Purkinje cell dendrites	10 days	Cerebellar cortex	Avella et al. (2006)	All mechanisms
	Increased cell apoptosis and decreased cell division	Not specified	Subventricular, hippocampus, corpus callosum	Dietrich et al. (2006)*	All mechanisms
	Decreased spine density and cell death	8 days 1 day	Cerebellar granule neurons Hippocampal neurons	Wick et al. (2004)* ° Andres et al. (2014)*	All mechanisms
	Apoptosis, altered granule cell migration and Purkinje cell dendrite growth	10 days	Cerebellum	Cerri et al. (2011)	All mechanisms
	Loss of neuronal activity, accompanied by cell apoptosis	embryo	Auditory cortex cells	Gopal et al. (2012)*	All mechanisms
	Increased BBB permeability, brain necrosis	adult	Hypothalamus, auditory cortex and caudal putamen	Sugimoto et al. (1995)	Direct neurotoxicity
	Cytoarchitectural changes and decrease in immunoreactivity for neurotransmitter markers	10 days	Hippocampal neurons	Piccolini et al. (2012)	Immune dysregulation
	DNA damage due to increased oxidative stress	adult adult	Not specified	Turan et al. (2014) Gulec et al. (2013)	DNA damage & oxidative stress
Vincristine (anti-mitotic)	Dose-dependent apoptosis	8 days	Cerebellar granule neurons	Wick et al. (2004)* °	All mechanisms

Note. * Direct administration of agent to neuroepithelial stem cell/precursor brain cell (neuron/support cell) cultures
  ° Administration in combination with other agents

As could be concluded from Table 1.2 some of the animal studies specifically have evidenced biomarkers for inflammation [67,73,79] and oxidative stress [77,81,85–87]. We will now discuss how these markers are related to specific neurotoxic pathways.

1.3   Possible neurotoxic mechanisms

According to Saykin and colleagues [20,40] five main pathways of chemotherapy-induced neurotoxicity can be distinguished, namely direct neurotoxic effects, immunological responses, hormonal changes, genetic factors and DNA damage (see Figure 1.3). In Table 1.2 we associate these potential mechanisms with existing animal studies for the three specified chemotherapeutic agents (i.e. methotrexate, alkylating agents, vincristine).
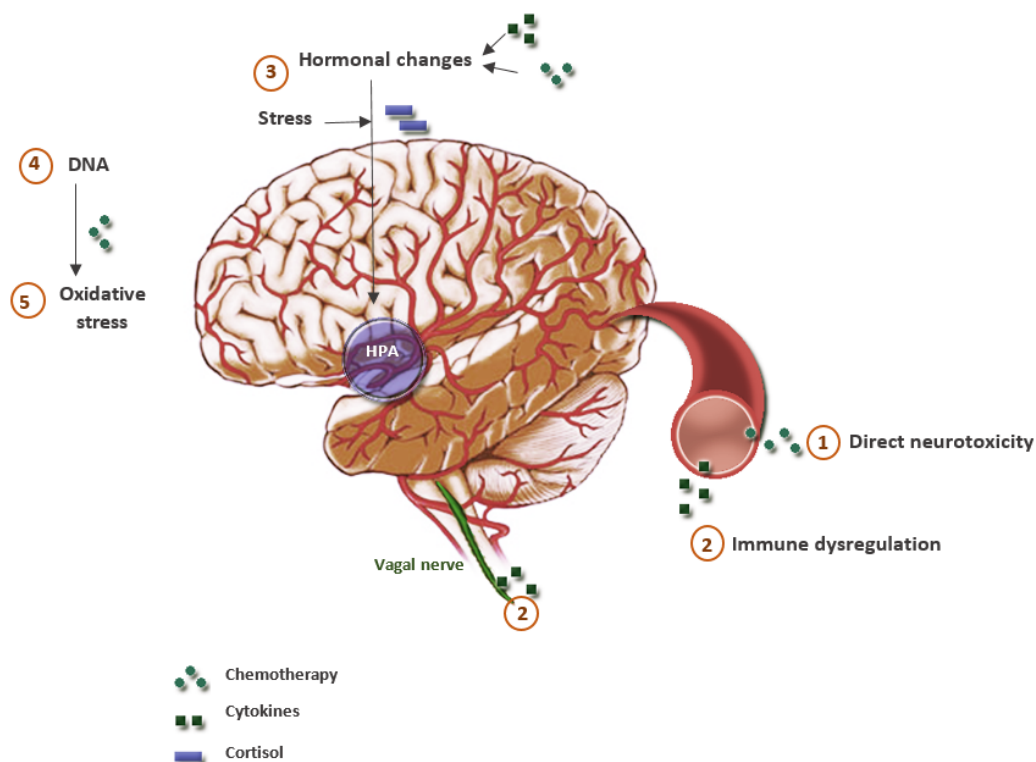
Figure 1.3 Potential neurotoxic pathways of chemotherapy

Note. This figure illustrates the five main neurotoxic mechanisms and possible interactions between them: (1) Direct neurotoxicity: chemotherapy crosses the blood-brain barrier immediately, (2) Immune dysregulation: immune signals such as cytokines could become neurotoxic through neuroinflammation, (3) Hormonal changes (e.g. alterations in estrogen and testosterone) are associated with cognitive functioning and functional changes within the brain, (4) Genetic predisposition: polymorphisms of specific genes (e.g. BDNF, APOE, …) are related to neurotoxic vulnerability and neural repair after chemotherapy, (5) DNA damage (e.g. by oxidative stress): chemotherapy can induce DNA damage in neurons directly or through oxidative stress.

1.3.1 Direct neurotoxicity of chemotherapeutic agents

Several chemotherapeutic agents can cause central neurotoxicity by crossing the BBB readily [88]. Direct damage to the BBB was shown in animal studies for agents such as cisplatin [80] (see Table 1.2). This may lead to grey matter (GM) apoptosis and/or white matter (WM) demyelination.

1.3.2 Immune dysregulation

In response to the disease itself[89] or to surgery [90,91] or to immunotherapy [92] the human body reacts with an increased immune response. Tissue damage activates peripheral immune responses that can cause neuroinflammation either directly or indirectly. On the one hand, peripheral cytokines (e.g. IL-1β, TNF-α, CRP) can directly bind to brain receptors, and cause damage to the BBB [93]. In this way they can directly invade the brain and induce neurotoxicity.

The indirect mechanism on the other hand, can be through stimulation of the vagal nerve [94], or through cytokine production and transition of macrophages within the brain [95], which induces functional brain changes in an indirect way. Evidence for neuroinflammation in the case of solid non-CNS tumors was found by Kesler and colleagues (2013) [96]. They demonstrated higher levels of cytokines, as well as reduced hippocampal volume in breast cancer survivors. Elevated levels of cytokines and simultaneous demyelination of the WM in response to chemotherapy in rodents [67] also suggest that neurological alterations can be induced by peripheral cytokines.

In addition to anatomical changes, cytokines can affect hormonal processes, by altering hypothalamus-pituitary-adrenal (HPA)-axis functioning [97–99]. Such hormonal changes can also influence cognitive functioning [100], which is discussed in the next section.

1.3.3 HPA-axis functioning: hormonal changes and stress

Since sex-related hormones (e.g. estrogen and testosterone) increase during adolescence, and influence brain development, the question arises as to what extent these changes are modified by chemotherapeutic agents. Sex- and stress-related hormones are mainly regulated by the HPA-axis [101]. Because some chemotherapeutic treatments (e.g. in ALL patients) include glucocorticosteroids, treatment may directly suppress HPA-axis activity. The investigation of chemotherapy-induced alterations of HPA-axis function is an active area of research[99,102]. Some studies have demonstrated longer HPA-axis suppression during treatment of childhood ALL and brain tumors [102–107]. Changes in HPA-axis activity were shown to lead to learning and memory difficulties in animals [100].

1.3.4 Genetic predisposition

Polymorphisms that are associated with cell metabolism, DNA repair or brain development, can affect the CNS vulnerability to chemotherapy-induced toxicity. The MTHFR-gene and the APOE-gene genotypes have been investigated most extensively [88]. The MTHFR-gene encodes for methylenetetrahydrofolate reductase, which is related to the folate metabolism. Given that disturbance of the folate metabolism may eventually result in demyelination, as well as

in endothelial damage and in intensive stimulation of N-methyl-D-aspartate (NMDA) receptors in the brain [88], the association between these polymorphisms and neurotoxicity due to MTX has been extensively investigated [108,109]. For instance, with regard to the MTHFR1298-gene, patients with the AC/CC genotype scored lower on the Trail Making Test than those with the AA genotype. The APOE-gene on the other hand, encodes for Apolipoprotein E, a glycolipoprotein that plays an important role in neuronal repair and neuroplasticity [110]. More specifically, patients who carry an ε4 allele show increased neurotoxic vulnerability to chemotherapy when compared to the ones who do not [111].Polymorphisms of the BDNF (Brain-Derived-Neurotrophic-Factor)-gene were recently also associated with neuroprotection against the toxic effects of chemotherapy [112].

1.3.5 DNA damage and oxidative stress

Finally, neuronal DNA damage can lead to transcription inhibition and subsequent changes in neurotransmission [113]. Since chemotherapeutic agents interfere with DNA synthesis, neurotoxicity might also be more pronounced when DNA repair mechanisms are weakened. As mentioned in Table 1.2, Xiao and colleagues reported neural DNA damage due to cyclophosphamide. One specific mechanism of DNA damage is oxidative stress. The production of free radicals during cell metabolism causes neurodegeneration [114]. Furthermore, increased oxidative stress was also discovered after the administration of MTX [86,87], cisplatin [77,81,115] and cyclophosphamide [85] in rodent studies. Recently, Caron and colleagues (2009) [116] showed elevated levels of oxidized phospholipids in the CSF (i.e. indication of oxidative stress) in combination with decreased executive functioning in pediatric ALL patients. Cole and colleagues (2015) also demonstrated that specific gene polymorphisms related to oxidative stress, were associated with lower neurocognitive scores in ALL patients [117]. These studies indicate the important role of oxidative stress in neurocognitive development during cancer. According to Wang and colleagues (2015) [98], inflammatory cytokines may not only cross the BBB and induce hormonal changes, but can also cause free oxygen radicals. This illustrates the interdependency between the previous mechanisms.

1.4 Possible influence in pediatric population

1.4.1 Neurotoxicity in a developing brain

Given that postnatal brain development occurs during childhood, children could be particularly vulnerable for treatment-induced neurotoxicity [118]. More specifically, cognitive functioning including domains of attention, verbal and visual (working) memory, processing speed, language, visuomotor functioning exponentially increase throughout development. From a neurobiological point of view, structural development of brain regions and their connections is crucial for daily life functioning. It has been widely assumed that neural development mainly implies decreases in cortical GM and increases in WM between the age of 4 and 20 [119–121]. We discuss GM and WM development separately, even though their development is interdependent [122,123].

1.4.2 Grey matter development

GM consists of neuronal cell bodies. Maturation of the GM follows a curved pattern: its density increases until young adolescence (between 12 and 20 years) and from then on it declines again [119,123–126]. These curves differ between brain areas. As reported by Gogtay and colleagues, lower-order somatosensory and visual cortices mature first, which is followed by higher-order association cortices and frontal cortex, which integrate the incoming information (i.e. parietal, frontal and superior temporal cortices) [122]. This developmental pattern matches the phylogenetical pattern (see Figure 1.4). Hence, integration of the higher-level cortical regions results in better cognitive performance on more demanding tasks. Cortical development and synapse elimination is thus heterochronous.
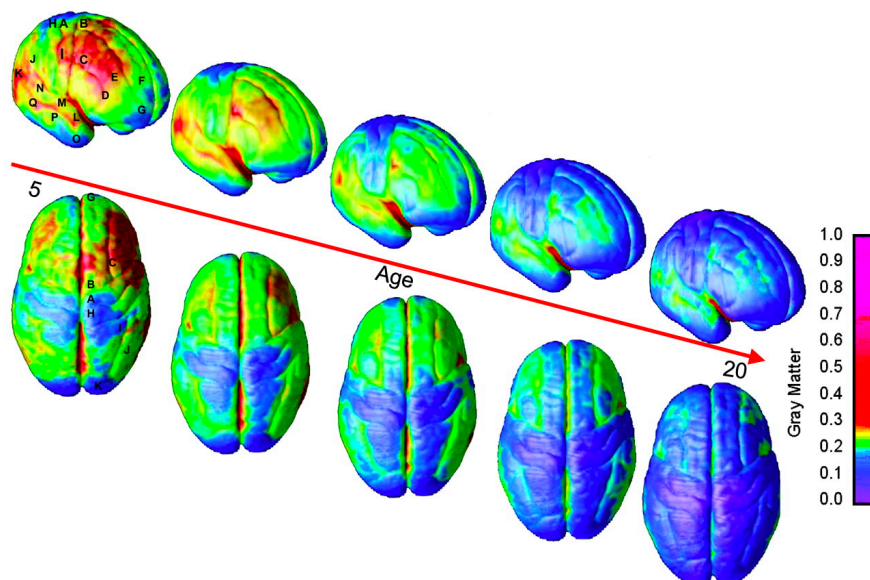
Figure 1.4 Cortical development of GM volume throughout childhood.
Adapted from Gogtay et al. [122]

An important GM structure located deeper in the brain is the hippocampus. This structure is mainly responsible for (episodic) memory function. Hippocampal development is influenced by stress-related hormones [127,128]. Since chemotherapy induces hormonal changes

(see previous section about neurotoxic mechanisms), this may indirectly cause structural changes in the hippocampus. In a recent review, Dietrich and colleagues [129] found that chemotherapy-induced direct cellular toxicity, inflammation and oxidative stress (i.e. indirect toxicity) all had a negative impact on hippocampal function.

Prefrontal regions, which are related to executive functioning, develop later. As a result, behavioral symptoms such as lack of self-control could appear if development is disturbed during the maturation process of this region. Such disturbances could arise before as well as during adolescence. With regard to sex-related differences, Giedd and colleagues (1999) showed that GM development peaks earlier for women than for men. This suggests hormonal effects on brain development. More specifically, elevated levels of testosterone were related to higher GM density for males [130].

Given the neurobiological evidence of neuron apoptosis in animal models, the question is whether age-dependent damage to the GM, can result in specific cognitive or behavioral symptoms.

1.4.3 White matter development

Besides this spatiotemporal pattern of the grey matter, white matter tracts which connect the grey matter areas (mainly containing glial cells and axons), also mature (i.e. myelinate and sprout) until young adolescence [131,132] . Whereas most GM development peaks in childhood, the amount of WM, which contains glial cells and myelinated axons, continues to increase until young adolescence [120,124] and remains stable until mid-adulthood. Besides volumetric studies of the WM, diffusion tensor imaging (DTI) is commonly used for investigating WM properties at a more microstructural level. DTI studies have found increasing anisotropy with age in brain regions associated with attention, motor skills, cognitive ability, and memory. Such increases in anisotropy, suggest more spatially organized WM fiber bundles. Notably, higher anisotropy in prefrontal and parietal regions has been correlated with working memory and reading abilities [133].

As is the case for GM development, patterns of maturation differ between both sexes [124]. WM increases more strongly for males, which suggests the influence of hormonal differences. Given that animal studies as well as studies in adult cancer patients have found changes in WM [67,134], an important question to address is whether chemotherapy during childhood may cause behavioral and cognitive sequelae. In this context, Schuitema and colleagues found WM changes that correlated with cognitive dysfunction in ALL survivors 20-30 years after diagnosis [134].

Due to these maturation processes, potential toxicity of medication and related mechanisms highly depend on the age of the child. Furthermore, as developmental demands increase with age, such induced cognitive deficits can tremendously affect academic performance, job success, social functioning and mental health over time [6].

1.4.4 Hormonal influences

Hormonal changes (e.g. stress-related changes) affect brain development in several ways, such as functional and structural changes of the hippocampus and limbic structures due to maltreatment and early stress (see Teicher et al. for a review [128]). The most widely investigated hormone is cortisol, regulated by the HPA-axis. Functional changes of this axis due to stress [135,136] or due to chemotherapy may cause long-term brain damage. In this context, most evidence of brain damage has been found for the hippocampal region [137,138]. Chemotherapy induced HPA-axis alterations during childhood can impact negatively on the quality of life of young cancer patients. For example, dysregulated activity of the HPA-axis in children has been associated with depression [139] as well as disruptive behavior [140,141]. Although research is abundant regarding the dysregulation of the reproductive system due to chemotherapeutic agents [142,143], potential dysfunctioning of the HPA-axis remains unclear. Since the HPA-axis is mainly responsible for hormonal regulation, we see the urge to expand investigations of chemotherapy-induced alterations of the HPA-axis.

1.5   Evidence of neurotoxicity in pediatric solid non-CNS tumors

1.5.1 Neurocognitive studies

In this section of our review, we discuss studies since 1990 which specifically included patients who were treated for non-CNS tumors during childhood, as control group or as patient group, if no radiotherapy was administered. Notably, solid non-CNS tumor patients were mostly considered as a control group in childhood studies, not as the group of interest. In a recent study, Bornstein and colleagues (2012) demonstrated that children who were treated for solid non-CNS tumors obtained motor and cognitive functioning scores which were similar to leukemia patients but lower than healthy controls [28]. Also other studies confirmed equal IQ scores for both patient groups [144–146]. Accordingly, a large study of Kadan-Lottick and colleagues (2010), revealed comparable scores for task efficiency and emotional regulation for several cancer survivor groups (i.e. osteosarcoma survivors, Acute Myeloid Leukemia, ALL and non-Hodgkin-lymphomas survivors), which were significantly lower than their siblings. However, they did not find significant differences for soft tissue and Ewing sarcomas [147].

In contrast, some studies do report lower cognitive scores for ALL patients treated with intrathecal chemotherapy in comparison to solid non-CNS tumor patients [148]. Brown and colleagues (1996) did not encounter such differences at diagnosis, but did find lower IQ scores in ALL patients 3 years later [149]. Also visuomotor functioning appeared lower in ALL patients who were treated with intrathecal chemotherapy compared to solid tumor patients [150,151]. Similarly, significant cognitive complaints (e.g. for concentration, working speed, task efficiency or memory) were mostly found in CNS tumors, cranial irradiation [152] and leukemia survivors [153]. Recently however, in a series of 58 patients, Mohrmann and colleagues (2015) reported that one out of three childhood solid non-CNS tumor patients had at least one cognitive complaint [9]. Furthermore, Edelman and colleagues also demonstrated that osteosarcoma survivors score significantly lower than controls for processing speed as well as memory, reading and attentional functioning. However, in their study this was only related to endocrine

and cardiac alterations, but not to MTX dose [154]. Concludingly, a limited number of studies investigated cognitive functioning of pediatric solid non-CNS tumor patients. To date, no study has been performed with cognitive assessments in only childhood solid tumor patients vs. control participants.

1.5.2 Neuroimaging studies

Similar to the existing neurocognitive studies, most imaging studies for solid tumor patients which investigate chemotherapy-induced neurotoxicity, were conducted for adult breast cancer patients [155–157]. They described both structural as well as functional neural changes. On the one hand, structural imaging studies demonstrated decreased GM densities in frontal, temporal, and cerebellar regions [158], as well as reduced hippocampal volumes [96,159]. On the other hand, also microstructural WM differences were observed between patients and control participants in multiple regions [23,24,160].With functional MR studies researchers also found reduced activation in prefrontal regions during executive tasks [24,155,161–163] as well as hyperactivation during verbal memory tasks [163].

In contrast to several studies in adults, brain developmental changes associated with the treatment of childhood cancer have so far only been investigated in ALL. Cranial irradiation is known to cause cognitive sequelae. As a consequence, chemotherapy combined with radiotherapy induces stronger morphological brain alterations than chemotherapy alone [164]. Nevertheless, recent studies with ALL patients showed brain changes due to chemotherapy alone. Neuro-anatomical findings in non-irradiated survivors leukemia which might explain such deficits, range from overt white matter (WM) hyperintensities to more subtle changes in grey and white matter volumes [15,165–167]. For example, using quantitative morphometry, Lesnik and colleagues (1998) [168] found smaller GM volumes in prefrontal and cerebellar regions of ALL survivors, who were treated only with intrathecal MTX and high dose IV MTX. Furthermore, DTI studies have shown WM alterations in the ALL survivor group [15,134]. According to Pääcko and colleagues (2000) the most notable WM changes were found in younger children [169]. Besides such morphological changes, recent resting-state fMRI studies also found decreased functional connectivity in ALL survivors [18,170].

In this regard, we also recently demonstrated functional connectivity to be reduced in leukemia survivors in the attention-related *Default Mode Network* (DMN), even years after treatment [170] (see Figure 1.5). Such functional brain changes might contribute to executive dysfunctioning, which was predominantly reported as a cognitive sequel in leukemia patients.

Although these studies suggest long-term neurotoxic effects, social contexts, such as higher parental education, and patients' baseline cognitive reserves are protective factors for potential neurotoxicity. This was shown by Kesler and colleagues, who associated the amount of neural reorganization of the WM with maternal education level [171]. So far, no neuroimaging studies exist for pediatric solid tumor patients.
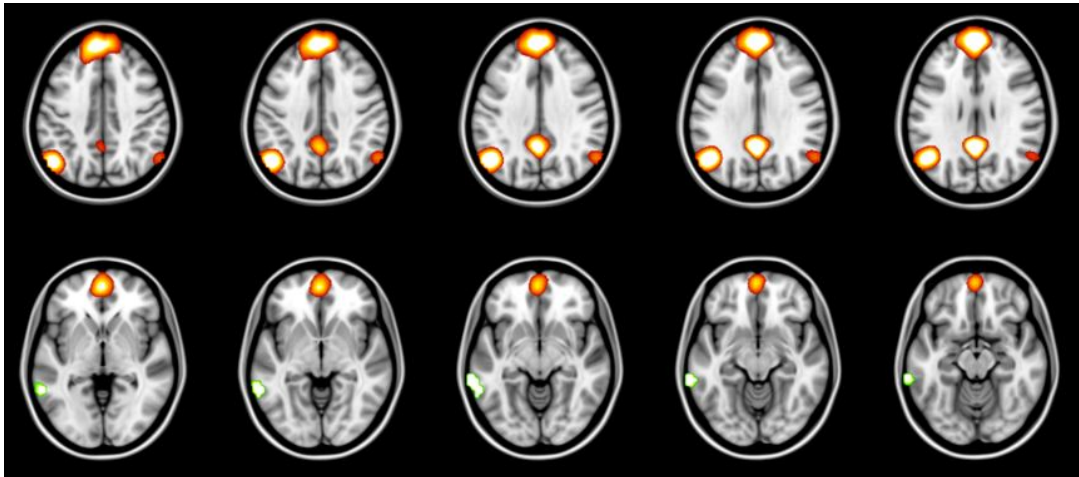
Figure 1.5 Functional connectivity Default Mode Network leukemia survivors vs. controls.
Adapted from Billiet et al. [170]
The group-average Default Mode Network is depicted in orange. The region which showed lower functional connectivity with the DMN in leukemia patients, is indicated in green (i.e. Inferior Temporal Gyrus).

1.6 Concluding remarks and future directions

Given that survival rates of solid non-CNS tumors have increased during the last few years, late psychosocial effects are of increasing interest and importance. So far, only physical rehabilitation has received primary attention in solid tumors, since these complaints are more common for solid tumor patients. Also, the sample size of these patient group is rather small and heterogeneous (e.g. treatment protocols, tumor type, tumor locations, age at diagnosis, etc.). This way it is challenging to perform high level research with these patient groups, and to draw firm conclusions with regard to their functioning. However, we reported histological and clinical evidence suggesting clear neurotoxicity of chemotherapeutic agents in the treatment of pediatric solid non-CNS tumors. Such acute neurological conditions and neural damage can lead not only to motor dysfunctioning, but also altered cognitive processes. Hence, understanding how neurocognitive functioning is altered is equally important, and acute cognitive screening assessments are highly recommended. We reported the potential pathways through which chemotherapy elicits damage, its impact on brain development and the long-term sequelae in pediatric cancer patients so far.

From animal and adult studies, we know that functional as well as structural neurological changes can appear after non-CNS directed chemotherapeutic treatment. Hence, the question whether and at what age brain development can be affected in pediatric solid non-CNS tumor patients, becomes crucial to address.

Although neurocognitive research demonstrates altered brain development for pediatric ALL and brain tumor patients, only a limited number of studies have been performed in pediatric solid non-CNS tumor patients. Ideally, such future studies should combine neurocognitive and imaging methods to assess neurodevelopment of pediatric solid tumor patients. Since treatment of the former patient groups include CNS-directed chemotherapy and irradiation respectively, it remains unclear whether non-CNS-directed chemotherapy can have a similar impact on brain development.

During development, gender and age play a major role in brain development, which interacts with hormonal processes. One of the potential neurotoxic pathways of chemotherapy is through hormonal pathways, such as modification of the HPA-axis. Such alterations may result in emotional and behavioral changes, depending on the gender and age of the patient. Furthermore, the different maturation patterns of brain regions at a specific age suggest different neurotoxic effects between patients of different ages. Given that frontal GM regions develop later in life than parietal regions, the largest impact of chemotherapy could be expected in frontal regions, with attentional and executive problems later in life. To address whether either younger patients or adolescents are more vulnerable, we recommend prospective designs in future studies. This way changes over time can be linked to dose, or to duration of treatment, and age at diagnosis. Since cognitive reserves may also play a role, it is highly recommended to include socioeconomic information in future studies.

Besides direct damage to the BBB, we discussed potential indirect toxic pathways of inflammation and DNA changes. It is possible that certain DNA polymorphisms related to brain development (i.e. APOE, BDNF, …) may provide protection against neurotoxicity during development. As it remains uncertain which immunological mechanisms and genotypes are involved in chemotherapy-induced neurotoxicity, studies including measurements of such biomarkers should be prioritized.

In comparison to ALL patients, childhood solid non-CNS tumors are a heterogeneous group with different diagnoses, staging and treatment protocols. To be able to distinguish between the potential neurotoxic effects of certain chemotherapeutic agents, differences in treatment protocols including non-CNS-directed chemotherapy should be investigated thoroughly. Although most studies only include a small number of patients, the acquisition of meaningful data from homogeneous populations requires large sample-size longitudinal multicenter studies. Given the evidence for acute neurotoxicity in childhood solid non-CNS tumor patients, the limited number of studies for long-term effects is remarkable.

Ideally, longitudinal study designs should be used which include measurements at diagnosis and after therapy. Given that this could be challenging, survivor studies would also provide valuable information. Only based on the results of these studies, will it be possible to construct international guidelines for further educational help, and for remediation, as well as to correctly inform and advise affected children and their parents [172]. In the event that no evidence for long-term neurotoxicity will be found, clinicians will be able to communicate this valuable and reassuring information to their patients and families.

In conclusion, whilst some advances have been made in our understanding of the neurotoxic effects of chemotherapy, there remains an urgent need for more research investigating how neurodevelopment is altered by chemotherapy in childhood and how this impacts on future cognitive and psychosocial function.

2 Objectives and outline

2.1 Objectives

The main aim of this PhD project was to gain knowledge about potential neurotoxicity in childhood cancer patients using state-of-the art neurocognitive and neuroimaging assessments. As previously mentioned, childhood cancer treatments are typically individualized, according to the diagnosis (i.e. type of cancer), location of the tumor, risk group (i.e. aggressiveness), and age at diagnosis. Hence, possible neurocognitive impairment highly depends on the treatment constituents as well as subject-specific risk factors (e.g. SES, age, cognitive reserves, ….).

Based on our literature review (Chapter 1), it was hypothesized that even (high-dose) intravenous chemotherapy (which is non-CNS-directed) could be neurotoxic. Still, underlying mechanisms probably cover a wide range, and are still to be unraveled (see Figure 2.1). Furthermore, subject-specific risk factors such as age at diagnosis, SES, depression, therapy doses and genetic predispositions are to be investigated.

Given that treatment-induced neural changes and subject-specific risk factors remain poorly understood, we addressed the following main research questions:

1. How does neurocognitive functioning develop throughout childhood leukemia patients, treated with intrathecal (i.e. CNS-directed) methotrexate and high-dose intravenous methotrexate? (Chapter 4)
2. Does high-dose intravenous (non-CNS-directed) chemotherapy induce long-term neurotoxicity in non-CNS sarcoma patients?
   a. Do we detect long-term observable leukoencephalopathy? (Chapter 5)
   b. Is white matter microstructure altered at intra-voxel level? (Chapter 6)
   c. Is grey matter structure and functional coherence affected? (Chapter 7)
3. How does neurocognitive functioning and leukoencephalopathy develop in current childhood non-CNS sarcoma patients treated with high-dose intravenous chemotherapy (Chapter 8)
4. Can we optimize subject-specific neuroimaging techniques in case of extensive neural damage (e.g. due to CNS tumors)? (Chapter 9)
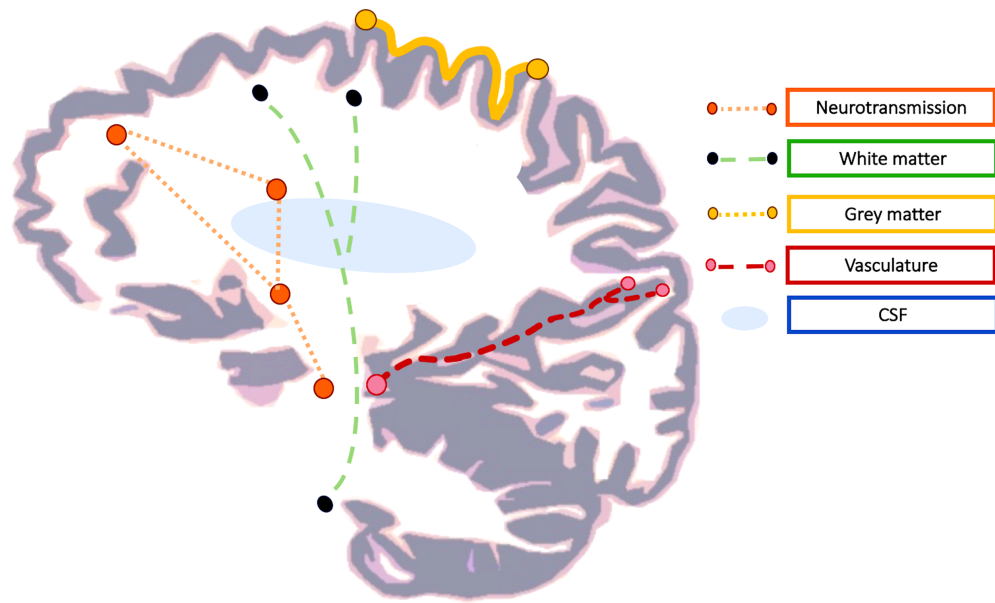
Figure 2.1 Schematic overview of neural anatomical systems involved in potential neurotoxicity

2.2 Outline

To address these questions, a variety of MRI sequences and neurocognitive assessments were obtained in current childhood cancer patients and survivor subgroups. Methods that were implemented across different studies will be discussed in more detail In Chapter 3. The different populations and applied methods to address the abovementioned questions are discussed for each chapter below.

As mentioned in the introduction, leukemia patients receive CNS-directed prophylaxis in addition to high-dose methotrexate, to prevent CNS metastases. This treatment was associated with acute encephalopathy, as well as long-term neurocognitive and neuroimaging changes. Nevertheless, evidence from longitudinal designs is still limited and developmental patterns remain hypothetical. Hence, in **Chapter 4** we investigated longitudinally acquired intelligence assessments (WISC-R) in 94 childhood leukemia patients, who were treated with CNS-prophylaxis in addition to high-dose intravenous methotrexate between 1990 and 1997. We hypothesized that educational background of the parents and age at diagnosis were important predictors in intelligence scores.

Based on the literature study, we also concluded a lack of neurotoxicity investigations in case of high-dose intravenous chemotherapy during childhood. Therefore, **Chapters 5, 6, 7** aimed to clarify the imaging features of long-term neurotoxicity in adult survivors of childhood non-CNS solid tumors. These chapters were based on our cohort study of survivors (n=34) who were treated with high-dose chemotherapy only (and local surgery and possibly RT). We explored the potential long-term impact of this treatment in childhood cancer survivors (n=34), compared to healthy controls (n=34), using FLAIR MRI, DWI, T1-weighted MRI, rsfMRI combined with neurocognitive assessments and genetic polymorphisms.

- **Chapter 5:** Observable leukoencephalopathy
This chapter investigated long-term lesions which are visually detectable on FLAIR MRI scans in the survivor cohort study. As previously mentioned, such lesions can be induced by toxic medical treatments. We discussed the odds ratios of these lesions in the survivor cohort, and hypothesized potential risk factors including the ApoE and MTHFR genotype, chemotherapy doses, age at diagnosis. Finally, we investigated the association between leukoencephalopathy, diffusion-weighted MRI, myelin-water imaging and neurocognitive outcomes in these patients.

- **Chapter 6:** Microstructural white matter alterations
Besides macroscopic visually observable lesions, diffusion-weighted MRI provides more detailed estimation of the white matter microstructure at a microscopic level, thanks to its directional information. Previous DWI studies have shown compromised white matter integrity following systemic chemotherapy in adult cancer patients. However, this has not been investigated in childhood solid tumors yet. In addition, more recent advanced diffusion models were not yet implemented in cancer patients. In this chapter, we applied the most recent diffusion analysis techniques (i.e. fixel-based analysis and NODDI model) to our survivor cohort.

- **Chapter 7:** Grey matter structure and functioning
Chapter 7 aimed to investigate grey matter structure and functional connectivity based on the T1-weighted MRI and rsfMRI scans, respectively. A voxel-based and surface-based approach was implemented to estimate grey matter density and cortical thickness, resp. Additionally, functional connectivity was estimated for regions which show lower cortical thickness, and these connectivity estimates were compared with healthy participants.

In order to explore neurodevelopmental and neurotoxic patterns throughout treatment in current childhood non-CNS tumor patients, **Chapter 8** demonstrates a longitudinal study in 15 pediatric cancer patients, of whom neurocognitive data and neuroimaging data were assessed. This chapter demonstrates odds ratios of leukoencephalopathy, and development in neurocognitive scores.

Given that the abovementioned studies yielded leukoencephalopathy due to chemotherapy, and cognitive problems are frequently present in case of clear neural damage, subject-specific neuroimaging becomes an interesting research field. Hence, we discussed a variety of DWI neuroimaging analyses to investigate white matter microstructure and topological organization in case of extensive neural damage in **Chapter 9,** specifically in survivors of fossa posterior tumors. Using a voxel-based, fixel-based and graph theoretical approach, we estimate not only local neural integrity, but also possible topological reorganization of the network.

Chapter 10 provides a general discussion of all abovementioned studies.

3 | Methods

3.1 Daily life questionnaires

Psychological complaints in oncology patients can cover a wide range of symptoms, including cognitive, emotional and behavioral problems. However, the assessment of such symptoms is a very complicated task in childhood cancer patients. Answering questionnaires about such complaints, is challenging for children since their cognitive abilities are still in development. Hence, a limited number of questionnaires were acquired in children, but were expanded to a wider range of questionnaires in the adult survivor study.

3.1.1 Children

In our current childhood non-CNS cancer study, we acquired one executive questionnaire (BRIEF) [173] and the Health-Related Quality of Life Questionnaire (HRQoL) from all children above 10 years old, and from all parents (also for children with younger ages) [174,175]. It was possible to acquire a larger range of questionnaires in our adult study.

3.1.2 Adults

In adult participants (i.e. childhood cancer survivors and healthy controls), we assessed questionnaires covering a variety of domains such as anxiety, depression, cognitive and executive functioning, daily quality of life including physical complaints and social functioning. The selection of questionnaires was based on a similar previous study in adult survivors of childhood leukemia [176], to be able to match data and compare findings.

First, anxiety was addressed using the State-Trait Anxiety Inventory (STAI) [177]. This questionnaire aims to estimate state and trait anxiety levels. The questions with regard to the trait anxiety domain covered long-term, general symptoms of anxiety, whereas state anxiety items address current, situation-related, contemporary symptoms. The questionnaire consisted of 40 multiple choice questions with a 4-point Likert scale. Second, depressive symptoms were estimated using the Beck Depression Inventory (BDI) [178]. This questionnaire was composed of 21 multiple choice items, which belong to three different dimensions (i.e. affective (5 items), cognitive (7 items) and somatic (9 items) dimension)). The questions were regarding the participant's feeling during the past two weeks, which was again to be answered with a 4-point Likert scale. Third, to measure the degree of daily-life self-reported cognitive difficulties, we made use of the Cognitive Failures Questionnaire (CFQ) [179]. This questionnaire included 25 items, which can be categorized into four subscales (i.e. absentmindedness, absentmindedness in social situations, names and words and orientation). Each question was addressed with a 5-point Likert scale. Fourth, the Behavior Rating Inventory of Executive Function (BRIEF) [180] was implemented to investigate subjective difficulties in daily life executive

functioning (i.e. behavioral regulation). The questionnaire consisted of 75 items which covered the nine domains of inhibition, flexibility, emotion-regulation, self-evaluation, taking initiative, working-memory, planning and organizing, task-evaluation and tidiness. The items were rated with a 3-point Likert scale. Fifth, we included the Pediatric Health Related Quality of Life Inventory (HRQoL)[181] to investigate general daily life functioning. 23 questions were posed with regard to four different domains: physical complaints, emotional complaints, social and education complaints.

3.2 Neurocognitive assessments

Besides subjective questionnaires, objective elaborate neurocognitive assessments (+/- 2.5-3.5 hours) were acquired to investigate neurocognitive functioning (see Table 3.1). These assessments were used to estimate intelligence, verbal and visual memory, attention and visuomotor functioning, optionally language tasks including word fluency and object naming. The neurocognitive protocols for children were previously implemented and demonstrated to be valuable in chronic pediatric diseases [182,183]. The protocols for adults were previously validated in adult survivors of childhood leukemia [176].

Table 3.1 Overview of the acquired neuropsychological assessments

Domain	Children (7-16 years)	Adults (>16 years)
Intelligence	WPPSI-III, WISC-III	WAIS-IV
Verbal memory	CMS (word pairs)	AVLT (15 words)
Visual memory	CMS (dots)	RVDLT (15 figures)
Attention	ANT	ANT
Visuomotor functioning	VMI	/
Language assessment	/	COWAT, PPVT

3.2.1 Children

First, we implemented the Wechsler Preschool and Primary Scale of Intelligence (WPPSI-III-NL)[184] and the Wechsler Intelligence Scale for Children (WISC-III-NL) [185] to estimate intelligence in children <6 years old and 6-16 years old, respectively. These assessments yielded a full scale IQ score, verbal IQ score and performance IQ score. Additionally, the WPPSI-III included an additional general language index. The verbal scale covered the tasks of information (i.e. general knowledge questions), vocabulary (i.e. provide definitions for words) and word reasoning (i.e. provide concept which is being described). The performance scale comprised block design (i.e. construct presented patterns with two-color blocks), matrix reasoning (i.e. complete an incomplete matrix of patterns with multiple choice options) and picture concepts (i.e. select pictures with a common characteristic).

With regard to the WISC-III, additional subscales included verbal comprehension, processing speed and perceptual organization. The verbal scale of the WISC-III consisted of information (i.e. general knowledge questions), similarities (i.e. provide conceptual similarity between two concepts), mathematics (i.e. calculations by heart), vocabulary (i.e. provide definitions for words) and comprehension (i.e. explain the logical reasoning for specific situations). The performance scale comprised the tasks of uncompleted figures (i.e. point to

missing part of the figure), coding (i.e. fill in the correct symbol matching a specific number), pictures order (i.e. order pictures of stories correctly), block design (i.e. construct presented patterns with two-color blocks), visual puzzles (i.e. construct puzzle).

Second, the Children 's Memory Scale (CMS)[186] was assessed to address verbal and visual memory. In the verbal memory task, 15 word pairs were presented auditory 3 times. After each presentation, the child was asked to provide the associated word for each of the 15 words (i.e. immediate recall). A 20 minutes time interval was then planned, during which non-verbal tasks of the remaining test assessment were acquired. After this time interval, the child was again requested to provide as many word pairs as he/she remembers (i.e. delayed recall). Finally, the child was asked whether word pairs were presented previously or not (i.e. delayed recognition). The visual memory task of the CMS is a spatial location test. More specifically, dots were presented in a matrix, of which the child the location needs to retain. This presentation occurs 3 times. Each time, the child needed to reconstruct the pattern with available dots. A second matrix was presented only once, after which the child needed to reconstruct the latter matrix as well as the first matrix (i.e. interference task). Again, after an interval of 20 minutes (during which verbal tasks are acquired), the child was requested to reconstruct the first pattern once more (i.e. delayed recall).

Third, the computerized Amsterdam Neuropsychological Tasks (ANT) [187] were acquired to investigate processing speed. To investigate baseline reaction times, focused attention, divided attention, sustained attention, and inhibitory control and flexibility, multiple subtasks were acquired according to the age of the child. More specifically, for children <9 years old, Baseline Speed (BS), Focused Attention for Objects (FA4O), Memory Search for Objects (MSO2), Response Organization Objects (ROO), Sustained Attention for Objects (SAO2) and Tapping (TP) were acquired. By contrast, for children above 9 years old, Focused Attention for Letters (FA4L), Memory Search for Letters (MSL), Shifting Attentional Set-Visual (SSV) were acquired in addition to the BS, ROO and TP.

Fourth, visuomotor functioning was assessed using the Beery developmental test of Visual-Motor Integration (VMI) [188]. During this test, the child was asked to copy figures (i.e. free drawing), match geometric figures visually (i.e. check the figure which is exactly the same as prototype), and draw lines within the predefined figure edges (i.e. restricted drawing). Using these three tasks, we addressed the Beery motor scale, visual perception scale and motor coordination scale, respectively.

3.2.2 Adults

The selection of test assessments was similar to a previous study in adult survivors of childhood leukemia [176] to retain the option of data merging and comparisons of results. First, the Wechsler Adult Intelligence Scale (WAIS-IV-NL) was administered to estimate intelligence[189,190]. The WAIS-IV-NL (Wechsler, 2012) provides a full scale IQ, and subscales of verbal comprehension, perceptual reasoning, working memory and processing speed. The subscale verbal comprehension was based on the subtests information (i.e. general knowledge questions) and vocabulary (i.e. explain the meaning of words). On the other hand, perceptual

reasoning covered the tests block design (i.e. in construct complex figures with 4 or 9 blocks with white, red or both colored surfaces) and matrix reasoning (i.e. complete figure rows with multiple choice options). Working memory was estimated using the digit span task (i.e. repeat sequences of digits in the presented order, the inverse order or rank them according to size). Processing speed included the tests of symbol search (i.e. check matching symbols) and coding (i.e. fill in the correct symbol matching a specific number).

Second, the Auditory Verbal Learning Test (AVLT)[191] was used to assess verbal memory functioning. In this test, first a list of 15 unrelated words (list A) was auditory presented 5 times. Then a second list (list B) was presented only once. After each presentation, the participant was asked which words he remembered, to estimate learning, retro- and proactive interference and confabulations. The abovementioned presentations were then followed by a break of 20 minutes (during which non-verbal tasks of the other assessments are acquired). After this break, the participant was again requested to name all words he remembered (i.e. delayed recall). In addition, words were auditory presented which the participant needed to categorize whether they were part of the first list, the second list or absent (i.e. delayed recognition).

Third, the Rey Visual Design Learning Test (RVDLT)[192] was acquired to investigate learning capacity with regard to visual information, thus short-term and long-term visual memory. Similar to the AVLT, 15 figures were shown to the participant 5 times, after which participants were asked to redraw as many figures as possible. Again, a break of 20 minutes was planned (during which verbal tasks of the remaining tests were acquired), and the participant needed to draw as many figures retained once more (i.e. delayed recall). Finally, 30 figures were presented which the participant needed to categorize either as 'being presented before' or not (i.e. delayed recognition).

Fourth, to investigate attentional functioning and processing speed, the computerized Amsterdam Neuropsychological Tasks (ANT)[187] were assembled. This test assessment included Baseline Speed (BS), Focused Attention for Letters (FA4L), Memory Search for Letters (MSL), Shifting Attentional Set-Visual (SSV), Response Organization Objects (ROO) and Tapping (TP), to measure baseline reaction times, focused attention, divided attention and memory, and inhibitory control and attentional flexibility, respectively. Mean reaction times and error rates, and related norm scores were calculated.

Fifth, we assessed word fluency using the Controlled Oral Word Association Test (COWAT)[193]. This task required the participant to spontaneously produce as many words as possible during one minute which belong to a certain semantic category (e.g. jobs and animals) or starting with a specific character (e.g. N, A, K).

Finally, to explore object naming and object-term semantics, the Peabody Picture Vocabulary Test (PPVT-III-NL) was implemented [194]. Here, participants were instructed to select the image of the object that was verbally named. The total error score (i.e. summation of all items that were answered incorrectly) and normative total scores (i.e. according to the age range) were calculated.

In summary, normative values were calculated for intelligence assessments, CMS, VMI, ANT and PPVT-III-NL. For these assessments, specifications of the normative samples are provided in Table *3.2*. On the one hand, normalizing the data is advantageous to obtain normally distributed data, which optimizes this specific assumption for many statistical tests. Furthermore, patients can be compared to a specific threshold and scores can be interpreted as a "clinical" value in case of one standard deviation below the mean. On the other hand, the normative samples are often historical, and hence lose their 'normative' value by time. Given that normative data become older the longer an assessment is used, participants are compared to outdated datasets (i.e. norm tables), which not only increases the normalized scores of the participants, but can also change the relative positions between participants. The increases in normalized scores are typically explained by the so-called Flynn effect. This effect is defined as the rise in IQ scores over generations and time, with an increase of 3 IQ points per decade on average [195]. As a result, historical norms become outdated and normalized scores can represent overestimated scores, which could decrease sensitivity to detect differences between clinical patient groups to healthy controls. Still, for the abovementioned assessments, normative scores were preferred throughout the thesis given the relatively recent and geographically (i.e. Dutch and Flemish) and age-matched normative data.

Table 3.2 Psychometric properties of implemented assessments

	Test-retest reliability (correlation)	Internal consistency (cronbach's alpha)	Norm group size	Norm group characteristics
STAI [196]	.54-.86	.86-.95	NA	Raw scores
BDI [197]	.93	.91	NA	Raw scores
CFQ [198]	/	.88	NA	Raw scores
BRIEF	.70-.79	.70-.94	815	Dutch, healthy
HRQoL [175]	.68-.88	/	NA	Raw scores
WISC-III	.52-.92	.55-.95	225	Flemish, healthy
WPPSI-III	.35-.86	.67-.93	524	Flemish, healthy
CMS [199]	.88-.98	.88-.93	1000	U.S., healthy
VMI	.85-.88	.81-.82	1737	U.S., healthy
WAIS-IV	.86-.98	.79-.97	510	Flemish, healthy
AVLT [200,201]	.51-.86	>.90	NA	Raw scores
RVDLT [202]	.46-.80	.51-.83	NA	Raw scores
ANT	.70-.84	/	6776	International
COWAT [193]	.40-.60	/	NA	Raw scores
PPVT	.94	.90-.97	2032 children + 1573 adults	Dutch, healthy

Note. Values were either derived from the original handbook, or from a specified reference.
/ indicates that the data were not available. NA=not applicable since raw scores were used.

3.3   MR neuroimaging

Magnetic Resonance Imaging (MRI) is the imaging technique relying on magnetic properties of the biological tissue. More specifically, atomic nuclei consist of protons, which possess electromagnetic features, and consequently behave as tiny magnets with a north and south pole. Given that the human body mainly consists of water and fat, hydrogen protons are abundant, and of main interest in medicine for the application of MRI.

Due to their natural spin around their main axis, hydrogen protons obtain magnetic properties, which makes them sensitive to changes in a magnetic field. Without any external magnetic field, magnetic signals resulting from spinning protons within the human body neutralize each other due to their random orientation distribution. In other words, a balance is met (i.e. net magnetization of approximately zero). However, when biological tissue is placed in the MRI scanner (i.e. a strong static magnetic field (B0)), the spins align along the main scanner axis (i.e. along the main axis of this (B0) magnetic field). This axis is in most cases the z-axis (foot to head axis of the human body). For the majority of the protons, the direction of the alignment is according to the magnetic field (i.e. low-energy spin-up state), while others are opposite to this magnetic field (i.e. high-energy spin-down state). Due to this difference, the longitudinal (i.e. along the z-axis) magnetization becomes nonzero (Mz), which is the sum of the nuclei precessing along that direction. The precession frequency of the spins parallel to the direction of B0, is called the Larmor frequency (ω0). This frequency is characteristic for the nucleus and it is proportional to the magnetic field strength. The precession frequency of hydrogen is 42.6MHz/Tesla (i.e. in a 1-Tesla magnetic field) (γ). However, this is altered by the surrounding tissue (cf. infra).

Lamor Frequency

$$\omega 0 = \gamma Bo$$

During an MRI acquisition, radiofrequency (RF) pulses are applied with the same Larmor frequency as hydrogen. By absorbing the energy from the pulse, these spins are excited. Some low-energy spin-up spins will suddenly transform into high-energy spin-down spins. Hence, the net longitudinal magnetization decreases (z-axis), while the transverse magnetization increases (xy plane). All excited spins will start rotating with the same phase. Once the RF pulse is ended, the protons gradually return to their original state (i.e. equilibrium, aligned with the static magnetic field), which is called 'relaxation'. This process comprises two subprocesses of relaxation, including spin-lattice relaxation (i.e. T1 or longitudinal relaxation) and spin-spin relaxation (i.e. T2 or transverse relaxation). First, the spins release energy to the surrounding elements (spin-lattice) as the protons return to their original low energy state. The longitudinal magnetization recovers (characterized by an exponential positive T1-curve). Second, due to different local magnetic fields (depending on the chemical environment), the precession frequencies of the spins differ (spin-spin), which causes loss of phase coherence and transverse magnetization (characterized by an exponential T2 decay curve).

Different tissue properties in biological organs result in different environments of the protons, so the durations of these relaxation processes highly depends on the location of the hydrogen protons. For instance, protons in CSF release their energy very slowly (i.e. long T1) and do not interact as strongly with other protons (long T2) as they would in the white matter (i.e. shorter T1 and T2).

In the application of MRI, a sequence of MR pulses can control different combinations of longitudinal and/or transverse relaxation. In addition, timing of the pulses can be modified in order to affect relaxation times. In this regard, repetition time (TR) is the time interval between RF pulses. Echo time (TE) is the interval between the RF pulse and the peak of the signal in the coil. Based on the information of T1 and T2 relaxation times of different tissue types, an MRI sequence can be used to obtain the contrast in the image. The MRI scan provides the necessary information about the anatomical structure or function of the organ. This study focuses on T1-weighted MRI, DWI, T2 FLAIR, RsfMRI (see Figure 3.1).
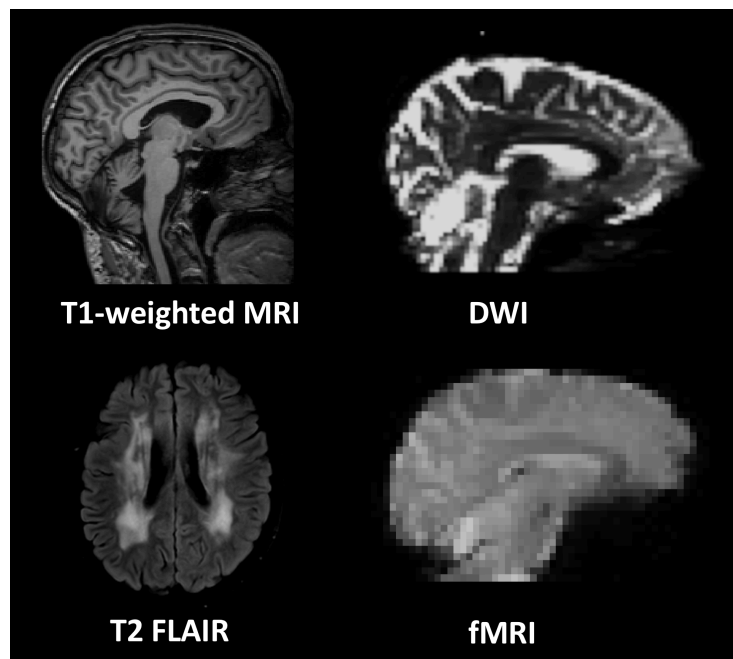
Figure 3.1 Overview of images of main interest in this study
Note. MRI=Magnetic Resonance Imaging, DWI=Diffusion-weighted (MR) imaging, FLAIR= Fluid Attenuation Inversion Recovery, fMRI=functional MRI.

3.3.1 T1-weighted MRI

As the term T1-weighted MRI suggests, the contrast of this MR image is mainly determined by T1 properties of the tissue, given that both TR and TE are short. Protons in fat easily realign. Hence, these protons have a short spin-lattice or T1 relaxation, and fat appears bright on a T1-weighted image. By contrast, realignment of spins in water takes longer, so water shows a low signal (i.e. appears dark). If longer TR would be applied, all the protons would recover their original state in the main magnetic field. As a result, the image intensities would be uniform. A TR shorter than the recovery times of the tissues allows us to differentiate between them (i.e. tissue contrast) (see Figure 3.2). This way, T1-weighted MRI provides a clear neuroanatomical image.
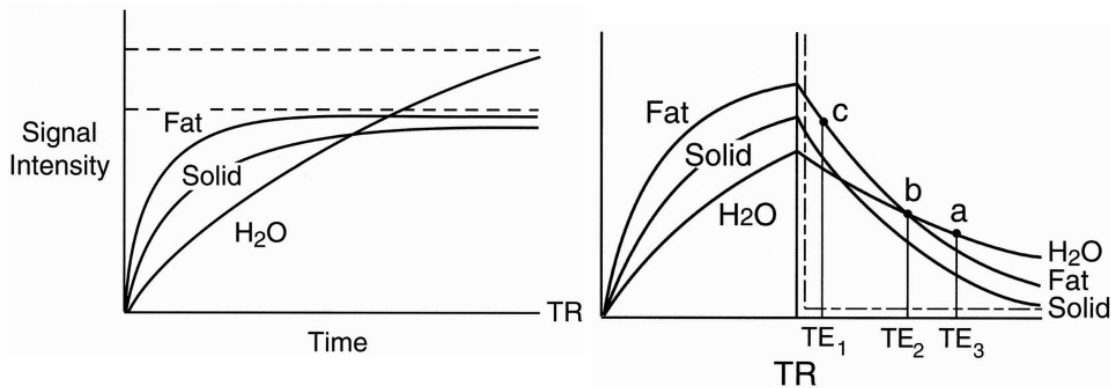
Figure 3.2 Decay curves of T1 (left) and T2 (right) in fat, water and solid tissue.
Adapted from [203]
Note. This figure depicts the relaxation curves for the different tissue subtypes. Based on these curves, a T1-weighted MRI scan with a short TE and short TR can easily dissociate different tissue type, so the anatomical information of CSF, grey and white matter in the brain can clearly be derived.

3.3.2 Diffusion-weighted imaging

To investigate microstructure of anatomical components with clear directionality information, more specifically anatomical "tracts", diffusion-weighted MRI (DWI) imaging is typically applied. Within the brain, this is specifically relevant for estimations of white matter tracts.

In DWI, the spontaneous motion of water molecules due to collisions is assumed as informative for directionality estimations. Although this movement cannot be measured at proton level, the macroscopic bulk result of microscopic random motion can be estimated. In a homogeneous collection of unrestricted water, the molecular motion may be truly random (all directions have an equal chance, is called "isotropic") and the displacement of particles follows a Gaussian distribution. However, in case of anatomical microstructure, such displacement is not random, but water molecules are impeded in their movement by the natural barriers (e.g. cell membranes, neurofilaments, myelin, etc.). In contrast to random movement, strong directional dependence of movement is called "anisotropic". With regard to the brain, the CSF can thus be assumed to show isotropic movement, whereas the water molecules show anisotropic movement in the white matter, and the grey matter is situated somewhere in between.

The most common approach to measure diffusion is to use a spin-echo acquisition scheme. Using a diffusion-weighted spin-echo sequence, spins that diffuse along the gradient direction experience a different gradient strength at two time points (resulting in net dephasing). More specifically, diffusion weighting can be produced by implementing a set of strong magnetic field gradients in equal direction and duration, but opposite magnitude prior to and after the 180° rephasing pulse. The first gradient will dephase all nuclear spins, while the second gradient will rephase only those spins that remained stationary. Hence, if water molecules move along the direction of the diffusion gradient, the rephrasing of the spins becomes incomplete, as they experience a different magnetic field during the second gradient. The measured signal is decreased.

This results in a local signal attenuation that is proportional to the (apparent) diffusion coefficient (ADC) and the applied gradient. This resulting signal can be expressed as follows (See equation 1.1).

$$S = S_0 e^{-b.ADC}$$ (1.1)

With S representing the measured signal; S_0 the non-diffusion-weighted signal (no additional gradients applied); ADC representing the diffusion constant (called 'apparent' given that it is affected by surrounding tissue); and b describes the degree of diffusion-weighting (caused by the diffusion-weighted gradients) and depends on gradient amplitude, duration and time between gradients.

ADC values are usually highest in CSF, bit lower in gray matter and lowest in white matter. Hence, CSF is depicted with high intensity on an ADC map (given the high ADC values). It is called 'apparent' because it differs from pure water due to the presence of microscopic barriers.

Besides a basic ADC calculation, Diffusion Tensor Imaging (DTI) is a model which expands the distribution of random displacement along a single direction to a random displacement in 3D. In other words, it is not a tensor of the first order (i.e. vector) that is estimated, but a tensor of the second order (i.e. matrix, see equation 1.2).

$$D = \begin{bmatrix} D_{xx} & D_{xy} & D_{xz} \\ D_{xy} & D_{yy} & D_{yz} \\ D_{xz} & D_{yz} & D_{zz} \end{bmatrix}$$ (1.2)

The diagonal elements represent the displacements along three orthogonal axes (xyz). The non-diagonal elements are correlations between displacements along any of the 2 relevant axes. To estimate this tensor a minimum of 6 diffusion-weighted images are required with non-collinear gradients. Once the tensor is estimated, a visual representation of this tensor is plausible using an ellipsoid (see Figure 3.3). This shape can be fully characterized by 6 parameters: 3 eigenvalues (λ1, λ2, λ3, the length of the axes, representing the magnitude of the diffusion) and 3 eigenvectors (the angles of the reference coordinate system 's axes, i.e. the direction of the diffusion). In other words, the tensor displays the average diffusion distance in each of the three principal directions during the applied diffusion gradient.

The most widely investigated scalar that can be derived from the diagonalized diffusion tensor is fractional anisotropy (FA). FA is the ratio of the standard deviation and quadratic mean of the eigenvalues. It has a value between 0 and 1 with 0 representing isotropic (i.e. equal in all directions) and anisotropy (i.e. diffusion along a single direction), respectively. The more the ellipsoid deviates from a sphere, the higher the FA.

Higher FA values suggest more white matter tracts going into the same direction. Hence, it is also used in order to delineate white matter tracts (i.e. tractography, see Figure *3.4*). FA values depend on multiple microstructural white matter factors (including white matter thickness, white matter integrity, myelination, crossing fibers, etc.). The

highest FA values can be found in central WM bundles such as the corpus callosum and the corticospinal tract. Due to pathological processes such as inflammation (edema), widening or shrinkage of the extracellular space or axonal loss, these diffusion-weighted metrics are affected which suggests microstructural tissue reorganization. More advanced models are discussed in Chapter 5.
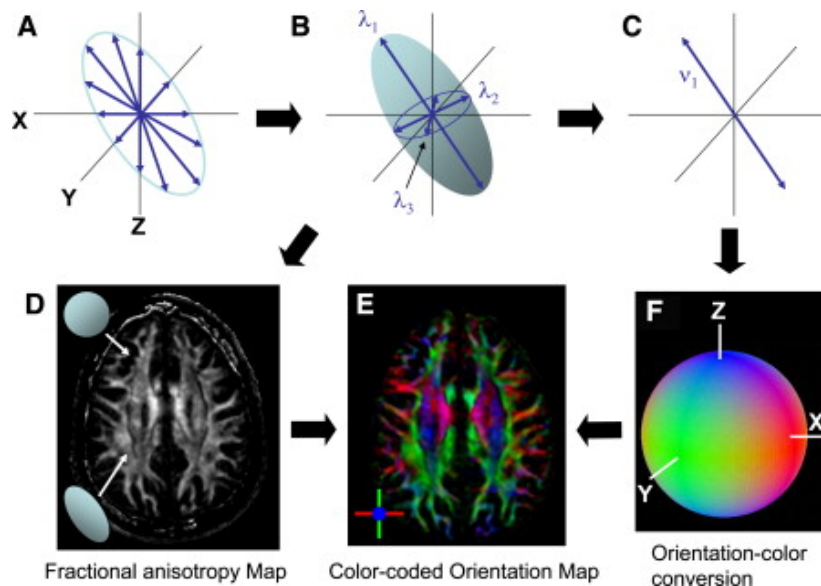
Figure 3.3 Visual representation of a diffusion tensor ellipsoid.
Adapted from Mori et al. [204]

Note. (A) From diffusion estimations along multiple gradient directions, orientation and shape of the "diffusion ellipsoid" is estimated. Based on the ellipsoid (B), the orientation of the longest axis can be found (C), which is assumed to represent the main local fiber orientation within this voxel. (D) An anisotropy (FA) map can be estimated: dark regions are isotropic (spherical) whereas bright regions are anisotropic. This orientation of the main axis can be converted to a color (F) at each pixel. By weighing color (F) by the anisotropy map (D), a color-coded orientation map is created (E).
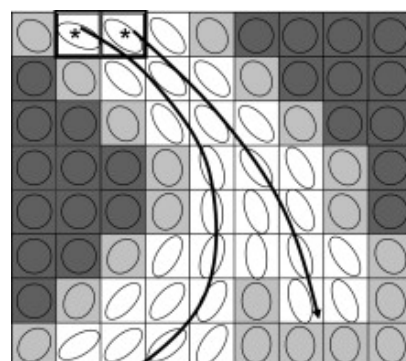
Figure 3.4 Scheme representing the tensor-based reconstruction of white matter tracts.
Adapted from Mori et al. [204]
Note. Based on anisotropy in each voxel, the average fiber orientation is estimated which is used to propagate a line voxel to voxel, until low anisotropy is reached (dark voxels).

3.3.3 T2-FLAIR imaging

Fluid Attenuation Inversion Recovery (FLAIR) is a sequence with an inversion recovery, which is a conventional (spin-echo) pulse, preceded by an inversion pulse. This is typically implemented to selectively null the signal from specific tissues. The function of the inverting pulse is to flip the initial longitudinal magnetization (Mo) of all tissues opposite to the direction of the main magnetic field (Bo). Next, these inverted tissues undergo T1 relaxation as they variably seek to re-establish magnetization along the z-direction. If then the conventional 90°-pulse is applied and spin echo signal generation begins, the initial longitudinal magnetizations of different tissues are now separated based on their different T1 relaxation times. The degree of image contrast depends on the inversion recovery time. In case of the FLAIR sequence, a long inversion time is implemented, so the signal of the CSF is canceled out.

Hence, (subtle) peripheral lesions or in periventricular regions close to CSF can be detected. More specifically, toxic leukoencephalopathy due to the use of certain medicinal drugs (e.g. antineoplastic, immunosuppressive, antimicrobial drugs), psychopharmacological stimulating drugs, cranial irradiation and environmental toxins (e.g. CO, As, CCl_4), predominantly affects the white matter and can easily be discovered based on a FLAIR MRI scan. A case example of leukoencephalopathy detected on a FLAIR MRI scan after chemotherapy, was presented previously (see Figure 1.2).

3.3.4 Resting state fMRI

Besides anatomical MRI scans, functional measurements of the brain can be obtained using functional MRI imaging (fMRI). Functional magnetic resonance imaging provides a non-invasive way to measure brain activity indirectly. Activation within the brain requires an increase in local oxygen metabolism. In addition, this neuronal activity is closely linked to local hemodynamic cerebral microcirculation, which is called the neurovascular coupling and can be modeled with the hemodynamic response function (see Figure 3.5). More specifically, elevated oxygen consumption yields a local drop in oxygen concentration, which motivates the body to supply more blood to the activated area.

Oxygen is transported by iron-containing hemoglobin in the blood. Using the differences in magnetic properties between oxy- and deoxyhemoglobin in the capillaries near the active neural zones as contrast, the blood oxygenation level dependent (BOLD) contrast visualizes this hemodynamic response to neuronal activation. More specifically, the magnetic state of the iron in hemoglobin depends on the amount of oxygen. Iron is paramagnetic if hemoglobin is depleted of oxygen (deoxyhemoglobin), since the iron molecule is more freely exposed to the magnetic field in this case. However, iron becomes diamagnetic when the hemoglobin molecule is saturated (oxyhemoglobin). Given that deoxyhemoglobin is paramagnetic, it introduces local inhomogeneity, which shortens T2* of the surrounding tissue and reduces the MRI signal. This leads to a decrease in image intensity. By contrast, oxyhemoglobin is weakly diamagnetic and therefore only affects image intensity to a small extent. When the concentration of oxyhemoglobin increases, which occurs a few seconds after neuronal activation, the local field inhomogeneity is reduced. Hence, T2* elongates again, and

the measured signal (T2*-weighted pulse sequence), increases. This way, T2* of blood depends on the degree of oxygenation of the blood; and BOLD fMRI techniques primarily measure changes in the local inhomogeneity of the magnetic field, resulting from local changes in blood oxygenation. The most well acknowledged model of the hemodynamic response suggests three phases of the BOLD response to a short-term increase in neuronal activity. First, the initial period of oxygen consumption leads to a drop in signal (due to increased deoxyhemoglobin/oxyhemoglobin). Second, an increased blood flow causes an important increase in the oxygen concentration. However, this supply is overcompensating the oxygen demand. Third, after the oversupply of oxygenated blood, it takes some time for the blood volume to diminish and return to baseline. Besides these changes in ratios of deoxyhemoglobin/oxyhemoglobin, the BOLD signal is also affected by inflowing additional blood, which was not similarly excited by the RF pulse. This inflow effect also adds to the increasing oxyhemoglobin/deoxyhemoglobin ratio in the second phase and further increases image intensity.

To acquire fMRI images, an Echo-Planar Imaging (EPI) is the typically implemented MRI sequence to generate T2*-weighted images. EPI allows the collection of an entire 2D MR image from one single excitation in about 40 to 100ms. The technique allows acquiring multiple adjacent slices efficiently. The entire brain can be imaged within 2 to 3 seconds. This time efficient acquisition helps us to understand the dynamic processes of the active brain.

In resting state fMRI studies, subjects do not have to perform a task. Instead, they are asked to relax and close their eyes for several minutes. During such acquisition, low frequency fluctuations (~ <.1 Hz) in oxy- and deoxyhemoglobin can be measured, which are presumably caused by spontaneous neuronal activation changes. These spontaneous signal fluctuations show a high degree of temporal correlation across widely separated brain regions. Hence, resting state studies examine the level of co-activation between the functional time series of anatomically separated brain regions during rest. Such co-activation is believed to reflect the so-called *functional connectivity* between these brain areas. By detecting such correlations, functional cortical networks have been extensively described, including the motor, language, auditory and visual network [205]. These so-called resting state networks typically correspond to critical brain 'states' or functions, as their specific names already suggest (e.g. language network is highly important for language functioning, …).

If no specific cognitive function is hypothesized to be affected in the participant group, it can be challenging to select an appropriate task for an active fMRI scan. Hence, resting state fMRI is particularly interesting, since this technique does not depend on task selection, nor on the participant's performance. Given that findings about neurocognitive difficulties in cancer patients remain heterogenous, we opted for resting state fMRI acquisitions in the current childhood cancer study (see Chapter 8) and adult survivor studies (see Chapters 5,6,7).
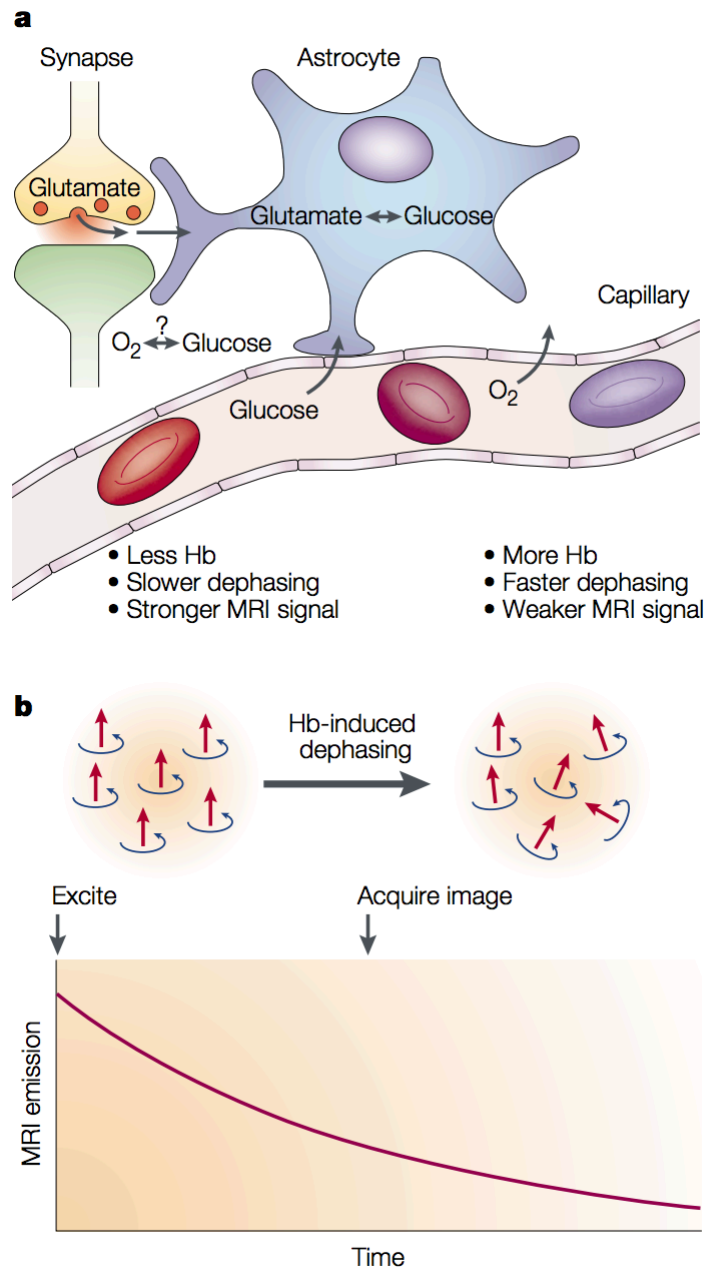
Figure 3.5 Fundamental principle of fMRI BOLD signal.

Adapted from Heeger et al. [206]

Note. The figure shows the assumed relationship between activity, neurotransmitter recycling and metabolic demand (Panel A), and the effect of deoxyhemoglobin on the MRI signal (Panel B).

4   Neurocognition in childhood ALL treated with intrathecal and intravenous methotrexate

Abstract

In childhood Acute Lymphoblastic Leukemia (ALL), radiotherapy for CNS prophylaxis is not used in frontline therapy anymore. Standard treatment for ALL currently consists of polychemotherapy. Therefore, assessment of potential chemotherapy-induced cognitive side effects becomes important. Although neurotoxicity was demonstrated in cross-sectional studies, longitudinal studies remain scarce. We evaluated intellectual development of 94 pediatric ALL patients between 1990 and 1997, diagnosed between the ages of 2 and 12 years old, treated according to the EORTC CLG 58881-protocol. Three assessments of the WISC-R were performed, according to age. Using repeated measures regression analysis, we investigated the effect of gender, (low vs. increased) risk group, parents' education, age at diagnosis, IQ subscale (verbal (VIQ) vs performance (PIQ) intelligence), and test session. PIQ scores were significantly lower than VIQ at baseline (-5.3 points on average, p=.0032), yet PIQ increased more strongly (PIQ: +3.9 points per test session; VIQ: +.8, p=.0079), so this baseline difference disappeared (p=.0079). There were no clear effects of gender (girls: +.6 points; p=.78), or risk group (low risk: +1.5 points; p=.49), but IQ scores were significantly higher when one parent had followed higher education (+9.5 points, p<.0001). Finally, diagnosis at younger age predicted lower IQ scores (-1.3 points/year, p=.0009). Given that IQ scores did not decline, our findings demonstrate a stable pattern. However, the lower PIQ scores at baseline may indicate that performance functioning is vulnerable to acute neurotoxicity. Also, lower scores for younger patients, highlight the stronger impact of the disease and/or treatment at younger age.

Keywords: *Acute Lymphoblastic Leukemia, Intelligence, Follow-up, Development, Performance vs Verbal intelligence*

4.1 Introduction

The remaining physical [2] and psychological symptoms [3] often affect daily life of pediatric cancer survivors to a large extent. Since survival rates of pediatric cancer patients continue to increase, factors that influence their quality of life, increasingly receive attention. During childhood, one important factor that influences daily life is performance at school [207]. School results often decline once a child is diagnosed with cancer [208]. The disease as well as the treatment can have an important impact on cognitive development. On the one hand, it is possible that cancer and/or chemotherapy induce physiological neurotoxic mechanisms. On the other hand, due to intensive treatment, also functioning at school can be delayed. For pediatric cancer patients it was shown that cognitive deficits thoroughly limit their overall functioning in daily life [4]. Brown and colleagues for instance demonstrated that children treated for ALL obtained lower scores on intelligence tests than control participants [11].

During the last few years, evidence for potential treatment-induced neurotoxicity in pediatric oncology is increasing. So far, most evidence exists for brain tumor and ALL patients [5,6]. However, these neurotoxic effects are mostly induced by radiotherapy (RT) [13,14,209]. Also in ALL patients neurocognitive functioning was mostly reduced in case of chemotherapy in combination with RT [15,134,210]. To limit RT-induced neurotoxic adverse effects, therapies changed throughout time towards chemotherapy-only treatments. Given that ALL is generally treated with chemotherapy only and prophylactic Central-Nervous-System-(CNS-)directed RT is abandoned, the long-term effects of chemotherapy become more important to address [12,211]. Chemotherapy for ALL includes CNS-directed prophylaxis, i.e. intrathecal (IT) chemotherapy, as well as high dose intravenous methotrexate (HD-MTX). High dose MTX can however cause serious acute neurological symptoms in patients [35]. Also animal studies evidenced neurotoxic effects, affecting both behavior as well as neurophysiology [65,79,86,87]. For chemotherapy only, Magnetic Resonance (MR) imaging studies indicated smaller grey matter volumes [168,212] as well as decline in white matter (WM) integrity [15,134] and WM hyperintensities [169] in ALL survivors compared to controls.

So far, survivor studies including neuropsychological assessments of chemotherapy-only treated patients, showed impairment of several neurocognitive functions. These include memory [213], specific attentional skills [214], visuomotor control [150], as well as verbal, and nonverbal functioning [8]. However, evidence for such specific deficits remain inconsistent [145,215]. Furthermore, general IQ scores of ALL patients also remain within the normal range [216].

All of the previously mentioned studies used a cross-sectional design. Although they showed neurocognitive sequelae, it remains unclear how cognitive functioning of the children evolves throughout their development. Given that this has important consequences for education and academic functioning of these patients later in life, longitudinal designs are essential to acquire a better understanding of cognitive and intellectual development over time in children treated for ALL. Only a few longitudinal studies were performed. Brown and colleagues (1999) concluded a decrement in intellectual functioning in children receiving CNS-prophylactic chemotherapy for leukemia [11]. In a small series of 16 CNS-directed treated patients (including Acute Lymphoblastic Leukemia, Acute Myeloid Leukemia, T-cell lymphoma)

and 10 non-CNS treated patients, they acquired IQ scores yearly from diagnosis for 5 years. Later, Kingma and colleagues (2002) investigated a broader range of functions, by assessing IQ scores as well as memory and attentional functioning [217]. Unpaired t-tests resulted in a significantly lower VIQ and executive performance for patients, but only 5 years after diagnosis. Recently, Halsey and colleagues (2011) demonstrated significantly lower IQ scores for ALL patients throughout development compared to controls, independently from MTX dose [218]. These researchers used intervals of .5, 3 and 5 years after diagnosis. Jansen and colleagues did not encounter such differences between patients and siblings, not at baseline, nor after treatment [219]. All of these longitudinal studies used different IQ measurements during their study, and variable assessment schedules according to the patient's age. In our study, we used one consistent intelligence test for a large population. Intelligence scores were assessed three times with an average interval of three years.

4.2   Methods

4.2.1 Patients

This was a cohort study of 94 Belgian Dutch speaking childhood ALL patients between the age of 2 and 12 years at diagnosis, who were newly diagnosed with ALL between 1990 and 1997 at the University Hospitals of Ghent and Leuven in Belgium. Out of 144 childhood leukemia patients, 50 patients were excluded because of predefined exclusion criteria: exceeding the age range (n=17, < 2 years old or > 12 years old at diagnosis), other diagnosis (n=25, high risk ALL, CNS involvement, mature B-cell ALL, or relapse), early death (n=1), missing data (n=5), refusal of the parent (n=2). Data were only complete if all subscales of the IQ test were acquired. The median age at diagnosis was 4.4 years (range 2.0-11.9 years). The majority of the patients was younger than 6 years old at diagnosis (n=60). All of the patients were treated according to the European Organisation for Research and Treatment of Cancer Children's Leukemia Group (EORTC-CLG) 58881 trial [220,221], a BFM-based protocol, which consisted of CNS prophylaxis with intrathecal methotrexate (IT-MTX) and HD-MTX (5g/m²). No one received cranial RT. Only patients from the low (n=53) and increased (n=41) risk group were included, whereas high risk patients (i.e. corticoresistent after prophase therapy; did not achieve complete remission after induction therapy; undifferentiated immunophenotype with absence of B-cell, T-cell, myeloid markers or CALLA; certain cytogenetic characteristics: t(9;22), t(4;11) or near-haploidy) were excluded, given their elevated risk of relapse during the first year of therapy [220,221].

4.2.2 Design

We used the Dutch translated version of the Wechsler Intelligence Scale for Children Revised (WISC-R). Given that we attempted to test with consistent materials throughout the study, and the WISC-R test can only be performed between 6 and 17 years old, first assessments were only established once patients had reached the age of 6 years old. A schematic overview of our design is presented in Figure 4.1. Cognitive functioning was evaluated at three time-points, according to their age. Given the age range limitations of the test, only patients younger than 12 years at diagnosis were included. We excluded patients younger than 2 years old, to avoid too large intervals between diagnosis and the first neuropsychological assessment.

All patients between 2 and 6 years old at diagnosis were tested at baseline (T1), as soon as they reached the minimal age (i.e. 6 years) for testing. For all other ages, baseline testing was executed at diagnosis if the patients were in a good clinical condition. Assessments were acquired within 12 months after diagnosis, avoiding periods when steroids were administered. Two- and three-year-old patients at diagnosis had their second and third assessment 6 and 9 years after diagnosis, respectively. All other patients' second and third neuropsychological assessment was planned 3 (T2) and 6 (T3) years after diagnosis. As a consequence, the interval between diagnosis and T2 was larger than 3 years (max 6 years) for the two- and three-year-old patients. For a detailed time schedule for all subjects, (see Figure 4.1).
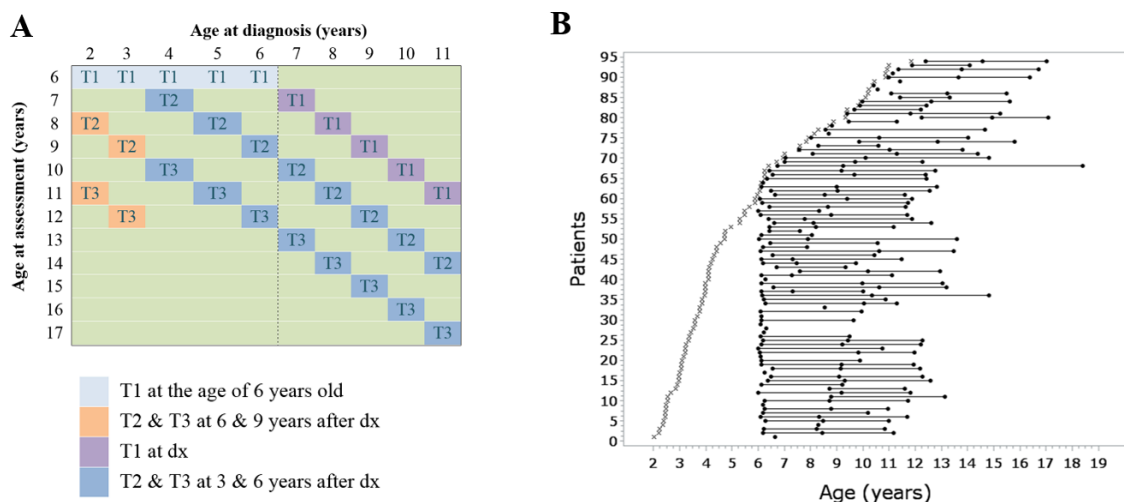
Figure 4.1 Design for longitudinal assessments in leukemia patients

Note. (a) The longitudinal design of the study: three neuropsychological assessments over time (T1), (T2), and (T3), for each age at diagnosis (dx). Patients who were diagnosed younger than 6 years old were tested once they reached the age of 6 years. Two-year-old and three-year-old patients were tested a second and third time 6 years after diagnosis and 9 years after diagnosis, respectively. Patients between 4 and 6 years old were tested a second and third time 3 and 6 years after diagnosis, respectively. Patients older than 6 years old were tested within the first year after diagnosis, 3 and 6 years after diagnosis. (b) The schedule of assessments (for each patient separately): age at diagnosis (x) is plotted against each test session (dots). Patients are sorted by age at diagnosis.

Socioeconomic status was defined by the educational level of the parents. We defined educational level as a binary variable. Education was considered as 'high' if one parent had obtained a degree of higher education after high school.

4.2.3 Statistical analysis

Socio-demographic predictors such as socioeconomic status (SES) [222] and gender [223] can affect intellectual outcome in children. Hence, we selected the following predictors a priori for the multivariate model to predict IQ scores: gender, risk group, education of the parents, age at diagnosis, IQ scale (verbal vs performance), and test session (1st, 2nd, 3rd). The last two variables were repeated measures (within-subjects variables). First, we evaluated the correlations between these predictor variables to address their possible interdependence before setting up our model.

Second, given the different approach for children diagnosed before vs after the age of 6 (see Design section), we investigated whether age at diagnosis had a different effect on IQ for the patients who were diagnosed before the age of 6 than for patients who were diagnosed after the age of 6 (i.e. a 'piecewise effect' for age at diagnosis). This was done to account for the different procedure for children younger than 6 years old who had already received or even completed chemotherapy, whereas for older children the first measurement was at diagnosis.

Third, we decided a priori to only assess interaction effects of test session with gender, IQ scale, and age at diagnosis. One joint likelihood ratio test was used to test for statistical significance at the 5% alpha level when adding all three interaction terms. If significant, the strongest interaction term was added and a second joint test was performed for the remaining two. We used fixed effects repeated measures regression with PROC MIXED in SAS v9.4 (SAS Institute, Cary, NC, USA). The first order autoregressive covariance structure was used to model the longitudinal effect of test session.

4.3   Results

4.3.1 Descriptive statistics

Descriptive statistics of predictors and outcomes are presented in Table 4.1. From the 94 the study was discontinued for thirty-eight patients (40%), of which 11 (29%) was due to death, 24 (63%) due to refusal for further participation and three (8%) due to relapse or second malignancy. The median verbal IQ was 105 (interquartile range (IQR): 96-115) at the first testing, and 108 (IQR: 97-119) at the third testing. The median performance IQ was 99 at the first testing (IQR: 88-111), and 109 at the third testing (IQR: 99-122).

Table 4.1 Patient characteristics and descriptive data longitudinal leukemia study

	N	Percentage
Girls vs. boys	46 vs. 48	49% vs. 51%
Low vs. increased risk	53 vs. 41	56% vs. 44%
Higher vs. lower education of parents	45 vs. 49	48% vs. 52%

	N	Median (IQR*)	Range
Age at diagnosis (years)	94	4.4 (3.2-7.0)	2.0-11.9
Age at testing (years)			
Testing 1	94	6.4 (6.1-8.3)	6.0-12.4
Testing 2	70	9.5 (8.7-10.6)	7.3-14.9
Testing 3	56	12.3 (11.6-13.9)	9.7-18.4
VIQ			
Testing 1	94	105 (96-115)	79-145
Testing 2	70	106 (95-120)	76-150
Testing 3	56	108 (97-119)	76-143
PIQ			
Testing 1	94	99 (88-111)	71-150
Testing 2	70	104 (97-116)	76-137
Testing 3	56	109 (99-122)	74-137
TIQ			
Testing 1	94	102 (94-115)	79-142
Testing 2	70	108 (96-121)	78-141
Testing 3	56	108 (100-122)	78-139

Note. * indicates Inter Quartile Range (IQR) = middle 50% of the data

4.3.2 Selection of predictors

We checked whether the effect of age at diagnosis was different before and after 6 years, given the different approach for children diagnosed before and after the age of 6. There was little evidence of such a 'piecewise' effect for age at diagnosis (p=.44).

Regarding the selection of interaction terms, the joint likelihood ratio test for the three a priori selected interaction terms was statistically significant (p=.007), resulting in the inclusion of the interaction between IQ scale and test session into the final regression model. The joint test for the remaining two interaction terms was not statistically significant (p=.25), such that these latter interactions were not considered further.

4.3.3 Repeated measures regression analysis

Concerning the demographic factors, IQ scores had a weak relationship with gender (girls: +.6 points on average; p=.78) and with risk group (low risk: +1.5 points; p=.49) (Table 4.2). Parental education by contrast, was significantly related to differences in intelligence scores. More specifically, children of whom at least one parent finished higher education obtain an IQ score which is on average 9.5 points higher (p<.0001).
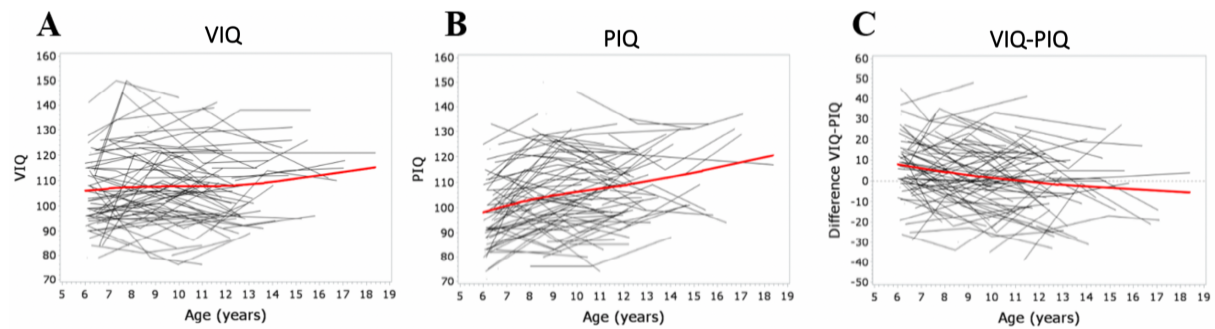
Figure 4.2 Spaghetti plots for developmental IQ patterns in leukemia patients
Note. The red line shows the average relationship between IQ and age (obtained with spline smoothing). (a) Spaghetti plot of Verbal IQ scores. (b) Spaghetti plot of the Performance IQ scores. (c) Spaghetti plot of the difference between VIQ and PIQ (positive result means verbal IQ was higher than performance IQ).

Furthermore, patients who were diagnosed at a younger age obtained lower IQ scores at baseline, with an average decrease of 1.3 points per year (p=.0009). Notably, a different pattern was observed for the two IQ subscales (i.e. performance IQ vs. verbal IQ). More specifically, at baseline assessment VIQ was higher than PIQ (+5.3 points; p=.0032). In addition, there was an interaction effect between IQ subscale and test session (p=.0079): whereas VIQ scores increased only to a limited extent (+.8 points per session; p=.39) (see Figure 4.2), PIQ scores increased more strongly (+3.9 points per session). As a result the difference between PIQ and VIQ at baseline disappeared over time. (Detailed descriptive data of the subscale scores at each assessment are reported in Table 4.3).

Table 4.2 Results of mixed model regression analysis predicting IQ scores

Predictor	Coefficient	SE	95% CI	P
Intercept	103.0	3.55		
Boy vs Girl	-.6	2.16	-4.9 to 3.7	.78
Low vs increased risk	1.5	2.16	-2.8 to 5.7	.49
Lower vs Higher education	-9.5	2.19	-13.9 to -5.2	<.0001*
Age at diagnosis (per year)	1.3	.40	.6 to 2.1	.0009*
PIQ vs VIQ [b]	-5.3	1.78	-8.9 to -1.8	.0032*
Test session (0, 1, 2) [b]	.8	.94	-1.1 to 2.7	.39
Test session by IQ scale interaction [a,b]	3.1	1.14	.8 to 5.3	.0079*

Note. [a] this refers to interaction effects with age at testing. [b] due to the interaction effects with age at testing, these effects represent the effect at the reference level (i.e. the main effect of IQ scale represents the difference between PIQ and VIQ at first test session; the main effect of test session represents the increase in average IQ score for VIQ. The interaction term coefficient represents the increase in average IQ score per test session for PIQ)

Table 4.3 Mean scores (with standard deviations) for each subscale

Subscale WISC-R	Mean score at assessment (SD)		
Time	1	2	3
Number of participants	N=94	N=70	N=56
Information	10.12 (2.74)	10.09 (2.92)	10.30 (2.87)
Similarities	11.60 (3.25)	12.00 (3.21)	12.29 (3.77)
Arithmetic	10.00 (3.24)	10.19 (3.15)	10.18 (3.05)
Vocabulary	11.68 (2.84)	11.50 (3.07)	11.96 (4.63)
Comprehension	11.87 (3.03)	12.61 (2.71)	12.54 (2.59)
Digit Span	9.04 (2.99)	10.07 (2.80)	10.17 (2.99)
Picture Completion	10.62 (2.99)	11.23 (3.15)	11.88 (2.67)
Picture Arrangement	10.61 (3.08)	11.14 (2.59)	11.41 (2.56)
Block Design	10.13 (3.45)	10.46 (3.29)	10.66 (2.89)
Object Assembly	8.98 (3.62)	10.17 (3.06)	11.04 (3.13)
Coding	10.44 (3.48)	11.27 (3.16)	11.00 (2.84)
Mazes	10.13 (2.72)	10.63 (2.85)	10.71 (2.90)

4.4 Discussion

In this longitudinal study, we investigated the potential neurotoxic effects of chemotherapy-only treatment in ALL patients without CNS involvement. For these patients, we did not encounter decrements (or lack of increase) in IQ scores. After controlling for the effect of parental education as indicator of socioeconomic status, we observed that VIQ scores increased only limitedly for ALL patients throughout and after treatment. However, we found that PIQ scores were lower than VIQ at baseline and increased more strongly. Furthermore, we encountered lower IQ scores for patients who were diagnosed at younger age. Seeing the different approach for children diagnosed before vs after the age of 6 (see Design section), the youngest patients already finished their therapy before their first assessment. Given that the most intensive phase of IT-MTX and intravenous HD-MTX is scheduled during the first 6 months of treatment [220,221], lower PIQ scores at baseline may indicate a stronger acute vulnerability to chemotherapy of performance functioning, with the youngest patients being the most vulnerable. The lower PIQ scores at baseline and stronger impact for younger patients, can both be due to the chemotherapy as well as to the disease itself. To further explore this hypothesis, performal functioning was plotted against duration between first assessment and diagnosis (see Figure 4.3).
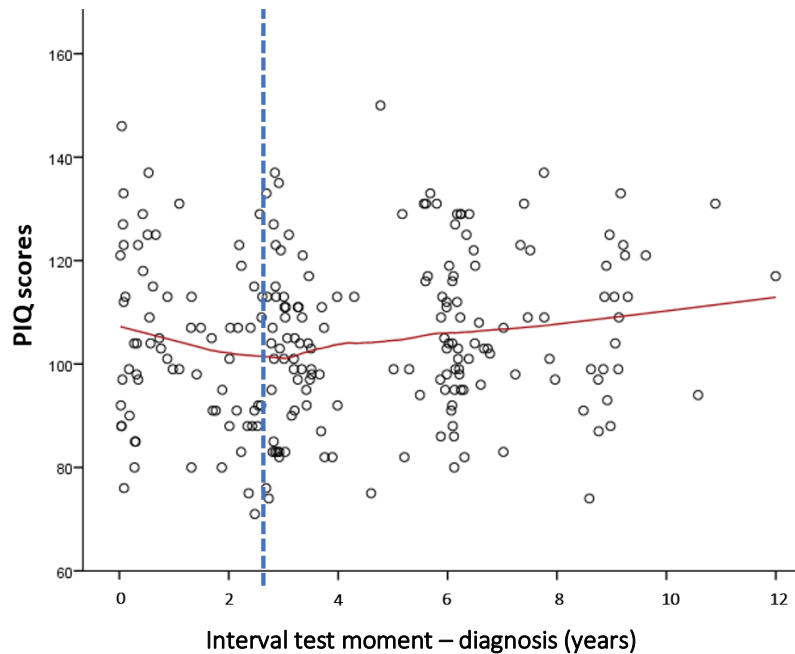
Figure 4.3 Scatterplot with PIQ scores for different time intervals between diagnosis and test assessment

As could be visually observed, a local regression curve fit (LOESS) suggests an acute decrease during the first 2 years, while patients who were tested at least 2.5 years after diagnosis at first assessment, show an increasing trend in scores. However, given the high variability in these data, not any non-linear regression model supported significant prediction of PIQ scores based on these intervals.

Given that tumor burden reflected by low vs. increased risk did not result in different IQ scores, and CNS positive patients were excluded, we suggest that lower PIQ scores in an acute stage should be assigned to the treatment rather than to the disease burden. Notice that treatment protocols between both risk groups also did not differ to a large extent (see Table 4.4).

Table 4.4 EORTC – CLG 58881: Treatment protocol for low vs. increased risk patients

	Dose	Days of administration
Induction: protocol IA		
Prednisolone (PO)	60 mg/m^2	1-7 (prephase)
Prednisolone (PO)	60 mg/m^2	8-28, + over 9 days
Vincristine (IV)	1,5 mg/m^2 (max 2,5 mg)	8, 15, 22, 29
Daunorubicin (IV)	30 mg/m^2	8, 15, 22, 29
Methotrexate (IT)	12 mg	1, 8, 22
According to randomisation		
E. coli asparaginase (IV) or	10 000 IU/m^2	12, 15, 18, 22, 25, 29, 32, 35
Erwinia asparaginase (IV)	10 000 IU/m^2	12, 15, 18, 22, 25, 29, 32, 35
Consolidation: protocol IB		
Cyclophosphamide (IV)	1 000 mg/m^2	36, 63
Cytarabine (IV)	75 mg/m^2	38-41, 45-48, 52-55, 59-62
6-Mercaptopurine (PO)	60 mg/m^2	36-63
Methotrexate (IT)	12 mg†	38, 52
Interval therapy		
6-Mercaptopurine (PO)	25 mg/m^2	1-56
Methotrexate (24 h) with leucovorin rescue at h36	5 000 mg/m^2 12 mg/m^2/6h	8, 22, 36, 50
Methotrexate (IT)	12 mg	9, 23, 37, 51
According to randomisation for increased risk pts		
Cytarabine (IV)	1 000 mg/m^2	9, 10, 23, 24, 37, 38, 51, 52
Reinduction: protocol II		
Dexamethasone (PO)	10 mg/m^2	1-21 + over 9 days
Vincristine (IV)	1,5 mg/m^2 (max 2,5 mg)	8, 15, 22, 29
Doxorubicin (IV)	30 mg/m^2	8, 15, 22, 29
Methotrexate (IT)	12 mg	38
Cyclophosphamide (IV)	1 000 mg/m^2	36
Cytarabine (IV)	75 mg/m^2	38-41, 45-48
6-Thioguanine (PO)	60 mg/m^2	36-49
According to randomisation		
E. coli-asparaginase (IV) or	10 000 IU/m^2	8, 11, 15, 18
Erwinia asparaginase (IV)	10 000 IU/m^2	8, 11, 15, 18
Maintenance (up to 2 years after day 1 of induction)		
6-Mercaptopurine (PO)	50 mg/m^2	daily
Methotrexate (PO)	20 mg/m^2	weekly
According to randomisation		
6- Mercaptopurine (IV)	1 g/m^2	monthly

Note. PO=Per Os; IV=intravenous; IT=intrathecal

Importantly, most ALL patients are diagnosed between 3 and 5 years old [224]. Yet, for these ages IQ testing is less reliable. Therefore, although patients differed in their treatment progress, this design permitted us to use the same test materials (WISC-R) and consistent norms for all patients. Despite a dropout of 40% after the second measurement, we could still acquire intelligence scores for a second time for 70 patients, of which 56 patients participated a third time. We mention that for the dropout group (n=38), the majority of the patients had lower education of the parent (60.53%). Given that education of the parents was a significant predictor in our analysis, this specific dropout might have resulted in a stronger positive trend of the remaining data.

Considering the earlier neuropsychological longitudinal studies, other studies did show decrements in IQ scores [11,87,218]. However, notice that in these earlier studies, IQ materials changed for some patients throughout time, and analyses did not include covariates. By contrast, Jansen et al. [219] also showed rather stable IQ scores of chemotherapy-only treated ALL patients. Still, they also demonstrated that PIQ was lower for younger patients (at diagnosis). Our finding of lower PIQ at baseline suggests an acute decline in performance cognitive functioning for ALL patients, whereas verbal functions are preserved. Consistent with the results of Jansen and colleagues, the most strongly affected patients in our study appeared to be the younger patients at diagnosis. Other studies with regard to brain vulnerability during development, also evidenced stronger vulnerability in younger children, such as early pediatric head injury and RT in ALL patients [35]. Although Halsey and colleagues [218] did not find differences between IT-MTX + HD-MTX vs. IT-MTX only, they did encounter lower IQ scores for patients than control participants at second (i.e. 3 years after diagnosis) and third (i.e. 5 years after diagnosis) assessment. More specifically, scores of control participants increased throughout development, whereas these of the patient groups (treated with either HD-MTX, IT-MTX or RT) remained stable. The increase in these scores for control participants could partly be explained by the Flynn effect (i.e. the observed rise in norm IQ scores over time, with an estimated increase of 3 IQ points per decade [195]). As a result, norms become obsolete. Therefore, the stability of patients' scores could indicate an inhibition of such growth in intelligence. Comparably, in our study, the increase in IQ scores that we observed in patients, could also have been stronger if no chemotherapy was administered. Given that we did not have data available about premorbid intellectual functioning, nor from control groups, it remains difficult to estimate the impact of the Flynn effect on these results. Unfortunately, premorbid screening for IQ and exact timing of control assessments, remains challenging to acquire in time.

With regard to the increase of IQ scores throughout development, we encountered the strongest increase in performance functioning with time (i.e. 'measurement') in comparison to verbal functioning. This suggests that for the lower PIQ scores at first assessment, compensation arises throughout development. In this context, Anderson and colleagues discussed plasticity of the younger brain [225]. In their review they report the potential regeneration of new neurons as well as new connections (i.e. so-called sprouting). The stronger increase in PIQ scores might be due to stronger practice or rehabilitation effects for PIQ than for VIQ, as Halsey and colleagues earlier suggested [218]. However, in our study we did not

register whether patients attended specialized rehabilitation programs (e.g. with physiotherapists, speech therapists, teachers) or special care. If this information could be accounted for in the future, the distinction between rehabilitation effects will become much clearer.

Finally, it is important to mention that we used general IQ measurements. Besides our longitudinal study and the study of Jansen and colleagues [219], also cross-sectional studies generally show average IQ scores for ALL patients compared to norm scores. By consistently using more specific measurements of attention, memory and executive functioning, as well as including control groups, chemotherapy-induced sequelae could be investigated in more detail.

4.5 Conclusion

In contrast to the existing evidence for long-term neurotoxicity due to RT, we showed that IQ scores of chemotherapy-only treated ALL patients increase only a little for VIQ, but increase more strongly for PIQ. Still, lower IQ scores for patients who were diagnosed at younger ages, highlight the stronger impact of the disease and/or treatment at younger age. Given that the tumor burden reflected by low vs. increased risk did not meaningfully affect IQ scores, we would assign this effect to treatment rather than to the disease burden. Although comparable to the normative range, PIQ was lower than VIQ at baseline. Given that patients already started therapy at first assessment, this could indicate that performance functioning is most vulnerable to acute neurotoxicity at baseline, specifically for patients diagnosed at younger age. Nevertheless, patients appear to catch up with a stronger increase in PIQ scores, which possibly indicates that PIQ is being trained more easily than VIQ. Still, given earlier evidence for delay in development of specific cognitive functions from cross-sectional studies, new longitudinal studies measuring more specific cognitive functioning will be required to address this question in the future. Also to investigate the impact of disease vs. treatment on cognition, it is recommended to implement neuro-imaging and behavioral assessments at baseline before treatment starts.

5 Long-term leukoencephalopathy in childhood sarcoma survivors treated with high-dose intravenous chemotherapy

Abstract

Knowledge is limited regarding the prevalence and persistence of chemotherapy-induced leukoencephalopathy in childhood cancer. This study explored the presence, clinical relevance and potential risk factors of leukoencephalopathy in childhood bone and soft tissue sarcoma survivors, treated with high-dose intravenous chemotherapy only. We acquired cross-sectional neurocognitive data in adult survivors (n=34) and healthy age-matched controls (n=34) (median age at diagnosis=13.32 years, age range=[16-35] years). Additionally, MR imaging included T2-weighted FLAIR (leukoencephalopathy Fazekas rating), multiexponential T2 relaxation (MET2) and multishell diffusion weighted MRI (DWI), to estimate myelin-related metrics and fluid movement restrictions, respectively. Finally, chemotherapy subgroups (methotrexate, alkylating agents or combination), age at diagnosis, the Apoε and MTHFRC677T polymorphisms were explored as potential risk factors for leukoencephalopathy.

At group level, quality of life, working memory, processing speed and visual memory were significantly lower in patients compared to controls. Furthermore, this is the first study demonstrating long-term leukoencephalopathy in childhood sarcoma survivors (27.2%), which was related to attentional processing speed. Lesions were related to diffusion-derived, but not to myelin-sensitive metrics. A significant interaction effect between age at diagnosis (AaD) and chemotherapy group demonstrated more lesions in case of high dose methotrexate (HD-MTX). However, patients treated with alkylating agents (without HD-MTX) also showed lesions in younger patients. Genetic predictors were non-significant. This study suggests long-term leukoencephalopathy with possibly underlying changes in vasculature or axonal structure, rather than long-term demyelination. Such lesions could affect processing speed, and as such long-term daily life functioning of these patients.

Keywords: Leukoencephalopathy, neurocognition, bone and soft tissue sarcoma survivors

5.1 Introduction

Cranial irradiation and chemotherapy can lead to neurocognitive alterations in childhood brain tumor [226,227] and acute lymphoblastic leukemia (ALL) patients, respectively [228–230]. Underlying neural processes for such cognitive changes are increasingly investigated. With regard to clinical neuroimaging, acute leukoencephalopathy was demonstrated in approximately 20% of ALL patients [231].

Besides such clinical (e.g. FLAIR) MRI images which show leukoencephalopathy, advanced neuroimaging techniques are currently implemented to investigate microstructural brain changes. More advanced neuroimaging studies demonstrated functional [232] and structural [134] neural changes in ALL survivors. However these patients are treated with high-dose methotrexate (HD-MTX) and intrathecal therapy. By contrast, limited research was conducted in childhood cancer patients treated with high-dose intravenous chemotherapy only [19]. Given that osteosarcoma patients are treated with high doses of intravenous chemotherapy (i.e. methotrexate), the question arises to which extent this could affect brain development during childhood. In this regard, Edelmann and colleagues evidenced deficits in reading, attentional and processing speed in pediatric osteosarcoma survivors [154]. Similarly, Mohrmann and colleagues also reported that 1 out of 3 solid non-central nervous system (CNS) childhood tumor patients experience cognitive difficulties later in life [9]. However, neural underpinnings of such behavioral differences are currently unknown in childhood solid tumor patients.

Multiple radiological case reports demonstrated acute MTX-induced [233] and ifosfamide-induced [234] leukoencephalopathy [231] in solid tumor patients. However, long-term persistence of such lesions, their neurobehavioral impact and underlying pathological processes, were not documented yet. So far, advanced neuroimaging studies were only performed in adult cancer patients (e.g. breast cancer [24,157,235,236], testicular cancer [237]), suggesting neural alterations due to non-CNS directed chemotherapy as well. For instance, to investigate white matter (WM) microstructure, diffusion-weighted neuroimaging is usually implemented. Derived parameters of this neuroimaging technique (e.g. fractional anisotropy (FA), apparent diffusion coefficient (ADC)) reflect diffusion restriction, which could be related to multiple underlying neural processes (e.g. axonal loss, demyelination, crossing fibers, fluid retention etc.)[238]. These parameters were repeatedly shown to be affected in adult cancer patients [23,239]. However, such investigations are absent in childhood cancer patients. Furthermore, diffusion-derived metrics are insufficiently specific for myelination estimations. Recently, estimations of myelin water fraction (MWF) based on so-called myelin water imaging became available [131]. Neurodevelopmental patterns of these estimates are assumed to correspond better to histological changes in myelination, compared to diffusion-weighted MRI measurements.

Besides the lack of evidence for underlying pathological processes in leukoencephalopathy, subject-specific risk factors to develop leukoencephalopathy were not yet investigated. Previously hypothesized risk factors for treatment-induced neurotoxicity include genetic predisposition, age at diagnosis, hormonal changes, therapy doses, … [20]. Multiple genetic polymorphisms have been hypothesized to play an important role in treatment-induced neurotoxicity [117,240]. So far, most evidence was provided for the methylene

tetrahydrofolate reductase (MTHFR) genotype in ALL [241], given its important role in methotrexate metabolism; and genes associated with brain development, including the apolipoprotein (Apoε) E genotype [110]. More specifically, the Apoε4 (arg112, arg158) allele is associated with elevated risk for both cerebrovascular [242] and Alzheimer's disease [243], as well as with cognitive difficulties in adult cancer patients (breast cancer [244], lymphoma [111], testicular cancer [237], brain tumors [245,246]).

Given that case reports showed acute leukoencephalopathy after administration of HD-MTX and/or ifosfamide, we investigated the risk for long-term leukoencephalopathy and neurocognitive functioning in survivors of bone and soft tissue sarcoma, who were treated with multi-chemotherapy during childhood. To clarify potential underlying pathology of such observable lesions, we correlated the level of leukoencephalopathy with diffusion-derived and myelin-sensitive metrics. Finally, we explored potential risk factors including the Apoε4 and MTHFR677T genotype, chemotherapy subgroups, age at diagnosis (AaD), socio-economic status (SES) and depression rates for survivors.

5.2 Methods

5.2.1 Subjects

Consulting the database of the Pediatric Hemato-Oncology Unit of the University Hospitals Leuven, 65 patients treated between 1991 and 2014 were eligible for this study. These patients were at least 2 years off therapy, non-cranial-irradiated, more than 16 years old at time of assessment, treated according to MMT89, MMT95[247], EORTC2001, EuroEwing99[248], EURAMOS01[249], RMS05, NRSTS05[250] for ewing sarcoma, osteosarcoma, rhabdomyosarcoma or non-rhabdomyosarcoma soft tissue sarcoma. 52% of all eligible patients participated in our study (n=34). Patients who did not participate were not motivated because of time consumption or distance. 34 adult control participants were age- and gender-matched at group level, and recruited through internal hospital announcements. Informed consents were obtained from all participants. This study was approved by the ethical committee of the University Hospital Leuven.

5.2.2 Data acquisition

5.2.2.1 Imaging acquisition

MRI images were acquired on a 3T Philips Achieva ds MRI scanner with a 32-channel phased-array head coil. First, MR-imaging included T2-weighted-Fluid-Attenuated Inversion Recovery (T2-FLAIR), which was evaluated for leukoencephalopathy[251] (TR/TE=9000ms/120ms, 28 slices, in-plane resolution of .685mm x .685mm, slice thickness of 5mm). T2-FLAIR images were visually classified by a trained neuroradiologist A.R. according to the Fazekas rating scale, and independently re-evaluated by a second neuroradiologist S.S. [252]. The radiologists were blinded to the other acquired imaging modalities, to subjects group and cognitive performance data. The Fazekas rating scale resulted in four patient subgroups (Fazekas rated 0-3; see Figure 5.1).
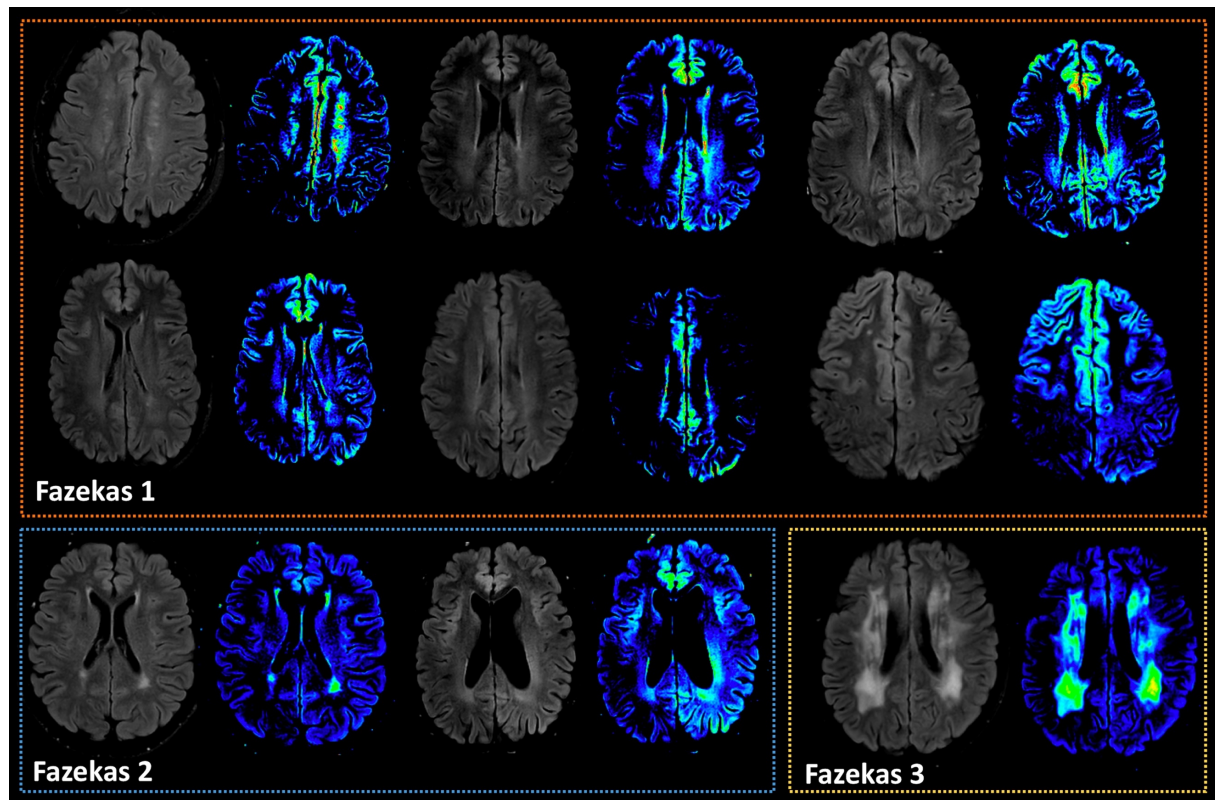
Figure 5.1 Cases showing white matter lesions, rated according to the Fazekas rating scale
Note. Lesions were highlighted using an intensity thresholded color map with higher intensities depicted in yellow-red

Second, Apparent Diffusion Coefficient (ADC) and Fractional Anisotropy (FA) maps were derived from diffusion-weighted MRI data (echo-planar, multi-shell imaging b-values 700, 1000 and 2800 s/mm^2, applied along 25, 40 and 75 directions, 10 b = 0 images [71], voxel size 2.5 x 2.5 x 2.5 mm^3, TR/TE = 7800 ms/90 ms, 50 axial slices). These values represent the estimated magnitude of diffusion (of water molecules) in a voxel, and the degree of this movement in one principal direction, respectively. Both can be affected by multiple neurotoxic processes e.g. demyelination, inflammation, microbleeds, axonal loss, … Therefore, more recent myelin-sensitive maps of Myelin Water Fraction (MWF) and Intra-Extra cellular Water Fraction (IEWF) were estimated based on a 3D GraSE sequence (voxel size .96 x .96 x 2.5 mm^3, ETL=32, TE=10, 20, … , 320ms, TR=1s, 32 slices, EPI factor 3, acceleration factor 2) (see example maps for one case, Figure 5.2) [253]. For both modalities, images were non-linearly registered to a population-based template. Metric averages were calculated for each subject (based on FA-thresholded maps for DWI maps, and TE1 segmentation for MWI maps) within the population-based WM masks (see Figure 5.2).
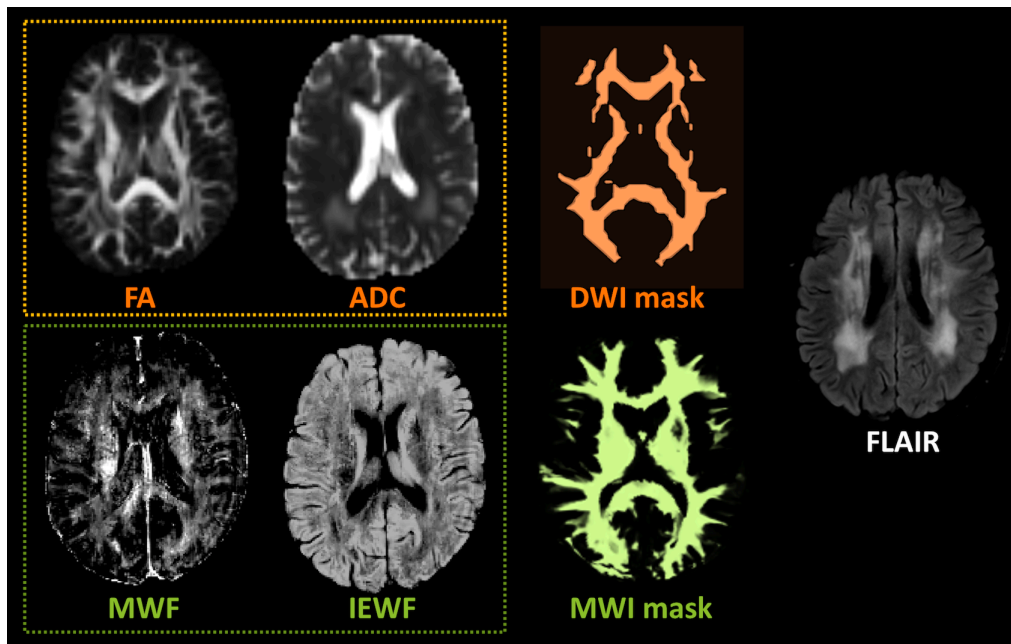
Figure 5.2 Example of diffusion- and myelin- derived metric maps to link with lesions

Note. DWI- and MWI-derived metric maps are shown for case who showed most extreme lesions (Fazekas was rated 3). Based on Diffusion-weighted MRI scans, Fractional Anisotropy (FA) and Apparent Diffusion Coefficient (ADC) maps were estimated. The multiexponential T2 relaxation (MET2) images were used for estimations of Myelin Water Fractions (MWF) and Intra- Extra-cellular Water Fraction (IEWF). For both image modalities, the white matter mask was segmented to estimate the average values DWI and MWI per subject (depicted in orange and green, respectively).

5.2.2.2 Medical assessments

Medical records included cardiotoxicity and neurotoxicity during treatment, MTHFRC677T genotyping (CC, CT and TT) and Apoε genotyping (ε2, ε3, ε4 allele, resulting in five subgroups: ε2/ε2, ε2/ε3, ε3/ε3, ε3/ε4, ε4/ε4; ε2/ε4 was not observed), AaD and time since start of treatment. Cumulative chemotherapy doses were recorded for methotrexate, ifosfamide, cyclophosphamide, cisplatin and doxorubicin (detailed patient characteristics and cumulative doses are shown in Table 5.1). One survivor was eventually excluded from analyses due to irradiation of the skull base.

Table 5.1 Patient characteristics sarcoma survivors

	Osteosarcoma		Ewing	Rhabdomyosarcoma		Non-rhabdomyosarcoma
TREATMENT	EORTC2001	EURAMOS1	EuroEW99	MMT95	RMS2005	NRSTS2005
NUMBER	3	13	7	6	3	2
AGE DIAGNOSIS	12-15years	10-18years	12-15years	4-15years	9-16years	11-14years
TIME SINCE THERAPY	14-15years	2-13years	4-15years	12-20years	4-8years	2-20years
MTX (G/M^2)	0-45	96-144	0	0	0	0
IFOS/CYCLO (G/M^2)	0-36	0-87	0-102	0-54	24-102	33-36
DOXO (MG/M^2)	450	450	180-360	0	0-375	210-240
CISPLATIN (MG/M^2)	600	240-480	0	0	0	0
FAZEKAS RATING	0,1	0,1,2,3	0,1	0,1	0,1	0

5.2.2.3 Neurocognitive assessment

We acquired data for intelligence, verbal and visual memory, and attentional functioning. An extensive battery included the Dutch versions of the WAIS-IV intelligence test, Auditory Verbal Learning Test, Rey Visual Design Learning Test and Amsterdam Neuropsychological Task battery. Subjective daily life experiences were acquired using the State Anxiety Inventory (STAI), Beck Depression Inventory (BDI), Behavior Rating Inventory of Executive functioning (BRIEF), Cognitive Failure Questionnaire (CFQ) and Quality of Life (QoL) Questionnaire. All data were acquired on the same day.

5.2.3 Data analyses

First, subjective complaints and objective neurocognitive measurements were predicted in one multivariate ANOVA (MANOVA) model by the predictors patient vs. control, lesion Fazekas rating, corrected for SES and depression rates as covariates [254–256]. Second, white matter average DWI- and MWI-derived metrics were predicted by the Fazekas lesion rating scale (i.e. one-way ANOVA). Third, odds ratios of white matter (WM) lesions were compared between HD-MTX administration (vs. no administration), the MTHFR and Apoε polymorphisms (likelihood ratio (LR)). Finally, in order to investigate the impact of AaD on the presence of WM lesions in survivors, the interaction effect of chemotherapy subgroup (i.e. HD-MTX, alkylating agents (i.e. ifosfamide or cyclophosphamide), patients who received both) and AaD was investigated (i.e. two-way ANOVA). For each model, p-values were assumed significant at α=.05. Statistical analyses were performed using SPSS v20.

5.3 Results

5.3.1 Behavioral functioning patients vs. controls

Median AaD was 13.32 years (IQR:4), time since start of treatment = 8.95 years (IQR: 8), age range=[16-35] years). Diagnoses included Ewing sarcoma (n=7), osteosarcoma (n=16), rhabdomyosarcoma (n=8) or non-rhabdomyosarcoma soft tissue sarcoma (n=2).

The comparison of subjective functioning between patients and controls shows significant decreases in overall QoL (F=5.070, p=.029) (complete statistical output of the multiple (uncorrected) ANOVAs, see Table 5.4). Furthermore, cognitive measures of WAIS working memory (F=6.485, p=.014), WAIS processing speed (F=5.619, p=.022) and RVDLT total (F=8.117, p=.007) were significantly lower in the patient group.

5.3.2 White matter lesions, pathology & functional outcome

Fazekas ratings for leukoencephalopathy were significantly related to DWI-derived metrics (i.e. FA: F=3.967, p=.012, and ADC: F=3.929, p=.012), but not to the myelin-sensitive metrics (i.e. MWF: F= 2.216, p=.095 and IEWF: F=.579, p=.631). More specifically, higher ADC and lower FA was found in subjects with higher Fazekas ratings. Furthermore, higher Fazekas levels were associated with longer attentional reaction times within the patient group during basal, focused, divided and sustained attention tasks (p<.05; see complete statistical model in Table 5.4).

5.3.3 Exploration of potential risk factors for leukoencephalopathy

As shown in in Figure 5.1, WM lesions were detected in nine out of the 33 patients (27.2%), in contrast to two out of 34 matched controls (6%, limited to Fazekas 1; *LR*=4.018, *p*=.045).

Within patients, white matter lesions were more often present in case of HD-MTX administration (*LR*=2.977, *p*=.084), albeit non-significant. Percentages of WM lesions were approximately 40% (n=6/16) in HD-MTX-treated patients, while only 18% (n=3/17) in non-MTX treated patients (see Figure 5.3). The highest levels on the Fazekas rating scale (level 2 and 3) were reached for three osteosarcoma survivors, treated with high dose MTX (144g/m^2) without ifosfamide/cyclophosphamide.

Furthermore, the interaction effect between chemotherapy subgroup and AaD was significant (*F*=3.434, *p*=.047; see Table 5.2). As shown in Figure 5.4, HD-MTX treated patients (without alkylating agents) were older at diagnosis (median 14.98 years), but leukoencephalopathy also occurred in patients treated with ifosfamide/cyclophosphamide only, but mainly in younger patients at diagnosis (median 8.65 years).

With regard to polymorphism subgroups, 30% of the lesions was found in the ε3/ε3 Apoε-genotype subgroup (see Figure 5.5; Table 5.3), whereas the ε2/ε2, ε2/ε3 group did not show any lesions. Nonetheless, these ratios were not significantly different (*LR*=2.468, *p*=.650). For HD-MTX treated survivors (n=16), patients showing white matter lesions carried at least one T allele of the MTHFR polymorphism (100%), possibly showing a trend (*LR*=5.214, *p*=.074), but non-significant association.

Table 5.2 Univariate ANOVA results WM lesions predicted by MTX administration, age at diagnosis and interaction effect

	Type III Sum of Squares	df	Mean Square	F	Sig.	η^2
Intercept	.198	1	.198	1.127	.298	.041
MTX/IFO/COMBI	.907	2	.453	2.583	.094	.155
Age at diagnosis	.426	1	.426	2.425	.131	.080
Interaction effect	1.206	2	.603	3.434	.047*	.199

Note. MTX= methotrexate. IFO=ifosfamide. COMBI=combination of both agents. WM lesion grade (Fazekas rated) was implemented as primary outcome.

Table 5.3 Percentages of white matter lesions in patient group, categorized by Apoε genotype and MTHFRC677T

		Apoε subgroup						MTHFRC677 subgroup			
		ε2/ε2	ε2/ε3	ε3/ε3	ε3/εE4	ε4/ε4	Total	CC	CT	TT	Total
WM lesions	Absent	1 (100%)	2 (100%)	14 (70%)	6 (75%)	1 (50%)	24 (72.7%)	3 (100%)	6 (66.6%)	1 (25%)	10 (62.5%)
	Present	0 (0%)	0 (0%)	6 (30%)	2 (25%)	1 (50%)	9 (27.3%)	0 (0%)	3 (33.3%)	3 (75%)	6 (37.5%)
Total		1 (100%)	2 (100%)	20 (100%)	8 (100%)	2 (100%)	33 (100%)	3 (100%)	9 (100%)	4 (100%)	16 (100%)
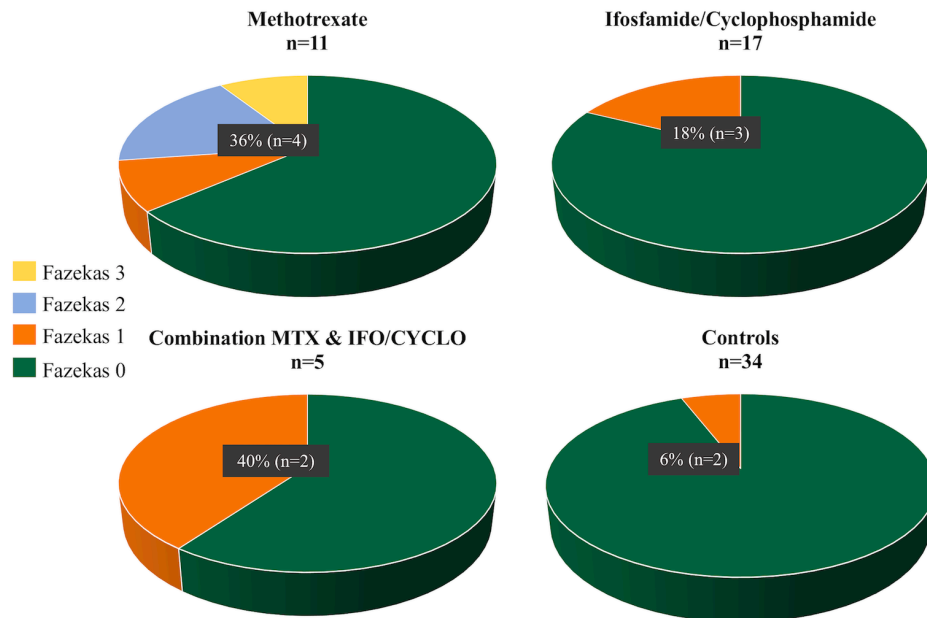
Figure 5.3 Percentages of patients with leukoencephalopathy,
classified by Fazekas rating scale

Note. HD-methotrexate and ifosfamide/cyclophosphamide are administered with the highest
cumulative doses of all agents within the specified treatment protocols. Ratios of WM lesions
rated according to the Fazekas rating scale, are shown for each subgroup treated with one or
both of these agents. HD-MTX (n=11+5) was only administered in osteosarcoma patients
(12g/m2 over four or six hours IV per course). Treatments for Ewing sarcoma and (non-
)rhabdomyosarcoma included ifosfamide/cyclophosphamide (without MTX administration,
n=17). Note that all patients received these agents in multi-agent chemotherapy protocols (see
Table 5.1).
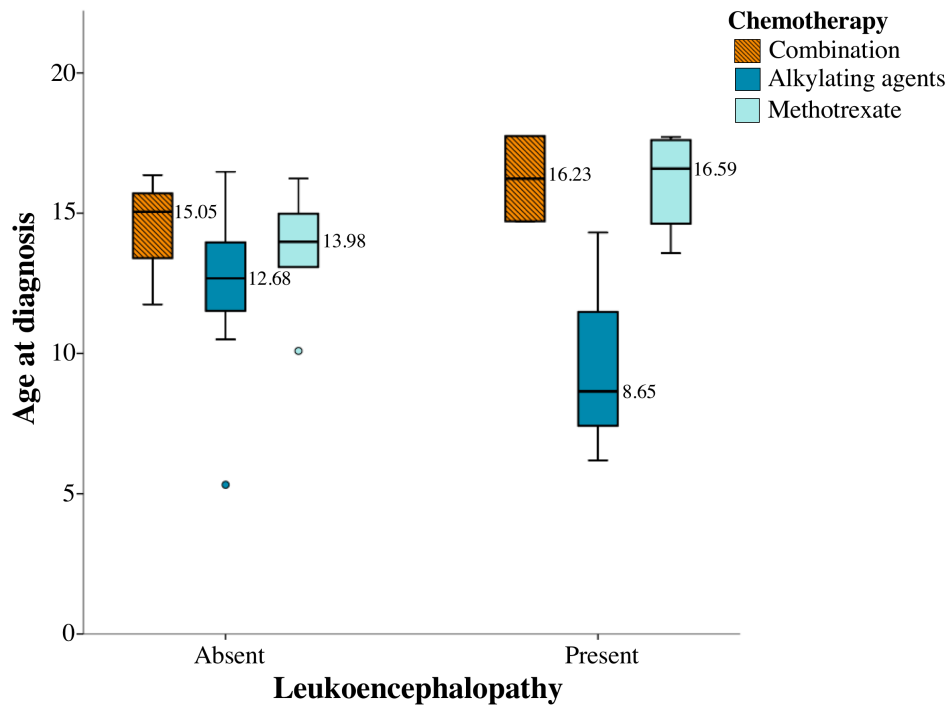
Figure 5.4 Boxplots for age at diagnosis, lesions and chemotherapy subgroups

Note. In the group of patients showing no lesions, n=3 had received combination therapy, n=16 ifosfamide/cyclophosphamide, n=5 methotrexate only. In the group of patients showing lesions, these numbers were n=2, n=3, n=4, resp. Error bars represent standard deviations of the values.
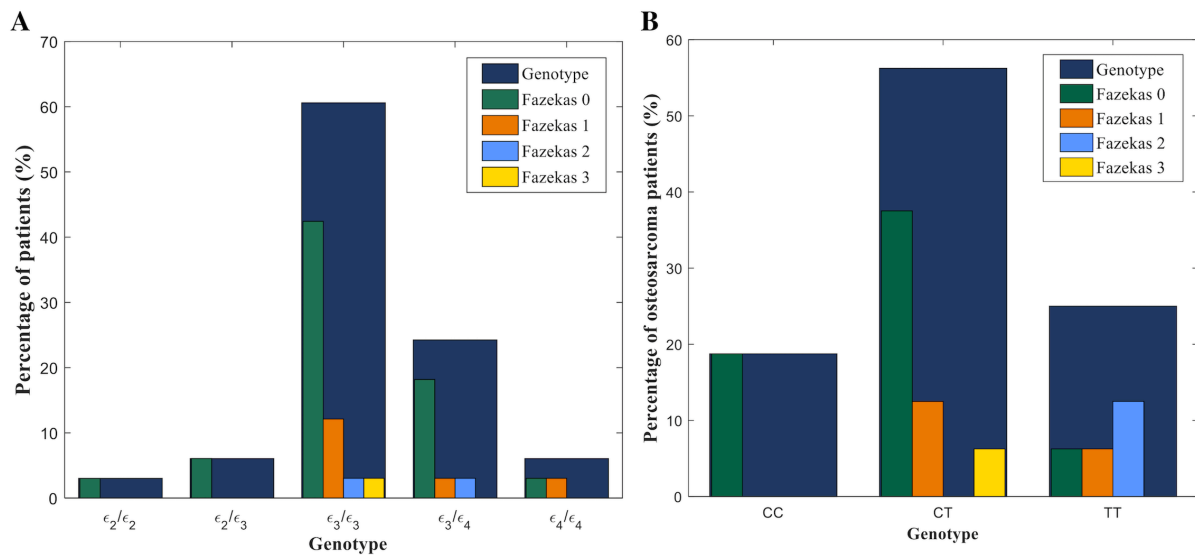
Figure 5.5 Percentages of patients with lesions for each polymorphism

Note. Percentages of patients in each subgroup are depicted. The distribution of the polymorphism variants is shown in dark blue. Within each polymorphism subgroup (Panel A: Apoε genotype, Panel B: MTHFR genotype), the distribution of Fazekas rated WM lesions is shown in green, orange, light blue and yellow for rating 0, 1, 2 and 3, respectively.

Table 5.4 MANOVA Subjective & objective scores predicted by WM Fazekas rating lesions

Dependent Variable	Patient vs. Control			WM lesions Fazekas			SES			Depression		
	F	Sig.	η^2	F	Sig.	η^2	F	Sig.	η^2	F	Sig.	η^2
BRIEF Total	1.626	.209	.036	1.391	.258	.087	1.036	.314	.023	3.677	.062	.077
PedsQL Total	5.070	.029*	.103	2.453	.076	.143	.056	.814	.001	28.665	<.001***	.394
STAI Total	1.033	.315	.023	1.021	.393	.065	2.221	.143	.048	48.940	<.001***	.527
CFQ Total	3.345	.074	.071	1.206	.319	.076	.105	.748	.002	.271	.605	.006
WAIS FSIQ	1.958	.169	.043	.576	.634	.038	4.055	.050	.084	.369	.547	.008
WAIS VCI	.659	.421	.015	1.235	.308	.078	3.799	.058	.079	.205	.653	.005
WAIS PRI	.027	.870	.001	.447	.720	.030	1.447	.235	.032	.072	.790	.002
WAIS WMI	6.485	.014*	.128	.690	.563	.045	5.112	.029*	.104	2.150	.150	.047
WAIS PSI	5.619	.022*	.113	.458	.713	.030	.015	.904	<.001	4.190	.047*	.087
AVLT Total	.044	.835	.001	.454	.716	.030	1.165	.286	.026	.994	.324	.022
AVLT immediate recall	.510	.479	.011	.450	.719	.030	.419	.521	.009	.084	.773	.002
RVDLT total	8.117	.007**	.156	.312	.816	.021	.252	.618	.006	12.116	.001**	.216
RVDLT immediate recall	3.742	.060	.078	.403	.751	.027	.025	.874	.001	1.914	.173	.042
AVLT recognition	.782	.381	.017	.627	.602	.041	.020	.888	<.001	.075	.785	.002
RVDLT recognition	.598	.443	.013	2.859	.048*	.163	.301	.586	.007	5.325	.026	.108
ANT reaction time baseline	.718	.401	.016	3.910	.015*	.210	1.035	.315	.023	.449	.506	.010
ANT stability reaction time baseline	.013	.911	<.001	3.797	.017*	.206	.002	.966	<.001	4.201	.046*	.087
ANT reaction time focused attention	.029	.866	.001	6.827	.001**	.318	.459	.502	.010	1.234	.273	.027
ANT focused attention: effect of distractors	.780	.382	.017	1.084	.366	.069	1.347	.252	.030	.507	.480	.011
ANT focused attention: effect of memory load	.224	.638	.005	4.244	.010*	.224	.056	.815	.001	.384	.538	.009
ANT reaction time divided attention	.493	.486	.011	8.770	<.001***	.374	.147	.704	.003	.912	.345	.020
ANT reaction time divided attention one distractor	.182	.672	.004	.802	.499	.052	<.001	.983	<.001	.268	.608	.006
ANT reaction time divided attention two distractors	.103	.750	.002	.645	.590	.042	.083	.775	.002	1.329	.255	.029
ANT reaction time compatible task	.754	.390	.017	.207	.891	.014	.643	.427	.014	.294	.590	.007
ANT set shifting: inhibition effect	3.465	.069	.073	5.708	.002**	.280	9.071	.004**	.171	.179	.674	.004
ANT set shifting: cognitive flexibility effect	.303	.585	.007	.281	.839	.019	1.141	.291	.025	.250	.620	.006
ANT reaction time sustained attention	.106	.746	.002	2.807	.051	.161	.078	.782	.002	1.384	.246	.031
ANT stability reaction time sustained attention	2.462	.124	.053	4.452	.008**	.233	.142	.708	.003	.020	.887	<.001

Note. *indicates p<.05, ** indicates p<.01, *** indicates p<.001

5.4 Discussion

Long-term neurotoxicity of intravenous chemotherapy was investigated using FLAIR-images, neurobehavioral assessments, DWI- and MWI-derived parameters and exploration of DNA polymorphisms in childhood sarcoma survivors. This study is the first study reporting long-term leukoencephalopathy in 27.2% of survivors, with highest frequency in HD-MTX treated patients (40%). Lesions were associated with diffusion-weighted imaging (i.e. water molecule movement), but not to more myelin-sensitive parameters. The presence of long-term leukoencephalopathy was related to longer reaction times, while on a group level, survivors performed worse on QoL, processing speed, working memory and visual memory.

Behavioral measures at group level

Patients reported lower QoL in comparison to controls. Such vulnerability in cancer patients has consistently been reported in earlier psychosocial studies in childhood cancer patients and survivors[257]. Besides these subjective reports, our neurocognitive test assessment demonstrated lower performances on processing speed (i.e. WAIS processing speed), working memory (i.e. WAIS working memory) and visual memory (RVDLT total), which could have an important impact on QoL of these patients. These findings confirm earlier attentional and processing speed alterations that were encountered in osteosarcoma survivors by Edelmann et al. (2016) [154]. In addition to their behavioral findings, this study importantly added the detection and potential impact of long-term leukoencephalopathy in these patients. However, one should note that the significance levels of behavioral comparisons between patients and controls in our study remained low, and would not survive stringent corrections for multiple comparisons.

Although behavioural investigations in cancer patients often focus on neurocognition independently of personality or coping mechanisms, factors such as depression and SES can largely affect cognitive functioning. Hence, we included both factors as covariates. We note that if depression would not have been included as covariate, anxiety (STAI) also appeared significantly higher in patients, and only working memory remained different at group level (while processing speed and visual memory did not). This demonstrates the possible impact of depression rates on decreased processing speed, which suggests the importance of detecting also emotional vulnerability as a potential risk factor early on during childhood, in order to improve neurodevelopment (e.g. information processing).

Imaging & cognition

Reaction times during baseline attention, focused, divided and sustained attention, were longer in patients showing leukoencephalopathy. Similarly, Cheung et al. (2016) reported acute leukoencephalopathy in leukemia and their experience of decreased task organization [230]. We note that scores in our study were obtained using a computerized task, recording reaction times in detail. As these scores only reached a clinical threshold in case of highest lesion load (Fazekas 3), such decreases in processing speed could be more subtle in case of smaller lesions or cerebrovascular damage [258].

With regard to underlying pathology, Cheung et al. (2018) recently associated elevated cerebrospinal values of total tau and myelin basic protein with development of leukoencephalopathy [259]. This suggests underlying neural damage, which could be axonal injury (e.g. demyelination). Nevertheless, the current study did not demonstrate a link between leukoencephalopathy and myelin-water fraction, as an estimation of axonal myelin content in sarcoma patients. To our knowledge, myelin-metrics were only implemented in two previous studies with cancer patients so far [170,260]. Similarly, these studies showed no differences in MWF 3-4 years after breast cancer treatment [260], nor 15 years after treatment for leukemia [170], which is consistent with our findings in childhood sarcoma survivors. Although they showed acute changes in diffusion metrics (i.e. decreased FA), these values normalized years after treatment [260]. Still, in the current study, diffusion changes remained clearly associated with lesion ratings, even years after treatment. Confirmingly, some adult cancer studies previously showed long-term diffusion changes in case of high-dose chemotherapy administration (i.e. including cyclophosphamide of 6g/m^2) [236]. Given that the majority of patients with lesions in our population (66%) had also received highest cumulative doses of methotrexate (of >45g/m^2), this could explain the observed long-term diffusion changes (measured with FA and ADC). Previous cancer studies focused either on WM lesions [230] or on diffusion images [156], but did not report both modalities. The link between diffusion changes and lesions could suggest axonal reorganization/loss, interstitial fluid, but also microscopic vascular damage [261]. Even increased blood-brain-barrier permeability was linked to hyperintensities in vascular cognitive impairment [262]. Hence, early detection of leukoencephalopathy and attentional assessments, will become informative to investigate daily life functional outcomes in these patients.

Potential predictors of leukoencephalopathy

Leukoencephalopathy was most frequent in HD-MTX-treated patients, showing the highest lesion load (Fazekas 2 and 3). HD-MTX combined with intrathecal administration was previously associated with acute leukoencephalopathy in ALL patients [230,263] (16%-27% in asymptomatic [230,231] vs. 58% of symptomatic patients) [231]. However, the question remains how persistent such lesions are. One study showed long-term lesions in 68% of ALL survivors (2.6-7 years after treatment) treated with triple intrathecal therapy (vs. 22% in case of intrathecal MTX) (n=66)[264]. We demonstrated such long-term leukoencephalopathy in 27% of childhood sarcoma survivors who did not receive CNS-directed treatment in contrast to ALL patients. ALL patients receive less intensive treatments of intravenous HD-MTX (3-5g/m^2/course over 24-36 hours (cumulative doses of 20g/m^2)) [228] compared to osteosarcoma patients (12g/m^2/course over 4-6 hours (cumulative doses MTX of 144g/m^2)), which could explain the higher frequency of lesions in the latter group (40%, n=6/16).

In our study, an interaction effect between chemotherapy subgroup and AaD, suggested that leukoencephalopathy was more pronounced in younger patients after treatment with alkylating agents (cumulative doses 24-102g/m^2). This could suggest that not only HD-MTX induces long-term leukoencephalopathy, but alkylating agents could yield similar effects in young patients. Importantly, median ages at diagnosis were 14.98 years, 12.31 years,

and 15.05 years for patients who received only HD-MTX, only ifosfamide/cyclofosfamide, or the combination, respectively.

Finally, with regard to genetic predisposition, three out of the six HD-MTX-treated patients showing WM lesions, were carriers of the MTHFRTT variant and showed the highest Fazekas rating (2 and 3). This could suggest a potential role of the MTHFRTT in developing lesions. Furthermore, approximately 30% of Apoε3/ε3 and Apoε4 carriers showed WM lesions, whereas no Apoε2 carrier showed WM lesions. This finding might be complementary with earlier demonstrated cognitive dysfunction in Apoε4 carriers in adult cancer populations [111,237,244–246]. Nevertheless, both polymorphisms were non-significant and currently limited to draw firm conclusions.

<u>Limitations and future directions</u>
Although this is the first study evidencing long-term leukoencephalopathy in childhood bone and soft tissue sarcoma patients, the number of patients showing lesions (n=9/34) remained limited to draw firm conclusions regarding possible risk factors. This study provided an exploration of risk factors including age at diagnosis, MTHFR and Apoε polymorphisms, and type of chemotherapy. Nevertheless, the low absolute number of cases showing lesions might partly explain the absence of significant results. Given the small cohort, larger studies including wider age ranges and inclusions in genetic subgroups, are necessary to confirm such subject-specific factors for neural damage in detail. Furthermore, we assumed lesions to be probably caused by the high dose chemotherapy, given earlier case reports. Nonetheless, baseline data were not available in this study. A longitudinal study with childhood patients is therefore highly recommended (see Chapter 8). Finally, given that lesions are heterogeneous between patients, underlying pathology and the impact of such lesions could be subject-specific, which will again require larger sample sizes and biochemical investigations in future research. More advanced imaging analyses could also investigate whether patients with large lesions (e.g. Fazekas 2 or 3), also demonstrate clear brain network changes (see Chapter 9). Larger samples of cases showing such lesions will therefore be required.

5.5 Conclusion

Survivors of childhood solid bone and soft tissue sarcoma treated with intravenous chemotherapy show an elevated risk for leukoencephalopathy, which was associated with increased attentional reaction times. The association with diffusion metrics suggests long-term microstructural tissue changes (e.g. vasculature, inflammation, axonal loss), but not necessarily long-term demyelination. Although only reaction times were related to lesion load, lower QoL, lower working memory, processing speed and visual memory was also detected at group level, which can highly affect patients' long-term daily life functioning. In order to address risk factors in more detail and improve neurodevelopment, future longitudinal studies are highly recommended including large samples.

6   White matter microstructural changes in childhood sarcoma survivors treated with high-dose intravenous chemotherapy

Abstract

With the increase of survival rates of pediatric cancer patients, the number of children facing potential cognitive sequelae has grown. Previous adult studies suggest that white matter (WM) microstructural changes may contribute to cognitive impairment. This study aims to investigate WM microstructure in childhood bone and soft tissue sarcoma.

Differences in (micro-)structure can be investigated using diffusion weighted MRI (DWI). The typically used diffusion tensor model (DTI) assumes Gaussian diffusion and lacks information about fiber populations. In this study, we compare WM structure of childhood bone and soft tissue sarcoma survivors (n=34) and matched controls (n=34), combining typical and advanced voxel-based models (DTI and NODDI model, resp.), as well as recently developed fixel-based models (for estimations of intra-voxel differences, Apparent Fiber Density (AFD) and Fiber Cross-section (FC)). Parameters with significant findings were compared between treatments and correlated with subscales of the WAIS-IV intelligence test, age at diagnosis, age at assessment and time since diagnosis. We encountered extensive regions showing lower fractional anisotropy, overlapping with both significant NODDI parameters and fixel-based parameters. In contrast to these diffuse differences, the fixel-based measure of AFD was reduced in the cingulum and corpus callosum only. Furthermore, AFD of the corpus callosum was significantly predicted by chemotherapy treatment and correlated positively with time since diagnosis, visual puzzles and similarities task scores.

This study suggests altered WM structure of childhood bone and soft tissue sarcoma survivors. We conclude global chemotherapy-related changes, with particular vulnerability of centrally located WM bundles. Finally, such differences could potentially recover after treatment.

Keywords: White matter, Childhood solid tumors, non-CNS directed chemotherapy, Diffusion-weighted imaging

6.1 Introduction

As survival rates increase for oncological patients, potential late aversive effects of the treatment become important to address [4,265]. In children specifically, brain development could be challenged during cancer, due to the disease and/or treatment. Hence, it becomes essential to trace potential neurotoxic mechanisms. In pediatric oncology, cranial irradiation was evidenced to lead to cognitive deficits in brain tumor patients [226,227] and leukemia patients [148,216,228,266]. Consequently, treatment for leukemia patients was replaced by CNS-directed chemotherapy.

Still, evidence also exists for cognitive decline due to CNS-directed chemotherapy, even without radiotherapy [10,266,267]. Most difficulties were reported for executive functioning [116,147,216]. In line with these cognitive studies, recent neuroimaging studies have also evidenced white matter [15,134,268–270] and grey matter changes due to CNS-directed chemotherapy [271–273]. In contrast to the large number of reports about late neurocognitive sequelae in leukemia [274], only limited research has been conducted on childhood solid non-CNS tumors [19]. Recently, a few studies have reported cognitive outcomes of childhood solid non-CNS tumor survivors. Mohrmann and colleagues have shown that one-third of solid non-CNS tumor patients experience cognitive complaints later in life [9]. For rhabdomyosarcoma, a recent survivor study also evidenced higher risk for depression and task efficiency problems [275]. Patients using psychopharmaca for anxiety or depression appeared to be most vulnerable. In addition, a recent study performed by Edelman and colleagues, demonstrated lower reading skills, attention, memory and processing speed in survivors of osteosarcoma [154].

Not only the number of behavioral studies remains limited for these patients, neuroimaging studies in childhood non-CNS solid tumor survivors have not been performed yet. Still, adult studies have reported alterations of the white matter microstructure in solid tumor patients (including breast and testicular cancer) [156,158,235,237,276]. Currently, MR diffusion-weighted neuroimaging is used to characterize the WM microstructure, and assess possible changes after treatments. These studies typically implement the diffusion tensor imaging (DTI) model, modeling the diffusion of water molecules in each voxel as a 3D Gaussian distribution [277].

In the cancer patient groups previously described, DTI-derived parameters such as fractional anisotropy or mean diffusivity often showed differences in multiple regions, scattered throughout the brain [134,155,278–280]. However, the cellular microstructure in biological tissue can lead to hindered, non-Gaussian diffusion, for which the DTI model is inadequate. Hence, advanced models should include information of more specific microstructural compartments of the tissue. One of these compartment models is Neurite Orientation Dispersion and Density Imaging (NODDI) [281]. This is a three-compartment model of white matter microstructure: intra-axonal space, extra-axonal space, and the cerebrospinal fluid. According to the model, water movement in the intra-axonal space depends on the orientation dispersion of tracts. Anisotropic and isotropic Gaussian distributions of movement are assumed for the extra-axonal space and cerebrovascular fluid, respectively. Using these biophysical assumptions, the NODDI model derives parameters for Neurite Density, Orientation Dispersion Index and Isotropic volume fraction to characterize white matter microstructure.

Still, these parameters are voxel-based, while white matter voxels are typically occupied by multiple fiber populations, resulting in crossing fibers [282]. In other words, changes measured by voxel-based parameters (i.e. based on the DTI or NODDI model), are not fiber-specific. To overcome this limitation, Raffelt and colleagues have recently developed the so-called 'Fixel-based' analysis [283]. Instead of calculating voxel-based parameters, the concept "fixel" was introduced to refer to individual fiber populations within a voxel, segmented from the fiber orientation distribution within a voxel. Hence, fiber-specific white matter microstructure can be modeled in each direction, and provide more detailed information about specific fiber bundles. Specifically, fixel-based parameters can model changes at both microstructural level (e.g. apparent fiber density, AFD) and macroscopic level (e.g. fiber cross-section, FC).

In this study, we compare WM microstructure between childhood bone and soft tissue sarcoma survivors and healthy matched controls, by using both fixel-based and voxel-based analyses. In addition, we investigate the link between IQ subscales and diffusion metrics. This way, we aim to investigate the white matter microstructure as underlying neural substrate for cognitive functioning in more detail. We hypothesize that if WM development is affected by chemotherapy during childhood, differences are expected in the diffusion-derived parameters. Specifically, if WM differences are different at macroscopic vs. microscopic level, the fixel-based analysis could demonstrate such distinctions and show fiber-specific changes.

6.2 Methods

6.2.1 Participants

This study included the same cohort as Chapter 5. We acquired DWI in 34 survivors of pediatric solid non-CNS tumors and 34 healthy age- and gender-matched controls. The patient group consisted of survivors of bone and soft tissue sarcomas (n= treated according to the chemotherapy protocols EURAMOS1 (n=13), RMS2005 (n=3), NRSTS2005 (n=1), Euro-Ewing99 (n=7), MMT95 (n=5), EORTC2001 (n=3), IVAD (n=1), which included intravenous chemotherapy only (1 survivor was excluded due to cranial irradiation). Adult survivors were included at least 2 years after treatment at the University Hospitals Leuven. The age at diagnosis ranged between 4.00-17.75 years (mean=12.97 years, SD=3.33). Healthy age-matched control participants were recruited using local electronic advertisements. All participants were aged between 16.14-35.28 years (mean=22.51, SD=3.97) at the moment of acquisition. Time since diagnosis ranged between 2.08-19.92 years (mean=9.92, SD=4.72). The study was approved by the Ethical Committee of University Hospitals Leuven and conducted according to the Declaration of Helsinki.

6.2.2 Data acquisition

Images were acquired on a 3T Philips Achieva MRI scanner with a 32-channel phased-array head coil. The echo-planar, multi-shell diffusion imaging scheme consisted of b-values 700, 1000 and 2800 s/mm^2, applied along 25, 40 and 75 uniformly distributed gradient directions respectively, in addition to 10 non-diffusion-weighted images (b=0). This multi-shell scheme including a high b-value, allowed us to apply advanced diffusion models. For all diffusion series,

the following acquisition parameters were constant: TR/TE=7800ms/90ms, 50 slices, voxel resolution of 2.5mm x 2.5mm x 2.5mm. The total acquisition time for the diffusion-weighted scans was approximately 25 minutes.

In addition to the neuroimaging data, the WAIS-IV intelligence test was acquired in all subjects on the same day. The main subscales were investigated as neurocognitive outcome of interest, including Verbal Comprehension Index subscales (i.e. Similarities, Vocabulary, Information), Perceptual Reasoning Index (i.e. Block Design, Matrix Reasoning, Visual Puzzles), Working Memory (i.e. Digit Span and Arithmetic) and Processing Speed (i.e. Symbol Search and Coding). Descriptive statistics of the main scales for this population and included data, see Table 6.1).

Table 6.1 Descriptive statistics of subgroups patients & controls

Measurement	Patients		Controls	
	Range	Mean (SD)	Range	Mean (SD)
Cognitive outcome				
FSIQ	73-133	100.58 (13.86)	89-137	109.91 (11.76)
PRI	70-135	102.24 (16.01)	85-139	101.74 (13.13)
VCI	70-131	100.55 (13.63)	74-134	108.97 (13.63)
WM	77-143	97.94 (13.58)	80-143	109.12 (13.92)
PS	63-122	99.45 (14.02)	81-134	107.38 (14.23)
Demographic variables				
Age at diagnosis (years)	5-18	13.24 (2.97)	NA	NA
Time since diagnosis (years)	2-20	9.80 (4.74)	NA	NA
Age at assessment (years)	16-35	23.04 (4.31)	16-30	22.12 (3.60)
Socio-economic status	11.5-60.5	35.19 (12.71)	19-66	47.58 (12.83)
DWI parameters				
FA significant regions	.56-.65	.61 (.02)	.62-.70	.65 (.19)
AFD corpus callosum	.25-.41	.32 (.04)	.27-44	.35 (.04)

Note.
FSIQ=Full Scale IQ, PRI=Perceptual Reasoning Index, VCI=Verbal Comprehension Index, WM=Working Memory, PS=Processing Speed. SES* was measured using the Hollingshead Four Factor Index of Social Status. NA=Not applicable. FA=Fractional Anisotropy, AFD=Apparent Fiber Density.

6.2.3 Data processing

To investigate the white matter of survivors in detail, both voxelbased and fixelbased analyses were used. For a schematic overview of these analyses, see Figure 6.1.
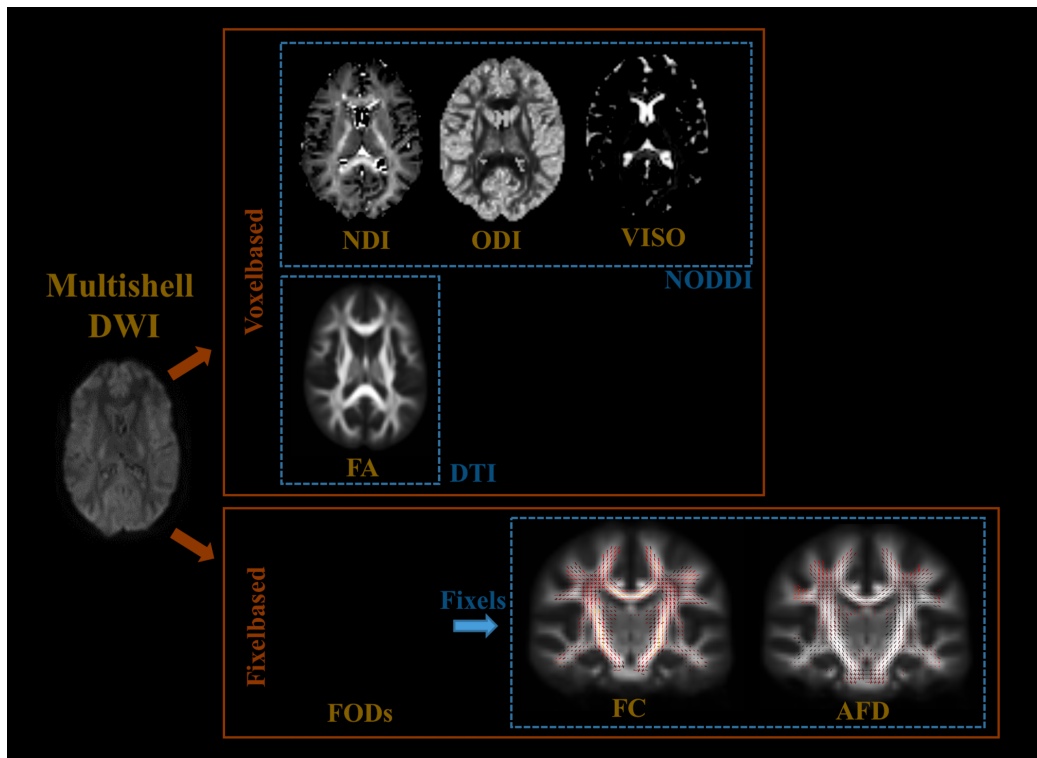
Figure 6.1 Schematic overview of voxel-based and fixel-based parameter maps
Note. NDI=Neurite Density Index, ODI=Orientation Dispersion Index, VISO=Isotropic Volume fraction, FA=Fractional Anisotropy. For fixelbased analyses, FODs=Fiber Orientation Distributions are used to calculate fixel-based parameters including: FC=Fiber Cross-section, AFD=Apparent Fiber Density.

6.2.3.1 Voxelbased analyses

DWI preprocessing including motion- and eddy current induced distortion correction was performed using ExploreDTI [284], DWI bias field correction [285] and global intensity normalization [286] was performed using MRtrix3 [287]. The corrected DWI images were then fitted with the (1) diffusion tensor model to generate fractional anisotropy (FA) maps using MRtrix3 and (2) the NODDI model using the NODDI Matlab toolbox [281], resulting in three additional parameter maps: neurite density index (NDI), isotropic volume fraction (Viso), orientation dispersion index (ODI).

The corrected DWI images were then used to compute fiber orientation distributions (FODs), using robust constrained spherical deconvolution [288] with a group average response function (based on the highest shell data (b=2800)). To be able to make interindividual comparisons at group-level, individual maps should be registered to the same space. Hence, individual FODs were registered diffeomorphically to a population-based FOD-atlas [289], which was created based on 20 individual FOD-maps (10 patients and 10 controls; mean age of subgroup: 20.83 years old (range 16.14-25.69)) (see Figure 6.2). This selection was required to limit the duration of the atlas calculation. Transformation fields of these registrations were applied to individual FA-, NDI-, ODI- and VISO-maps.
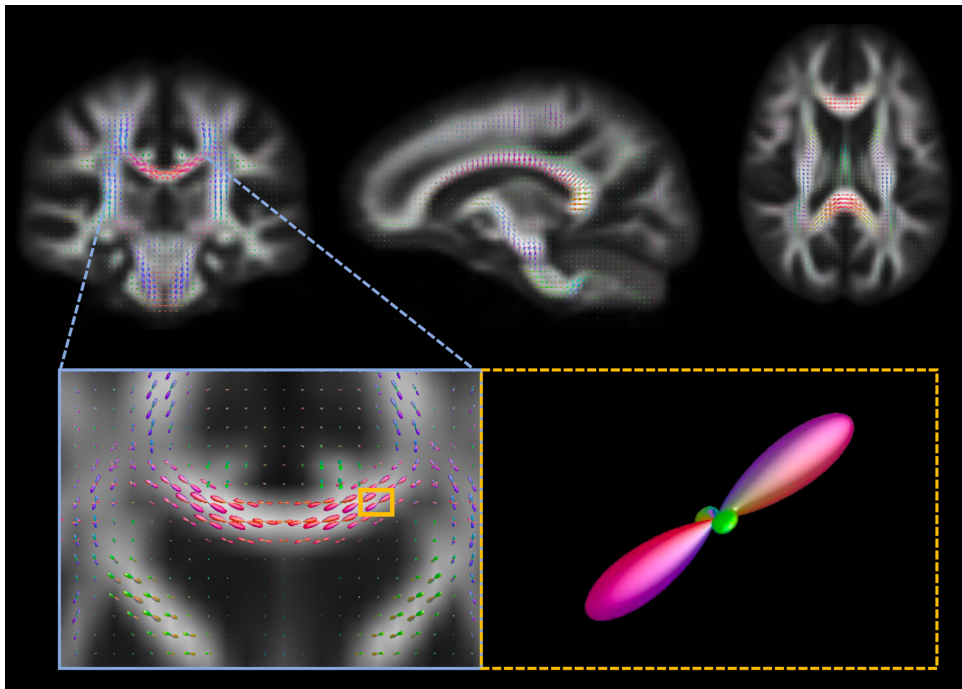
Figure 6.2 Population-based atlas of Fiber Orientation Distributions (FODs)

Note. To be able to make interindividual comparisons, individual Fiber orientation distributions (FODs) were calculated, using robust constrained spherical deconvolution [288]. Individual FOD maps were diffeomorphically registered to the population-based FOD-atlas.

6.2.3.2 Fixel-based analyses

Fixel-based parameters were calculated as described by Raffelt and colleagues, using MRtrix3 [290]. FODs were used to segment the fiber populations (fixels) in each voxel. More specifically, the first fixel-based parameter, apparent fiber density (AFD), was calculated as the integral of each FOD lobe [286]. This measure is correlated with the relative intra-axonal volume of fibers along the main direction of that lobe. The second fixel-based parameter, fiber bundle cross-section (FC), is a macroscopic measure representing changes in the number of voxels that a specific tract bundle occupies. FC was computed based on the non-linear FOD registration step, as the cross-sectional change in the plane perpendicular to the fixel orientation. Smoothing and cluster enhancement was applied in a fixel-based manner, instead of voxel-based [290].

6.2.4 Statistics

White matter microstructure was compared between the solid non-CNS tumor survivor group and healthy controls by using multiple T-tests ($p < .05$). Threshold-free cluster enhancement was applied for voxel-based parameters (i.e. FA-, ODI-, NDI- and VISO- maps)[291] and connectivity-based fixel enhancement for measures of FD and FC in all white matter fixels (i.e. AFD, FC). 12 T-tests tests were performed (i.e. FA, ODI, NDI, VISO, AFD and FC (6) * patients > controls and vice versa (2)). P-values were calculated for each fixel using non-parametric permutation testing (5000 permutations), and family-wise error corrected for multiple comparisons. Finally, stringent bonferroni-correction ($p < .05/12$) was applied to investigate most significant differences in more detail. In Figure 6.3, we depict the expected value changes in case of specific white matter changes.
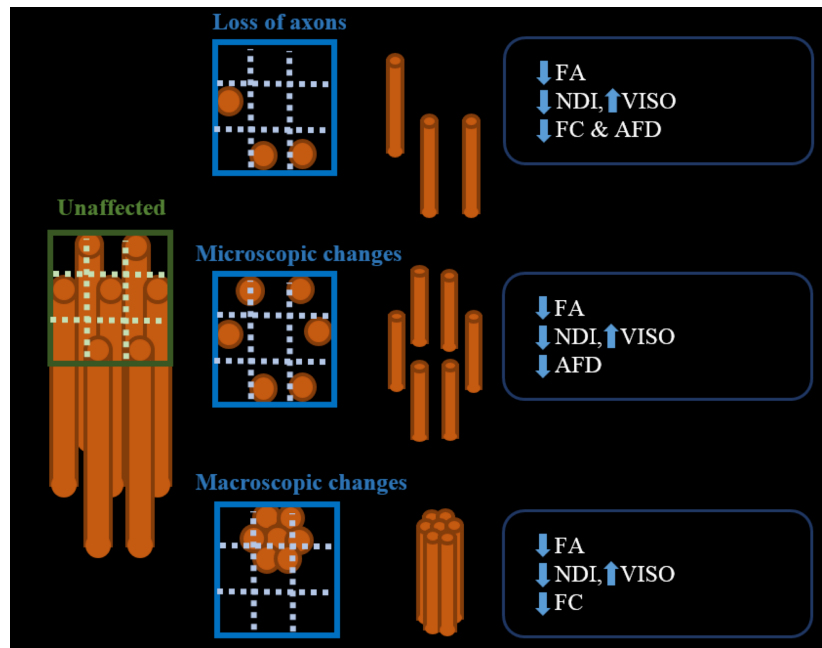
Figure 6.3 Schematic presentation of potential WM changes after therapy and expected DWI parameter changes

Note. In case of chemotherapy-induced WM microstructural damage, parameters derived from diffusion models, are expected to change. In voxelbased analyses, typically lower FA (DTI model), lower NDI and higher VISO (NODDI model) are expected. In fixel-based analysis, FC and AFD are expected to change, according to macroscopic and microscopic changes, respectively. NDI=Neurite Density Index, ODI=Orientation Dispersion Index, VISO=Isotropic Volume fraction, FA=Fractional Anisotropy, FC=Fiber Cross-section, AFD=Apparent Fiber Density.

In addition, to investigate the link between clinical data and diffusion parameters, Pearson correlation analyses were performed. More specifically, the region showing most significant differences in diffusion parameters was selected for further analyses with clinical measures within the patient group. The most significant parameter in this region was correlated with age at diagnosis, time since treatment, age at assessment, task scores on the subscales of the WAIS-IV assessment (Matrix Reasoning (MR), Visual Puzzles (VP), Similarities (S), Vocabulary (V), Information (I), Digit Span (DS), Arithmetic (A), Symbol Search (SS), Coding (C)), and was compared between chemotherapy protocols (SPSS toolbox, v.23).

6.3   Results

6.3.1   Voxelbased analyses

Voxelbased analyses based on the NODDI model, demonstrated significant group differences for the neurite density index (NDI) and isotropic volume fraction (VISO). More specifically, elevated VISO was encountered distributed throughout the central white matter in the patient group, even after Bonferroni-corrections. These regions surrounded a small region of higher NDI in the corticospinal tract. Additionally, FA was lower in similar white matter regions (see Figure 6.4).
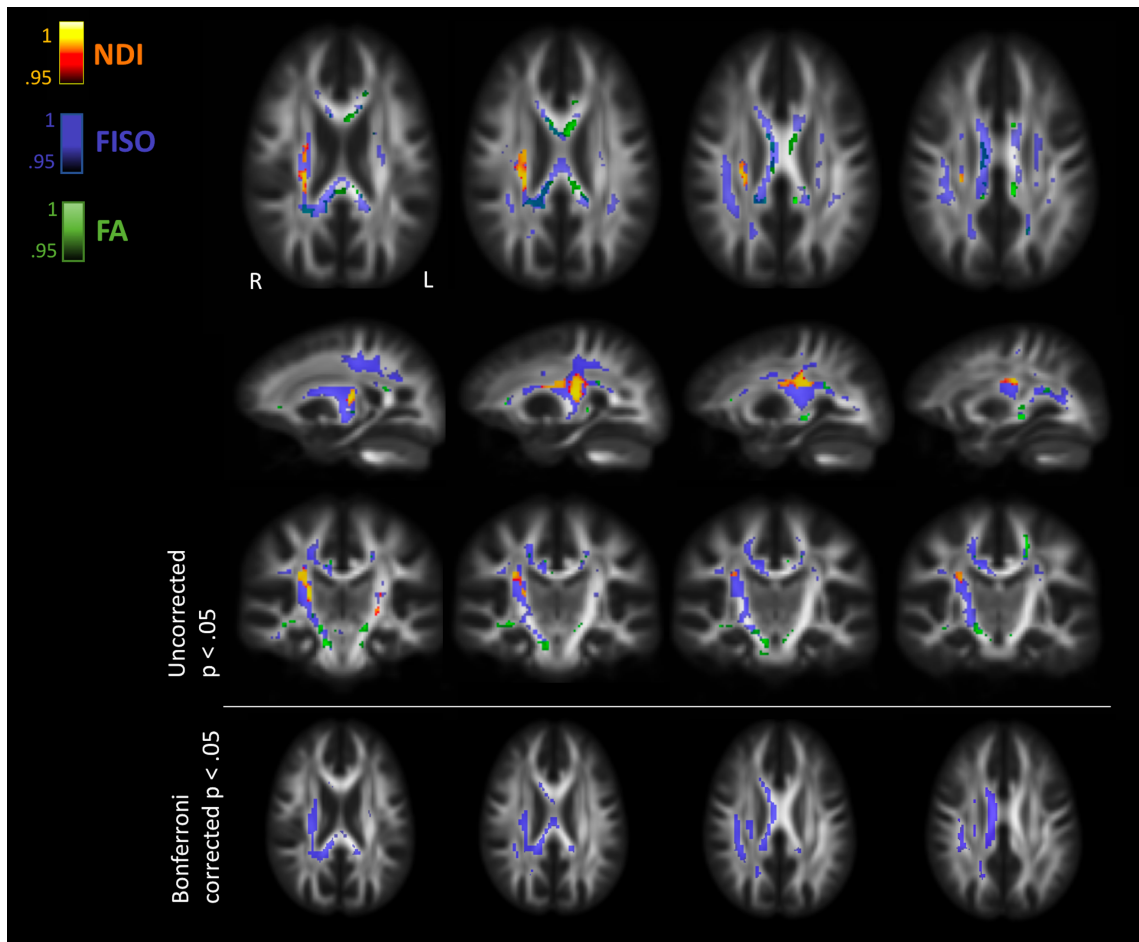
Figure 6.4 Voxelwise group comparisons of DWI metrics

Note. Regions showing significant different white matter paramaters in bone and soft tissue sarcoma survivors when compared to healthy matched controls using voxel-wise permutation testing with threshold-free cluster enhancement (FWE-corrected p<.05). Upper panel shows original results. Lower panel shows results after stringent additional Bonferroni corrections (adapted for 12 tests). Significant higher NDI and VISO in patients is depicted in orange and purple, resp. Lower FA is shown in green.

6.3.2 Fixelbased analyses

Given that the typical single-tensor (i.e. DTI) measures can be affected by the amount of fiber populations in the voxels, fixel-based analysis was performed. Similar to the widespread differences of FA and VISO, fiber cross-section (FC) was also lower throughout the brain in the patient group. As shown in Figure 6.5, this measure overlapped with lower FA, higher VISO and higher NDI values. By contrast, apparent fiber density (AFD) was lower in specific tracts, including the corpus callosum, the cingulum and a small part of the corticopontine tract. In conclusion, the scattered differences of FA and VISO overlapped with both fixel parameters fiber cross-section and fiber density, but differences in AFD seemed limited to single tracts (see Figure 6.6). AFD in the corpus appeared most significantly different, which remained after Bonferroni corrections. Finally, the fixel-based and voxel-based parameters indicated additional significant regions, which were not detected by the other modality (i.e. voxel-based and fixel-based, resp.).
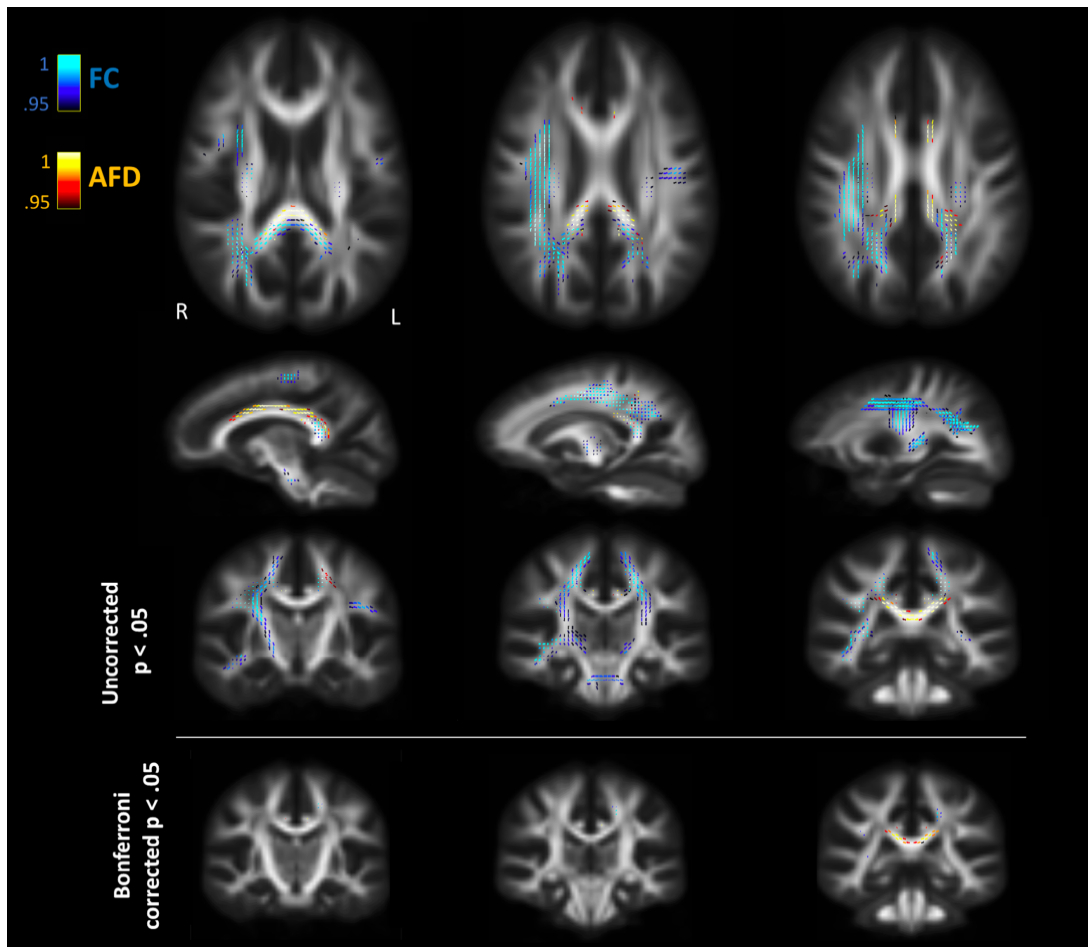
Figure 6.5 Fixel-based group comparisons of AFD and FC

Note. Regions with lower Apparent fiber density (AFD) in the corpus callosum and cingulum of patients compared to controls (p<.05) are depicted in orange. Lower Fiber Cross-Section (FC) is presented in blue. In the lower panel, results of the group comparisons are shown after stringent Bonferroni corrections (adapted for 12 tests)
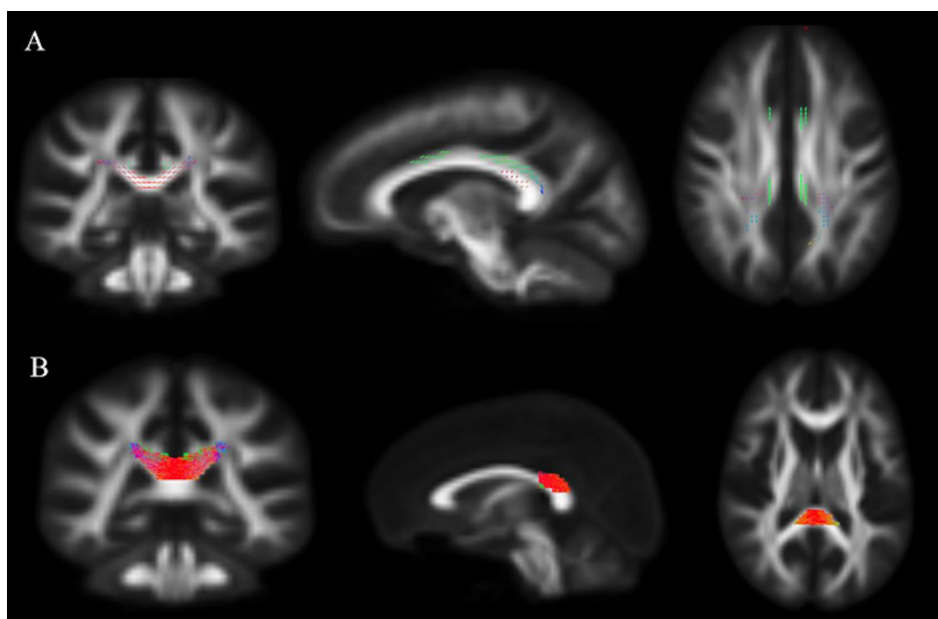
Figure 6.6 Results of fixel-based group comparison of AFD

Note. Panel A: Lower apparent fiber density (AFD) in survivors is depicted (colored by direction: left-right, anterior-posterior and superior-inferior are represented by red, green, blue, resp.) (p<.05). Panel B: A mask was created in the corpus callosum, for the significant region of AFD only, in order to calculate mean AFD values in this region for all subjects. These mean values were correlated with timing variables (time since diagnosis, age at diagnosis and age at assessment)

6.3.3 WM structure, intellectual outcome, therapy dose and timing

The region showing significant differences ($p < .05$) in the most diffusion parameters, was the posterior part of the corpus callosum body (Figure 6.5 and Figure 6.6). AFD was most significant in this region (most significant fixels in this region showed $p < .01$). Hence, this parameter was calculated for each individual within this region. The mean AFD was specifically calculated within the central part of the corpus callosum (coronal view), which showed significantly lower AFD. Probabilistic fiber tracking in this region was performed, based on the FOD template, to use as mask (see Figure 6.6). This specific AFD measure was compared between chemotherapy protocols (using a univariate ANOVA) and used to correlate with timing variables: age at diagnosis, time since treatment and age at assessment, as well as with the subscales of the WAIS-IV. First, AFD was significantly predicted by the treatment protocol ($F(7,1)= 3.080$, $p=.008$). More specifically, AFD appeared lowest for patients treated according to the EURAMOS1 and RMS05 treatment (see Figure 6.7). However, for specific chemotherapy doses within these protocols, no clear associations were encountered (see Figure 6.8).

Second, correlations were calculated within the patient group between mean AFD in the CC, timing variables and IQ subtask scores. Mean AFD did not correlate significantly with age at diagnosis, age at assessment ($r=-.068$, $p=.708$; $r=.030$, $p=.809$, respectively; See Figure 6.9), nor with most subscales of the WAIS (see Table 6.2). In contrast, time since diagnosis and task scores on visual puzzles and similarities were positively correlated with mean AFD ($r=.366$, $p=.036$; $r=.262$, $p=.032$; $r=.288$ $p=.018$, resp.; See Figure 6.7).

Table 6.2 Correlations between AFD corpus callosum and WAIS subscale scores

Main Scale	Subscale	Correlation (p)
Perceptual Reasoning Index	Block Design	.072 (.562)
	Matrix Reasoning	.123 (.321)
	Visual Puzzles	.262* (.032)
Verbal Comprehension Index	Similarities	.288* (.018)
	Vocabulary	.080 (.519)
	Information	.222 (.071)
Working Memory	Digit Span	.112 (.368)
	Arithmetic	.030 (.810)
Processing Speed	Symbol Search	-.074 (.550)
	Coding	.050 (.687)

Note. Each subscale of the WAIS intelligence assessment was correlated with AFD in the corpus callosum. The subscales of Visual Puzzles and Similarities were significantly correlated with AFD. For these subscales, scatterplots are included in Figure 7 in the main manuscripts. * indicates significant correlations (p<.05).
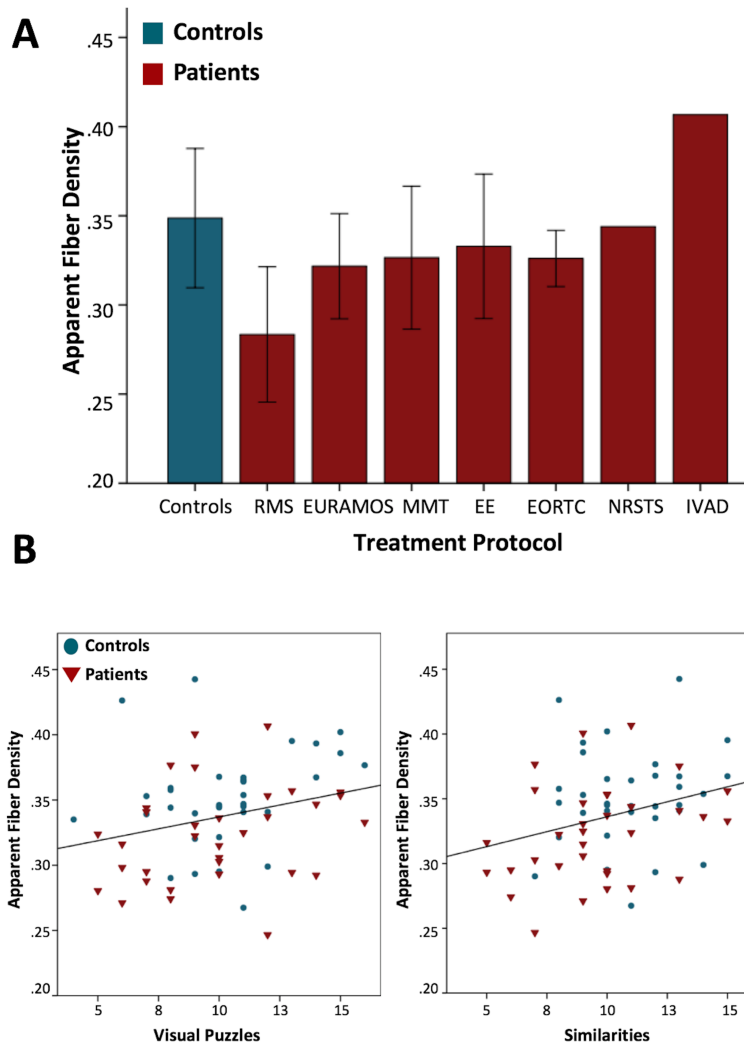
Figure 6.7 Apparent Fiber Density, treatment protocol and cognitive outcomes

Note. Panel A: Bar plots with average AFD values for the control group in blue (n=33). The red bars represent equivalent values for patients, treated according to the following chemotherapy protocols: RMS05 (n=3), EURAMOS1 (n=13), MMT95 (n=5), EuroEwing99 (n=7), EORTC2001 (n=3), NRSTS05 (n=1), IVAD (n=1)

Panel B: Scatter plots indicating the significant linear associations between IQ subscales and AFD, for both controls and patients
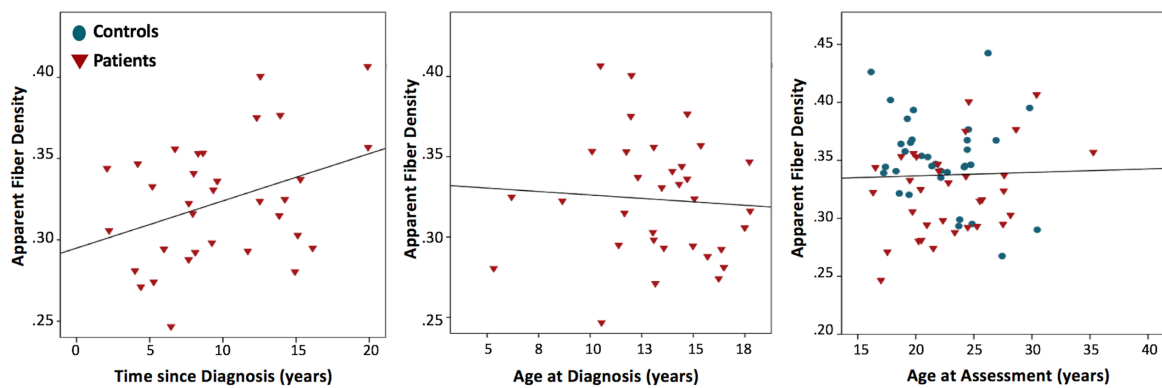
Figure 6.8 Scatter plots depicting the relationship between timing and AFD of the corpus callosum

Note. Timing variables including time since diagnosis, age at diagnosis and age at assessment are depicted against apparent fiber density that was measured in the significant region within the corpus callosum
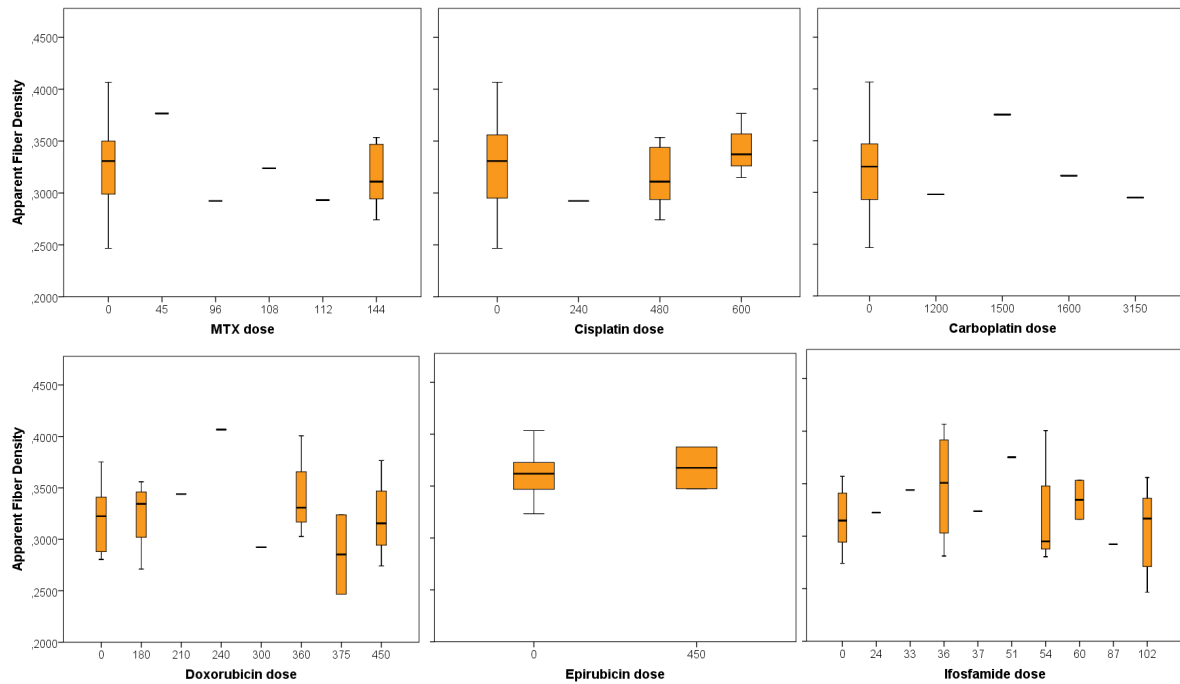
Figure 6.9 Boxplots showing AFD in the corpus callosum against chemotherapy doses
Note. No clear linear relationship was encountered between chemotherapy doses and AFD in the corpus callosum.

6.4 Discussion

This study showed the first findings of potential WM alterations in childhood solid non-CNS tumor survivors (i.e. bone and soft tissue sarcomas), on average 10 years after chemotherapy-treatment, when compared to healthy controls. This was the first childhood cancer survivor study investigating long-term microstructural changes using advanced imaging methods. By expanding the standard voxel-based analyses of fractional anisotropy (i.e. based on the DTI model) to NODDI and fixel-based analysis, distinctions could be made between different origins of white matter changes. This study showed widespread differences between patients and controls, with lower values of fractional anisotropy (DTI), increased isotropic volume fraction (NODDI) and reduced fiber cross-section in patients, while lower apparent fiber density appeared only in specific WM tracts in patients (FBA). However, after stringent Bonferroni corrections, only widespread VISO and AFD in the corpus callosum remained significant. The fiber density measure also appeared to be related to time since diagnosis and verbal and visual subtask scores. Using these advanced methods, we demonstrated microstructural changes even in cases who did not show white matter lesions.

Widespread differences in voxel-based measures
First, voxel-based comparison of FA-maps showed lower FA in multiple brain regions in survivors when compared to matched controls. This finding is in line with previous findings in cancer survivors [235,280,292] describing reduced FA linked with impaired cognitive performance suggestive for decreased WM integrity. In earlier studies, regions showing lower FA values were also heterogenous, suggesting widespread WM microstructural changes. One hypothesis of

chemotherapy-induced neurotoxicity is accelerated aging of fiber populations due to chemotherapy [268]. Healthy aging studies typically report decreases in FA values throughout lifespan after the age of 30 years [293]. The differences in FA did not remain after Bonferroni correction. However, this correction could be a rather stringent method in this case, given that the NODDI analyses showed an overlap between lower FA and higher VISO. This latter measure clearly remained significant after corrections. A recent study of Billiet and colleagues yielded comparable results related to aging throughout lifespan, with increases in VISO and NDI and decrease in FA [253]. Similar to our study, they did not encounter differences in ODI. Since ODI did not differ between our survivor group and controls, we assume that the diffuse pattern of higher VISO and lower FA is not due to increased neurite dispersion but due to the relative amount of fluid in the extra-cellular space.

Such elevated levels of extra-cellular fluid could suggest widespread changes due to white matter atrophy or cerebral edema. Periventricular changes related to fluid retention, could also explain altered NDI of the corticospinal tract. Neurotoxic mechanisms including ischemic hypoxia, encephalopathy, cardiac arrest, inflammatory processes, etc. [294] could result in elevated interstitial fluid. Although the VISO parameter suggests increased interstitial fluid, voxelbased parameters are affected by multiple underlying tissue changes, including axonal loss, axonal density, axon diameter, myelination, gliosis etc., which cannot be easily disentangled [295]. Furthermore, in crossing fiber regions, the degeneration of tracts can even lead to higher anisotropy, which makes the interpretation of voxelbased measures difficult. Tensor-derived metrics, such as FA are also more dependent on periventricular partial volume effects given the remaining csf signal in lower b-values. Given that only the higher shell b=2800 data were used for CSD-derived metrics, these effects should be smaller. Therefore, we assume the fixel-based measure to be less dependent on the overall amount of white matter, and partial volume fractions. By using fixel-based analyses, we could provide essential additional information in this study.

Distinction between global and local differences in fixel-based measures

In accordance with the diffuse differences in VISO and FA, the fixel-based measure of the fiber-cross-section also appeared to be widely decreased. The lower fiber cross-section values support the hypothesis of decreased axon bundle thickness, which could be due to atrophy or interstitial fluid retention. In contrast, with regard to the microstructural measure of apparent fiber density, differences were encountered only in the single tracts of the corpus callosum, the cingulum and the corticopontine tract. Since AFD is different in specific fiber populations, it could be hypothesized that these centrally-located tracts are specifically vulnerable for microstructural changes in pediatric chemotherapy. The vulnerability of central tracts could be explained by their dense axonal packing and their high vascular supply [296]. More specifically, after Bonferroni corrections, AFD appeared only significant in the corpus callosum. As described by Garg and colleagues (2015), the corpus callosum would be especially vulnerable to demyelination and inflammatory processes, which could reduce the intra-axonal compartment volume fraction in these regions. This region was already suggested to be

vulnerable to toxicity earlier due to chemotherapy [156], but also due to alcohol abuse as well [297,298]. Such specific sensitivity of the corpus callosum could explain the observed decrease in AFD in this region. Although metrics derived from higher shell data (b=2800) are less affected by CSF volume effects, one should note that highly variable partial volumes in small structures might affect significance levels. By contrast, larger structures such as the corpus callosum would be influenced by such volume effects to a smaller extent [299].

Microstructural differences, intelligence scores, chemotherapy and timing

Finally, the specific measure of fiber density in the corpus callosum was associated with chemotherapy protocol, time since diagnosis and intelligence subtask scores. Specifically, survivors treated according to the EURAMOS1 and RMS05 protocol, showed lower apparent fiber densitiy in the corpus callosum. Similarly, Stouten-Kemperman and colleagues [236] showed that patients exposed to higher doses of chemotherapy are probably more vulnerable to neurotoxicity. However, the protocols included in our study prescribe different chemotherapy agents. The first protocol mainly includes methotrexate, cisplatin and doxorubicin [249,300], whereas the second protocol mainly prescribes ifosfamide, vincristine and actinomycin [301].

As our survivor group was limited to 33 subjects, this study was not able to investigate the effects of specific agents included in these protocols. Multiple chemotherapy protocols were included in this study, which resulted in heterogeneity in the patient group. Still, all treatments included at least one high-dose chemotherapy agent (methotrexate and/or ifosfamide). Furthermore, as higher chemotherapy doses are administered in case of larger, more aggressive tumors, or metastases, these factors could also indirectly be related to potential neurotoxicity. Nevertheless, additional figures did not show clear trends in AFD related to cumulative chemotherapy doses (see Figure 6.9). This suggests that neurotoxicity probably arises in case of certain combinations of agents, and depending on an individual's vulnerability, rather than due to only the dose of one specific agent. In addition, the significant group difference in AFD was measured between survivors and control participants, at group level. During recruitment of patients, 52% of the existing database of patients (inclusion criterium: treated according to the predefined chemotherapy protocols, >2 years out of treatment) participated. Given that times since diagnosis were similar between the participating and non-participating patients, we assume that this dataset was representative for all patients. Nonetheless, we note that the ratio of osteosarcoma patients was higher in participating than in non-participating patients. Given that these patients often receive high-dose chemotherapy, we cannot exclude this higher ratio to have affected our results.

Furthermore, although this study showed group-based effects for bone and soft tissue sarcoma patients, larger samples are necessary to investigate vulnerability of specific subgroups and differentiate between specific chemotherapy agents. At this stage, it remains uncertain which individual factors play a role in therapy-induced toxicity affecting the WM. Besides neurotoxicity, also differences in SES could have an important impact on brain development during childhood. In this regard, one should note that SES scores were significantly lower in patients. This might highly affect the group comparison results. Although

it is complicated to investigate the independent effect of this measure on imaging values or any cognitive value, since these are highly correlated, additional analyses showed that significant group differences in diffusion metrics still remain after statistical correction for SES. With regard to cognitive measures, visual puzzles and similarities subtask scores were positively correlated with corpus callosal fiber density. Both these subtasks require matching skills and logical reasoning. Puzzles require visuospatial matching and manual coordination. Previous studies have clearly indicated the important role of the corpus callosum in bimanual coordination[302] . By contrast, the ability to find similarities between words depends more on conceptual matching (cognitive semantics). As our measure of AFD was derived from the posterior part of the corpus callosum, we mainly investigated the link between parietal and occipital lobe connectivity and intellectual outcome. This region could play an important role in conceptual and visual matching skills. However, we cannot exclude that the global macrostructural changes (as measured with VISO, FA and fiber cross-section) can affect multiple other cognitive domains as well.

Finally, we encountered a significant correlation between time since diagnosis and AFD of the corpus callosum, suggestive of a recovery pattern after treatment. In this respect, Armstrong and colleagues recently summarized the processes of axon regeneration and remyelination in case of brain injury [303]. They demonstrate the natural tendency of the WM to remyelate after inflammation or vascular damage [304]. Since chemotherapy could induce such neurotoxic processes [19,305], leading to microstructural changes, recovery processes could arise in childhood cancer patients as well. Furthermore, recently a similar potential recovery was detected in FA values 3 years after treatment in breast cancer patients [253]. This would explain a positive trend in apparent fiber density throughout time. Although a positive trend with age at diagnosis was expected as well, this correlation was not significant. Still, other pediatric oncology (i.e. brain tumor and leukemia) studies also evidenced higher neurotoxic vulnerability of the younger patients at diagnosis [116,145,216,228]. Patients in our study were on average 13 years old at diagnosis. Although the age at diagnosis ranged between 5 and 18 years, the majority of the patients were older than 10 years at diagnosis (91%). It can be assumed that underrepresentation of this younger patient group would explain the lack of correlation between age at diagnosis and AFD. If future studies would show similar lack of correlation between age at diagnosis and diffusion parameters in younger patients at diagnosis as well, recovery processes could provide a possible explanation.

<u>Future directions</u>

By using multiple analysis methods, we aimed to distinguish between several potential tissue changes. First, based on voxel-based analyses, we showed elevated isotropic fractions and lower fractional anisotropy, presumably due to interstitial edema. Second, based on the fixel-based analyses, we showed diffuse macroscopic WM morphological changes (as measured by FC), while microscopic changes (as measured AFD) were limited to densely packed WM tracts. In summary, these findings suggest that densely packed WM tracts are mainly vulnerable for microscopic changes, while macrocopic changes are diffuse. Both types of WM changes could

lead to lowered ability to transfer information efficiently. In this respect, lower FA values were related to lower processing speed [280] and attentional functioning [235,253] in breast cancer patients. To investigate which type of WM change leads to specific cognitive difficulties, and processing speed in particular, future studies will be necessary including behavioral measurements. Furthermore, this is the first pilot study showing potential long-term white matter microstructural changes in children treated with chemotherapy, using advanced diffusion imaging. Hence, this patient group covered a variety of subgroups of patients (i.e. bone as well as soft tissue sarcoma), treated according to different chemotherapy protocols. In this study, we did not report a relationship between chemotherapy dose and diffusion metrics. Since exploratory analyses did not show differences in AFD of the corpus callosum according to the cumulative doses of individual chemotherapy agents (i.e. methotrexate, cisplatin, carboplatin, doxorubicin, epirubicin or ifosfamide), statistical analyses were not included in this study to investigate this in detail. Additional diffusion-weighted MRI studies will be necessary to draw firm conclusions about potential predictors for neurotoxic vulnerability. Although this prospective study suggests potential WM changes due to treatment, the underlying physiological processes cannot be identified using DWI alone. Not only are some chemotherapeutic agents more toxic than other agents, also individual risk factors in patients should be further investigated, such as therapy metabolism, cardiotoxicity, and genetic predisposition. Finally, we suggest to implement longitudinal studies to investigate potential recovery processes in more detail, since this study only included a cross-subject correlation between time since diagnosis and AFD.

6.5 Conclusion

In summary, our study provides the first evidence of changes in the WM structure of childhood survivors of bone and soft tissue sarcoma. We showed widespread differences in diffusion parameters, suggesting macroscopic changes. Furthermore, microscopic differences in centrally-located tracts could suggest specific vulnerability to vascular or inflammatory mechanisms after disease or treatment, associated with chemotherapy protocol, visual and verbal matching task scores, and time since diagnosis. Advanced diffusion models, such as fixel-based analyses bring additional insights in the mechanisms of disease- or therapy-induced neurotoxicity and enabled us to differentiate between WM toxicity at the macroscopic vs. microscopic level. Still, histological animal and post-mortem studies are necessary to complement these findings.

7   Grey matter structure and function in survivors of childhood sarcoma treated with high dose intravenous chemotherapy

Abstract

Research with regard to grey matter development in childhood non-CNS cancer patients is currently limited. However, as behavioral studies showed cognitive as well as emotional complaints in childhood cancer patients and survivors, structural as well as functional neuronal changes could be hypothesized. In order to investigate long-term cortical developmental in survivors of childhood non-CNS tumors, we analyzed high-resolution structural (T1-weighted) MRI and resting state functional MRI (Rsfmri) scans, to derive structural and functional cortical information in survivors of sarcoma, respectively.

Images of these patients, who had received high doses of intravenous chemotherapy during childhood (n=33), were compared to matched healthy control participants (n=34).

Cortical density was investigated using a voxel-based morphometry analysis (VBM), while cortical thickness comparisons were based on a vertex-wise surface-based morphometry (SBM) approach. Significant regions showing lower density or thickness were further investigated as seeds of interest for Rsfmri-derived functional coherence investigations. Finally, we explored whether cortical thickness was associated with cumulative doses of chemotherapy (i.e. methotrexate and ifosfamide), and age at diagnosis; and the link between functional regional strength, neurocognitive assessments and subjective daily life complaints. We conclude lower grey matter density and cortical thickness in frontal brain areas, of which the orbitofrontal area appeared associated with age at diagnosis. Furthermore, cortical thickness of the parahippocampal area appeared lower in survivors, but only if the group comparison was not controlled for depression. This region specifically also showed lower functional coherence in survivors, which seemed associated with lower processing speed.

This neuroimaging study integrating structural and functional information of the cortex in survivors of childhood solid non-CNS tumors, suggests cortical thinning as well as decreased density of frontal and parahippocampal areas. These brain areas could be important for attentional functioning and emotion/reward, which could provide an explanation of long-term complaints in daily life. Frontal brain areas might specifically be vulnerable during adolescence.

Keywords: Grey matter, cortical structure and coherence, non-CNS directed chemotherapy

7.1 Introduction

Evidence for treatment-related changes in emotional and cognitive functioning in daily life of cancer patients is dramatically increasing. However, underlying neural mechanisms remain largely inconsistent and hypothetical. It is hypothesized that neural signaling is altered due to cancer treatment, which could explain cognitive and behavioral changes. So far, neural signaling was mainly investigated using active [24,163] or resting state functional MRI [18,170,306] in adult non-CNS cancer patients. Such functional neural changes can be attributed to psychosocial risk factors such as adverse early life events [307,308], fatigue [306], as well as to anatomical cortical damage (e.g. atrophy) [309]. Given that childhood cancer patients suffer from both stress and chemotherapeutic treatments, it is extremely important to investigate brain developmental patterns in these patients. However, such research is currently lacking.

So far, grey matter cortical thickness or density in childhood cancer patients has only been investigated in case of cranial radiotherapy [310] and intrathecal chemotherapy [167,271,311–313], in brain tumors and leukemia respectively. Nonetheless, increasing evidence exists for similar anatomical changes in adult cancer patients treated with intravenous chemotherapy only (i.e. no CNS prophylaxis) [292]. Cortical decreases in grey matter volumes and density were consistently reported in adult breast cancer [155,314–319], ovarian cancer [320], testicular cancer [321], lung cancer [322] patients. Such changes appeared distributed across the brain (e.g. frontal, parahippocampal, cingulate gyrus, and precuneus). However, a surface-based approach was not implemented yet to investigate cortical thickness. What is more, the functional impact of such anatomical changes was not always reported.

Unfortunately, similar investigations of grey matter pathological mechanisms during childhood brain development are non-existing to date, and as such, they are highly recommended. So far, a few studies reported altered neurocognitive functioning in childhood non-CNS solid tumor patients [9] or survivors [154] (who only received intravenous chemotherapy). These existing studies demonstrated lower intelligence scores in preschool patients [323], as well as long-term complaints of reduced memory, processing speed [154], task efficiency [147] and difficulties at school in around 1/3 non-CNS tumor patients [9]. Using an EEG paradigm, also decreased auditory processing speed was evidenced [324]. Besides such cognitive changes, other mental complaints of discomfort including post-traumatic symptoms [325,326], fatigue [327], anxiety and depression [328], highly affect long-term mental health in childhood cancer patients [329].

In order to investigate long-term cortical development changes, we analyzed structural and functional cortical information in adult survivors of childhood non-CNS tumors (osteosarcoma and soft tissue sarcomas), who had received high doses of intravenous chemotherapy during childhood. First, anatomical cortical changes were investigated using both a voxel-based morphometry analysis (VBM) as well as a vertex-wise surface-based morphometry (SBM) approach. Second, significant regions of lower grey matter density and cortical thickness were used as seeds of interest for resting state functional coherence investigations. Finally, we investigated whether cortical thickness was associated with cumulative doses of chemotherapy, and age at diagnosis; and the link between functional regional strength, neurocognitive assessments and subjective daily life complaints.

7.2 Methods

7.2.1 Participants

This study included the same cohort as Chapters 5 and 6. Survivors of childhood bone and soft tissue sarcomas (n=33), who were treated with intravenous chemotherapy only (protocols EURAMOS1, RMS2005, NRSTS2005, Euro-Ewing99, MMT95, EORTC2001, IVAD) were recruited in this study. Their treatment consisted of multimodal chemotherapy including high-dose methotrexate either combined with ifosfamide or not. Patients were >2 years out of treatment. Time since diagnosis ranged between 2.08-19.92 years (mean=9.92, SD=4.72). Thirty-four healthy control participants were age- and gender-matched. All participants were aged between 16.14-35.28 years (mean=22.51, SD=3.97) at the moment of acquisition. The study was approved by the Ethical Committee of the University Hospitals Leuven.

7.2.2 Data acquisition

First, high-resolution whole brain T1-weighted MRI scans were acquired for anatomical cortical analyses (i.e. voxel-based (VBM) and surface-based morphometry (SBM)), and for anatomical reference. Acquisition parameters were as follows: MPRAGE, resolution=.98x.98x1.2mm, TE=4.6 ms, TR=9636 ms, FOV=192x250x250mm, 160 slices with slice thickness=1.2mm. Second, resting state functional MRI scans were obtained using a T2*-weighted echo-planar imaging (EPI) sequence. Parameters were: resolution=3.6x3.6x4mm, TE=33 ms, TR=1700 ms, FOV=230x230x120mm; 30 slices with slice thickness=4mm. Both scan sequences were obtained within one scanning session on a 3T Philips Achieva MRI scanner with a 32-channel phased-array head coil.

Besides MRI imaging, questionnaires were obtained assessing emotional values (anxiety (STAI) and depression (BDI)), cognitive failure (CFQ) and quality of life (PedSql). An extensive neurocognitive test battery covered the domains of intelligence (WAIS), verbal (AVLT) and visual memory (RVDLT), and computerized attention tasks (ANT). Based on previously reported behavioral group comparisons (see Chapter 5), only processing speed, working memory (measured with the WAIS-IV) and attentional reaction times (ANT computerized tasks) were extracted and analyzed in the current study.

7.2.3 Data preprocessing

First, T1-weighted MRI images were skull-stripped using FSL brain extraction [330], and bias field corrected using ANTs [285]. These images were further processed in CAT12 (SPM) toolbox for VBM and SBM investigations using standard settings [331]. In this process, images were segmented using a 6-tissue probability map (including the grey and white matter, and CSF), smoothed with a kernel of 12mm, and non-linearly registered to MNI template space for group comparisons. The grey matter maps are further processed for grey matter density (based on VBM) and cortical thickness estimations (based on SBM).

Second, resting state fMRI images were preprocessed using FSL (realignment, brain extraction, spatial smoothing of 2mm, intensity normalization). Signal denoising and nuisance regression of the CSF and white matter were performed, using FSL and its add-on ICA-AROMA

toolbox. Finally, a high pass filter of .01Hz was applied. Using Freesurfer, subject-specific parcellations were estimated based on the T1-weighted MRI image, applying the Desikan-Killiany atlas. This atlas was both used to localize significant VBM and SBM results (CAT), and for subject-specific parcellations which were rigidly coregistered in native space (ANTs) to the Rsfmri data, in order to construct a functional connectome. These subject-specific connectomes consisted of the Desikan-Killiany atlas nodes (see Figure 7.1) and positive partial correlations between their average BOLD signals as their edge weights (in-house matlab scripts).
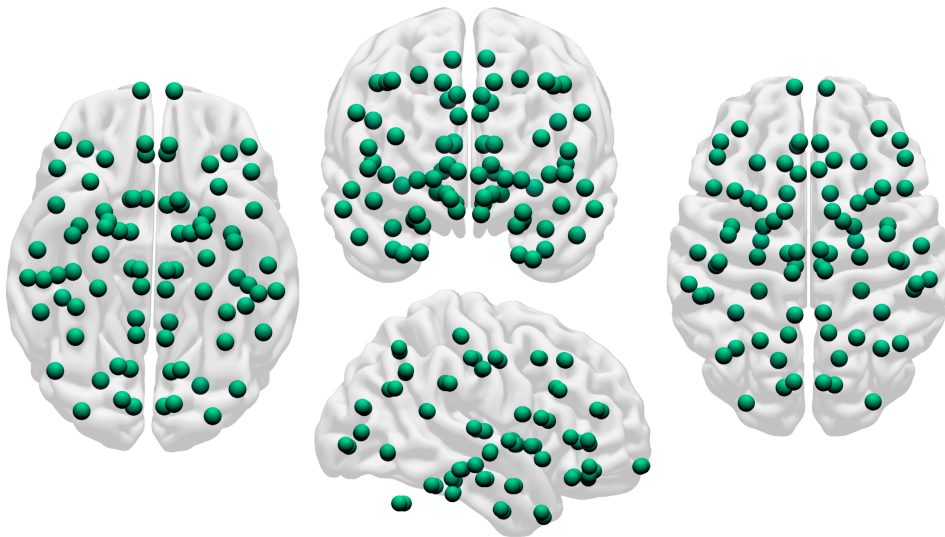
Figure 7.1 Included nodes for connectome construction based on the Desikan-Killiany atlas

Note. The Desikan-Killiany atlas consisted of 68 nodes, which were complemented with 9 additional nodes from the whole-brain freesurfer parcellation in each hemisphere, resulting in 84 nodes in total.

7.3 Statistical analyses

First, outlier T1-weighted and Rsfmri data were excluded from analyses (based on the Mahalanobis distance (n=1), and movement parameters (>2mm framewise displacement, n=3), respectively. Second, whole-brain anatomical group comparisons (patients vs. controls) were performed for grey matter density (GMD) at voxel-level (VBM) using a GLM model (patients<controls and vice versa; with SES and total intracranial volume as covariates). In addition, cortical thickness (SBM) was compared between the two groups (patients<controls and vice versa; with SES and age at assessment as covariates).

Third, these models were complemented with the predictor of depression (BDI) to address the association between anatomy and depression in addition to neurocognitive outcome. Group comparisons were assumed significant at cluster-level with FWE-corrected p-values <.05, combined with a threshold of p <.001 uncorrected at voxel-level.

Fourth, the Desikan-Killiany atlas-based connectivity graph (see Figure 7.1) was used to calculate functional graph theoretical efficiency values at whole-brain level (i.e. global efficiency), local level (i.e. local efficiency) and nodal level of the selected regions only (i.e. nodal strength (nodal degree only in case of significantly different nodal strength) of significant VBM

and SBM regions) (BCT toolbox). These values were compared between patients vs. controls for a range of network density thresholds (0-50%).

In order to demonstrate potential local functional impact, possibly driving the nodal strength values, group average partial correlations (of the SBM-selected regions showing significant differences in nodal strength) were depicted. Finally, cortical thickness values of significant SBM regions were correlated with cumulative chemotherapy doses of methotrexate and ifosfamide, and age at diagnosis. Functional nodal strength values of significant nodes were correlated with the abovementioned functional outcomes (i.e. BDI, STAI, CFQ, working memory, processing speed). All correlations were calculated within the survivor group, and assumed significant at p<.05.

7.4 Results

7.4.1 T1-weighted MRI: VBM and SBM group comparisons

Based on the voxel-based analysis, lower grey matter density was found in the frontal lobe (1 cluster) and in the cerebellum (1 cluster) (see Figure 7.2, panel A). After correction for depression, these regions remained significant and a third region appeared in the cerebellum (see Figure 7.2, panel B). No significant differences were found in the opposite directions (i.e. patients > controls).
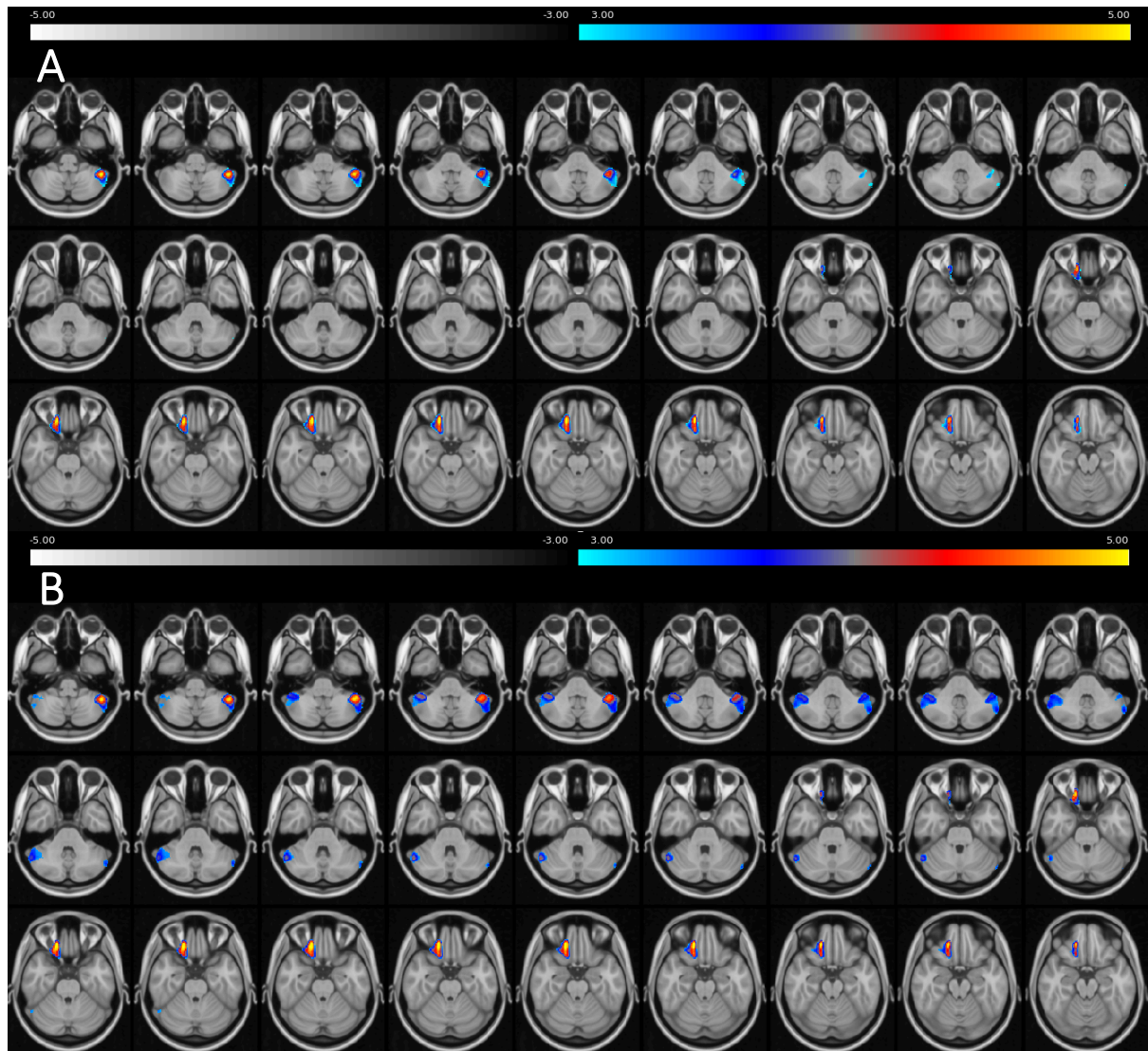
Figure 7.2 ANOVA group comparison results of GMD (patients < controls)

Note. Panel A depicts the significant group difference patients < controls, corrected for SES and age at assessment; panel B shows the results after additional correction for BDI.

Comparably, based on SBM, cortical thickness appeared lower in patients than in controls in the right orbitofrontal region (2 clusters), left medial frontal region and left parahippocampal region (see Figure 7.3, panel A). After additional correction for depression, all frontal regions remained significant. By contrast, the parahippocampal region was no longer significant, while a second cluster in the left medial frontal appeared significant after adding this predictor (see Figure 7.3, panel B).

Again, no regions were detected with higher cortical thickness in patients than controls.
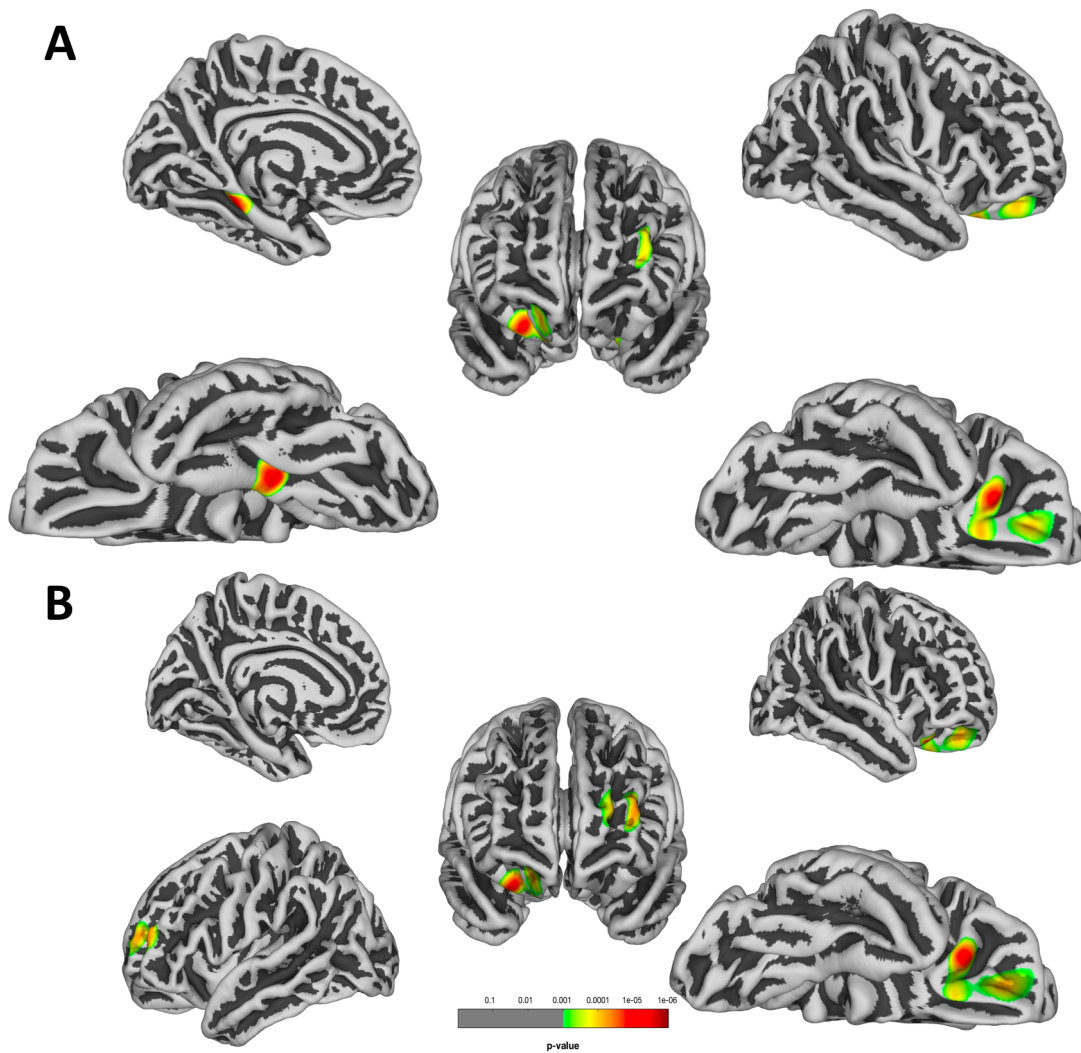
Figure 7.3 ANOVA group comparison results of cortical thickness

Note. Panel A depicts the significant group difference patients < controls, corrected for SES and age at assessment; panel B shows the results after additional correction for BDI.

7.4.2 Rsfmri: nodal strength

With regard to the functional graph theoretical measures, global and local efficiency measures across the entire brain were not significantly different between patients versus controls.

By contrast, functional strength at nodal level (calculated for significant VBM and SBM regions) appeared only significantly different in the left parahippocampal volume. This region showed decreased nodal strength in patients compared to controls, which remained the case for any network threshold (see Figure 7.4).

By contrast, the cerebellum, left and right rostral middle frontal region and left lateral orbitofrontal region did not show any significant differences in functional nodal strength between patients and controls. Furthermore, nodal degree (i.e. the number of functional connections) was only significantly different in the parahippocampal region between patients and controls, if the network was thresholded extracting the strongest connections only (<10% network density).

In order to visually explore whether the abovementioned group differences in parahippocampal nodal strength could be driven by specific connections, group average partial correlations between this region and other brain regions (at threshold correlations >.05) were depicted in Figure 7.4. As could be inferred from this figure, most connections seem rather similar between patients and controls. However, some specific parahippocampal associations appeared particularly different, which might affect the overall nodal strength measures and their group differences. More specifically, correlations between the left parahippocampal region and right orbitofrontal region, right pericalcarine region, right superior temporal area, and right supramarginal region remained at this threshold in the control participant group, but not in the patient subgroup; which could partly drive the higher overall nodal strength of the parahippocampal region in controls. Still, this remains a merely visual interpretation.

7.4.3 Risk and outcome of cortical thickness and functional nodal strength

Finally, correlations between cortical thickness, cumulative methotrexate and ifosfamide doses and age at diagnosis were calculated for the frontal areas (given that cortical thickness of these regions remained significantly lower after correction for depression) (see Table 7.1).
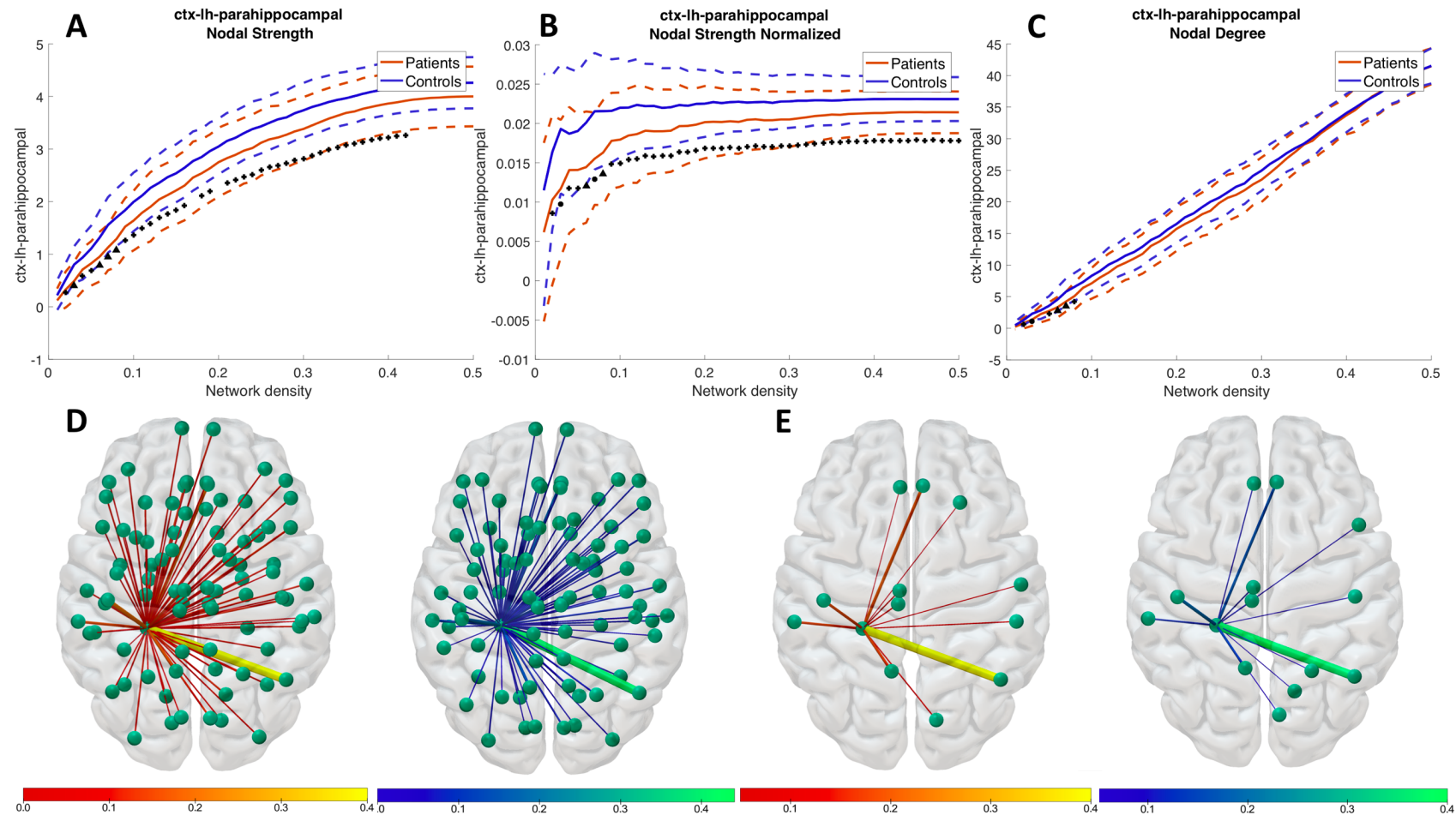
Figure 7.4 ANOVA group analysis results of functional strength values in the left parahippocampal region

Note. Panel A depicts the results of the ANOVA group comparison of nodal strength values between patients and controls, for a range of network densities between 1-50% thresholds. This network density range represents the proportionally thresholded network with an increase of .01% (e.g. network density .1 means the subject-specific networks were thresholded at 10% strongest connections). Panel B depicts the results of the ANOVA group comparison of normalized nodal strength values. These values represent the nodal strength of the parahippocampal region, proportional to the entire subject-specific network. Panel C depicts the results of the ANOVA group comparison of nodal degree values (i.e. the total number of existing connections). Panel D represents the group average partial correlations of the parahippocampal region, patients are depicted in red, control participants in blue. Panel E represents the thresholded (i.e. correlations > .05) group average partial correlations of the parahippocampal region. This figure shows correlations that remain in both subgroups, and some that remain in only one of them. More specifically, correlations between the left parahippocampal region and right orbitofrontal region, right pericalcarine region, right superior temporal area, and right supramarginal region remained at this threshold in the control participant group, but not in the patient subgroup; whereas correlations that remain in patients but not in controls include the left parahippocampal region with right cuneus, lingual region, pars opercularis, superior parietal and transverse temporal region.

Table 7.1 Bivariate correlations between cortical thickness of SBM-selected regions, chemotherapy dose and age at diagnosis.

Region of interest	Correlation (p-value)		
	cumulative MTX dose	cumulative IFO dose	age at diagnosis
Left rostral middle frontal	.028 (.881)	.058 (.751)	-.079 (.666)
Right rostral middle frontal	.160 (.382)	-.008 (.967)	.065 (.724)
Right lateral orbitofrontal	.333 (.063)	-.121 (.510)	.478 (.006)**

Note. * indicates p<.05; ** indicates p<.01. MTX=methotrexate, IFO=ifosfamide
Regions of interest were selected based on the SBM results (significant regions with different cortical thickness at group level, corrected for BDI, SES and age).

As could be inferred from Table 7.1, cortical thickness of the right lateral orbitofrontal region positively correlated with age at diagnosis. In other words, older age at diagnosis was associated with higher cortical thickness of the right lateral orbitofrontal region. No chemotherapy dose-dependency of the cortical thickness was detected.

Furthermore, the abovementioned behavioral (subjective and objective) outcomes and parahippocampal nodal strength were correlated. As shown in Table 7.2, the nodal strength of the parahippocampal region correlated significantly with processing speed of the intelligence test assessment.

Table 7.2 Bivariate correlations between functional nodal strength of the parahippocampal region and behavioral outcome measures

Scale	Correlation (p-value) with parahippocampal nodal strength
PedSql	-.011 (.957)
STAI	.163 (.399)
BDI	.262 (.170)
CFQ	.059 (.761)
WAIS working memory	-.080 (.675)
WAIS processing speed	.438 (.015)*
ANT reaction time baseline	-.002 (.991)
ANT reaction time divided attention	-.334 (.076)
ANT set shifting: inhibition effect	-.326 (.085)
ANT stability reaction time sustained attention	-.055 (.782)

Note. * indicates p<.05

7.5 Discussion

This is the first neuroimaging study integrating structural and functional neuroimaging of the grey matter in survivors of childhood sarcoma. We demonstrated lower grey matter density and cortical thickness in frontal areas, and lower grey matter density in the cerebellum. We did not observe dose-dependency of cortical thickness in these frontal areas, but cortical thickness of the right orbitofrontal area was correlated with age at diagnosis. The additional predictor of depression appeared to play a role in group differences in cortical thickness of the parahippocampal area. Besides these structural grey matter differences, only the latter region showed significantly lower nodal strength in patients, which correlated with lower processing speed in patients.

Structural cortical changes and risk factors

The medial- and orbitofrontal brain regions with lower GM density (based on the VBM analysis), also showed lower cortical thickness (based on the SBM analysis). These findings could suggest cortical thinning of the cortical layer, as well as decreased density at voxel-level in childhood cancer survivors. Previously, Hakamata and colleagues (2007) also showed lower GM volumes in the orbitofrontal regions, but specifically in adult cancer survivors suffering from a post-traumatic stress disorder [309]. In our study, even after correction for depression, group differences between patients and controls still remained significant in these regions.

By contrast, the parahippocampal area only showed lower cortical thickness, if not corrected for depression. In other words, higher depression rates in patients might partly explain lower cortical parahippocampal cortical thickness in this group. Previously, we detected higher depression levels in the patient cohort compared to controls (see Chapter 5). Therefore, we now aimed to investigate the group comparison for grey matter anatomy, both corrected and uncorrected for depression. In cancer patients specifically, one study by Yoshikawa and colleagues (2007) demonstrated smaller amygdala volumes in breast cancer patients who had experienced a depressive episode, compared to control breast cancer patients [308]. In this regard, earlier studies also demonstrated lower cortical thickness of the orbitofrontal cortex and temporal lobe areas in non-cancer patients who suffer from major depressive disorders [332], depending on the age of depression onset [333]. Specifically, patients with a depression onset at younger age, showed lower hippocampal volumes. These researchers previously hypothesized age-dependent stress-related remodeling. In childhood cancer patients in specific, traumatic experiences during cancer treatment could yield similar developmental changes, resulting in long-term cortical changes up to adulthood in this specific region. Recently, such neurobiological *double hit hypothesis* (i.e. effect of treatment combined with stress) was posed by Marusak and colleagues (2017), suggesting specific vulnerability of the hippocampus [334]. Our current findings seem to be in line with this proposed hypothesis.

Unfortunately, we did not have any stress-related subjective, nor objective, measures available during treatments. In this regard, higher stress levels (i.e. so-called allostatic load) during cancer treatments and inefficient coping strategies, have been hypothesized to affect the HPA-axis, and as such, indirectly affect emotional and cognitive side effects [335].

The important impact of hormonal processes on the cerebral cortex was not only evidenced by post-traumatic and depression studies in non-cancer patients, but also in cancer studies including hormonal treatments [336]. More specifically, glucocorticoid responses to a physiological stressor [337], as well as memory recall [337] in breast cancer patients appeared to depend on specific hormonal treatments (e.g. gonadotropin-releasing hormone agonist, anti-estrogen). Similarly, androgen deprivation for prostate cancer in men was associated with lower frontal grey matter volumes [338]. Hence, implementation of stress-related measures (both subjective and biochemical markers) in future neuroimaging research, would yield additional insights into potential interactions between chemotherapy doses and stress-related hormonal responses at neurobiological level. Stress responses can additionally be affected by socioeconomic environment [339], which can have an important impact on cortical development. For instance, parental education was previously associated with increased cortical thickness of frontal areas [340]. This can partly be explained by increased parental stimulation [341]. In order to investigate cancer treatment-related effects, SES and BDI were included as covariates. Given that the encountered group differences in frontal areas still remained after correction, we assume that cancer (and its treatments) could decrease grey matter thickness and density.

With regard to age-dependency, we specifically showed frontal cortical thickness to negatively correlate with age at diagnosis. Frontal brain areas are known to develop later throughout neurodevelopment. More specifically, across the brain, the amount of grey matter, cortical thickness and cortical complexity in general decrease throughout development [342,343], while the latter mainly increases in frontal areas [344]. This is thought to be an adaptive process with increased selective pruning and decreased synaptogenesis, leading to improved executive functioning throughout childhood [345]. Given that the majority of our patients were treated during adolescence (median age of 13.32 years old), this finding could demonstrate specific vulnerability of frontal regions during treatment, possibly leading to inefficient pruning and decreased cortical thickness.

In contrast to the surface-based approach in our study, earlier studies only investigated grey matter volumes and grey matter densities using a voxel-based approach in adult oncology patients (using a binary and weighted GM map, resp.). Evidence for decreased grey matter volumes and density were consistently reported in adult breast cancer [155,314–319], ovarian cancer [320], testicular cancer [321], lung cancer [322] patients. However, cortical thickness (based on SBM) was not yet explored, neither were these approaches implemented for childhood cancer survivors before. Given that the SBM analysis in our study also yielded significant lower values in frontal areas, cortical thinning could be hypothesized in addition to decreased GM density during childhood cancer, with specific vulnerability during adolescence.

Functional cortical changes and functional outcomes
Besides the lower cortical thickness of the parahippocampal region in patients, this region also showed lower functional nodal strength. Furthermore, this appeared to correlate with processing speed values in the survivor subgroup. Given that the parahippocampal cortical

thickness appeared lower in patients, only as long as it was not controlled for depression, this region could potentially play a role in depressive scores as well.

The results of our surface-based analyses as well as nodal strength group comparisons yielding the left parahippocampal area to appear as a significant region, might suggest a structural as well as functional sensitivity of this region. We note that only 5 regions were extracted for the functional nodal comparisons, based on the voxel- and surface-based results, to limit the number of statistical tests. However, functional strength could be reduced rather globally, and the difference in parahippocampal strength might not be as specific as was hypothesized. In order to validate this specificity, the prevalence of significant group differences in nodal strength of the remaining 80 rois was explored (with additional post-hoc group comparisons of nodal strength across all regions, non-corrected). This additional exploration yielded only 7 regions with different nodal strength values between the two groups, including the left parahippocampal region. Such limited number of significant regions strengthens the hypothesis of a specific vulnerability of the parahippocampal area. It is hypothesized that the association between stress, hormonal alterations by the HPA-axis, and structural and functional changes of the hippocampus, is mediated by high-affinity glucocorticoid receptors in the hippocampus [346]. By mediating the feedback inhibition of the HPA-axis [347], the hippocampus is assumed to be vulnerable for glucocorticoid-induced atrophy [348], known as the *glucocorticoid cascade hypothesis* [349,350].

The functional nodal strength of the parahippocampal area appeared associated with survivors' processing speed. Although this region was historically mainly associated with memory encoding and retrieval, hippocampal and parahippocampal subregions are proposed to relate to multiple functional systems and behavioral outcomes [351,352]. Given that the parahippocampal strength was related to processing speed, the parahippocampal-prefrontal system could be particularly of interest. The stronger thresholded connectivity between the left parahippocampal area and the right orbitofrontal area in controls, could be in line with this hypothesis. Consistently with our findings, an EEG study in childhood cancer survivors earlier demonstrated lower processing speed in an auditory task [324]. However, their study included 19 survivors, treated for leukemia with cranial RT. Our study extends these previous findings with decreased resting-state fMRI connectivity of the parahippocampal area in survivors of solid tumors who did not receive any cranial RT.

Furthermore, previous psychological research demonstrated the negative impact of depression and stress on information processing speed in children [353] as well as in adults [256]. Given that the survivor group showed elevated depression scores, this could specifically affect processing speed in cases with clinical depression scores.

<u>Absence of network efficiency differences</u>

Functional efficiency measures were not significantly different between patients and controls. Similar to our findings, Kesler and colleagues (2017) recently demonstrated no group differences in global efficiency in breast cancer patients, and only subtle differences in local efficiency (at uncorrected p-level) [354]. Based on structural networks, Amidi and colleagues (2017) also did not encounter global efficiency differences, but did encounter lower local efficiency in testicular cancer patients [355]. This suggests that (functional) networks are probably not profoundly reorganized, but overall functional coherence might be lower in patients.

<u>Limitations and future directions</u>

Based on our study, we only reported lower density in cerebellar regions, but could not provide information about the thickness of the cerebellar cortical layer. Unfortunately, using the current techniques we applied, we were unable to derive the cortical thickness of the cerebellum. Furthermore, to estimate functional coherence in the brain, we calculated positive partial correlations between atlas-based areas. The calculation of partial correlations is currently a standard implemented approach to estimate coherence between regions, as they would remove sources of shared variance in oscillations with other brain areas [356]. Furthermore, we regressed out the CSF and WM signals and denoised the data from noise components. However, we did not regress out global BOLD signal, and ignored anti-correlations (i.e. negative correlations). For both decisions pros and cons are disputable [356]. Regression of the global signal might help remove non-neural related covariance between regions (e.g. movement, respiration). However, it can also result in spurious artefactual anti-correlations. In this study, we focused on positive correlation values in the connectomes only, since it remains unclear whether anti-correlations in BOLD signal are biologically meaningful or not. Furthermore, negative partial correlations in our dataset were limited to a very low correlation range (<.2). As a consequence, we cannot exclude the possibility that negative values might still appear valuable in future studies, once a biological interpretation of negative correlations would become available. In addition, to investigate excitatory and inhibitory effects of regions to other brain regions, dynamic analyses of the BOLD signals could provide more detailed temporal information, as compared to partial correlations. Partial correlations provide a static measure of coherence of regions across the entire fMRI acquisition (7mins). However, using a specific time-window (i.e. dynamic analyses, dynamic changes in these networks (rather than the size or strength of nodes and networks) might be affected during cancer treatments as well.

We focused mainly on nodal strength measures of brain regions showing lower density or cortical thickness. This yielded lower strength of the parahippocampal region only. However, studies often investigate all of the existing partial correlations between regions to regions, to clarify specific localized "connection" differences. Given that 84 nodes were included in our analyses, such approach would have resulted in 6972 connection comparisons. This would have elevated the risk for type I errors, due to the high number of tests and possibly random coincidence. Therefore, in order to limit the number of statistical tests, we only focused on nodal strength of each node as a more robust measure, rather than ROI-to-ROI specific

correlations. Nevertheless, we cannot exclude the possibility of brain area-specific differences in functional coherence, which did not necessarily differ in nodal strength. Using our method, specific connectivity changes could therefore have been missed.

Finally, this study investigated a group of solid tumor survivors, who were treated according to different chemotherapeutic protocols. As these treatments and different ages at diagnosis result in a heterogenous population, investigations of more complicated interaction effects (e.g. between chemotherapeutic agents, and individual risk factors) require larger sample studies.

7.6 Conclusion

This neuroimaging study of childhood cancer survivors integrated structural and functional grey matter investigations, which suggested long-term cortical changes of cerebellar, frontal and the parahippocampal area. With regard to the parahippocampal region, both cortical thickness and functional strength appeared lower in patients, of which the latter seemed associated with lower processing speed. Furthermore, cortical thickness of orbitofrontal areas correlated with age at diagnosis. Based on this exploratory cohort study, we assume that treatment- or stress-related neurotoxicity could depend on the age and emotional coping mechanisms of the child, with frontal areas possibly being vulnerable during adolescence and parahippocampal areas might depend on depressive symptoms. As previous oncology studies mainly reported changes in attention, our findings of structural frontal and functional parahippocampal brain alterations, could support the hypothesis of underlying neuronal remodeling during development.

Longitudinal follow-up of childhood sarcoma patients:
                                                     interim analyses

Abstract

Neuroimaging and neuropsychological investigations in adult cancer patients increasingly report treatment-induced neurotoxicity, resulting in cognitive changes. However, no longitudinal studies exist in childhood solid non-CNS tumor patients who are treated with high-dose intravenous chemotherapy without CNS-prophylaxis. Although case reports and our survivor cohort study suggest leukoencephalopathy, the incidence and neurocognitive outcomes are largely unknown. In this study, we acquired longitudinal MRI scans and neurocognitive assessments in childhood bone and soft tissue sarcoma patients (aged between 2.17 and 18.33 years old (M=12.00, SD=4.46)). Test assessments were acquired at diagnosis and 2 years after diagnosis in 24 bone and soft tissue sarcoma patients in total. Additionally, MRI was acquired in 12 children at the start and end of treatment, of whom 6 were also scanned 2 years after diagnosis. This interim study of preliminary data demonstrated acute leukoencephalopathy in 6/12 of the included patients at the end of treatment. However, neurocognitive assessments did not significantly change from baseline to follow-up. This study suggests stable age-equivalent cognitive values, up to 2 years after diagnosis. This study will be continued and more patients will be recruited, in order to address more subject-specific risk factors for leukoencephalopathy. Future studies are highly recommended to also explore emotional or fatigue outcomes, which were not included in this study. Finally, advanced multi-modal neuroimaging techniques in larger sample childhood cancer studies could yield additional insights in underlying biochemical mechanisms and neurodevelopmental patterns.

Keywords: Acute leukoencephalopathy, non-CNS directed chemotherapy, childhood sarcoma

8.1 Introduction

Although evidence for high-dose chemotherapy-induced neurotoxicity is slowly increasing based on cross-sectional studies, the amount of longitudinal studies remains limited [357]. With regard to childhood cancer, longitudinal neurocognitive studies were only performed in childhood leukemia patients so far. These studies yielded subtle declines in intelligence scores [358], fine motor functioning [359], verbal fluency [360], working memory [17], attentional and school difficulties [228,361,362]. Often the intelligence scores appear lower than healthy controls, but are still within the normal range [16,228]. With regard to neuroimaging, clinical MRI scans have evidenced acute leukoencephalopathy in leukemia patients as well. For instance, Reddick and colleagues (2009) showed bilateral hyperintensities in leukemia patients on longitudinally acquired T2-weighted MRIs [363]. According to these researchers, such white matter damage could initially lead to decreased processing speed, and other neurocognitive outcomes could be affected in a secondary stage [364]. Similarly, in adult leukemia survivors such acute lesions were recently associated with long-term difficulties in task organization and initiation [230].

Although the evidence of subtle decreases in attention and leukoencephalopathy are increasing in leukemia patients, such investigations were not reported in solid non-CNS tumor patients yet. Important to note is that leukemia patients receive IT-MTX (i.e. CNS-directed chemotherapy) combined with HD-MTX, which is not the case in solid non-CNS tumor patients. Hence, both components could induce encephalopathy. However, some subgroups of non-CNS tumor patients (e.g. osteosarcoma patients) also receive high doses of intravenous chemotherapy (e.g. methotrexate, alkylating agents), which has been evidenced to induce acute neurological symptoms and neurobiological toxicity [19].

Longitudinal neuroimaging studies in solid non-CNS tumor patients were only more recently performed in adult cancer patients. These studies suggested structural as well as functional brain changes after multi-agent chemotherapy treatments. Such neural alterations were predominantly investigated in breast cancer [24,235,315,318,365–371], but also testicular cancer [321,355] and gastric cancer patients [372]. With regard to anatomical changes, widespread reduced grey matter densities (in frontal [318,321], parietal [321], occipital [315] and temporal [366] areas) and altered white matter microstructure [235,355] were encountered throughout the brain. Furthermore, a number of functional MRI studies in adults evidenced altered fMRI BOLD signal during rest [372], or during an active task [24,367,369,370,373]. These studies most consistently reported signal changes in frontal regions during tasks which require working memory.

Although the amount of longitudinal imaging studies is increasing for adult cancer patients, longitudinal studies are very rare in childhood non-CNS tumor patients. Still, case reports of childhood cancer patients treated with high-dose intravenous chemotherapy also showed treatment-induced leukoencephalopathy [233]. Unfortunately, the prevalence of acute leukoencephalopathy in childhood non-CNS tumor patients, and its clinical relevance currently remains unknown. Hence, we launched a longitudinal study to explore developmental patterns in leukoencephalopathy in current childhood bone and soft tissue sarcoma patients based on preliminary data of FLAIR MRI neuroimaging, in combination with a comprehensive neurocognitive test battery. Here, we present interim results of currently included patients. We

explored whether significant evolution occurred in leukoencephalopathy and cognitive measurements, whether age at diagnosis or MTX administration could be important risk factors, and whether leukoencephalopathy was associated with neurocognitive outcomes.

8.2 Methods

8.2.1 Participants

In this study, 24 childhood bone and soft tissue sarcoma patients were recruited at diagnosis, treated with multi-agent intravenous chemotherapy regimens including high-dose agents (i.e. either HD-MTX or high-dose alkylating agents). 12 of these patients were treated for osteosarcoma who received high-dose MTX. The other patients were treated for ewing sarcoma (n=6), rhabdomyosarcoma (n=5) and non-rhabdomyosarcoma (n=1) with treatments including high-dose alkylating agents (i.e. ifosfamide or cyclophosphamide). Patients were aged between 2.17 and 18.33 years old (Mean=12.00, SD=4.46). For detailed patient characteristics, see Table 8.1.

Table 8.1 Patient characteristics

DIAGNOSIS	Osteosarcoma	Ewing sarcoma		Rhabdo-myosarcoma	Non-rhabdomyosarcoma
TREATMENT	EURAMOS1	EE08	EE12	RMS2005	NRSTS2005
NUMBER	12	4	2	6	1
AGE DIAGNOSIS	5.25-17.8	6.44-14.99	14.71-14.97	2.93-17.21	14.42
MTX (G/M^2)	132-144	0	0	0	0
IFO (G/M^2)	0-60	54-102	54-84	51-54	33
CYCLO (G/M^2)	0	0-12	4.5-12	4.2-8.4	0
DOXO (MG/M^2)	450	0	0	0-240	225
CISPLATIN (MG/M^2)	480	0	0	0	0

Note. EE=EUROEWING. MTX=methotrexate, IFO=ifosfamide, CYCLO=cyclophosphamide, DOXO=doxorubicin. 1 patient received combined multi-agent treatments of EURAMOS and RMS.

8.2.2 Data acquisition

Of all included patients (n=24), 18 patients underwent a comprehensive neurocognitive assessment at diagnosis, and 2 years after diagnosis. MRI scans were independently obtained at diagnosis and end of treatment in 12 patients, of whom 6 underwent a third MRI scan combined with the second neurocognitive test assessment (see Figure 8.1). These data were used for preliminary analyses.

MRI scans included FLAIR images, which were visually rated by a neuroradiologist for the level of leukoencephalopathy according to the Fazekas rating scale (see Chapter 5). These ratings range between 0 (no lesions present) and 3 (most extensive white matter lesions). The radiologist was blinded to the participant groups (scans were anonymized and randomly organized). With regard to neurocognitive values, age-dependent assessments included intelligence assessment (WPPSI-III, WISC-III, WAIS-IV), visual and verbal memory assessment (CMS), visuomotor functioning (VMI) and attentional tasks (ANT) (as described in detail in section 3.2.1). All scores that were extracted, were age-equivalent scores (i.e. compared to the age-dependent norms).
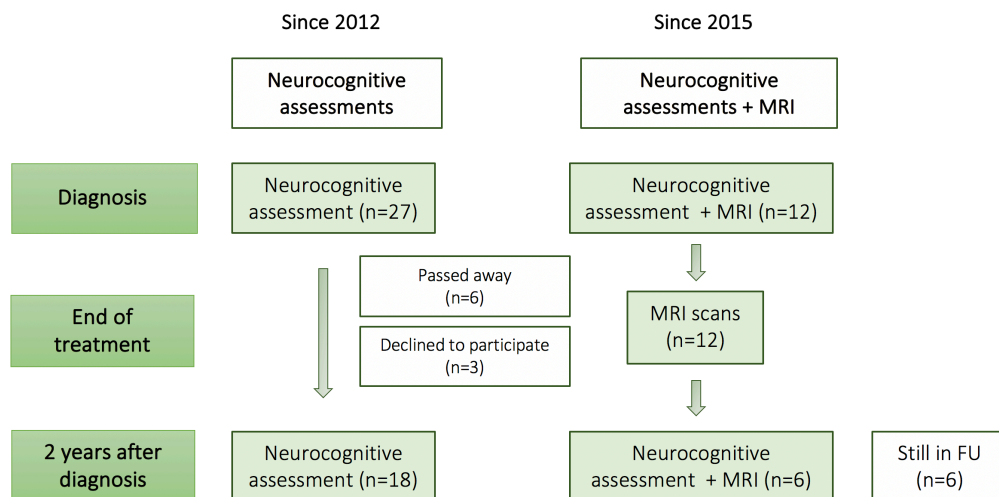
Figure 8.1 Schematic overview of the available (preliminary) data for analyses

Note. Since 2012, neurocognitive assessments were acquired at diagnosis and 2 years later. These data were used for preliminary analyses of the behavioral data. In addition, since 2015 MRI scans were acquired at diagnosis, end of chemotherapy, and 2 years after diagnosis. In total, 24 (18+6) patients were included in behavioral analyses, while 12 patients were included for lesion classifications.

8.2.3 Data processing

First, evolution of both (ordinal) leukoencephalopathy ratings, and (continuous) cognitive measures throughout time was investigated using the Wilcoxon signed rank test.

Second, the possible impact of age at diagnosis and MTX administration (vs. no MTX) on change in these outcomes (i.e. difference scores between ordinal Fazekas ratings T2-T1, and continuous cognitive scores T2-T1) was investigated with Spearman correlations, and Mann Whitney U tests respectively. Similarly, changes in cognitive values were correlated with lesion rating changes using Spearman correlations. All analyses were performed using SAS software v9.4.

8.3 Results

8.3.1 Leukoencephalopathy Fazekas rating

The Wilcoxon signed rank test demonstrated a significant increase in Fazekas ratings (p=.0313) (see Table 8.2). Out of the 12 patients who were scanned at diagnosis and end of treatment, 6 patients (50%) showed an increase in Fazekas score with ≥ 1 grade difference. For 6 patients who were also scanned 2 years after diagnosis, this rating remained stable.

Such change occurred in 4/7 (50%) of patients treated according to EURAMOS2001, 1/1 (100%) treated according to RMS, and 1 out of 4 treated (25%) according to EUROEWING.

Out of the patients who showed increased hyperintense FLAIR signal (i.e. more extensive lesions), the majority (n=4/6) ratings increased with 1 grade (see Figure 8.2). For the remaining 2 patients this increase reached even 2 (n=1) and 3 (n=1) grades of difference between start and end of treatment. The latter patients were both treated with high-dose MTX regimen.
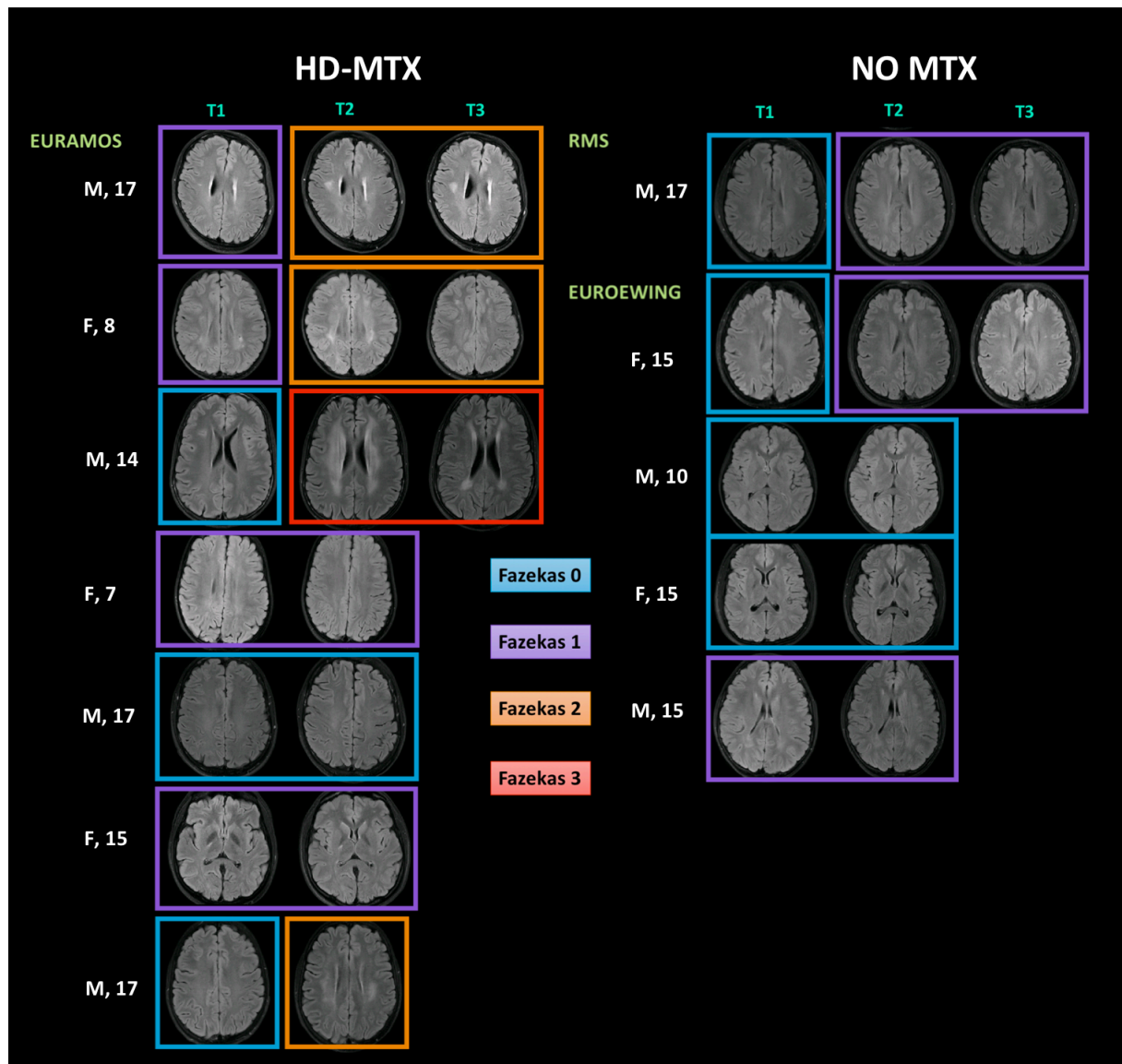
Figure 8.2 Fazekas rated FLAIR MRI scans for all patients at T1, T2, T3.
Note. T1 is at diagnosis, pre-treatment; T2 is end of therapy (i.e. approximately one year after diagnosis); T3 is 2 years after diagnosis. Fazekas rating 0 is indicated in blue, rating 1 in purple, rating 2 in orange and rating 3 in red. F=female, M=male.

Table 8.2 Descriptive statistics Fazekas ratings in childhood sarcoma patients

Outcome				T1					T2			
	N	Mean	SD	Med	Min	Max	Mean	SD	Med	Min	Max	P
	12	.42	.51	.00	.00	1.00	1.17	.94	1.00	.00	3.00	.0313*
FLAIR Fazekas				T1					T3			
	N	Mean	SD	Med	Min	Max	Mean	SD	Med	Min	Max	P
	6	.33	.52	.00	.00	1.00	1.50	1.05	1.50	.00	3.00	.0625

Note. T1=first MRI scan at diagnosis, T2=second MRI scan at end of therapy, T3=third MRI scan 2 years after diagnosis; N=number of inclusions, SD=standard deviation, MED=median value, Min=minimum value, Max=maximum value, p=p-value from Wilcoxon signed rank test comparing FLAIR rating at T1 vs. T2, and T1 vs. T3, * indicates p-value <.05.

8.3.2 Neurocognitive functioning

The Wilcoxon signed rank tests comparing first and second neurocognitive assessments did not show any significant changes in age-equivalent neurocognitive scores (see Table 8.3). Only one borderline non-significant decrease was observed in age-equivalent reaction times on the divided attention task with highest memory load (MS3, p=.0781). In addition, age at diagnosis was not significantly associated with change in cognitive values, nor with Fazekas lesion increases (see Table 8.4). Nevertheless, effect sizes (i.e. correlation values) reached relatively higher values ($\rho \geq .50$) for correlations between age at diagnosis and VIQ (ρ=-.525) and divided attention with memory load (ρ=-.643). Similarly, lesion load increases were not significantly correlated with cognitive value changes (see Table 8.4). However, again regarding the effect sizes , notice a relatively higher correlation between lesion increase and changes in PIQ (ρ=-.632), baseline attention (BS, ρ=-.707), focused (FA, ρ=-.676) and divided attention task specifically (MS, ρ=.676).

Finally, MTX administration (see Table 8.5) did not significantly predict cognitive changes or lesion increase. Although stronger increases in Fazekas ratings were observed in case of MTX administration, lesions also occurred in case of no MTX administration.

Table 8.3 Descriptive statistics neurocognitive tests childhood sarcoma patients T1 and T2

Test Subscale		N	Mean	SD	Median	Min	Max	Mean	SD	Median	Min	Max	P
					T1					T2			
Intelligence (WPPSI, WISC and WAIS)	VIQ	13	104.20	12.68	105.00	85.00	121.00	98.08	16.28	99.00	69.00	122.00	.1052
	PIQ	13	99.46	19.78	98.00	68.00	133.00	101.20	17.75	104.00	73.00	128.00	.9854
	FSIQ	18	101.40	14.53	103.5	80.00	122.00	99.67	16.08	103.50	78.00	123.00	.3460
	PS	16	92.88	24.61	92.50	22.00	124.00	94.56	12.50	92.50	70.00	117.00	.8306
Visual memory (CMS)	Learn	12	10.25	2.45	10.00	7.00	14.00	11.42	2.61	12.00	7.00	15.00	.2852
	Short	12	10.75	2.22	12.00	7.00	13.00	11.67	1.37	12.00	8.00	13.00	.2813
	Long	12	10.33	2.46	11.50	5.00	13.00	9.83	3.10	12.00	3.00	12.00	.7578
Verbal memory (CMS)	Learn	12	9.75	2.96	10.00	6.00	15.00	9.00	2.17	9.00	5.00	12.00	.4102
	Short	12	9.50	3.66	9.50	5.00	19.00	9.42	3.15	10.50	4.00	13.00	1.000
	Long	12	8.50	2.24	9.00	4.00	13.00	8.42	3.26	9.50	3.00	13.00	.7490
Visuomotor (VMI)	Visual	14	108.6	11.29	102.50	97.00	128.00	101.60	12.39	105.00	77.00	123.00	.0554
	Motor	14	99.29	11.06	100.00	74.00	123.00	102.40	12.04	102.00	77.00	132.00	.3843
	VM	16	99.94	7.81	99.50	86.00	111.00	100.40	11.00	100.00	75.00	117.00	.9142
Attention (ANT)	BS	15	.14	1.28	-.30	-1.33	2.96	.45	.97	.15	-.85	2.31	.4883
	FA	13	.23	.97	.18	-1.40	1.86	-.45	.91	-.56	-2.13	1.34	.1272
	FA2	13	-.20	1.13	-.49	-1.69	2.17	-.36	.70	-.31	-1.42	.95	.4973
	FAm	14	.01	1.06	.06	-1.24	2.70	3.53	8.49	.19	-1.23	27.55	.1775
	FAfp	14	.36	1.41	.04	-1.07	3.29	1.57	5.09	-.59	-1.07	18.42	.6838
	MS	13	-.37	.66	-.22	-1.87	.42	-.32	.76	-.48	-1.33	1.64	.6233
	MS2	13	-.20	1.13	-.49	-1.69	2.17	-.36	.70	-.31	-1.42	.95	.4973
	MS3	8	.39	1.22	.16	-1.23	2.35	-.46	.70	-.42	-1.69	.56	.0781
	MSm	13	-.19	.90	-.22	-1.12	2.19	-.12	.96	-.23	-1.18	1.97	.9460
	MSfp	8	.23	1.28	.22	-1.67	2.18	-.40	.79	-.60	-1.20	.79	.1094

Note. Neurocognitive scores are age-equivalent for each assessment (Intelligence (Mean=100, SD=15), Memory (Mean=10, SD=3), Visuomotor (Mean=10, SD=3), and Attention (Z-scores)). T1=first assessment at diagnosis, T2=second assessment 2 years after diagnosis; N=number of inclusions, SD=standard deviation, Min=minimum value, Max=maximum value, VIQ=verbal IQ, PIQ=performance IQ, FSIQ=full scale IQ, PS=processing speed, Learn=learning phase of dot positions or word pairs in visual or verbal memory task resp., Short=short-term recall, Long=long-term recall, VM=visuomotor task, BS=baseline speed, FA=focused attention, FA2=focused attention with memory load, FAm=focused attention number of misses, FAfp=focused attention false positives, MS=memory search (divided attention), MS2 and MS3= memory search with increased memory load; p=p-value from Wilcoxon signed rank test comparing test scores at T1 vs. T2, * indicates p-value <.05.

Table 8.4 Correlations between change in cognitive values, age at diagnosis and lesion rating

Development in values	Age at diagnosis				Lesion rating difference 2y after dx			
	N	ρ	95% CI	P	N	ρ	95% CI	P
Lesions end treatment	12	-.011	(-.581;.567)	.9727				
Lesions 2y after dx	6	.169	(-.752;.858)	.7675				
VIQ change	13	-.525	(-.828;.058)	.0649	4	.500	(-.904;.984)	.5828
PIQ change	13	-.055	(-.587;.513)	.8615	4	-.632	(-.989;.867)	.4560
FSIQ change	18	.061	(-.419;.512)	.8129	6	-.338	(-.896;.672)	.5422
Processing Speed change	16	.030	(-.474;.517)	.9151	5	-.707	(-.975;.532)	.2126
BS change	15	-.172	(-.625;.379)	.5483	6	-.676	(-.955;.360)	.1546
FA change	13	.126	(-.461;.630)	.6878	5	.447	(-.745;.948)	.4962
MS change	13	-.382	(-.764;.229)	.2027	6	.676	(-.360;.955)	.1546
MS2 change	13	-.643	(-.875;-.116)	.0158	6	.338	(-.672;.896)	.5422
MS3 change	8	-.310	(-.826;.522)	.4742	5	.447	(-.745;.948)	.4962

Note. For each 'change' value, a difference score in cognitive values was calculated between testing 2years after diagnosis and testing at diagnosis. 'Lesions (end of treatment and 2y after dx)' represent the differences between lesion rating scores at these timepoints and the baseline lesion rating scores (at diagnosis). This value was correlated with age at diagnosis. ρ=Spearman correlation, CI=confidence interval.

Table 8.5 Prediction of developmental changes by MTX vs. no MTX

Development in values	No MTX			MTX			
	N	Mean	SD	N	Mean	SD	P
Lesions end treatment	5	.40	.548	7	1.00	1.155	.426
Lesions 2y after dx	3	.67	.577	3	1.67	1.155	.302
VIQ change	8	-3.75	13.677	5	-10.00	6.964	.509
PIQ change	8	4.38	13.627	5	-2.40	5.941	.509
FSIQ change	10	-1.20	10.871	8	-2.38	8.314	.859
Processing Speed change	8	-.13	9.643	8	3.50	31.555	.958
BS change	8	.47	1.847	7	.13	.960	.908
FA change	6	-.82	.860	7	-.55	1.564	.943
MS change	6	.03	1.212	7	.08	.457	.431
MS2 change	6	-.16	.929	7	-.15	1.525	1.00
MS3 change	3	-1.20	1.021	5	-.64	1.069	.371

Note. For each 'change' value, a difference score in cognitive values was calculated between testing 2years after diagnosis and testing at diagnosis. This value was predicted by MTX vs. no MTX using Mann Whitney U Tests.

8.4 Discussion

This interim analysis of the ongoing study demonstrated acute leukoencephalopathy in 6/12 of the included sarcoma patients at the end of treatment, which remained stable in patients who were scanned 2years after diagnosis (n=6). Age-equivalent neurocognitive values remained stable. No significant changes throughout time were encountered, nor did these values reach clinical thresholds. Changes in scores were not significantly related to lesion extent, age at diagnosis or MTX administration, but effect sizes could suggest some subtle trends.

With regard to leukoencephalopathy, MTX administration vs. no administration did not result as a significant predictor of lesion increase. Still, the highest lesion ratings were detected in two patients who were treated with high-dose intravenous MTX (i.e. app. $144g/m^2$ cumulative dose), as compared to patients treated with multi-agent regimens without MTX. Although these intravenous doses are mostly higher than in leukemia treatments, more leukoencephalopathy studies were conducted in leukemia patients so far. This is mainly due to their CNS-directed chemotherapy treatment. Nevertheless, acute neurological symptoms during chemotherapy were previously frequently reported in osteosarcoma patients [35]. Also, higher doses of IV-MTX was earlier related to higher risk for leukoencephalopathy in leukemia [263]. Therefore, HD-MTX-treated patients such as osteosarcoma patients could specifically be at risk. Still, similar to our adult survivor cohort study (see Chapter 5), we also encountered leukoencephalopathy in current childhood patients treated with other chemotherapeutic agents excluding MTX (n=2). These patients (n=2) had both received multi-agent chemotherapy containing ifosfamide, which is known for neurotoxicity in animal models (i.e. $54g/m^2$ cumulative dose,). So, lesions not only appeared in case of MTX administration and were not limited to either younger or older patients. Besides these findings, some adult cancer studies also evidenced leukoencephalopathy after multi-agent chemotherapeutic treatment [373,374]. For instance, increases in Fazekas rating (+1) was recently demonstrated by Menning and colleagues (2017) in breast cancer patients [239]. However, these ratings remained limited to Fazekas 1 and 2, and were not significantly higher compared to healthy age-matched controls.

Furthermore, it could be noticed that some patients were rated Fazekas 1 at diagnosis in our population. Fazekas > 0 indicates hyperintensity of the white matter on the T2-FLAIR image. This MRI scan typically demonstrates a change from hyperintensity towards hypointensity of the white matter between 0 and 2 years old [375,376]. Still, terminal zones of myelination can remain hyperintense up to 4 years old [377]. Therefore, Fazekas is typically rated 0 in children older than 4 years old. Given that all patients were at least 7 years old, one would expect Fazekas rating 0 at diagnosis. Although Menning and colleagues did not encounter more Fazekas 1 ratings in breast cancer patients prior to treatment, compared to controls; they did also show a few cases showing Fazekas 2 at diagnosis, which was not observed in controls [373]. In childhood leukemia studies however, no baseline data prior to treatment were available to compare to our baseline ratings [263]. Whether subtle underlying neural damage is already present at baseline will therefore require advanced imaging future studies. Also, quantitative analyses of the lesions will become increasingly valuable in future research, as such methods

are less dependent on inter-rater variability. Such quantitative estimations of lesion loads could include automatic segmentation of lesion volumes.

After the earlier childhood cancer studies which focused on leukemia patients treated with HD-MTX, this is the first prospective study in childhood patients treated with other intravenous agents. Nevertheless, the sample size of patients showing lesions in this interim analysis, currently remains too small (i.e. 6/12) to address the risk of specific agents or additional risk factors. Given that not all patients showed leukoencephalopathy, subject-specific mediating factors are still highly probably. Biological mediators that could play an important role in leukoencephalopathy occurrence, include metabolism alterations [259], inflammatory processes [259], vascular supply changes [378], …, which were not acquired in the current study. To address such underlying mechanisms, biochemical measurements or multi-modal neuroimaging could add information in future research.

Furthermore, although leukoencephalopathy visually appeared to decline throughout time, the rating categories (as categorized by the clinical neuroradiologist) remained stable. In contrast to such stable visual ratings, previous quantitative diffusion-weighted MRI studies have shown recovery patterns in diffusion metrics in adult breast cancer [260,374] and lymphoma [37] patients, as well as adult survivors of childhood sarcoma in our previous cohort study [379]. Such recovery patterns could be dose- and interval-dependent. In the breast cancer patients, recovery was encountered 3-4 years after treatment. Therefore, additional follow-up assessments including advanced neuroimaging techniques would be interesting to address temporal patterns of neurobiological mechanisms and underlying pathology. Given that not only high-dose MTX-treated patients showed lesions, such longitudinal studies could become important to implement in multiple childhood cancer populations (treated with multi-agent regimens).

With regard to neurocognitive functioning, no significant findings were encountered. Given that this study was only an exploratory analysis, with a limited amount of data available, the reported p-values are to be interpreted with caution. On one hand, a large number of tests was performed which increases the risk of false positive results. On the other hand, a low number of observations is associated with lower sensitivity and could increase the risk of missing real underlying effects. Therefore, results are assumed only to be hypothesis-generating, and reported effect sizes might be more valuable compared to p-values.

Still, correlations between lesion change, decrease in PIQ, processing speed, divided attention and the negative association with improved baseline speed, could be assumed relatively high (i.e. >.50). Although this group is more heterogenous in age at test assessment, and we could not correct for SES or depression (given low number of inclusions), underlying associations between lesions and decreased attentional reaction times would confirm our findings of the adult cohort study (Chapter 5). Due to such acute neural damage (e.g. observed leukoencephalopathy), neurodevelopmental patterns could be affected with a delay later in neurodevelopment (e.g. decreased white and grey matter density as well as decreased processing speed in adulthood, which we encountered in the survivor cohort study). Still, the

non-significant p-values in the current study encourage to interpret the encountered effect sizes only very cautiously. Currently such interpretations remain very hypothetical.

Finally, although we did not detect change throughout time, we cannot exclude the possibility of delayed development, given that healthy controls were not included in the current study. Steeper learning curves could appear in healthy participants, which would then still suggest subtle delayed cognitive development. Furthermore, the observed leukoencephalopathy could induce other psychological complaints besides cognitive decline as well. Emotional complaints (e.g. depression, anxiety, …), fatigue, etc. could still occur due to neural damage, and possibly play a long-term role in (cognitive) functioning of adult survivors of childhood cancer. Therefore, future large sample longitudinal studies are recommended, including questionnaires, as well as sibling or healthy matched control data.

8.5 Conclusion

This study demonstrated acute leukoencephalopathy in 6 of 12 included current childhood sarcoma patients treated with different chemotherapy regimens. Nevertheless, age-equivalent cognitive values appeared rather stable from diagnosis up to 2 years after diagnosis. These interim results point towards acute lesions, but no obvious acute cognitive symptoms. However, these findings will need confirmation in the future (after sufficient data collection). Expansion of this research is recommended to address subject-specific risk factors for leukoencephalopathy, its underlying biochemical mechanisms, as well as emotional processes, which were not included in the current study, but could influence long-term outcomes in adult survivors. Finally, more advanced neuroimaging techniques in large sample childhood cancer studies could yield insights in microstructural neurodevelopmental patterns.

9 What the future might hold: the human connectome in case of neural damage

Abstract

We previously demonstrated the possible occurrence of leukoencephalopathy after chemotherapy in non-CNS tumor patients. In case of such visually observable and extensive neural damage, neural integrity could be not only reduced locally, but also induce secondary brain damage. Such cascade effects could possibly lead to profound reorganization of the underlying brain network, or the so-called 'connectome'. However, larger samples are required to investigate brain topology in childhood cancer survivors demonstrating clear long-term neural damage. Therefore, 21 childhood infratentorial tumor survivors were recruited in this final study, for whom a long-term infratentorial lesion (i.e. cavity) is consistently present. Based on diffusion-weighted MRI scans, multiple recent analyses were implemented to investigate microstructural reorganization and topology of supratentorial white matter (i.e. the well-known voxel-based approach, a more tract-specific (fixel-based) analysis, and finally a graph theoretical approach). In addition to previous findings of widespread decreases in FA (based on voxel-based analyses), fixel-based analyses enabled us to dissociate macro- from microstructural changes, in infratentorial vs. supratentorial brain areas, respectively. In addition, graph theoretical analyses evidenced that local reorganization mainly occured in core connected regions, which could suggest specific vulnerability of these areas. Based on this multi-method approach we discuss the differential findings, their link with intelligence subscales, and pros and cons of these methods in case of observable neural damage.

9.1 Introduction

This thesis mainly comprised neuroimaging and neurocognitive investigations of childhood cancer patients and survivors, who were treated for non-CNS tumors, with local treatment (surgery and possibly radiotherapy) and systemic chemotherapy. These patients did not experience CNS invasion or cranial radiotherapy. In other words, one would not expect direct neurotoxicity, given the presumably protective blood-brain-barrier and no CNS-prophylaxis was applied. Nevertheless, we demonstrated that high-dose intravenous chemotherapy could engender visually detectable leukoencephalopathy; and even if lesions are not visually detectable, subtle brain alterations could occur due to therapy.

Advanced neuroimaging techniques currently deliver the opportunity to estimate white and grey matter differences at more detailed (i.e. voxel) level, which are not easily detected by a clinician (on a clinical scan by the radiologist, or in asymptomatic patients by the oncologist). Such imaging methods were discussed in the previous chapters, in which we implemented well-known voxel-wise statistical group comparisons, comparing brain MRI images of non-CNS tumor survivors to healthy controls. These studies demonstrated multiple brain areas to be affected at microstructural level by high-dose intravenous chemotherapy. In all existing imaging studies to date, the extent of these regions partly depends on significance thresholds that are applied. More diffuse patterns are encountered in case of less stringent statistical thresholds. By applying a more stringent threshold, the most significant brain areas remain, which are most often interpreted as being 'most affected'. Linking these specific regions with behavioral outcomes, is in line with the localism view. In this context, the *double dissociation hypothesis* states a direct relationship between neurobiology and behavior: a lesion in region A is associated with lack of behavioral function A, while this behavioral function is preserved in case of a lesion in brain region B, whereas the latter lesion is associated with lack of behavioral function B, which is independent of the integrity of region A [381].

However, the brain is increasingly perceived as a complex network, consisting of interacting regions. More specifically, the *diaschisis hypothesis* suggests that damage to one brain region also results in secondary damage to another region [382]. Such cascade effects are even more probable in case of extensive neural damage, and could highly affect the underlying brain network. This has been evidenced previously in neurological conditions such as epilepsy, traumatic brain injury, stroke, … [383], which can result in a wide range of psychological sequelae or neurological syndromes.

In childhood cancer specifically, long-term neural damage and cascade effects are clearly evident in brain tumors. Two-third of these patients are diagnosed with a infratentorial brain tumor (i.e. located below the tentorium). These patients often suffer from neurocognitive deficits [384], given that their brain maturation is highly affected by the long-term lesion itself, as well as by each constituent of the treatment. Initially, the brain tumor leads to high intracranial pressure and related acute symptoms (e.g. nausea, headaches, loss of motor coordination, speech, …). Their treatments can include neurosurgery, additional (craniospinal and/or local) photon/proton beam radiotherapy (RT), and/or chemotherapy.

Due to neurosurgery, specific white matter tracts might be damaged, which can lead to

acute and long-term emotional, motor and speech deficits [385]. This might be explained by secondary (not only local) damage after surgery. More specifically, damage to the infratentorial region could also result in hypoperfusion of supratentorial regions [386,387]. From a functional connectivity perspective, functional cerebello-cerebral networks also demonstrated specific subregions of the cerebellum to be part of specific supratentorial networks [388,389]. This provides a possible explanation for cognitive difficulties (e.g. working memory) depending on the specific cerebellar tumor location [390]. From a structural connectivity perspective, also tractography studies evidenced fronto-cerebellar white matter tracts to be involved both in post-surgical mutism [391] as well as in working memory difficulties [392]. Besides the tumor (lesion) itself and neurosurgery, cranial radiotherapy was abundantly associated with widespread brain damage and an extensive range of long-term endocrine and neurocognitive symptoms [393–395]. Consequently, in infratentorial tumor patients, a large long-term impact on quality of daily life was reported [396].

To investigate underlying neural underpinnings of psychological symptoms, multiple neuroimaging approaches can be applied. Although previous studies have shown long-term widespread brain injury in childhood infratentorial tumors survivors, the microstructural reorganization of white matter tracts remains unclear given the heterogeneity in the applied methods. To investigate white matter microstructure, voxel-based analyses of diffusion tensor (DTI) metrics are most frequently applied. However, as demonstrated in Chapter 6, the DTI model is increasingly criticized for lack of sensitivity to microstructural changes (especially in crossing fiber areas). One alternative is the recently developed fixel-based analysis (presented in Chapter 6), which could dissociate micro- from macrostructural changes. Still, in case of a neural attack (such as the occurrence of a brain tumor), the brain network, or so-called *connectome*, can be highly affected, leading to reorganization of the brain connectivity and brain topology [383]. Such topological changes cannot be investigated using voxel- or fixel-based approaches only. In this regard, graph theoretical approaches now receive more attention. It is hypothesized that most densely connected regions (i.e. so-called hubs) might be specifically sensitive to neural damage in some diseases or toxic events [397]. For instance, we demonstrated strongest decreases in fiber density in the corpus callosum of non-CNS tumor survivors (Chapter 6).

To investigate whether specific brain regions are more vulnerable to treatment-induced toxicity, and their functional impact, we investigated diffusion-weighted MRI scans and neurocognitive outcomes in long-term survivors of childhood infratentorial tumors. The main aim of this study was to integrate information of multiple analysis techniques estimating structural connectivity in these survivors. These approaches included the well-known voxel-based approaches, as well as more tract-specific (fixel-based) analysis and finally a graph theoretical approach. We will discuss the subgroup comparison findings, their link with intelligence subscales, and differential interpretations of these different methods.

9.2 Methods

9.2.1 Participants

21 childhood infratentorial tumor survivors were recruited (median age at diagnosis 7.8 years, range: 2.8-18.4 years; median age at assessment 25.3 years, range 16.4-34.8 years; >2 years post-treatment), who were treated between 1991 and 2015 for a pilocytic astrocytoma (n=8), ependymoma (n=1) or medulloblastoma (n=12) at the Pediatric Hemato-Oncology Department of University Hospitals Leuven. Details of treatments are presented in Table 9.1. 21 age-, gender- and education-matched controls were recruited via online forums. The study was approved by the ethical committee of UZ Leuven. All participants (>18 years old) had signed the informed consents to participate in the study. Parents (of participants <18 years old) were also requested to give assent.

9.2.2 Data acquisition

9.2.2.1 MRI neuroimaging

Multishell DWI and T1-weighted MR-scans were acquired on a 3T Philips Achieva MRI scanner with a 32-channel phased-array head coil. The DWI imaging scheme consisted of b-values 700, 1000 and 2800 s/mm^2, applied along 25, 40 and 75 uniformly distributed gradient directions respectively, in addition to 10 non-diffusion-weighted images (b=0) (TR/TE=7800ms/90ms, 50 slices, 2.5mm x 2.5mm x 2.5mm).

T1-weighted MR-scans (TR/TE=4.6ms/9.6ms, 160 slices, .98 × .98 × 1.2mm) were used for anatomical reference. More specifically, the grey matter cortical layer from the T1-weighted MRI scan was used as the edge for diffusion-based tractography (i.e. so-called anatomy-constrained tractography) (see section 9.2.3.4 and 9.2.3.5). In addition, the anatomical T1-weighted MRI scan was also used for mapping of anatomical regions, in order to construct a structural brain network (i.e. connectome; see section 9.2.3.5).

9.2.2.2 Neurocognitive assessments

Besides MRI neuroimaging, neurocognitive assessments were acquired including estimations of intelligence, verbal and visual memory, attentional functioning, and language (abbreviated version of the WAIS-IV intelligence test [189], Auditory Verbal Learning Test (AVLT) [191], Rey Visual Design Learning Test (RVDLT) [192], Amsterdam Neuropsychological Task battery (ANT) [187], Peabody Picture Verbal Task (PPVT) [398], Controlled Oral Word Association Test (COWAT) [399]). Subjective experiences were estimated using self-reported questionnaires (the State Anxiety Inventory (STAI) [400], Beck Depression Inventory (BDI) [178], Behavior Rating Inventory of Executive functioning (BRIEF) [180], Cognitive Failure Questionnaire (CFQ) [179] and Quality of Life (QoL) Questionnaire [175]). All behavioral data were acquired on the same day as the MRI scan.

Table 9.1 Patient characteristics

Patient	Age at dx (years)	Time since treatment (years)	Tumor type	Surgery	Craniospinal RT	Posterior Fossa RT	Tumor bed RT	Multi-agent CT	Intraventricular MTX	HD-MTX	Fazekas FLAIR rating	Metastasis	Relapse
1	3.3	19.9	PA	+	-	-	-	-	-	-	1	-	-
2	11.1	15.0	MB	+	+	-	+	+	-	-	1	-	-
3	7.3	9.2	PA	+	-	-	-	-	-	-	1	-	-
4	4.6	22.7	MB	+	+	+	-	-	-	-	0	+	-
5	10.8	21.5	MB	+	+	+	-	-	-	-	1	-	-
6	2.9	19.5	MB	+	+	+	-	+	+	+	2	+	-
7	18.4	1.5	MB	+	+	-	+	+	-	-	0	-	-
8	10.2	20.0	PA	+	-	-	-	-	-	-	0	-	+
9	4.5	17.6	PA	+	-	-	-	-	-	-	0	-	-
10	7.8	17.0	PA	+	-	-	-	-	-	-	1	-	-
11	3.2	16.2	PA	+	-	-	-	-	-	-	0	-	-
12	13.3	17.2	MB	+	+	+	-	+	-	-	1	-	-
13	11.6	10.0	PA	+	-	-	-	-	-	-	0	-	-
14	8.8	15.6	PA	+	-	+	-	-	-	-	0	-	+
15	3.2	5.2	MB	+	+	+	-	+	+	-	0	+	+
16	7.1	21.9	MB	+	+	+	-	-	-	-	0	-	-
17	12.9	4.8	MB	+	+	+	-	+	-	-	1	-	-
18	7.2	16.8	MB	+	+	+	+	+	+	+	2	+	-
19	4.8	20.3	MB	+	+	+	-	+	+	+	1	+	+
20	8.0	26.0	EP	+	-	+	-	-	-	-	1	-	-
21	14.0	5.2	MB	+	+	+	+	+	+	+	3	+	-

Note. PA= pilocytic astrocytoma, EP= ependymoma, MB= medulloblastoma, dx= diagnosis, MTX= methotrexate, HD-MTX= high-dose methotrexate, RT= radiotherapy, CT= chemotherapy. Metastases that were detected, were located in the spine. As could be inferred, patients showing Fazekas lesion rating 2 or 3, were treated with intraventricular MTX combined with high-dose MTX in addition to cranial radiotherapy. + indicates the inclusion of the treatment constituent or symptom occurrence, - indicates the absence.

9.2.3 Data analyses

9.2.3.1 Behavioral analyses

One MANOVA analysis was performed to compare behavioral outcomes between the patient survivor group and healthy controls. Since SES did not significantly differ between the two groups, SES was not included as covariate. In order to restrict the number of analyses, we further focused on the link between imaging parameters and the subscales of behavior showing the most significant differences between groups only (p<.001).

9.2.3.2 Preprocessing

All preprocessing and analyses were performed using MRtrix3 [401]. First, DWI images were denoised using Marchenko-Pastur-Principal-Component-Analysis [402]. Gibbs ringing was removed [403]. Images were then corrected for motion and distortion, and bias field corrected using ANTs bias field correction [285]. Intensities of the images were normalized across the complete group. These preprocessed images were subsequently used for the following statistical group comparisons. 2 patients were excluded from the imaging analyses due to mechanical shunt artefacts.

9.2.3.3 Voxel-based statistics

First, Apparent Diffusion Coefficient (ADC) maps were calculated. Second, DTI-derived Fractional Anisotropy (FA) maps were computed. Voxel-wise group comparisons (patients vs. controls; irradiated patients vs. non-irradiated patients) were performed for both types of maps using a non-parametric approach in MRtrix3 (i.e. voxel-based permutation testing with threshold-free cluster enhancement).

9.2.3.4 Fixel-based statistics

Besides most often calculated DTI measures (e.g. FA), we applied the more recent CSD model, which yields fiber orientation distributions (FODs) (see Chapter 6). This enabled us to compute FOD-derived parameters, such as Apparent Fiber Density (AFD) and Fiber Cross-section (FC) (i.e. so-called *fixels*, see Chapter 6). As mentioned earlier, the so-called fixel-based approach was recently hypothesized to dissociate microstructural from macrostructural white matter properties, based on AFD and FC, respectively.

In this study, tissue-specific fiber orientation distributions (FODs) were estimated in each voxel of the DWI image, using multi-tissue constrained spherical deconvolution and T1-based tissue segmentations [404]. In order to achieve the latter, anatomical T1 images were first segmented in native space based on 6 tissue priors (i.e. grey matter, white matter, CSF, bone, soft tissue and background) using the CAT toolbox [331], subcortical grey matter was segmented using FSL [405]. These T1-images were rigidly registered to diffusion space (FSL, boundary based cost function). The FODs were then estimated for each tissue type separately, and the GM segmentation was later on used for anatomically constrained tractography. Similar to the voxel-wise comparisons, again non-parametric group comparisons of these fixel-based values were performed (patients vs. controls; irradiated patients vs. non-irradiated patients).

9.2.3.5 Connectome-based statistics
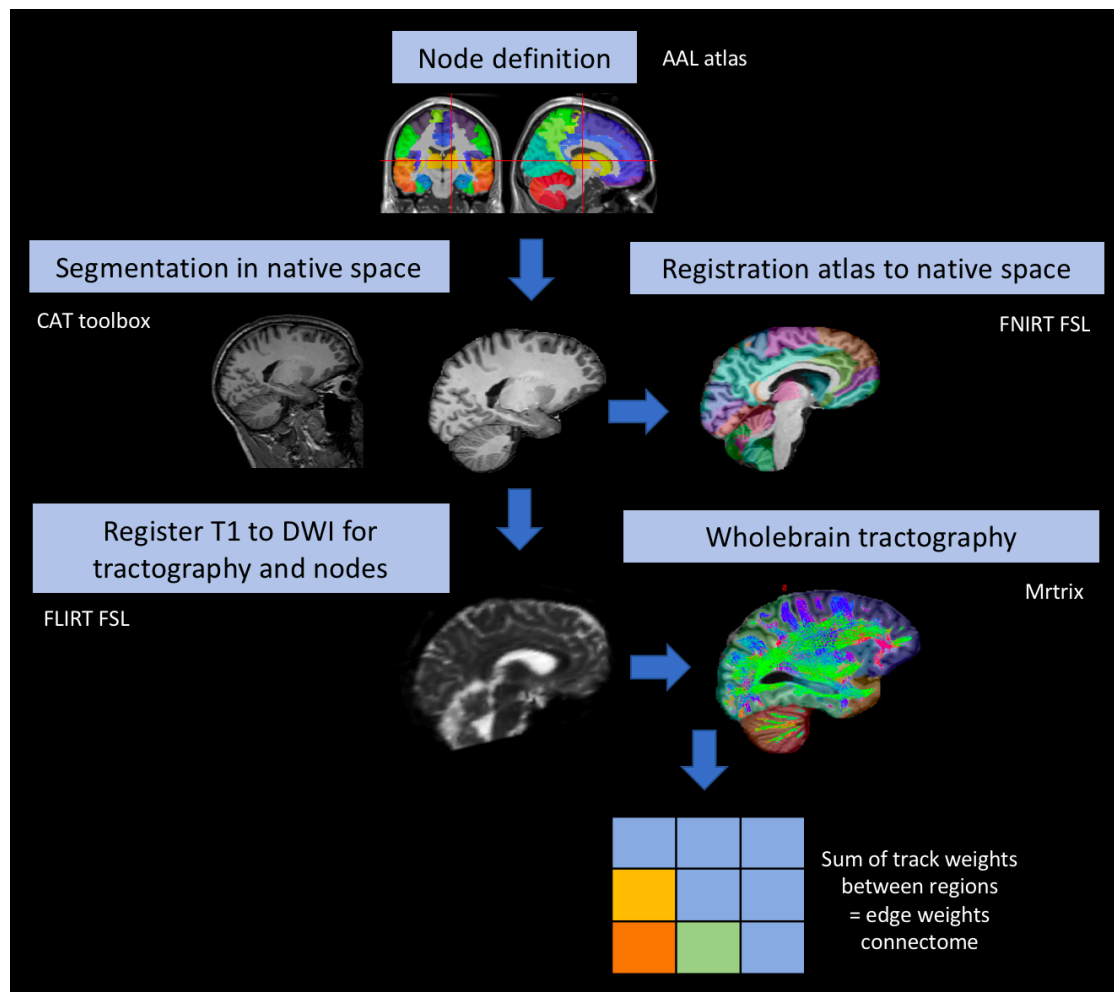
Figure 9.1 Graph construction based on tractography

Note. Structural connectivity graphs were constructed for all participants separately. First, the AAL atlas was non-linearly registered to subject-specific T1-weighted MRI scan. Second, T1-weighted MRI scans were segmented into tissue priors, in order to dissociate white and grey matter. Third, the AAL parcellations in subject space were linearly registered to diffusion-weighted MRI scans in order to dissociated brain regions in diffusion images. Fourth, wholebrain tractography was calculated for preprocessed diffusion-weighted MRI scans. Fifth, based on the regions of the AAL atlas and wholebrain tractography, graphs were constructed (using in-house matlab scripts) based on track weights (calculated using SIFT2). These track weights were then used to calculate graph theory parameters (using the matlab-based Brain Connectivity Toolbox). Graph theory parameters included global efficiency, local efficiency and average nodal strength.

Based on graph theory, a brain network (i.e. graph or connectome) can be constructed consisting of brain regions (so-called *nodes*) and connectivity values (so-called *edges*). The structural organization of the brain is perceived as efficient if a low number of brain regions (nodes) are densely connected to their subnetwork regions (i.e. within-module nodes), which is reflected in high so-called *global and local efficiency* [406].

For each subject, subject-specific connectomes (i.e. connectivity graphs) were constructed (see Figure 9.1). More specifically, to construct these connectomes, the AAL-atlas [407] was nonlinearly registered to individual brain-extracted T1-images, using FSL (mutual information cost function). Once in native space, these were rigidly registered to DWI space (boundary based cost function).

Based on the preprocessed DWI images, 10 million whole-brain tracks were generated using anatomically-constrained probabilistic tractography, based on the FODs [408]. The resulting tractography was further processed using Spherical-deconvolution Informed Filtering of Tractograms (SIFT2)[409], which weighs the tracts proportionally to the entire whole-brain tractography.

To construct the connectivity graph, connectivity (i.e. 'edge') values were calculated for the tracks connecting the supratentorial AAL regions only. These connectivity (i.e. 'edge') values represented the sum of the tract weights (i.e. relative contribution of the tract streamline to the FOD cross-section) [410]. Based on these values, graphs were constructed (using in-house matlab scripts), which were analyzed for graph theory parameters (using the matlab-based Brain Connectivity Toolbox). Graph theory parameters included global efficiency, local efficiency and average nodal strength. Global efficiency is defined as the inverse of the average shortest path length (i.e. number of edges connecting the nodes). Local efficiency is an equivalent measure for specific nodes and its neighbors. Finally, nodal strength is the total connectivity strength of a node (i.e. sum of all edge weights of a node).

These values were compared between patients vs. controls, for a range of network densities, as implemented previously [411].

9.2.3.6 Imaging, radiotherapy and behavior

Subject-specific imaging metrics were extracted from the abovementioned analyses (sections 9.2.3.3, 9.2.3.4, 9.2.3.5). More specifically, these included average FA and average microstructural AFD values of the significant group comparison resulting regions, as well as global efficiency and local efficiency. The latter two values were 'cost-integrated values' as they were averaged across a range of thresholded networks (i.e. network density). The minimal proportional threshold of this range was selected explaining at least 95% of the overall network connectivity for all subjects.

All of these derived final values (i.e. FA, AFD, global and local efficiency) were compared between irradiated (n=13) and non-irradiated patients (n=6), in order to detect the potential impact of radiotherapy. Second, these values were inter-correlated (to check interdependency) and correlated with behavioral subscales within the patient subgroup in order to check functional relevance of these measures. As mentioned in section 9.2.3.1, only most significantly different behavioral subscales between patients and controls were used for the latter analysis.

9.3 Results

9.3.1 Behavioral analyses

As could be inferred from Table 9.2, patients on average scored worse on a wide range of behavioral subscales. Most significant subscales included the intelligence scales acquired using the WAIS-IV, verbal learning and PPVT. In order to restrict the number of tests for associations between neuroimaging and behavior, we correlated the WAIS subscales with imaging metrics in section 9.2.3.6.

Table 9.2 Significant behavioral outcomes for patients vs. controls

Outcome	Patients		Controls		Group comparisons		
	Mean	SD	Mean	SD	*F*	*p*	η^2
WAIS-IV-NL subscale							
FSIQ	80.10	12.73	107.85	14.42	42.79	<.001**	.523
VCI	84.33	15.93	108.55	16.76	22.51	<.001**	.366
PRI	87.52	12.70	108.05	14.35	23.57	.<.001**	.377
WMI	80.90	19.63	103.80	13.98	18.35	<.001**	.320
PSI	78.00	13.87	102.80	13.79	32.95	<.001**	.458
AVLT subscale							
Learning phase	-1.98	1.01	-.875	1.35	8.77	.005*	.184
Delayed recall	-1.53	1.02	-.460	1.58	6.76	.013*	.050
RVDLT subscale							
Learning phase	-1.43	1.47	.376	1.55	14.67	<.001**	.273
Immediate recall	-1.35	1.70	.257	1.61	9.68	.003*	.199
PPVT	88.14	16.59	108.30	11.53	20.21	<.001**	.341
ANT divided attention°							
Reaction time	.64	1.77	-.49	1.17	5.73	.022*	.128
Number of errors	.74	2.01	-.48	.91	6.13	.018*	.136
BRIEF subscale emotion regulation	54.29	12.44	45.70	5.69	7.94	.008*	.169
PedsQL Physical	614.29	165.18	703.75	80.81	4.77	.035*	.109

Note. FSIQ=Full Scale IQ, VCI=Verbal comprehension Index, PRI=Perceptual Reasoning Index, AVLT=Auditory Verbal Learning Test, RVDLT=Rey Visual Design Learning Test, PPVT=Peabody Picture Vocabulary Test, ANT=Amsterdam Neuropsychological Tasks, BRIEF=Behavior Rating Inventory of Executive functioning, SD=standard deviation; * indicates p<.05, ** indicates p<.001, ° divided attention task of the ANT (MSL) with highest memory load, i.e. "look for 3 characters".

9.3.2 Voxel-based

As shown in Figure 9.2, widespread significant group differences were encountered with regard to FA and ADC in patients vs. controls. More specifically, lower FA and elevated ADC were found in white matter areas in patients in the corpus callosum, cortical spinal tract, cingulum and cerebellar tracts.
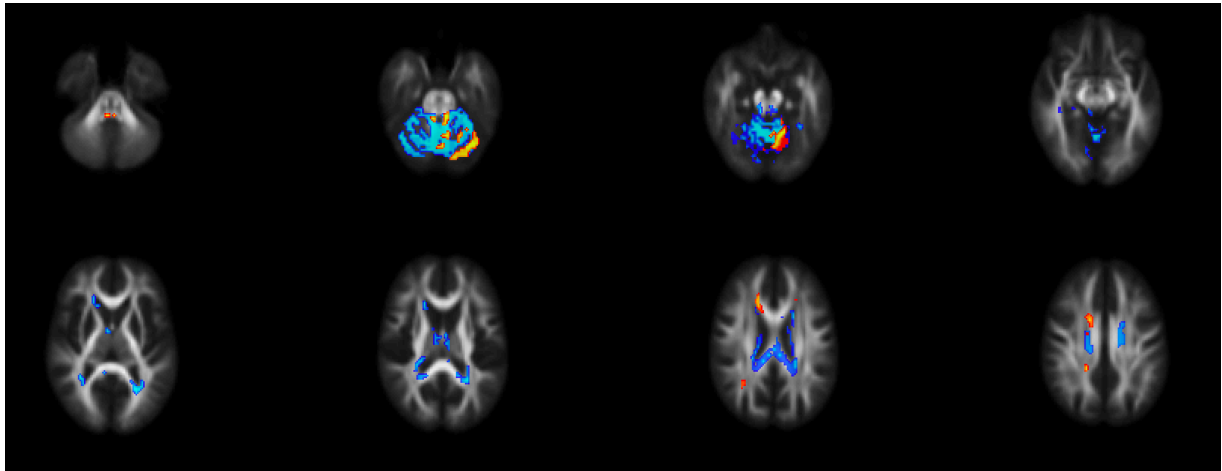
Figure 9.2 Voxel-wise group comparison results (patients vs. controls) FA and ADC

Note. Lower FA (fractional anisotropy) in patients is depicted in orange, higher ADC (apparent diffusion coefficient) in patients is depicted in blue (FWE-corrected, p<.05). No significance was found in the opposite directions.

9.3.3 Fixel-based

By contrast, based on the fixel-based group comparison (see Figure 9.3), microstructural alterations of AFD were found in supratentorial as well as infratentorial brain regions; whereas differences in FC were only encountered in the brainstem and cerebellum (i.e. infratentorial brain areas).
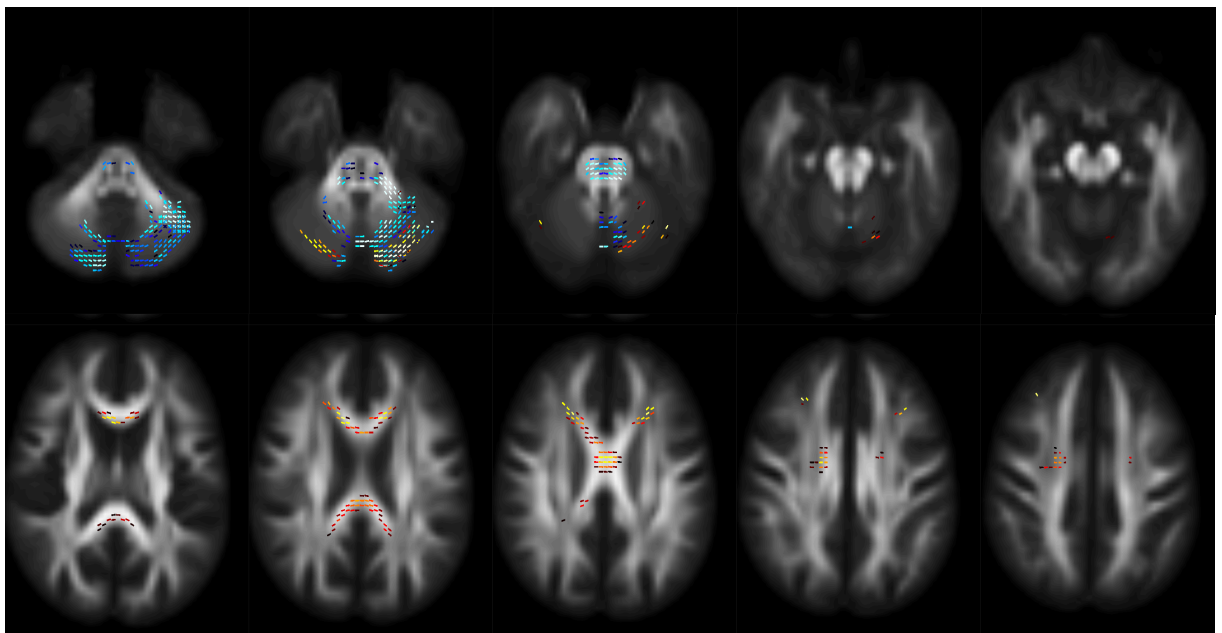

Figure 9.3 Fixel-based group comparison results (patients vs. controls) AFD and FC

Note. Lower AFD (microscopic, apparent fiber density) in patients is depicted in orange, while lower FC (macroscopic, fiber cross-section) in patients is depicted in blue (FWE-corrected, p<.05). No significance was found in the opposite direction.

Table 9.3 Statistical values of voxel- and fixel-based group comparisons

Outcome	Patients		Controls		Group comparisons
	Mean	SD	Mean	SD	Cluster size (# voxels)
Fixel-based analysis					
AFD	.4433	.0122	.5514	.0087	505
FC	.9036	.0393	1.1113	.0141	817
Voxel-based analysis					
FA	.3460	.0080	.4236	.0038	378
ADC	.0011	<.001	.0008	<.001	1762

Note. AFD=Apparent Fiber Density, FC=Fiber Cross-Section, FA=Fractional Anisotropy, ADC=Apparent Diffusion Coefficient. For statistical analyses of FC, logarithmic transformation of the data was performed, as suggested by Raffelt and colleagues. 10914 white matter voxels were included in the group comparison analyses.

9.3.4 Connectome-based

As the network density range of 1-28% explained at least 95% of the overall network connectivity for all subjects (see Figure 9.4), this range was used to calculate subject-specific average ('cost-integrated') values of global efficiency, local efficiency and average nodal strength, across these thresholded stronger networks (i.e. lower network densities). Based on the subject-specific connectomes, global efficiency appeared significantly lower in patients for the entire network density range (see Figure 9.5, panels A). By contrast, local efficiency as well as average nodal strength were also significantly reduced, but only for lower network densities, i.e. only for core network connections.
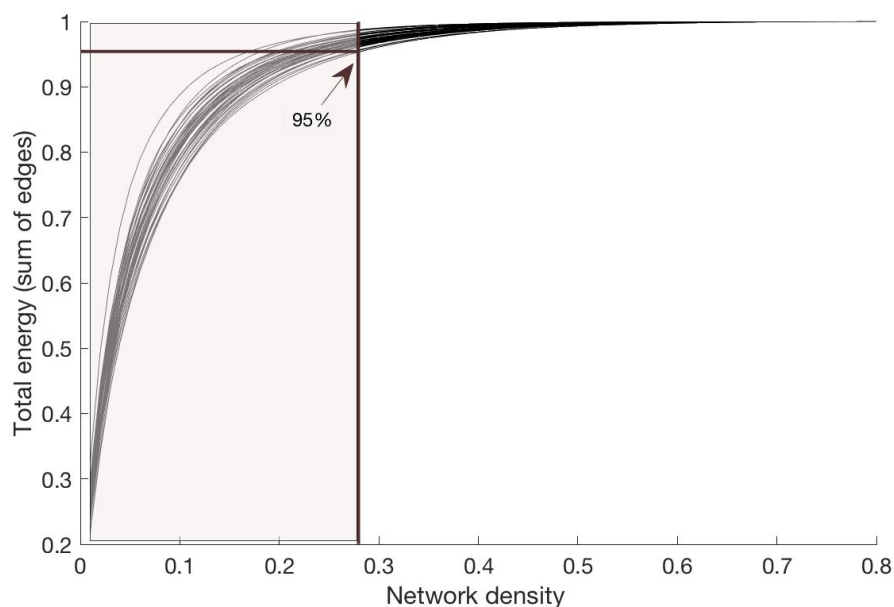
Figure 9.4 Percentage of total energy for each network density

Note. For all subjects, the percentage of energy (i.e. sum of edge weights) is depicted for each network density. The arrow indicates the position where 95% of the total energy is reached for the subject with the lowest energy-cost-function. This value appears to be 28% of network density. Hence, for cost-integrated values, graph theory metrics were averaged across the thresholded networks with 1-28% network density (i.e. area colored in grey).

Consequently, cost-integrated (i.e. averaged across the stronger 1-28% network density thresholds) global and local efficiency were significantly lower in patients in core connectomes (see Figure 9.5, panels B).
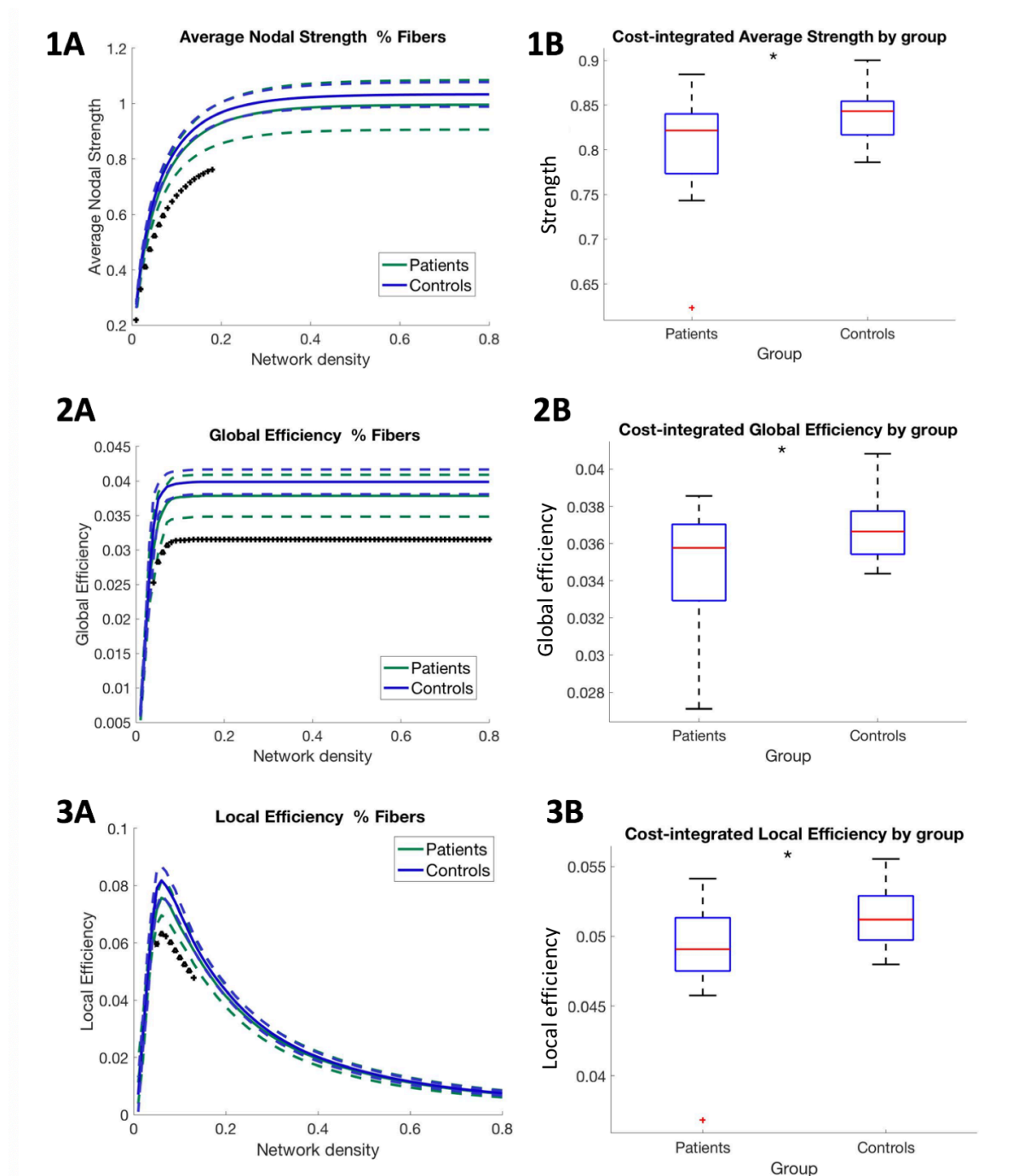
Figure 9.5 Global and local efficiency for each network density

Note. On the left, for each network cost (i.e. the selection of 1-80% strongest connections of the network), average nodal strength values, average global efficiency and local efficiency for each group are represented, in upper, middle and lower panel, resp. Black signs indicate p-values of one-way ANOVAs: + indicates p<.05, ∇ indicates p<.0, * indicates p<.001. On the right, boxplots show the group averages (and deviations) of these values, 'cost-integrated' (i.e. averaged) across the range of low network densities (<.28 network density, i.e. thresholded networks including core connections). For cost-integrated measures of average nodal strength, global efficiency, local efficiency, p-values of one-way ANOVA were *p*=.0289, *p*=.0178, *p*=.0114, respectively (* indicates p<.05).
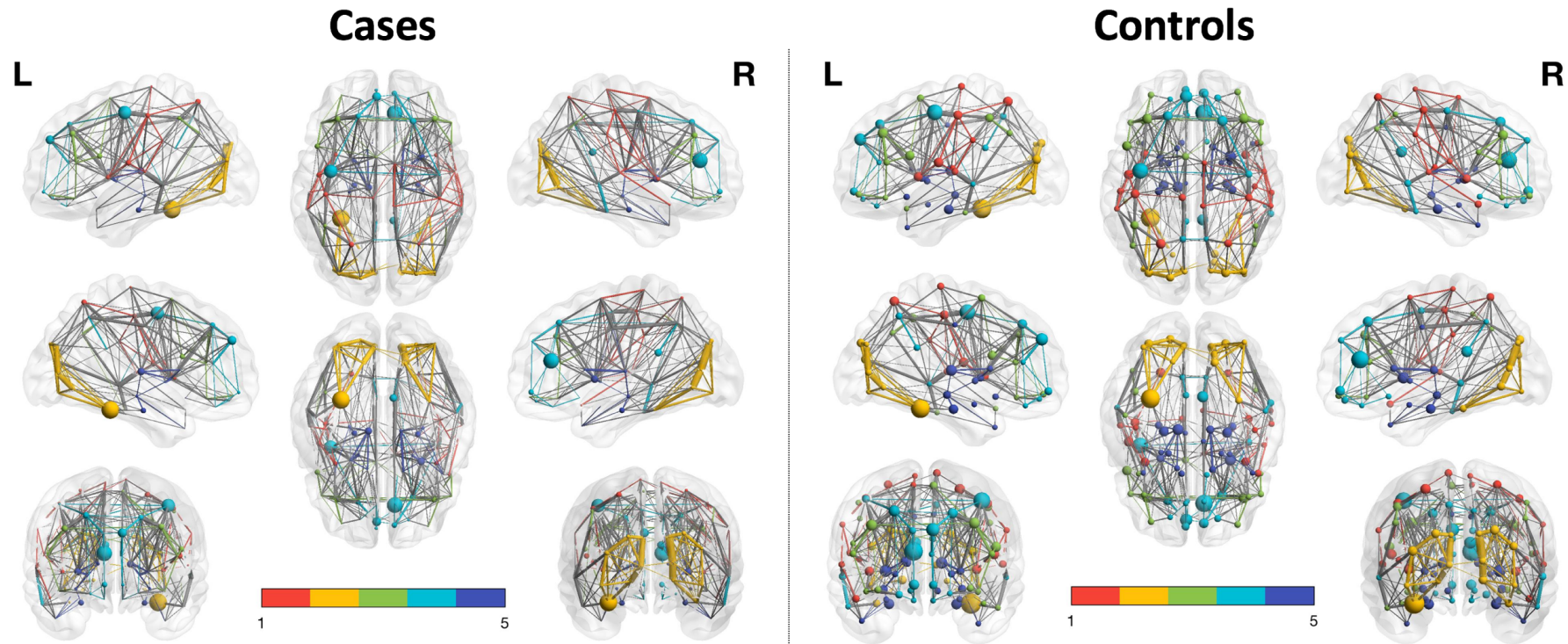
Figure 9.6 Thresholded average structural connectomes

Note. Group average networks based on trackweights between supratentorial AAL-regions (thresholded for 10 % of the strongest connections) in cases vs. controls, in left vs. right panel, resp. Colored modules in this figure were estimated in BrainNetViewer (n=5). Nodal size is proportional to its number of connections. Edge thickness is proportional to the edge value. As could be inferred from this graph, nodes show a lower number of (and less dense) connections in the average network of cases (on the left), compared to controls (on the right) (at network strength of 10%).

Average connectomes for patients and controls are depicted in Figure 9.6. As could be visually interpreted from this figure, nodes clearly appeared less densely connected in patients compared to controls. Although global efficiency appeared lower in patients compared to controls for the entire network cost range, local efficiency was only lower if connectomes were thresholded for subject-specific core (i.e. 'strongest') connections. This could suggest core connections to be (less efficiently) reorganized locally, while non-core (i.e. less dense) connections would not be locally modified in topology.

To investigate the hypothesis of vulnerability at nodal level, nodal strength (i.e. sum of track weights of the node) of all AAL atlas regions in patients vs. controls are depicted in Figure 9.7 . More specifically, all brain regions (nodes) were ordered according to their average nodal strength in healthy controls (i.e. assumed as "healthy regional connectivity strength"). This figure appears to confirm the hypothesis that most of the significant group differences in nodal strength mainly occurred in the regions that were most densely connected in healthy controls (towards the right side of the graph). These more densely connected regions could be viewed as railway stations (or 'hubs' in graph theory).
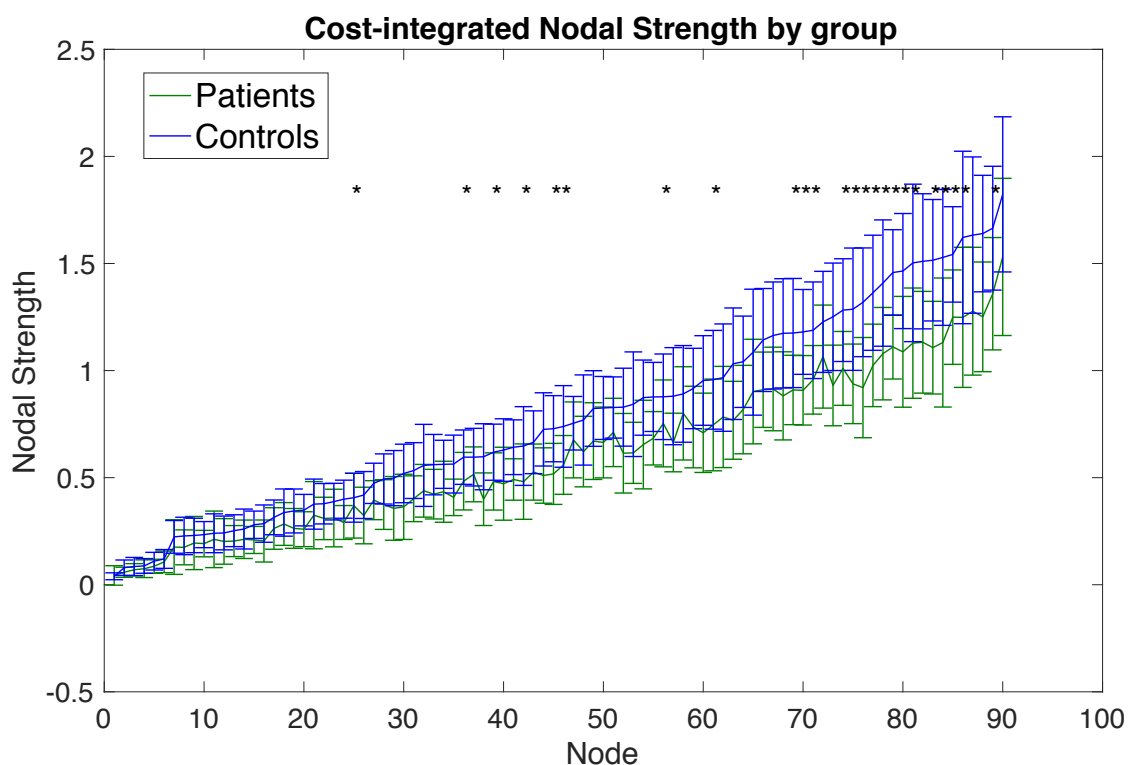
Figure 9.7 Nodal strength ANOVA group comparisons (patients vs. controls), ordered by nodal strength of healthy controls

Note. All 90 brain regions are ordered according to their average strength in healthy controls. Most of the significant group comparison results are located on the right of the graph, suggesting the most densely connected areas to be mostly affected in patients. Furthermore, more variance can be observed in the more strongly connected regions. * indicates $p < .01$, FDR-corrected for 90 nodes.

9.3.5 Imaging and radiotherapy

None of the group comparisons yielded significant differences between irradiated (n=13) vs. non-irradiated (n=6) patients. This was the case for voxel-wise comparisons, nor fixel-based comparisons, nor efficiency measures across density ranges.

Similarly, if we investigated nodal strengths for all atlas regions depicted for irradiated patients vs. non-irradiated patients (see Figure 9.8), one should note that variability in both groups largely overlapped for all of the brain regions, and no significance was encountered. Both groups showed high within-group variability in nodal strength, which appeared most often in patients who had received radiotherapy.
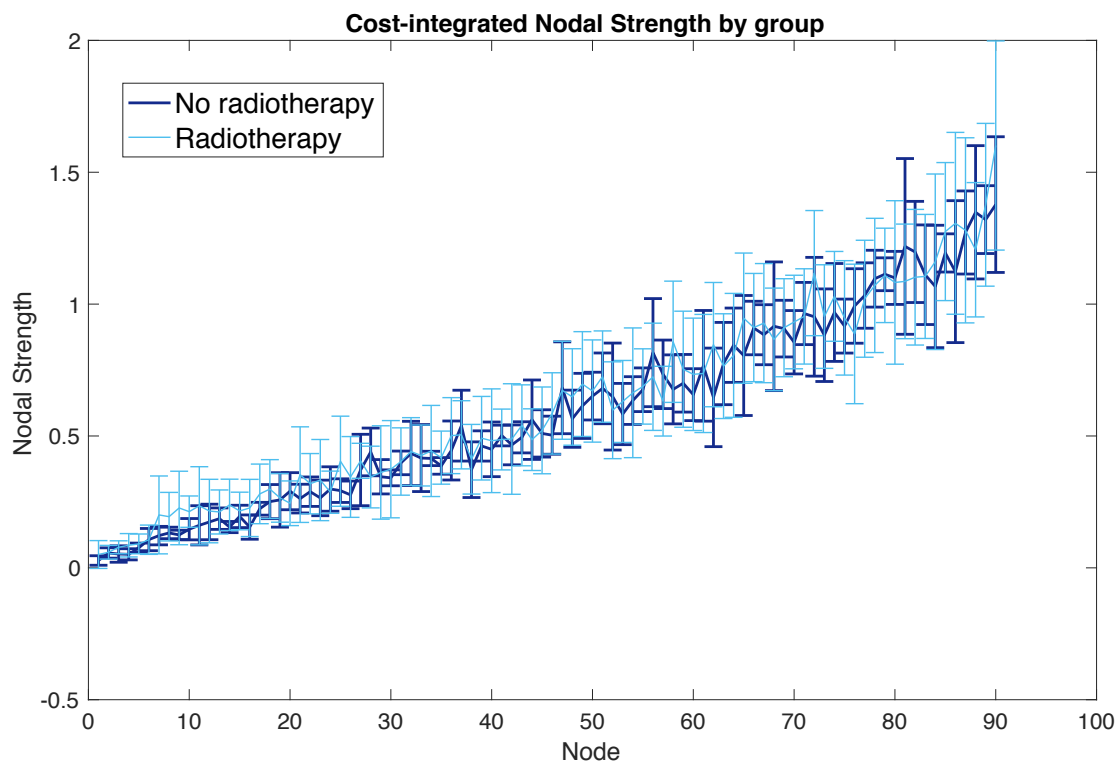
Figure 9.8 Nodal strength ANOVA group comparisons (irradiated patients vs. non-irradiated patients), ordered by nodal strength of healthy controls

However, the abovementioned group comparisons could be less sensitive to significance due to the low number of inclusions, and stringent correction for multiple tests (e.g. voxel-wise). By contrast, if the extracted values of average FA, average AFD (of regions showing significant group comparison results), and cost-integrated global and local efficiency were predicted by RT vs no RT in a basic one-way ANOVA model, a significant association wase found between RT and the diffusion-derived metrics of FA and apparent fiber density (F=6.167, p=.024; F=11.181, p=.004; F=.096, p=.760; F=1.069, p=.316). More specifically, irradiated patients showed lower FA and fiber density in significant regions compared to non-irradiated patients. A linear trend in median values according to cranial RT dose could be visually detected, although not tested due to low subgroup inclusion rates (see Table 9.4).

Table 9.4 Median values of extracted diffusion metrics for controls, and irradiated patient subgroups

Scale	Median values participant subgroups (SD)				
	Controls	0Gy	<23.4Gy	35-36Gy	40Gy
FA significant regions	.4209 (.01)	.3712 (.03)	.3385 (<.01)	.3228 (.03)	.3391 (.05)
AFD significant regions	.5490 (.04)	.4739 (.05)	.4550 (<.01)	.4155 (.04)	.4174 (.11)
Global efficiency	.0367 (<.01)	.0352 (<.01)	.0367 (<.01)	.0358 (<.01)	.0306 (<.01)
Local Efficiency	.0276 (<.01)	.0277 (<.01)	.0275 (<.01)	.0269 (<.01)	.0218 (<.01)

Note. This table demonstrates median values that were extracted from subject-specific diffusion data. Average FA and AFD were calculated for their significant group comparison resulting regions. Global and local efficiency were calculated for each subject-specific connectome (averaged across the 28% strongest thresholded connectomes of the subject = cost-corrected). Subgroups included n=21, n=8, n=2, n=7, n=2 participants in each of the subgroups, respectively. Gy=Gray unit of RT (total cranial dose).

9.3.6 Imaging and behavior

Finally, correlations between imaging extracted values (i.e. FA and AFD of significant group comparison results, global and local efficiency) and WAIS subscales were presented for all participants in Table 9.5. Highest correlations could be observed between diffusion metrics (FA and AFD) and intelligence scores. This was consistent for each of the intelligence subscales (see Figure 9.10). Global efficiency appeared only mildly correlated, while local efficiency was not significantly correlated. Finally, diffusion-derived metrics of FA and AFD were highly inter-correlated, as connectome-based metrics (i.e. global and local efficiency) were as well. As demonstrated in Figure 9.9, AFD seemed to most optimally dissociate non-irradiated, irradiated patients and healthy controls.

Table 9.5 Correlations between diffusion metrics and subscales of the WAIS intelligence test in all participants

Scale	FA significant regions	AFD significant regions	Global efficiency	Local Efficiency
FA	1			
AFD	.893**	1		
Global efficiency	.302	.368*	1	
Local Efficiency	.322*	.382*	.879**	1
FSIQ	.642**	.622**	.362*	.270
VCI	.464**	.473**	.336*	.246
PRI	.606**	.519**	.253	.184
WM	.595**	.560**	.362*	.307
PS	.576**	.638**	.334*	.277

Note. This table demonstrates correlations between the four selected metrics based on the diffusion-weighted MRI data. These metrics include average FA and AFD in the significant regions of the voxel-based and fixel-based group comparisons, respectively; and global and local efficiency (which were integrated across the 1-28% network density range). * indicates p<.05, ** indicates p<.01.
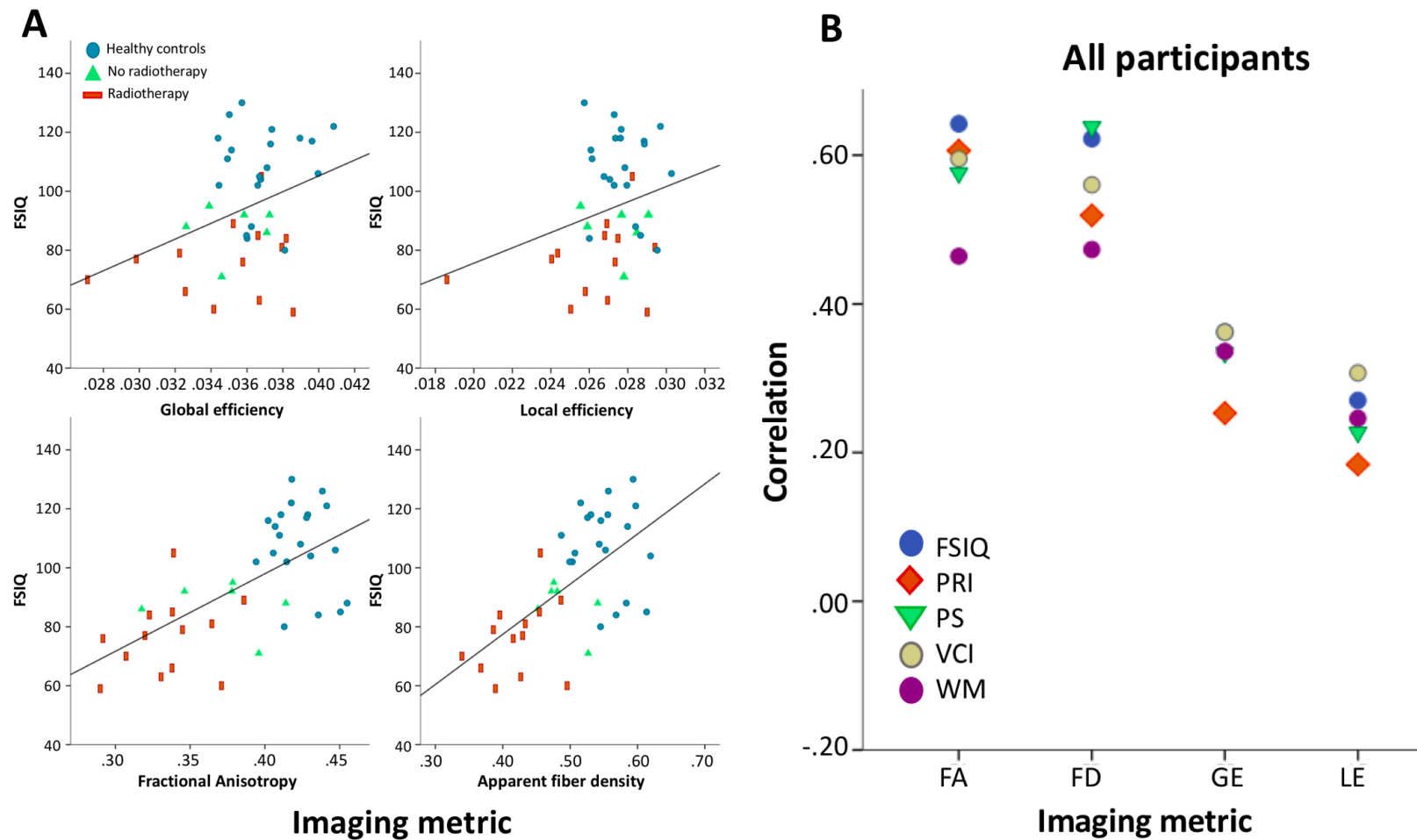
Figure 9.9 Scatterplots and correlations between intelligence and structural connectivity estimated values
Note. This figure presents the estimated linear associations between intelligence scores and diffusion-derived connectivity estimates.
Panel A demonstrates the distributed intelligence scores and derived imaging values. Panel B depicts the correlations between each intelligence subscale and imaging derived metric. FSIQ=Full Scale IQ, PRI=Perceptual Reasoning, PS=Processing Speed, VCI=Verbal Comprehension Index, WM=Working Memory. FA=Fractional anisotropy, FD=Fiber Density, GE=Global Efficiency, LE=Local Efficiency.

Figure 9.10 Scatterplots of intelligence subscale scores and imaging metrics
Note. This figure demonstrates all distributions of intelligence subscale scores and diffusion-derived connectivity estimated values. VCI=Verbal Comprehension, PRI=Perceptual Reasoning Index, WM=Working Memory, PS=Processing Speed.

9.4 Discussion

Using a multi-modal analysis approach, we evidenced white matter microstructural changes and possibly supratentorial reorganization in survivors treated for infratentorial tumors during childhood. Voxel-based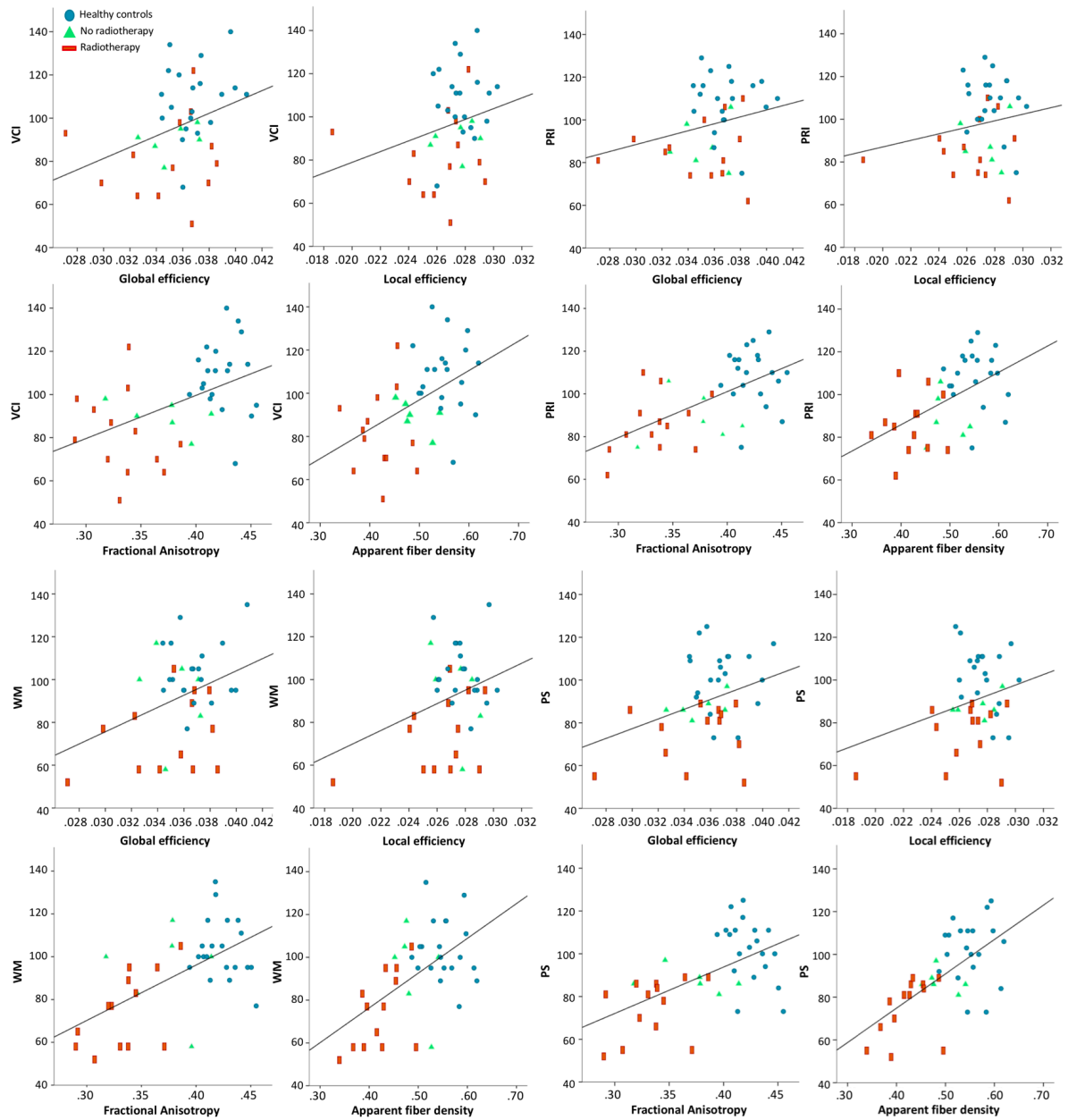 group comparisons yielded widespread group differences with higher ADC and lower FA in survivors compared to controls. By contrast, fixel-based analyses evidenced widespread lower fiber density across the brain, whereas lower fiber cross-section was only present in infratentorial areas (brainstem and cerebellum). Finally, using graph analysis, global efficiency appeared lower in patients for any network cost, while local efficiency of regions appeared only reduced for core connections (i.e. thresholded connectomes for highest network densities). More specifically, at sub-regional level, nodal strength appeared significantly lower in patients for the most strongly connected brain areas (i.e. *hubs*). Finally given the high correlations between voxel- and fixel-based 'integrity' estimations (i.e. FA and AFD), these values could be assumed as cognitive outcome predictors, albeit with possibly the *hub* areas being the most important.

From voxel-based to connectome-based

Studies previously evidenced a wide range of long-term behavioral impact of a brain tumor and its treatment [412,413]. From a localism perspective, multiple neuroimaging studies investigated lesion-symptom mapping, in order to associate the brain lesion with behavioral outcomes. In this regard, voxel-based lesion-symptom mapping was one possible approach, meaning that behavioral outcomes were predicted by each voxel of the remaining lesion or cavity [381]. Nevertheless, *the diaschisis hypothesis* now became common sense, which states that secondary brain damage in another brain region could occur due to underlying brain connectivity and dynamic interactions between brain areas [382]. In this context, earlier diffusion-weighted MRI studies demonstrated white matter alterations also in supratentorial brain regions in long-term survivors of infratentorial tumors [414,415], even in non-irradiated patients [416].

The question which brain areas are mostly affected, highly depends on the underlying toxic mechanisms, for which the applied modalities could provide complementary information. More specifically, applying a voxel-based or fixel-based approach, yielded widespread differences in FA and AFD, respectively. However, in contrast to the voxel-based approach, the fixel-based approach appeared capable of dissociating microstructural (fiber density) from macrostructural (fiber cross-section) changes. In contrast to widespread differences in microstructural changes (AFD), macrostructural brain changes only appeared in the cerebellum and brainstem (i.e. where the remaining lesion is located). This might demonstrate the validity of using the fixel-based analysis for dissociating microstructural and macrostructural changes of the white matter [283].

Nevertheless, both voxel-based and fixel-based approaches use a tensor or FOD model which estimate microstructure on a voxel-based-level. These approaches do not investigate brain topology or network organization. To address topology, recent graph theoretical approaches are increasingly implemented [406]. As recently suggested by Gleichgerrcht and

colleagues (2017), such approach could become specifically informative in case of observable neural damage [381]. To our knowledge, this the first study investigating supratentorial structural subject-specific connectomes in infratentorial tumor survivors.

This study demonstrated lower efficiency in patients compared to controls, at global as well as local level. This suggests that not only overall whole-brain connectivity is lower in patients, but also that the extents of such effects are different across brain areas, leading to local restructuring. More specifically, we observed that global efficiency of structural networks was diminished in survivors of childhood infratentorial tumors, independently from the overall network strength. By contrast, local changes depended on the extraction of networks at different density levels. Local efficiency and average nodal strength were significantly lower in patients when only considering core connections (<28% of network density), suggesting a local reorganization of the strongest connections.

We also demonstrated that the most densely connected regions (possibly so-called hubs), were most significantly lower in patients at nodal level. These findings are in line with previous studies, which suggest that global disorders and/or induced toxicity predominantly affect highly connected hubs, given that hubs are assumed to process most of the information [397]. Hence, these brain areas could possibly be important to spare with regard to radiotherapy and/or neurosurgery. Similarly, voxel-based and fixel-based comparisons also often yield highest significant group differences in regions that show highest 'integrity' or 'connectivity' estimates in healthy controls (e.g. regions with highest FA or highest AFD, resp.). However, densely connected regions (hubs) often contain multiple crossing fiber populations, which is problematic for voxel-based estimations (e.g. FA). Therefore, to estimate white matter connectivity in crossing fiber populations, nodal strength (as a sum of weights of tracts through the area) could partly solve this issue.

Cranial radiotherapy (and chemotherapy)

To date, cranial radiotherapy is strongly assumed to be neurotoxic in brain tumor patients [417]. In infratentorial tumors specifically, the medulloblastoma subgroup is known to experience such RT-induced neurocognitive problems [418]. However, for none of the voxel-based, fixel-based or graph theory measures, group differences appeared between irradiated (n=13) vs. non-irradiated (n=6) patients. Similar to these findings, Rueckriegel and colleagues (2010) also evidenced patterns of lower FA in non-irradiated (astrocytoma) survivors compared to irradiated (medulloblastoma) survivors of infratentorial tumors [416].

However, the numbers of inclusions in our subgroups are low, and the patient subgroup who received cranial irradiation showed high variability in nodal strength. Furthermore, the higher variability in nodal strength in irradiated patients could be due to subject-specific factors including age at irradiation and craniospinal RT doses, which might influence vulnerability of specific regions. Still, using a simple one-way ANOVA statistical model predicting the average imaging metrics by RT vs. no RT (instead of a voxel-wise comparison), did yield lower FA and fiber density in irradiated patients compared to non-irradiated patients, and a negative linear trend in these values associated with RT dose was observed. Similar to this finding, earlier

studies also evidenced lower FA in medulloblastoma patients specifically, who receive RT [415,419–423]. In addition to these earlier findings, our study suggests infratentorial tumor survivors to be at risk for white matter damage, not merely due to RT, but probably with an increased risk. We also note that although RT vs. no RT did not show differences in global and local efficiency, the patients who received highest craniospinal RT dose (40Gy) demonstrated the lowest efficiency scores. A specific minimal amount of radiotherapy might thus still result in reorganization of the connectome. Future larger sample studies will be required to confirm this hypothesis.

Finally, we focused on diffusion-weighted MRI and applicable models. Nevertheless, we need to mention that leukoencephalopathy was again detected on T2-FLAIR scans in some patients (ratings were included in the demographics table). Most extensive lesions were found in patients who had received cranial radiotherapy, as well high-dose MTX and intraventricular MTX (Fazekas>1, n=3). This is in line with our previous non-CNS tumor studies. However, the number of cases showing clear lesions again remained too limited for advanced neuroimaging group comparisons.

Functional relevance of imaging metrics

Multiple treatment-related risk factors in infratentorial tumor patients are associated with decreases in cognition, including post-surgical sequelae (e.g. *posterior fossa syndrome*) [412], chemotherapy- and radiotherapy-induced (leuko-)encephalopathy, as well as connectivity changes due to the remaining lesion. Each of these treatment constituents may result in widespread brain injury and impair maturation, leading to long-term behavioral difficulties across a wide range of neurocognitive domains.

At group level, we demonstrated patients to score lower on a wide range of neurocognitive tests. Earlier, Reddick and colleagues (2003) suggested that white matter damage initially leads to decreased attentional functioning, which then results in secondary neurocognitive difficulties in brain tumor patients, including decreased full scale intelligence [364]. Recent neuroimaging techniques to investigate white matter microstructure and structural connectivity are therefore highly recommended in this population [413].

Given that FA, AFD and nodal strength were lower throughout the brain, but not restricted to a specific brain area, this suggests global decreased integrity. These values of integrity were most strongly correlated with all intelligence subscales, while global and local efficiency measures were only mildly or not significantly correlated, respectively. Low variabilities in the latter measures could have contributed to their low correlations. Furthermore, the graph-derived connectivity measures, were at network level (i.e. global and local efficiency). However, at nodal level, we demonstrated the possible vulnerability of hubs, which could be specifically important in functional outcomes. Hence, the link between nodal values of integrity (particularly in hubs) (e.g. based on FA or AFD) and behavioral outcomes could become more informative in future studies. Still, correlations between nodal values of hubs (e.g. nodal strength, nodal degree) and behavior requires additional nodal investigations in order to determine the most 'important' or meaningful nodes (e.g. additional graph-derived estimations of betweenness and centrality to define hubs, based on topology).

<u>Limitations and future directions</u>

This study was performed to investigate the possible reorganization after extensive neural damage, and vulnerability of specific regions due to treatment. However, we note that the sample size of our groups remained relatively small, and treatments during childhood were heterogenous. The treatments of participating patients included neurosurgery in all cases, additional cranial radiotherapy in most cases (n=14), and additional chemotherapy in multiple cases (n=9)). Given that the patient population experiences a wide range of treatment-related side effects, multiple subject-specific risk factors could be hypothesized, including chemotherapy-induced leukoencephalopathy, age at diagnosis, RT dose, treatment subgroup, post-surgical complaints, hormonal deficiencies, etc. Therefore, larger multi-center sample populations are required to apply more complicated statistical models (e.g. mediating factors or interactions), in order to detect patients who are most at risk for reorganization of the network. Furthermore, longitudinal designs are recommended to dissociate the partial impact of each treatment constituent (i.e. surgery, chemotherapy and radiotherapy).

Finally, this study focused on structural connectivity in infratentorial tumor survivors. Although we correlated these structural metrics with behavioral outcomes, this study did not include functional MRI imaging. Integrating the link between structural and functional connectivity would be an intriguing next step in this research domain. Additionally, hubs might specifically need more attention for integrity estimations.

9.5 Conclusion

In summary, widespread microstructural changes were evidenced in supratentorial brain areas in survivors of infratentorial tumors. Besides such widespread changes, our study also suggests possible topological reorganization. This study highlights the complementarity of neuroimaging analyses in case of extensive neural damage. Earlier studies in infratentorial tumors consistently applied voxel-based approaches demonstrating lowered FA, but both recent techniques of fixel-based analysis and graph theory applications added new information to these findings. Fixel-based analyses enabled us to dissociate macrostructural brain alterations (fiber cross-section) that occur in infratentorial brain areas, and microstructural (apparent fiber density) alterations that occur throughout the brain. In addition, graph theoretical analyses evidenced global reorganization in survivors, whereas local reorganization mainly occurred in core connected regions, which might suggest specific vulnerability. Such supratentorial brain alterations and regional vulnerability is highly relevant for the impaired neurocognitive performance which is frequently observed following treatment for childhood infratentorial tumors.

<div style="border:1px solid #888; padding:1em;">

10

General discussion and future perspectives

</div>

The main aim of this doctoral research project was to explore potential neurocognitive and structural and functional brain changes after multi-agent chemotherapy (including high-dose agents) in childhood cancer. By combining neurocognitive assessments, genetic polymorphism analyses, clinical (treatment and symptom) features and advanced neuroimaging techniques in pediatric oncology patients, survivors, and matched healthy control participants, we aimed to discover new insights into neurodevelopmental patterns and related biomarkers during childhood cancer. This was an innovative project as childhood non-CNS tumor patients were investigated, compared to earlier studies in brain tumors and leukemia patients treated with CNS-directed prophylaxis (cranial irradiation and CNS-directed chemotherapy). By implementing extensive neurocognitive test batteries and advanced MRI neuroimaging, this project provided new insights into potential pathological pathways. In this discussion, we first review the main findings of our studies and link these with earlier findings. Second, we discuss current limitations and provide recommendations for future research directions.

10.1 Acute and long-term neurotoxicity in childhood cancer patients

At the start of this PhD project an extensive literature study was performed to summarize the existing evidence for chemotherapy-induced neurotoxicity in childhood non-CNS tumors. Based on these findings, it was hypothesized that high-dose chemotherapy could induce neural changes, and potential neurocognitive deficits. Most studies evaluating the impact of chemotherapy only were previously performed in ALL patients. Hence, in this doctoral project previously acquired longitudinal assessments in ALL patients were analyzed. This study showed that patients obtained IQ-scores within the normal range (**Chapter 4**), but younger patients and lower education of parents were associated with lower IQ scores, which might highlight a stronger impact of the disease and/or treatment. These findings were in line with previous studies [35,218]. Although these patients were treated with chemotherapy only (including high-dose methotrexate, no RT), leukemia is known to potentially invade the CNS system (i.e. lead to brain metastases). Therefore, leukemia patients receive CNS-prophylaxis in addition to intravenous chemotherapy (i.e. intrathecal methotrexate to date).

Given the findings of our literature review, it was remarkable that no neuroimaging, nor neurocognitive investigations were available in childhood non-CNS tumor patients who were treated with non-CNS-directed, high-dose intravenous chemotherapy only. Therefore, we performed three neuroimaging analyses in a cohort study of adult survivors of childhood solid sarcoma. In summary, we demonstrated both functional and structural brain changes occurring in survivors of pediatric cancer, even after high-dose intravenous chemotherapy without CNS

prophylaxis. These analyses demonstrated observable leukoencephalopathy (based on T2-FLAIR images), widespread microstructural white matter changes with strongest findings in the corpus callosum (based on DWI imaging), and frontal and parahippocampal cortical changes (in **Chapter 5, 6 and 7**, respectively). Such alterations could partly explain long-term neurocognitive as well as emotional daily life complaints of patients who were treated with intravenous chemotherapy during childhood.

Is (non-CNS-directed) intravenous chemotherapy neurotoxic in childhood sarcoma patients?
Single case reports previously evidenced acute leukoencephalopathy due to high-dose intravenous chemotherapy in childhood cancer patients [233]. Similarly, we encountered acute leukoencephalopathy in 50% of the currently included childhood non-CNS tumor patients (**Chapter 8**). However, persistence of these lesions remains unclear. We demonstrated that such leukoencephalopathy was still visually detectable in 27% of our survivor cohort multiple (2-20) years after treatment (**Chapter 5**). Although risk factors could only be limitedly explored given the low number of inclusions, administration of high-dose MTX appeared to result in the highest levels of lesions (i.e. Fazekas 2 and 3). Still, in case of administration of chemotherapeutic regimens containing alkylating agents but no MTX, younger patients were also suggested to be at risk for leukoencephalopathy (albeit showing more subtle lesions). The association between these lesions and diffusion metrics, could suggest multiple underlying pathological processes, including white matter organizational changes, but also cerebrovascular damage, which could both explain decreased processing speed [258]. The question if and why exactly younger patients could indeed be more vulnerable (possibly 'growing into deficit') for such long-term leukoencephalopathy, requires larger sample studies, and neurobiological developmental studies.

Which white matter microstructural alterations occur after high-dose chemotherapy?
Although the percentage of encountered leukoencephalopathy (i.e. 27%) was remarkable, the question remains whether more subtle brain alterations occur due to high-dose chemotherapy, even if lesions are not visually detectable. Advanced neuroimaging techniques currently deliver the opportunity to estimate white and grey matter differences at microscopic (i.e. voxel) level, which are not easily visually observable.

Using advanced DWI methods, we showed that such microstructural changes could occur throughout the brain, but that the measure of fiber density was specifically altered in centrally located WM bundles (**Chapter 6**). Based on the DTI model, previous studies also reported heterogenous findings with diffuse patterns of microstructural changes in survivors of childhood ALL [268,419], medulloblastoma [267], and adult solid non-CNS tumors [155,235]. By contrast, our study demonstrated the added value of applying more advanced diffusion models (i.e. CSD), compared to the previously applied models (i.e. DTI) [155,424]. Specific vulnerability of central white matter bundles (e.g. such as the corpus callosum) to loss in tract density, could be attributed to their high level of myelination and susceptibility to inflammatory processes [296]. Given that chemotherapy was associated with both processes in histological research [425,426],

we concluded the corpus callosum to be specifically sensitive to such neurotoxic mechanisms [156].

Which grey matter (structural and functional) alterations occur after high-dose chemotherapy?

In addition to the advanced analyses of white matter microstructure, investigations of the grey matter in these adult survivors of childhood non-CNS tumors, (using T1-weighted MRI and Rsfmri) provided interesting and new findings regarding cortical thinning and altered functional coherence throughout childhood neurodevelopment (**Chapter 7**). This study demonstrated reduced cortical thickness in frontal areas and the parahippocampal region, while frontal and cerebellar regions also showed lower cortical density.

Given that these findings were different either including the covariate of depression or not, we suggested the possibility of the *double hit hypothesis* [334]. This hypothesis states an increased impact of treatment-induced neurotoxicity in case of more stress- or depressive symptoms. The parahippocampal area could specifically be vulnerable to this double hit, given its high level of glucocorticoid receptors. Previously, Kesler and colleagues (2013) also demonstrated increased inflammatory levels (peripheral cytokines) and reduced hippocampal volume in breast cancer patients [96]. Furthermore, our study demonstrated lower functional nodal strength of this region, which could play a role in behavioral outcomes. If indeed treatment-related toxicity could be amplified by stress, emotional coping mechanisms of the child will become important to assess in similar future studies.

White and grey matter findings: neural cascade effects from (age-dependent) primary hits to extended damage?

Across the described neuroimaging studies, multiple imaging parameters (estimating specific structural or functional information of the tissue) appeared significantly different between patients and healthy controls in multiple brain areas.

First, the load and distributions of lesions in patients showing leukoencephalopathy appeared very heterogenous (**Chapter 5, Chapter 8**). Subject-specific biological mediators that could play an important role in leukoencephalopathy occurrence (and extent), can include metabolism alterations [259], inflammatory processes [259], vascular supply [378], ... It could be hypothesized that due to such underlying mechanisms, other neurodevelopmental patterns are affected with possible delay. Delayed long-term neurological outcomes could include decreased white and grey matter density in survivors, with specific initial targets (or 'hits').

Group comparisons of white matter microstructure (estimated with FA, based on the DTI model) demonstrated diffuse patterns of affected regions in patients. However, if more stringent statistical thresholds are applied, remaining significant regions mainly cover regions with high 'density' estimates (**Chapter 6**). Mainly the corpus callosum remained significant both in DTI-derived FA and CSD-derived fiber density. Many of the earlier mentioned adult DTI studies also provided evidence for decreased integrity of the corpus callosum [235,260,268]. This is not only a large fiber bundle, which elevates the risk of showing significant results statistically. The high level of myelination and fiber density of this fiber bundle might also result in specific

biological vulnerability of oligodendrocytes [83]. Similar to these findings in sarcoma survivors, we investigated fiber density in supratentorial brain areas in posterior fossa tumor survivors (**Chapter 9**). Although these patients show even lower values in fiber density throughout the brain (compared to non-CNS tumor patients), fiber density of the corpus callosum again remains most significantly altered if stronger statistical thresholds would be applied.

Concordant with the hypothesis of specific 'hits' or vulnerability of most dense structures, so-called 'hubs' (from a graph theoretical approach) are hypothesized to be affected the most. Recently, graph theoretical studies suggested specific vulnerability of such regions, since they process most of the information and could be viewed as important 'railwaystations' [397].

With regard to grey matter investigations, we encountered frontal cortical thickness to be different between patients and controls, after correction for depression (parahippocampal areas did not remain significantly different) (**Chapter 7**). The orbitofrontal brain area specifically appeared to correlate with age at diagnosis. This was the only age-at-diagnosis-related imaging finding across all studies. It could be hypothesized that brain regions which are most vigorously developing within specific age ranges, could specifically be vulnerable (and region of 'hit') to toxicity [176]. Given that the majority of these non-CNS tumor patients were adolescent during treatment, the neurotoxic 'hit' could be frontal brain areas in particular.

Other oncology patient populations have different median ages at diagnosis, for whom other brain areas could become more vulnerable to toxicity. Across the studies that were discussed in this project, median ages at diagnosis of included patients were 4 (range 2-12) years in childhood leukemia patients, 13.32 (4-18) years in solid non-CNS tumor survivors, and 7.8 years (2.8-18.4) years in infratentorial CNS tumor patients. As could be inferred, ages at diagnosis strongly relate to the specific type of cancer diagnosis and its treatment. In other words, specific cancer diagnoses occur more frequently within certain age ranges, compared to other cancer types. Even though age of brain injury is known to affect the impact of the injury on specific neurobehavioral outcomes, time-dependent neurotoxic effects of specific treatments are challenging to address. The neurotoxic 'hits' could be age-related, and even more, these could hypothetically be age-depending 'railwaystations' or 'hubs'.

Although earlier studies provided evidence for younger ALL patients to be more at risk for cognitive deficits (after cranial RT [35] or CNS-directed chemotherapy in ALL patients [219] (**Chapter 4**), age-dependent brain tissue- and region-specific developmental patterns are to be unraveled in more detail. Only then we will be able to estimate age-dependent vulnerability of more specific neurocognitive functioning, given the complicated neurobiological processes of brain development.

When does neurotoxicity occur, and is recovery possible?

Based on the survivor cohort study, we did not encounter a relationship between visually detectable leukoencephalopathy and time since diagnosis (**Chapter 5**). Even more, the highest lesion load (Fazekas 3) was encountered 8 years after treatment. By contrast, fiber density of the central white matter tracts did positively correlate with time since diagnosis, which could suggest recovery or 'catching up' patterns in diffusion metrics (**Chapter 6**). In contrast to

observable lesions in FLAIR images, underlying microstructural changes might thus still recover to normal (age-dependent) values. With regard to grey matter cortical thickness, no association with timing was found, which could suggest less plasticity. Given that developmental patterns of white and grey matter are highly different, microstructural stability and plasticity of these tissues could be rather distinct [427].

Although these cross-sectional data evidenced long-term neurotoxicity related to high-dose intravenous chemotherapy, we could not investigate fluctuations in microstructural changes throughout time, nor could we dissociate treatment from disease effects. No pre-treatment data were available in our cross-sectional survivor cohort study. To address time-dependency of lesions, longitudinal designs are required.

Two previous longitudinal diffusion MRI studies in adult solid tumor patients demonstrated decreases in diffusion metrics (e.g. FA) during the first months after treatment [235,355]. However, recently Billiet and colleagues (2018) expanded these findings showing recovery 3-4 years after treatment [260]. By contrast, longitudinal neuroimaging studies were not yet performed in current childhood non-CNS tumor patients.

By implementing a longitudinal design (**Chapter 8**), we demonstrated acute leukoencephalopathy at the end of treatment in multiple cases. However, the few cases for whom an MRI scan was acquired one year later, showed less extensive lesions, although Fazekas ratings remained stable. This could suggest that recovery indeed occurs, but such recovery is only subtly visible on FLAIR MRI scans. To investigate microstructural developmental patterns in more detail, more advanced analyses of MRI scans (e.g. including quantitative volumetric measures) could add such information in future studies. Such quantitative measures would be less rater-dependent than lesion classifications. Furthermore, based on DWI, VBM or SBM analyses, underlying microstructural changes or recovery of the white or grey matter could additionally be detected (e.g. fiber density, grey matter density, cortical thickness, ...), even in case of no observable leukoencephalopathy. Toxicity-induced changes in neurodevelopment of such microstructural properties, are still to be investigated in future studies.

What is the neuropsychological impact?
The different imaging modalities applied in non-CNS tumor survivors mainly showed associations between the derived imaging metrics (i.e. lesion load on FLAIR images (**Chapter 5**), fiber density of the corpus callosum in DWI (**Chapter 6**), parahippocampal nodal strength in Rsfmri (**Chapter 7**)) and attention- or processing speed-related subscales. Most evidence for cognitive dysfunction in adult cancer patients also exists for lower processing speed [176,214].

More specifically, patients with leukoencephalopathy showed longer reaction times on computerized attention tasks. This finding is concordant with the attentional model of Reddick and colleagues [364], stating that white matter damage initially leads to decreased processing speed, and other neurocognitive outcomes could be affected in a secondary stage. Similarly, microstructural fiber density of the corpus callosum was primarily related to the processing speed subscale of the intelligence assessment (not to other cognitive measures). Given the

association between leukoencephalopathy and diffusion metrics, their associations with attentional functioning are largely interdependent. On the other hand, this finding might suggest that even if no leukoencephalopathy is visually detected, a linear relationship could exist between more subtle microstructure changes (diffusion metrics, e.g. fiber density) and attentional scores. In this regard, previous diffusion-weighted MRI studies in cancer patients, also evidenced such linear associations with decreased attention and executive functioning in leukemia patients [268], as well as in breast cancer survivors [23].

These two abovementioned studies only covered structural information of the white matter. However, functional neuroimaging adds information of brain activity, and functional coherence ('collaboration') of multiple brain regions. Based on the RsfMRI data, we encountered an association between the parahippocampal functional strength and processing speed. Given that not only structural, but also functional coherence appeared associated with processing speed, either initial sensitivity of attentional functioning or common underlying pathways could be inferred. In this context, one previous survivor study of leukemia patients demonstrated lower functional connectivity of attention-related networks in patients, which could explain such behavioral effects in processing speed [170].

Lesions and targets of neurotoxicity: how to optimize neuroimaging in case of neural damage?
Clear lesions or observable brain damage induced by cancer treatment or CNS tumor processes, can highly influence advanced (microstructural) neuroimaging analyses. We demonstrated visually detectable leukoencephalopathy after high-dose chemotherapy, which is correlated with diffusion metrics (in **Chapter 5**). Hence, also advanced group comparison analyses are associated with such lesions (as performed in **Chapter 6**).

Furthermore, although hemodynamic changes were evidenced in multiple cancer studies using fMRI [161,170,428], limited research currently exists with regard to chemotherapy-induced microbleeds or vascular angiopathy. Still, susceptibility-weighted MRI (SWI) scans previously demonstrated chemotherapy-induced small vessel disease in breast cancer patients [378], as well as radiation-induced microbleeds in nasopharyngeal tumors [429]. In case of such microvascular damage, each of the microstructural neuroimaging findings which were encountered (i.e. leukoencephalopathy on FLAIR scans, microstructural changes measured by DWI, and T1-weighted intensities), as well as the neurovascular coupling (fMRI) could be affected [430].

Concludingly, quantitative measures of such observable lesions (e.g. leukoencephalopathy and/or microbleeds) based on clinical MRI scans (such as FLAIR and SWI), and their link with advanced analyses will become highly valuable in future advanced neuroimaging studies. To address primary targets or 'hits' of toxicity, the imaging information from these modalities is ideally combined.

To integrate structural and functional information of the brain, approaches such as graph theory could provide a possible solution, given that networks can be constructed with structural as well as functional connectivity estimates. In adult survivors of non-CNS tumors (**Chapter 7**), we encountered decreases in functional coherence, but not profound

reorganization of the functional network (i.e. no differences in global or local efficiency with healthy controls). This was in line with previous adult non-CNS cancer studies [355,431]. By contrast in case of clear neural damage (e.g. infratentorial tumors), graph theoretical analyses provided evidence for topological reorganization, in addition to global decrease in integrity (**Chapter 9**). This was mainly the case in most densely connected regions which might suggest specific vulnerability of these regions. Therefore, future studies are recommended to investigate the importance of so-called 'hubs', if these are also related to visually detectable lesions (i.e. microbleeds and/or leukoencephalopathy), and if they finally also appear most functionally relevant in daily life. Given that the absolute number of cases showing leukoencephalopathy in our studies remained limited, graph theoretical approaches in these patients were not explored yet. Still, to investigate profound reorganization of the network, and vulnerability of 'hubs' might particularly become important in larger populations showing such lesions.

10.2 Future directions

10.2.1 Towards expanded research

This PhD project yielded some new insights in potential chemotherapy-induced neurotoxicity during childhood. Still, we note several limitations that were encountered, and how future research could partly solve these issues.

10.2.1.1   Large longitudinal population studies

We aimed to investigate therapy-induced neural alterations in cancer patients compared to healthy controls. However, given that childhood cancer is rare, different pathologies, ages at diagnoses and treatment protocols were included. More specifically, in the non-CNS tumor studies, patients were treated for osteosarcoma, ewing sarcoma, non-rhabdomyosarcoma and rhabdomyosarcoma. Each of these patients had received multi-agent regimens containing either methotrexate, or alkylating agent(s), or a combination of both. Hence, we questioned whether such intravenous chemotherapy (known to be neurotoxic in animal studies and case reports) could induce comparable neurotoxic mechanisms as in adult cancer patients. Similarly, in the CNS tumor survivor study, patients were treated for astrocytoma, ependymoma and medulloblastoma, of whom the latter group mainly received whole-brain irradiation.

To differentiate between subject-specific risk factors, more complicated statistical models (including multiple predictors) will be required. All childhood cancer populations would therefore ideally be included in a longitudinal design with sufficient sample size. Besides treatment dose as predictor, also age at diagnosis (and thus time of neurotoxic hit), could then be included in prediction models of long-term outcomes of childhood cancer patients. As discussed previously, neurotoxic hits in a developing brain are possibly age-dependent (i.e. depending on the brain maturity) and result in different neurodevelopmental patterns and their long-term daily life experience.

Not only to address subject-specific risk factors, but certainly in neuroimaging analyses, large sample sizes are essential to reach sufficient statistical power. For voxel-wise analyses, a high number of statistical tests is performed, for which a stringent statistical threshold is

preferably implemented. Studies with small sample sizes have a large risk to result in too many false positive findings [432]. For this reason, we often applied non-parametric permutation testing [433] instead of parametric statistics [434] . Still, the possibility to implement such analyses, often depends on the neuroimaging toolboxes that are used.

10.2.1.2   Integration of valuable in vivo neuroimaging biomarkers

The discussed neuroimaging analyses (including DWI, Rsfmri, T1-weighted MRI) covered MRI data acquired in adult survivors of childhood cancer (in **Chapter 5, 6, 7 and 9**). We attempted to apply most recent analysis techniques, to estimate underlying microstructure and functioning most optimally. Still, a wide range of analysis (e.g. voxel-based, component based, tract-based, higher-order models, connectome-based, …) and remaining imaging modalities exist that could provide additional insights in neurotoxic mechanisms.

Age-informed selection of imaging parameters

With regard to analyses, we consistently correlated subject-specific imaging values (extracted from group comparison results in one imaging modality (e.g. DWI, T1, …)) with participants' behavior, clinical values, timing variables. However, as previously discussed (**Chapter 9**), the brain consists of complex networks and interactions, which probably require more complicated prediction models than correlation analyses only [435,436]. Also, these correlations highly depend on the imaging parameter which is extracted. For instance, grey matter structural parameters can be estimated based on T1-weighted MRI, such as cortical thickness, grey matter surface area, grey matter volume, grey matter density, … However, age-related developmental patterns are very different between these parameters [343,437]. While cortical thickness decreases, cortical density and surface areas increase throughout development [438]. Previously, it was hypothesized that decrease in cortical thickness correlated with synaptic pruning. However, change in synaptic density is currently assumed to change nonmonotonic, and brain-region-specific throughout childhood. Therefore, neurotoxic-induced micro- and macrostructural investigations not only depend on the brain maturity of the child, but certainly also on the selected parameter and on which brain region values are estimated. Future studies should therefore investigate such imaging parameters, and compare these with existing (and increasing) normative neurodevelopmental data as background knowledge. In this context, large international collaborations and developmental neuroimaging projects, such as the Developing Human Connectome Project [439], the ENIGMA project [440], … could provide such normative information of normal neurodevelopment and genetic predispositions acquired in large pediatric samples.

Time-varying functional coherence

With regard to functional imaging, we focused on static correlations between resting-state fMRI signals (**Chapter 7**). However, functional coherence and signaling between brain areas is increasingly hypothesized to be dynamic, or time-varying [441]. Therefore, dynamic analyses of functional imaging (or timeseries of signals) instead of static measures (i.e. correlation) could

add important information about time-dependent (and more causal) interactions between brain areas. More specifically, given that our studies mainly evidenced long-term changes in attention or processing speed, dynamic analyses (e.g. 'switching') of attention-related networks could specifically be of interest in childhood cancer populations. Such dynamic analyses become even more valuable in case of high temporal resolution, which is specifically the case in electroencephalography (EEG). Earlier studies investigating EEG during attentional tasks also demonstrated prolonged information processing in childhood cancer survivors [324] and lower elicited signals breast cancer patients [442]. Hence, EEG and active fMRI paradigms with attentional tasks could become valuable in future studies. Finally, functional neuroimaging analyses are now even evolving towards predictions of underlying neurobiological processes (e.g. metabolites, chemical or electrical signaling) [441]. Still, such prediction models need further improvements combining multi-modal (neuroimaging) data, before valuable implementation would be possible.

Integration of imaging modalities, and feasibility in children
In **Chapter 5**, we demonstrated the link between leukoencephalopathy and diffusion metrics, and in **Chapter 7**, we investigated the association between grey matter cortical thickness and functional coherence. Given that image values remain very rough estimates of underlying microstructure, integration of multiple image modalities become increasingly important.

The most basic method to integrate image information, is by spatial coregistration of the different images, and investigate their values in coregistered areas. However, local voxel-based values do not provide the global dynamic network information we might need. In **Chapter 9,** we discussed graph theory which could be applied on any image modality estimating connectivity. This could be a possible approach to predict functional connectivity estimations, based on structural connectivity [406]. Furthermore, the hypothesis of age-dependent 'hub' vulnerability and link with observable lesions, is to be addressed using multi-modal imaging. A wide range of other imaging modalities could yield additional insights into pathological mechanisms in pediatric cancer patients [424,443], including spectroscopy (MRS), glutamate imaging (CEST), perfusion images (e.g. ASL), susceptibility-weighted imaging (SWI), EEG, Positron Emission Tomography (PET) ..., as these provide estimations of neurobiological processes such as metabolic alterations, neurotransmission changes, or blood supply changes, resp.

In adult cancer patients, metabolic changes [155,444] and increased blood flow [365,368] were evidenced in breast cancer patients. Although the latter finding suggests hemodynamic and vascular changes, limited research currently exists with regard to microvascular damage. SWI scans could therefore be informative to add in a clinical follow-up design in order to detect potential microbleeds, certainly in case of RT. With regard to EEG, decreased potentials during sustained attentional tasks were detected in breast cancer patients after chemotherapy [442]. Given our findings of microstructural white matter changes and its association with decreased processing speed, the link with EEG signaling could particularly be valuable [445]. Furthermore, as cancer patients often complain about fatigue, sleep EEG could provide additional interesting

findings [446]. With regard to PET imaging, frontal activation changes were evidenced in breast cancer patients so far [447]. However, besides such activation estimates, PET might specifically become valuable to investigate the link with neurobiological mechanisms and toxic deposits, that can be estimated using multiple tracers in vivo [448].

In conclusion, in childhood cancer patients (**Chapter 8**), 3D FLAIR images could be implemented for lesion delineations, and SWI could be implemented to detect microbleeds. Besides these clinical scans, advanced scans (e.g. DWI and RsfMRI) could be added. However, given that a non-anesthesia MRI scanning protocol for a child is ideally limited to maximum 30-40minutes, additional modalities need to be selected. As children easily move, modalities of which the quality is less moving-dependent are preferred. For this reason, EEG and MRS are possibly more challenging. Furthermore, with regard to PET imaging, radiation doses are applied, for which the additional value of (as compared to MRI) currently still needs more evidence. Certainly with regard to chemotherapy-induced neurotoxicity, valuable tracers need more (pre-)clinical investigations before its application in childhood cancer patients.

10.2.1.3   Psychology-related biomarkers and germline assessments

Our studies focused on neuroimaging parameters to estimate underlying pathology. However, many biochemical side effects at cellular level can be induced by chemotherapeutic treatments, by the emotional situation, coping mechanisms, and by the disease itself, which we currently did not measure or associate with our neuroimaging findings.

Peripheral biomarkers

First, electrophysiological changes (e.g. peripheral sensory neurotoxicity) might occur due to chemotherapy administration. Although central and peripheral neurotoxicity due to chemotherapy are generally discussed separately [449], interactions between these two levels are highly probable. Sensory-motor axonal neuropathy (as measured with electromyography (EMG)), can also affect neurocognitive scores on tasks which require manual or fine motor execution [450]. Furthermore, this could also interact with cerebello-cortical networks [451]. However, such electrophysiological investigations have not yet been integrated in cancer patients. Similarly, although cardiotoxicity is known to be a possible chemotherapy-induced side-effect, and heart rate variability (HRV) is affected in stress situations, HRV was only limitedly investigated in adult cancer patients [452,453], but not in combination with neurocognitive research.

Second, multiple peripheral signaling biomarkers interact with the CNS system, either indirectly via the HPA-axis or directly via the lymphatic system. Biochemical measurements of interest could include inflammatory markers [454], neurotrophic factors [455], neurotoxic CSF values [259] as well as neuro-endocrine estimations [334,346,456].

In leukemia, CSF values are specifically valuable, given that CSF samples are consistently acquired in the clinical setting to detect CNS invasion. However, in non-CNS solid tumor patients, ethical issues come into play given that lumbar punctures are painful, and not required for cancer staging. Hence, such measures would mainly be applicable in leukemia

patients. Finally, given the close association between stress experience and endocrine values, not only these values would be interesting to link to neuroimaging, but also stress- and coping-related questionnaires are important, which are feasible to obtain in all patients.

Emotional and fatigue involvement

As we demonstrated in **Chapter 5,** survivors of childhood cancer showed elevated depression ratings, anxiety ratings and lower quality of life in general, compared to healthy controls. Furthermore, we showed different cortical thickness changes, which depended on correction for depression or not in **Chapter 7.** Given that emotional and traumatic experiences during childhood cancer can highly affect their quality of life [457], and possibly also brain maturation processes, emotion-, stress-, coping-, trauma-related questionnaires will be important to acquire in future studies. Constructive coping mechanisms during childhood cancer in particular are associated with their expression of positive affect [458]. The association between emotional processes, heart rate variability, neuro-endocrine measurements, and neuroimaging findings could particularly interesting, given their association with the vagal nerve [452]. This could profoundly evidence or falsify 'the double hit' hypothesis at endocrine, psychological and neural level. Not only would it be interesting to investigate emotion-related maturation processes, but also its impact on cognitive values. Often neurocognitive studies do not correct for emotional values, while it has clearly been documented that stress [459] and fatigue [460] highly affect attentional functioning in cancer patients. Even stress experienced by parents throughout treatment, can affect long-term cognitive functioning of childhood cancer patients [461]. It is therefore recommended to consistently screen for these values in combination with cognition investigations.

Genetic involvement

A large degree of interpatient variability in cognitive outcomes exists. Demographic and treatment variables can explain such variability to some extent [12,264,266,462–466]. However, a compelling need exists to identify the possibly involved genetic predisposition factors. In the sarcoma survivor study, we focused on the MTHFRC677T and Apoε genotypes (**Chapter 5**). Although polymorphisms of these SNPs were not significantly associated with the occurrence of leukoencephalopathy in survivors of childhood sarcoma, no lesions were detected in the MTHFR CC group, nor in the Apoε2 carriers, which could still suggest trends. Given its role in MTX metabolism, the MTHFR genotype could particularly be an interesting future biomarker for leukemia and bone tumor patients, since both groups receive high doses of MTX.

Emerging evidence indicates that multiple other germline genetic variants could modulate the risk of treatment-related neurocognitive deficits [467,468], via neural plasticity and repair [111,240,246,469], neuroinflammation and oxidative stress [117,470,471], neurotransmission [117,240,469,472], and folate metabolism [109,241,473]. These studies demonstrate the complexity of a probably polygenic susceptibility to treatment-induced neurotoxicity. However, brain development and its complexity are also assumed to be genome-dependent, which is particularly important in childhood brain development [474–476]. Hence, genes associated with

brain development could be particularly interesting to address in case of childhood treatment-induced neurotoxicity.

Selection of population-specific biomarkers, and feasibility in children

In order to limit data assessments in children independently from clinical settings, short feasible acquisitions are ideally applied in large childhood cancer populations. In this regard, abbreviated behavioral screening assessments (including neurocognitive screenings and subjective experience questionnaires) are ideally combined with standard MRI imaging in all childhood cancer patients. Besides leukemia and sarcoma, also Wilm's tumors, neuroblastoma, … patients could be included, since evidence is still lacking for these populations. Selection of additional biomarkers would in a next stage largely depend on the available clinical data, which is related to specific diagnoses and their treatment. For instance, CSF values could be informative to investigate for toxic markers in leukemia patients (as punctures occur in clinics), MTHFR genotypes would be informative in patients treated with high-dose MTX, and endocrine markers would initially be easily implemented in research for patients with hormone deficiencies (e.g. after radiotherapy). Finally, as all cancer patients receive cardiac follow-ups in the clinical setting, electrophysiological measures could be derived from existing data, and possibly associated with stress-related questionnaires.

10.2.2 Towards clinical interventions

10.2.2.1   (Neuro-)Psychological risk assessment and interventions

Our studies clearly evidenced neurotoxicity in childhood sarcoma patients (i.e. leukoencephalopathy, white and grey matter microstructural changes, lower task scores on processing speed). However, the question remains if (and how) some patients could recover from neurotoxicity after treatment. Time since treatment was related to the observed WM microstructural changes in the survivor study (**Chapter 6**), and the extent of leukoencephalopathy also declined after treatment in the childhood patients (**Chapter 8**). Furthermore, the impact of lesions on cognitive values in survivors only appeared to be subtle, and limited to reaction times on attentional tasks.

For these patients who do show attentional difficulties, attentional intervention programs could become interesting in the future [477]. However, their success rates remain inconsistent so far. As our follow-up study in leukemia patients suggested, patients at risk could include younger patients, as well as lower SES of the family [228]. The latter finding confirms higher education of the parents, or any other positive socio-economic predictor, to be important. Higher socio-economic environments generally provide more neurocognitive stimulation during childhood brain development. Such stimulation could build neurocognitive reserves, lowering the impact of disease or treatment on cognitive outcomes [478]. Therefore, in lower income households, school attending and stimulation of the child might be particularly important. One should note that non-CNS tumor patients in general do not reach clinical thresholds for deviant neurocognitive scores, nor do they complain themselves about cognitive

functioning in daily life. In our longitudinal study (**Chapter 8)**, normalized cognitive scores also did not decrease from baseline to follow-up.

By contrast, the adult survivors did show elevated depression ratings, anxiety ratings and lower quality of life in general. Given that some survivors still report such psychological complaints years after treatment, therapy-related effects on neuropsychological functioning is probably subject-specific. This highly suggests to apply early psychological screenings (including pain-, cognition-, emotion-, fatigue-, stress-, trauma-related, ... questionnaires), in order to improve psychosocial assistance and treatments. Screening instruments for psychosocial risk factors that now increasingly receive attention, include the Distress Thermometer (DT) and Psychosocial Assessment Tool (PAT), among others [479]. Based on such screening instruments, complaints could be detected early onwards (e.g. stress, anxiety, depressive thoughts, pain, attention, motor functioning, word finding ...), and psychosocial support could be individualized.

Given that long-term complaints of childhood non-CNS cancer patients mainly include emotional issues, coping mechanisms play a very important role in their quality of life [480]. Psychosocial interventions ideally improve these coping strategies, and are mostly recommended in vulnerable groups. Kazak and colleagues (2004) demonstrated the success of cognitive-behavior therapeutic interventions on intrusive thoughts in families of adolescent cancer patients and decreased arousal in these patients [481].

Besides psychosocial interventions, EEG neurofeedback could also hold promise to improve some of the abovementioned complaints. During neurofeedback, patterns of neuronal activity are represented on a computer screen, and altered by auditory or visual rewards when desired brain waves are present. This has only limitedly been investigated in adult cancer patients, but showed improvements in cognitive impairment [482], cancer-related pain [483] and neuropathy [484]. As relaxation is important to reduce stress, and psychosomatic complaints, alternative methods also increasingly receive attention. For instance, music therapy has been evidenced to result in relaxation (measured with EEG) [485]. Similarly, mindfulness has been evidenced to reduce stress-related cortisol and pro-inflammatory cytokines in adult breast cancer patients [486], and emotional distress in adolescent survivors of cancer [487]. However, these techniques were only limitedly studied so far. Given the neural plasticity in childhood, child-friendly neurocognitive techniques (e.g. hypnosis, mindfulness, yoga, ...), physical activity, language therapy, and research hold great promise to improve patient-specific complaints.

10.2.2.2   Towards innovative treatment investigations

During the last decades, neurocognitive difficulties were evident in brain tumor and leukemia cases, after treatment with whole brain irradiation. As survival rates increased by improvement of treatments, side effects are increasingly avoided by adapting treatments. Therefore, RT is now avoided in brain tumor patients <3 years old, and replaced by intrathecal chemotherapy in leukemia patients. With regard to cranial radiotherapy in childhood brain tumors, one future perspective is avoidance of irradiating specific brain areas, e.g. hippocampus [488]. However, the entire brain is currently assumed to be "eloquent", for which

any brain damage leads to certain loss of function. One hypothesis could be to avoid the previously discussed so-called 'hubs', or highly connected brain regions, from a connectionist perspective [381]. This has not been implemented in radiotherapy yet, nor in neurosurgery, but could hold great promise for future research and treatment applications [489]. In children specifically, developing brain areas in the age range of the patient could also be particularly vulnerable.

Systemic chemotherapy is one alternative to limit neurotoxicity in case of brain tumors or leukemia. However, leukoencephalopathy can still arise, as we demonstrated in non-CNS tumor patients. To date, clinical MRI scanning is part of standard care in brain tumor and leukemia patients. Still, this is not the case yet for non-CNS tumor patients. Given our findings of neurotoxicity in these patients, future standard care procedures could include longitudinal neurocognitive and emotional screenings combined with MRI scanning. This could be implemented to improve future personalized medical treatments [490]. For instance, a wider range of chemotherapeutic agents with lower doses could be administered, or fractionation of high-dose agents, in order to achieve similar survival rates, but decreased encephalopathy. Furthermore, new personalized treatments (e.g. immune therapy, molecularly targeted drugs) increasingly receive attention. These treatments also require (genetic) biomarkers in order to adapt treatments, and improve survival rates as well as long-term sequelae in childhood cancer patients.

Finally, additional neuroprotective medication has been explored in adult cancer patients with cognitive or fatigue complaints [491]. These studies were mainly performed in brain tumor, breast cancer and ovarian cancer patients. Investigated agents included antioxidants (e.g. d-Methionine)[72], stimulants modafinil [492,493] and methylphenidate [494], mood stabilizer lithium, acetylcholinesterase inhibitor donepezil [495,496], and NMDA antagonist memantine [497]. Animal research on potential psychopharmacological interventions still keeps increasing [491]. Although these studies suggest some positive results in cognitive functioning, the impact and possible side effects of such treatments remain largely unknown and open for debate in childhood cancer patients.

10.3 General conclusion

This doctoral research project aimed to explore the neural underpinnings of potential neurotoxicity in childhood cancer patients, receiving high-dose chemotherapy. Advanced MR neuroimaging techniques provided evidence for therapy-induced macro- and microstructural changes and potential risk factors such as age at diagnosis, time since treatment and depression rates. We demonstrated visually observable neural damage, as well as microstructural and functional changes that are not visually detectable on clinical MRI scans. Such microstructural and functional changes were repeatedly related to attentional or processing speed measures. Therefore, we would recommend future screenings of neurocognitive, as well as emotional, functioning early on in treatment in all current patients. These assessments could be further associated with advanced neuroimaging techniques in longitudinal designs. By implementing such investigations in standard care, innovative childhood cancer therapies (e.g. personalized molecular targeted treatments, chemotherapy dose reductions, protective medication, …) could be further improved to restrict neurotoxicity. Consequently, neurodevelopment and long-term quality of daily life of childhood cancer patients could be further improved in the (near) future.

Bibliography

1   Gatta G, Capocaccia R, Stiller C, Kaatsch P, Berrino F, Terenziani M. Childhood cancer survival trends in Europe: a EUROCARE Working Group study. J Clin Oncol 2005; 23: 3742–51.

2   Zebrack BJ, Landier W. The perceived impact of cancer on quality of life for post-treatment survivors of childhood cancer. Qual Life Res 2011; 20: 1595–608.

3   Kazak AE. Posttraumatic Stress Disorder (PTSD) and Posttraumatic Stress Symptoms (PTSS) in Families of Adolescent Childhood Cancer Survivors. J Pediatr Psychol 2004; 29: 211–9.

4   Kunin-Batson A, Kadan-Lottick N, Neglia JP. The contribution of Neurocognitive functioning to quality of life after childhood acute lymphoblastic leukemia. Psychooncology 2014; 23: 692–9.

5   Mulhern RK, Butler RW. Neurocognitive sequelae of childhood cancers and their treatment. Pediatr Rehabil 2004; 7: 1–6.

6   Moore BD 3rd. Neurocognitive outcomes in survivors of childhood cancer. J Pediatr Psychol 2005; 30: 51–63.

7   Krull KR, Hardy KK, Kahalley LS, Schuitema I, Kesler SR. Neurocognitive Outcomes and Interventions in Long-Term Survivors of Childhood Cancer. J Clin Oncol 2018; 33: JCO.2017.76.469.

8   Brown RT, Madan-Swain A, Walco GA, et al. Cognitive and academic late effects among children previously treated for acute lymphocytic leukemia receiving chemotherapy as CNS prophylaxis. J Pediatr Psychol 1998; 23: 333–40.

9   Mohrmann C, Henry J, Hauff M, Hayashi RJ. Neurocognitive Outcomes and School Performance in Solid Tumor Cancer Survivors Lacking Therapy to the Central Nervous System. J Pers Med 2015; 5: 83–90.

10 Moleski M. Neuropsychological, neuroanatomical, and neurophysiological consequences of CNS chemotherapy for acute lymphoblastic leukemia. Arch Clin Neuropsychol 2000; 15: 603–30.

11 Brown RT, Sawyer MG, Antoniou G, Toogood I, Rice M. Longitudinal follow-up of the intellectual and academic functioning of children receiving central nervous system-prophylactic chemotherapy for leukemia: a four-year final report. J Dev Behav Pediatr 1999; 20: 373–7.

12 Buizer AI, de Sonneville LMJ, Veerman AJP. Effects of chemotherapy on neurocognitive function in children with acute lymphoblastic leukemia: a critical review of the literature. Pediatr Blood Cancer 2009; 52: 447–54.

13 Campbell LK, Scaduto M, Sharp W, et al. A meta-analysis of the neurocognitive sequelae of treatment for childhood acute lymphocytic leukemia. Pediatr Blood Cancer 2007; 49: 65–73.

14 Duffner PK. Long-term effects of radiation therapy on cognitive and endocrine function in children with leukemia and brain tumors. Neurologist 2004; 10: 293–310.

15 Elalfy M, Ragab I, Azab I, Amin S, Abdel-Maguid M. Neurocognitive outcome and white matter anisotropy in childhood acute lymphoblastic leukemia survivors treated with different protocols. Pediatr Hematol Oncol 2014; 31: 194–204.

16 Iyer NS, Balsamo LM, Bracken MB, Kadan-Lottick NS. Chemotherapy-only treatment effects on long-term neurocognitive functioning in childhood ALL survivors: a review and meta-analysis. Blood 2015; 126: 346–53.

17 Kanellopoulos A, Andersson S, Zeller B, et al. Neurocognitive Outcome in Very Long-Term Survivors of Childhood Acute Lymphoblastic Leukemia After Treatment with Chemotherapy Only. Pediatr Blood Cancer 2016; 63: 133–8.

18 Kesler SR, Gugel M, Pritchard-Berman M, et al. Altered resting state functional connectivity in young survivors of acute lymphoblastic leukemia. Pediatr Blood Cancer 2014; 61: 1295–9.

19 Sleurs C, Deprez S, Emsell L, Lemiere J, Uyttebroeck A. Chemotherapy-induced neurotoxicity in pediatric solid non-CNS tumor patients: An update on current state of research and recommended future directions. Crit Rev Oncol Hematol 2016; 103: 37–48.

20 Ahles TA, Saykin AJ. Candidate mechanisms for chemotherapy-induced cognitive changes. Nat Rev Cancer 2007; 7: 192–201.

21 Kasper B, Harter C, Meissner J, et al. Prophylactic treatment of known ifosfamide-induced encephalopathy for chemotherapy with high-dose ifosfamide? Support Care Cancer 2004; 12: 205–7.

22   David KA, Picus J. Evaluating Risk Factors for the Development of Ifosfamide Encephalopathy. Am J Clin Oncol 2005; 28: 277–80.

23   Deprez S, Amant F, Yigit R, et al. Chemotherapy-induced structural changes in cerebral white matter and its correlation with impaired cognitive functioning in breast cancer patients. Hum Brain Mapp 2011; 32: 480–93.

24   Deprez S, Vandenbulcke M, Peeters R, et al. Longitudinal assessment of chemotherapy-induced alterations in brain activation during multitasking and its relation with cognitive complaints. J Clin Oncol 2014; 32: 2031–8.

25   Correa DD, Hess LM. Cognitive function and quality of life in ovarian cancer. Gynecol Oncol 2012; 124: 404–9.

26   Skaali T, Fossa SD, Andersson S, et al. Self-reported cognitive problems in testicular cancer patients: relation to neuropsychological performance, fatigue, and psychological distress. J Psychosom Res 2011; 70: 403–10.

27   Stouten-Kemperman MM, de Ruiter MB, Caan MWA, et al. Lower cognitive performance and white matter changes in testicular cancer survivors 10 years after chemotherapy. Hum Brain Mapp 2015; 36: 4638–47.

28   Bornstein MH, Scrimin S, Putnick DL, et al. Neurodevelopmental functioning in very young children undergoing treatment for non-CNS cancers. J Pediatr Psychol 2012; 37: 660–73.

29   Seigers R, Fardell JE. Neurobiological basis of chemotherapy-induced cognitive impairment: A review of rodent research. Neurosci. Biobehav. Rev. 2011; 35: 729–41.

30   Pratt WB. The anticancer drugs. Oxford University Press, 1994.

31   Quasthoff S, Hartung HP. Chemotherapy-induced peripheral neuropathy. J Neurol 2002; 249: 9–17.

32   Sioka C, Kyritsis AP. Central and peripheral nervous system toxicity of common chemotherapeutic agents. Cancer Chemother Pharmacol 2009; 63: 761–7.

33   Verstappen CCP, Heimans JJ, Hoekman K, Postma DTJ. Neurotoxic Complications of Chemotherapy in Patients with Cancer. Drugs 2003; 63: 1549–63.

34   Rollins N, Winick N, Bash R, Booth T. Acute methotrexate neurotoxicity: Findings on diffusion-weighted imaging and correlation with clinical outcome. Am J Neuroradiol 2004; 25: 1688–95.

35   Inaba H, Khan RB, Laningham FH, Crews KR, Pui CH, Daw NC. Clinical and radiological characteristics of methotrexate-induced acute encephalopathy in pediatric patients with cancer. Ann Oncol 2008; 19: 178–84.

36   Sánchez-Carpintero R, Narbona J, López De Mesa R, Arbizu J, Sierrasesúmaga L. Transient posterior encephalopathy induced by chemotherapy in children. Pediatr Neurol 2001; 24: 145–8.

37   Eichler AF, Batchelor TT, Henson JW. Diffusion and perfusion imaging in subacute neurotoxicity following high-dose intravenous methotrexate. Neuro Oncol 2007; 9: 373–7.

38   Tsang DSF, Khong PL. Diffusion magnetic resonance imaging findings in acute methotrexate neurotoxicity. J Hong Kong Coll Radiol 2005; 8: 250–3.

39   Terasawa Y, Nakane S, Ohnishi T, Harada M, Furutani K, Izumi Y, Kaji R. A case of methotrexate encephalopathy: Findings on diffusion tensor image and correlation with clinical outcome. Clin Neurol 2007; 47: 79–84.

40   Saykin AJ, Ahles TA, McDonald BC. Mechanisms of chemotherapy-induced cognitive disorders: neuropsychological, pathophysiological, and neuroimaging perspectives. Semin Clin Neuropsychiatry 2003; 8: 201–16.

41   Pratt CB, Green AA, Horowitz ME. Central nervous system toxicity following the treatment of pediatric patients with ifosfamide/mesna. J Clin Oncol 1986; 4: 1253–61.

42   Antunes NL, De Angelis LM. Neurologic consultations in children with systemic cancer. Pediatr Neurol 1999; 20: 121–4.

43   Di Cataldo A, Astuto M, Rizzo G, Bertuna G, Russo G, Incorpora G. Neurotoxicity during ifosfamide treatment in children. Med Sci Monit 2009; 15: CS22-5.

44   Dimaggio JR, Baile WF, Brown R, Schapira D. Hallucinations and ifosfamide-induced neurotoxicity. Cancer 1994; 73: 1509–14.

45   Bernard PA, McCabe T, Bayliff S, Hayes D. Successful treatment of ifosfamide neurotoxicity with dexmedetomidine. J Oncol Pharm Pract 2010; 16: 262–5.

46   Ames B, Lewis LD, Chaffee S, Kim J, Morse R. Ifosfamide-induced encephalopathy and movement disorder. Pediatr Blood Cancer 2010; 54: 624–6.

47   Epelman S, Gorender E, Beaugrand A, Meirelles P, Oliveira R, Melaragno R. Double alkylating agents treatment with ifosfamide (IFOS) and cyclophosphamide (CYCLO) for relapsed pediatric solid tumors. Pediatr Blood Cancer 2012; 59 (6): 1093.

48   Yule SM, Price L, Pearson ADJ, Boddy A V. Cyclophosphamide and ifosfamide metabolites in the cerebrospinal fluid of children. Clin Cancer Res 1997; 3: 1985–92.

49   Hagleitner MM, De Bont ESJM, Te Loo DMWM. Survival trends and long-term toxicity in pediatric patients with osteosarcoma. Sarcoma 2012; 2012. DOI:10.1155/2012/636405.

50   Ito Y, Arahata Y, Goto Y, et al. Cisplatin neurotoxicity presenting as reversible posterior leukoencephalopathy syndrome. Am J Neuroradiol 1998; 19: 415–7.

51   Verschraegen C, Conrad CA, Hong WK. Subacute encephalopathic toxicity of cisplatin. Lung Cancer 1995; 13: 305–9.

52   Pratt CB, Goren MP, Meyer WH, Singh B, Dodge RK. Ifosfamide neurotoxicity is related to previous cisplatin treatment for pediatric solid tumors. J Clin Oncol 1990; 8: 1399–401.

53   Tajino T, Kikuchi SI, Yamada H, Takeda A, Konno SI. Ifosfamide encephalopathy associated with chemotherapy for musculoskeletal sarcomas: Incidence, severity, and risk factors. J Orthop Sci 2010; 15: 104–11.

54   Toker E, Yenice Ö, Ögüt MS. Isolated abducens nerve palsy induced by vincristine therapy. J AAPOS 2004; 8: 69–71.

55   Burns B V, Shotton JC. Vocal fold palsy following vinca alkaloid treatment. J Laryngol Otol 1998; 112: 485–7.

56   Delaney P. Vincristine-induced laryngeal nerve paralysis. Neurology 1982; 32: 1285–8.

57   Legha SS. Vincristine Neurotoxicity: Pathophysiology and Management. Med Toxicol 1986; 1: 421–7.

58   Postma TJ, Benard B a., Huijgens PC, Ossenkoppele GJ, Heimans JJ. Long-term effects of vincristine on the peripheral nervous system. Clin Neurol Neurosurg 1992; 94: 80.

59   Aydogdu I, Ozturan O, Kuku I, Kaya E, Sevinc A, Yildiz R. Bilateral transient hearing loss associated with vincristine therapy: Case report. J Chemother 2000; 12: 530–2.

60   Lugassy G, Shapira A. Sensorineural hearing loss associated with vincristine treatment. Blut 1990; 61: 320–1.

61   Riga M, Psarommatis I, Korres S, et al. Neurotoxicity of vincristine on the medial olivocochlear bundle. Int J Pediatr Otorhinolaryngol 2007; 71: 63–9.

62   Dettmeyer R, Driever F, Becker A, Wiestler OD, Madea B. Fatal myeloencephalopathy due to accidental intrathecal vincristin administration: A report of two cases. Forensic Sci Int 2001; 122: 60–4.

63   Meggs WJ, Hoffman RS. Fatality resulting from intraventricular vincristine administration. J Toxicol - Clin Toxicol 1998; 36: 243–6.

64   Rzeski W, Pruskil S, Macke A, et al. Anticancers agents are potent neurotoxins in vitro and in vivo. Ann Neurol 2004; 56: 351–60.

65   Seigers R, Schagen SB, Beerling W, et al. Long-lasting suppression of hippocampal cell proliferation and impaired cognitive performance by methotrexate in the rat. Behav Brain Res 2008; 186: 168–75.

66   Wick A, Wick W, Hirrlinger J, et al. Chemotherapy-induced cell death in primary cerebellar granule neurons but not in astrocytes: In vitro paradigm of differential neurotoxicity. J Neurochem 2004; 91: 1067–74.

67   Briones TL, Woods J. Dysregulation in myelination mediated by persistent neuroinflammation: possible mechanisms in chemotherapy-related cognitive impairment. Brain Behav Immun 2014; 35: 23–32.

68   Andres AL, Gong X, Di K, Bota DA. Low-doses of cisplatin injure hippocampal synapses: a mechanism for 'chemo' brain? Exp Neurol 2014; 255: 137–44.

69   Avella D, Pisu MB, Roda E, Gravati M, Bernocchi G. Reorganization of the rat cerebellar cortex during postnatal development following cisplatin treatment. Exp Neurol 2006; 201: 131–43.

70   Cerri S, Piccolini VM, Santin G, et al. The developmental neurotoxicity study of platinum compounds. Effects of cisplatin versus a novel Pt(II) complex on rat cerebellum. Neurotoxicol Teratol 2011; 33: 273–81.

71   Christie LA, Acharya MM, Parihar VK, Nguyen A, Martirosian V, Limoli CL. Impaired cognitive function and hippocampal neurogenesis following cancer chemotherapy. Clin Cancer Res 2012; 18: 1954–65.

72   Gopal KV, Wu C, Shrestha B, Campbell KCM, Moore EJ, Gross GW. D-Methionine protects against cisplatin-induced neurotoxicity in cortical networks. Neurotoxicol Teratol 2012; 34: 495–504.

73   Piccolini VM, Cerri S, Romanelli E, Bernocchi G. Interactions of neurotransmitter systems during postnatal development of the rat hippocampal formation: Effects of cisplatin. Exp Neurol 2012; 234: 239–52.

74   Xiao R, Yu HL, Zhao HF, Liang J, Feng JF, Wang W. Developmental neurotoxicity role of cyclophosphamide on post-neural tube closure of rodents in vitro and in vivo. Int J Dev Neurosci 2007; 25: 531–7.

75   Yang M, Kim JS, Song MS, et al. Cyclophosphamide impairs hippocampus-dependent learning and memory in adult mice: Possible involvement of hippocampal neurogenesis in chemotherapy-induced memory deficits. Neurobiol Learn Mem 2010; 93: 487–94.

76   Briones TL, Woods J. Chemotherapy-induced cognitive impairment is associated with decreases in cell proliferation and histone modifications. BMC Neurosci 2011; 12: 124.

77   Gulec M, Oral E, Dursun OB, et al. Mirtazapine protects against cisplatin-induced oxidative stress and DNA damage in the rat brain. Psychiatry Clin Neurosci 2013; 67: 50–8.

78   Lee GD, Longo DL, Wang Y, et al. Transient improvement in cognitive function and synaptic plasticity in rats following cancer chemotherapy. Clin Cancer Res 2006; 12: 198–205.

79   Seigers R, Schagen SB, Coppens CM, et al. Methotrexate decreases hippocampal cell proliferation and induces memory deficits in rats. Behav Brain Res 2009; 201: 279–84.

80   Sugimoto S, Yamamoto YL, Nagahiro S, Diksic M. Permeability change and brain tissue damage after intracarotid administration of cisplatin studied by double-tracer autoradiography in rats. J Neurooncol 1995; 24: 229–40.

81   MI Turan, Cayir A, Cetin N, Suleyman H, SilteliogluTuran I, Tan H. An investigation of the effect of thiamine pyrophosphate on cisplatin-induced oxidative stress and DNA damage in rat brain tissue compared with thiamine: thiamine and thiamine pyrophosphate effects on cisplatin neurotoxicity. Hum Exp Toxicol 2014; 33: 14–21.

82   Lyons L, ELBeltagy M, Bennett G, Wigmore P. The effects of cyclophosphamide on hippocampal cell proliferation and spatial working memory in rat. PLoS One 2011; 6. DOI:10.1371/journal.pone.0021445.

83   Dietrich J, Han R, Yang Y, Mayer-Pröschel M, Noble M. CNS progenitor cells and oligodendrocytes are targets of chemotherapeutic agents in vitro and in vivo. J Biol 2006; 5. DOI:10.1186/jbiol50.

84   Tomiwa K, Hamaza F, Mikawa H, OMIWA K. Neurotoxicity of Vincristine after the osmotic opening of the blood-brain barrier. Neuropathol Appl Neurobiol 1983; 9: 345–54.

85   Bhatia AL, Manda K, Patni S, Sharma AL. Prophylactic action of linseed (Linum usitatissimum) oil against cyclophosphamide-induced oxidative stress in mouse brain. J Med Food 2006; 9: 261–4.

86   Rajamani R, Muthuvel A, Senthilvelan M, Sheeladevi R. Oxidative stress induced by methotrexate alone and in the presence of methanol in discrete regions of the rodent brain, retina and optic nerve. Toxicol Lett 2006; 165: 265–73.

87   Uzar E, Koyuncuoglu HR, Uz E, et al. The activities of antioxidant enzymes and the level of malondialdehyde in cerebellum of rats subjected to methotrexate: Protective effect of caffeic acid phenethyl ester. Mol Cell Biochem 2006; 291: 63–8.

88   Froklage FE, Reijneveld JC, Heimans JJ. Central neurotoxicity in cancer chemotherapy: pharmacogenetic insights. Pharmacogenomics 2011; 12: 379–95.

89   Dranoff G. Cytokines in cancer pathogenesis and cancer therapy. Nat. Rev. Cancer. 2004; 4: 11–22.

90   Rosczyk HA, Sparkman NL, Johnson RW. Neuroinflammation and cognitive function in aged mice following minor surgery. Exp Gerontol 2008; 43: 840–6.

91   Terrando N, Eriksson LI, Kyu Ryu J, et al. Resolving postoperative neuroinflammation and cognitive decline. Ann Neurol 2011; 70: 986–95.

92   Trask PC, Esper P, Riba M, Redman B. Psychiatric side effects of interferon therapy: Prevalence, proposed mechanisms, and future directions. J. Clin. Oncol. 2000; 18: 2316–26.

93   Wilson CJ, Finch CE, Cohen HJ. Cytokines and cognition - The case for a head-to-toe inflammatory paradigm. J Am Geriatr Soc 2002; 50: 2041–56.

94   Kelley KW, Bluthé RM, Dantzer R, et al. Cytokine-induced sickness behavior. In: Brain, Behavior, and Immunity. 2003. DOI:10.1016/S0889-1591(02)00077-6.

95   Morrow GR, Hickok JT, Andrews PL, Stern RM. Reduction in serum cortisol after platinum based chemotherapy for cancer: a role for the HPA axis in treatment-related nausea? Psychophysiology 2002; 39: 491–5.

96   Kesler S, Janelsins M, Koovakkattu D, et al. Reduced hippocampal volume and verbal memory performance associated with interleukin-6 and tumor necrosis factor-alpha levels in chemotherapy-treated breast cancer survivors. Brain Behav Immun 2013; 30: S109-16.

97   Nolten WE, Goldstein D, Lindstrom M, et al. Effects of cytokines on the pituitary-adrenal axis in cancer patients. J Interferon Res 1993; 13: 349–57.

98   Wang XM, Walitt B, Saligan L, Tiwari AFY, Cheung CW, Zhang ZJ. Chemobrain: A critical review and causal hypothesis of link between cytokines and epigenetic reprogramming associated with chemotherapy. Cytokine 2015; 72: 86–96.

99   Wilson KS, Gray CE, Lidgard GP, Parker AC. Recovery of hypothalamic-pituitary-adrenal function after intermittent high-dose prednisolone and cytotoxic chemotherapy. Postgrad Med J 1977; 53: 745–8.

100 Aisa B, Tordera R, Lasheras B, Del Río J, Ramírez MJ. Cognitive impairment associated to HPA axis hyperactivity after maternal separation in rats. Psychoneuroendocrinology 2007; 32: 256–66.

101   Spear LP. Neurodevelopment During Adolescence. Neurodev Mech Psychopathol 1987; : 62–83.

102   De Freitas Cunha C, Silva IN, Finch FL. Early adrenocortical recovery after glucocorticoid therapy in children with leukemia. In: Journal of Clinical Endocrinology and Metabolism. 2004: 2797–802.

103   Gordijn MS, Gemke RJ, van Dalen EC, Rotteveel J, Kaspers GJ. Hypothalamic-pituitary-adrenal (HPA) axis suppression after treatment with glucocorticoid therapy for childhood acute lymphoblastic leukaemia. Cochrane database Syst Rev 2012; 5: CD008727.

104   Kuperman H, Damiani D, Chrousos GP, et al. Evaluation of the hypothalamic-pituitary-adrenal axis in children with leukemia before and after 6 weeks of high-dose glucocorticoid therapy. J Clin Endocrinol Metab 2001; 86: 2993–6.

105   Mendoza-Cruz a C, Wargon O, Adams S, Tran H, Verge CF. Hypothalamic-pituitary-adrenal axis recovery following prolonged prednisolone therapy in infants. J Clin Endocrinol Metab 2013; 98: E1936-40.

106   Salem MA, Tantawy AA, El Sedfy HH, et al. A prospective study of the hypothalamic-pituitary-adrenal axis in children with acute lymphoblastic leukemia receiving chemotherapy. Hematology 2015; 20: 320–7.

107   Schmiegelow M, Feldt-Rasmussen U, Rasmussen AK, Lange M, Poulsen HS, Muller J. Assessment of the Hypothalamo-Pituitary-Adrenal Axis in Patients Treated with Radiotherapy and Chemotherapy for Childhood Brain Tumor. J Clin Endocrinol Metab 2003; 88: 3149–54.

108   Kamdar KY, Krull KR, El-Zein RA, et al. Folate pathway polymorphisms predict deficits in attention and processing speed after childhood leukemia therapy. Pediatr Blood Cancer 2011; 57: 454–60.

109   Linnebank M, Pels H, Kleczar N, et al. MTX-induced white matter changes are associated with polymorphisms of methionine metabolism. Neurology 2005; 64: 912–3.

110   Matura S, Prvulovic D, Jurcoane A, et al. Differential effects of the ApoE4 genotype on brain structure and function. Neuroimage 2014; 89: 81–91.

111   Ahles T, Saykin A, Noll W, et al. The relationship of APOE genotype to neuropsychological performance in long-term cancer survivors treated with standard dose chemotherapy. Psychooncology 2003; 12: 612–9.

112   Ng T, Teo SM, Yeo HL, et al. Brain-derived neurotrophic factor genetic polymorphism (rs6265) is protective against chemotherapy-associated cognitive impairment in patients with early-stage breast cancer. Neuro Oncol 2016; 18: 244–51.

113   Hetman M, Vashishta A, Rempala G. Neurotoxic mechanisms of DNA damage: Focus on transcriptional inhibition. J Neurochem 2010; 114: 1537–49.

114   Mariani E, Polidori MC, Cherubini A, Mecocci P. Oxidative stress in brain aging, neurodegenerative and vascular diseases: An overview. J. Chromatogr. B Anal. Technol. Biomed. Life Sci. 2005; 827: 65–75.

115   Joshi G, Sultana R, Tangpong J, et al. Free radical mediated oxidative stress and toxic side effects in brain induced by the anti cancer drug adriamycin: Insight into chemobrain. Free Radic Res 2005; 39: 1147–54.

116   Caron JE, Krull KR, Hockenberry M, Jain N, Kaemingk K, Moore IM. Oxidative stress and executive function in children receiving chemotherapy for acute lymphoblastic leukemia. Pediatr Blood Cancer 2009; 53: 551–6.

117   Cole P, Finkelstein Y, Stevenson K, et al. Polymorphisms in Genes Related to Oxidative Stress Are Associated With Inferior Cognitive Function After Therapy for Childhood Acute Lymphoblastic Leukemia. J Clin Oncol 2015; 33: 2205–11.

118   Stiles J, Jernigan TL. The basics of brain development. Neuropsychol. Rev. 2010; 20: 327–48.

119   Jernigan TL, Trauner DA, Hesselink JR, Tallal PA. Maturation of human cerebrum observed in vivo during adolescence. Brain 1991; 114: 2037–49.

120   Pfefferbaum A, Mathalon DH, Sullivan EV, Rawles JM, Zipursky RB, Lim KO. A quantitative magnetic resonance imaging study of changes in brain morphology from infancy to late adulthood. Arch Neurol 1994; 51: 874–87.

121   Reiss AL, Abrams MT, Singer HS, Ross JL, Denckla MB. Brain development, gender and IQ in children. A volumetric imaging study. Brain 1996; 119 (Pt 5: 1763–74.

122   Gogtay N, Giedd JN, Lusk L, et al. Dynamic mapping of human cortical development during childhood through early adulthood. Proc Natl Acad Sci U S A 2004; 101: 8174–9.

123   Sowell ER, Thompson PM, Holmes CJ, Jernigan TL, Toga AW. In vivo evidence for post-adolescent brain maturation in frontal and striatal regions [1]. Nat. Neurosci. 1999; 2: 859–61.

124   Giedd JN, Blumenthal J, Jeffries NO, et al. Brain development during childhood and adolescence: a longitudinal MRI study. Nat Neurosci 1999; 2: 861–3.

125   Sowell ER, Thompson PM, Tessner KD, Toga AW. Mapping continued brain growth and gray matter density reduction in dorsal frontal cortex: Inverse relationships during postadolescent brain maturation. J Neurosci 2001; 21: 8819–29.

126   Sowell ER, Peterson BS, Thompson PM, Welcome SE, Henkenius AL, Toga AW. Mapping cortical change

across the human life span. Nat Neurosci 2003; 6: 309–15.

127   Bremner JD, Narayan M. The effects of stress on memory and the hippocampus throughout the life cycle: Implications for childhood development and aging. Dev Psychopathol 1998; 10: 871–85.

128   Teicher MH, Andersen SL, Polcari A, Anderson CM, Navalta CP, Kim DM. The neurobiological consequences of early stress and childhood maltreatment. In: Neuroscience and Biobehavioral Reviews. 2003: 33–44.

129   Dietrich J, Prust M, Kaiser J. Chemotherapy, cognitive impairment and hippocampal toxicity. Neuroscience 2015; 309: 224–32.

130   Herve PY, Leonard G, Perron M, et al. Handedness, motor skills and maturation of the corticospinal tract in the adolescent brain. Hum Brain Mapp 2009; 30: 3151–62.

131   Deoni SCL, Dean DC, O'Muircheartaigh J, Dirks H, Jerskey BA. Investigating white matter development in infancy and early childhood using myelin water faction and relaxation time mapping. Neuroimage 2012; 63: 1038–53.

132   Dean DC, O'Muircheartaigh J, Dirks H, et al. Mapping an index of the myelin g-ratio in infants using magnetic resonance imaging. Neuroimage 2016; 132: 225–37.

133   Nagy Z, Westerberg H, Klingberg T. Maturation of White Matter is Associated with the Development of Cognitive Functions during Childhood. J Cogn Neurosci 2004; 16: 1227–33.

134   Schuitema I, Deprez S, Van Hecke W, et al. Accelerated aging, decreased white matter integrity, and associated neuropsychological dysfunction 25 years after pediatric lymphoid malignancies. J Clin Oncol 2013; 31: 3378–88.

135   Liu D. Maternal Care, Hippocampal Glucocorticoid Receptors, and Hypothalamic-Pituitary-Adrenal Responses to Stress. Science (80) 1997; 277: 1659–62.

136   Woon FL, Hedges DW. Hippocampal and amygdala volumes in children and adults with childhood maltreatment-related posttraumatic stress disorder: A meta-analysis. Hippocampus. 2008; 18: 729–36.

137   Lupien SJ, de Leon M, de Santi S, et al. Cortisol levels during human aging predict hippocampal atrophy and memory deficits. Nat Neurosci 1998; 1: 69–73.

138   O'Brien JT, Lloyd A, McKeith I, Gholkar A, Ferrier N. A longitudinal study of hippocampal volume, cortisol levels, and cognition in older depressed subjects. Am J Psychiatry 2004; 161: 2081–90.

139   Lopez-Duran NL, Kovacs M, George CJ. Hypothalamic-pituitary-adrenal axis dysregulation in depressed children and adolescents: A meta-analysis. Psychoneuroendocrinology. 2009; 34: 1272–83.

140   Sondeijker FEPL, Ferdinand RF, Oldehinkel AJ, et al. Disruptive behaviors and HPA-axis activity in young adolescent boys and girls from the general population. J Psychiatr Res 2007; 41: 570–8.

141   Van Goozen SHM, Matthys W, Cohen-Kettenis PT, Buitelaar JK, Van Engeland H. Hypothalamic-pituitary-adrenal axis and autonomic nervous system activity in disruptive children and matched controls. J Am Acad Child Adolesc Psychiatry 2000; 39: 1438–45.

142   Gradishar WJ, Schilsky RL. Effects of cancer treatment on the reproductive system. Crit Rev Oncol Hematol 1988; 8: 153–71.

143   Knopman JM, Papadopoulos EB, Grifo JA, Fino ME, Noyes N. Surviving childhood and reproductive-age malignancy: Effects on fertility and future parenthood. Lancet Oncol. 2010; 11: 490–8.

144   Moore BD 3rd, Copeland DR, Ried H, Levy B. Neurophysiological basis of cognitive deficits in long-term survivors of childhood cancer. Arch Neurol 1992; 49: 809–17.

145   von der Weid N, Mosimann I, Hirt A, et al. Intellectual outcome in children and adolescents with acute lymphoblastic leukaemia treated with chemotherapy alone: age- and sex-related differences. Eur J Cancer 2003; 39: 359–65.

146   Tamaroff M, Miller DR, Murphy ML, Salwen R, Ghavimi F, Nir Y. Immediate and long-term posttherapy neuropsychologic performance in children with acute lymphoblastic leukemia treated without central nervous system radiation. J Pediatr 1982; 101: 524–9.

147   Kadan-Lottick NS, Zeltzer LK, Liu Q, et al. Neurocognitive functioning in adult survivors of childhood non-central nervous system cancers. J Natl Cancer Inst 2010; 102: 881–93.

148   Giralt J, Ortega JJ, Olive T, Verges R, Forio I, Salvador L. Long-term neuropsychologic sequelae of childhood leukemia: Comparison of two CNS prophylactic regimens. Int J Radiat Oncol Biol Phys 1992; 24: 49–53.

149   Brown RT. A 3-year follow-up of the intellectual and academic functioning of children receiving central nervous system prophylactic chemotherapy for Leukemia. J Dev Behav Pediatr 1996; 17: 392–8.

150   Buizer AI, De Sonneville LMJ, van den Heuvel-Eibrink MM, Njiokiktjien C, Veerman AJP. Visuomotor control in survivors of childhood acute lymphoblastic leukemia treated with chemotherapy only. J Int Neuropsychol Soc 2005; 11: 554–65.

151   Copeland DR, Dowell RE, Fletcher JM, et al. Neuropsychological effects of childhood cancer treatment. J Child Neurol 1988; 3: 53–62.

152   Wengenroth L, Rueegg CS, Michel G, et al. Concentration, working speed and memory: Cognitive problems in young childhood cancer survivors and their siblings. Pediatr Blood Cancer 2015; 62: 875–82.

153   Prasad PK, Hardy KK, Zhang N, et al. Psychosocial and Neurocognitive Outcomes in Adult Survivors of Adolescent and Early Young Adult Cancer: A Report From the Childhood Cancer Survivor Study. J Clin Oncol 2015; 33: 2545–52.

154   Edelmann MN, Daryani VM, Bishop MW, et al. Neurocognitive and Patient-Reported Outcomes in Adult Survivors of Childhood Osteosarcoma. JAMA Oncol 2016; 2: 201–8.

155   De Ruiter MB, Reneman L, Boogerd W, et al. Late effects of high-dose adjuvant chemotherapy on white and gray matter in breast cancer survivors: Converging results from multimodal magnetic resonance imaging. Hum Brain Mapp 2012; 33: 2971–83.

156   Deprez S, Billiet T, Sunaert S, Leemans A. Diffusion tensor MRI of chemotherapy-induced cognitive impairment in non-CNS cancer patients: A review. Brain Imaging Behav. 2013; 7: 409–35.

157   Pomykala KL, de Ruiter MB, Deprez S, McDonald BC, Silverman DHS. Integrating imaging findings in evaluating the post-chemotherapy brain. Brain Imaging Behav 2013; 7: 436–52.

158   McDonald BC, Conroy SK, Ahles TA, West JD, Saykin AJ. Gray matter reduction associated with systemic chemotherapy for breast cancer: a prospective MRI study. Breast Cancer Res Treat 2010; 123: 819–28.

159   Schneiderman B. Hippocampal volumes smaller in chemotherapy patients. Lancet Oncol. 2004; 5: 202.

160   Stemmer SM, Stears JC, Burton BS, Jones RB, Simon JH. White matter changes in patients with breast cancer treated with high-dose chemotherapy and autologous bone marrow support. AJNR Am J Neuroradiol 1994; 15: 1267–73.

161   de Ruiter MB, Reneman L, Boogerd W, et al. Cerebral hyporesponsiveness and cognitive impairment 10 years after chemotherapy for breast cancer. Hum Brain Mapp 2011; 32: 1206–19.

162   Kesler SR, Kent JS, O'Hara R. Prefrontal cortex and executive function impairments in primary breast cancer. Arch Neurol 2011; 68: 1447–53.

163   Kesler SR, Bennett FC, Mahaffey ML, Spiegel D. Regional brain activation during verbal declarative memory in metastatic breast cancer. Clin Cancer Res 2009; 15: 6665–73.

164   Hertzberg H, Huk WJ, Ueberall MA, et al. CNS late effects after ALL therapy in childhood. Part I: Neuroradiological findings in long-term survivors of childhood ALL - An evaluation of the interferences between morphology and neuropsychological performance. Med Pediatr Oncol 1997; 28: 387–400.

165   Kingma A, van Dommelen RI, Mooyaart EL, Wilmink JT, Deelman BG, Kamps WA. Slight cognitive impairment and magnetic resonance imaging abnormalities but normal school levels in children treated for acute lymphoblastic leukemia with chemotherapy only. J Pediatr 2001; 139: 413–20.

166   Montour-Proulx I, Kuehn SM, Keene DL, et al. Cognitive changes in children treated for acute lymphoblastic leukemia with chemotherapy only according to the Pediatric Oncology Group 9605 protocol. J Child Neurol 2005; 20: 129–33.

167   Carey ME, Haut MW, Reminger SL, Hutter JJ, Theilmann R, Kaemingk KL. Reduced frontal white matter volume in long-term childhood leukemia survivors: A voxel-based morphometry study. Am J Neuroradiol 2008; 29: 792–7.

168   Lesnik PG, Ciesielski KT, Hart BL, Benzel EC, Sanders JA. Evidence for cerebellar-frontal subsystem changes in children treated with intrathecal chemotherapy for leukemia: enhanced data analysis using an effect size model. Arch Neurol 1998; 55: 1561–8.

169   Pääkkö E, Harila-Saari a, Vanionpää L, Himanen S, Pyhtinen J, Lanning M. White matter changes on MRI during treatment in children with acute lymphoblastic leukemia: correlation with neuropsychological findings. Med Pediatr Oncol 2000; 35: 456–61.

170   Billiet* T, Elens* I, Sleurs* C, Uyttebroeck A, Lemiere J, Deprez S. Brain Connectivity and Cognitive Flexibility in Nonirradiated Adult Survivors of Childhood Leukemia. JNCI J Natl Cancer Inst 2018; 110: 1–9.

171   Kesler SR, Tanaka H, Koovakkattu D. Cognitive reserve and brain volumes in pediatric acute lymphoblastic leukemia. Brain Imaging Behav 2010; 4: 256–69.

172   Trask CL, Welch JJG, Manley P, Jelalian E, Schwartz CL. Parental needs for information related to neurocognitive late effects from pediatric cancer and its treatment. Pediatr Blood Cancer 2009; 52: 273–9.

173   Gioia GA, Isquith PK, Guy SC, Kenworthy L. Behavior rating inventory of executive function. Child Neuropsychol 2000; 6: 235–8.

174   Varni JW, Limbers CA, Bryant WP, Wilson DP. The PedsQL multidimensional fatigue scale in pediatric obesity: feasibility, reliability and validity. Int J Pediatr Obes 2010; 5: 34–42.

175   Varni JW, Seid M, Rode CA. The PedsQL: measurement model for the pediatric quality of life inventory. Med Care 1999; 37: 126–39.

176   Elens I, Deprez S, Danckaerts M, et al. Neurocognitive Sequelae in Adult Childhood Leukemia Survivors Related to Levels of Phosphorylated Tau. JNCI J Natl Cancer Inst 2017; 109: 1–4.

177   Van der Ploeg HM. Validity of the Zelf-Beoordelings-Vragenlijst (A Dutch version of the Spielberger State-Trait Anxiety Inventory). Ned Tijdschr voor Psychol en haar Grensgebieden 1980; 35: 243–9.

178   Beck A, Steer R, Brown G. Beck Depression Inventory-II. San Antonio 1996; : 12–5.

179   Broadbent DE, Cooper PF, FitzGerald P, Parkes KR. The cognitive failures questionnaire (CFQ) and its correlates. Br J Clin Psychol 1982; 21: 1–16.

180   Roth RM, Isquith PK, Gioia GA. Behavior Rating Inventory of Executive Function®–Adult Version (BRIEF®-A). Psychol Assess Resour 2005. DOI:10.1093/arclin/act031.

181   Karimi M, Brazier J. Health, Health-Related Quality of Life, and Quality of Life: What is the Difference? Pharmacoeconomics 2016; 34: 645–9.

182   Sterken C, Lemiere J, Van den Berghe G, Mesotten D. Neurocognitive Development After Pediatric Heart Surgery. Pediatrics 2016; 137: e20154675.

183   Mesotten D, Gielen M, Sterken C, et al. Neurocognitive Development of Children 4 Years After Critical Illness and Treatment With Tight Glucose Control. JAMA 2012; 308: 1641.

184   Wechsler D. WPPSI-III administration and scoring manual. Psychol Corp 2002. DOI:10.1177/1073191102009001003.

185   Wechsler D. Manual for the Wechsler Intelligence Scale for Children-Third Edition (WISC-III). J Abnorm Child Psychol 1991.

186   Cohen MJ. Children's Memory Scale. J Psychoeduc Assess 2001; 19: 392–400.

187   De Sonneville L. Amsterdam neuropsychological tasks: a computer-aided assessment program. In: Cognitive ergonomics, clinical assessment and computer-assisted learning: computers in psychology. 1999: 187–203.

188   Beery KE, Beery NA. The Beery-Buktenica Developmental Test of Visual-Motor Integration (Beery-VMI) with supplemental Developmental tests of Visual Perception and Motor Coordination and Stepping Stones Age Norms from Birth to Age Six. 5th Ed Pearson Assessments, Minneapolis 2004.

189   Wechsler D. Wechsler adult intelligence scale–Fourth Edition (WAIS–IV). 2008.

190   Weiss LG, Saklofske DH, Coalson DL, Raiford SE. WAIS-IV Clinical Use and Interpretation. 2010 DOI:10.1016/C2009-0-01910-2.

191   Van der Elst W, van Boxtel MPJ, van Breukelen GJP, Jolles J. Rey's verbal learning test: normative data for 1855 healthy participants aged 24-81 years and the influence of age, sex, education, and mode of presentation. J Int Neuropsychol Soc 2005; 11: 290–302.

192   Foster PS, Drago V, Harrison DW. Assessment of nonverbal learning and memory using the Design Learning Test. J Psychol 2009; 143: 245–66.

193   Ross TP, Calhoun E, Cox T, Wenner C, Kono W, Pleasant M. The reliability and validity of qualitative scores for the Controlled Oral Word Association Test. Arch Clin Neuropsychol 2007; 22: 475–88.

194   Williams J. Test review: Peabody picture vocabulary test-third edition (ppvt-iii). Can. J. Sch. Psychol. 1999; 14: 67–73.

195   Trahan LH, Stuebing KK, Fletcher JM, Hiscock M. The Flynn effect: a meta-analysis. Psychol Bull 2014; 140: 1332–60.

196   Van der Ploeg HM. Zelf-Beoordelings Vragenlijst: een Nederlandstalige bewerking van de Spielberger State-Trait Anxiety Inventory. Lisse: Swets en Zeitlinger, 2000.

197   Van Der Does A, Willem J. BDI-II-NL: de Nederlandse versie van de Beck Depression Inventory. Amsterdam: Harcourt Test Publishers, 2002.

198   Ponds R, van Boxtel MP, Jolles J. De 'Cognitive Failure Questionnaire' als maat voor subjectief cognitief functioneren. Tijdschr voor Neuropsychol 2006; 2: 37–45.

199   Horton AM, Monahan MC, Fennell EB. Children's Memory Scale - Book and test review. Arch Clin Neuropsychol 2001; 16: 193–8.

200   Delaney RC, Prevey ML, Cramer J, Mattson RH. Test-retest comparability and control subject data for the rey-auditory verbal learning test and rey-osterrieth/taylor complex figures. Arch Clin Neuropsychol 1992. DOI:10.1016/0887-6177(92)90142-A.

201   de Paula JJ, Cunha Melo LP, Nicolato R, et al. Reliability and construct validity of the Rey-Auditory Verbal Learning Test in Brazilian elders. Rev Psiquiatr Clin 2012. DOI:10.1590/S0101-60832012000100004.

202   Wilhelm P, Van Klink M. Validity of the Rey Visual Design Learning Test in primary and secondary school children. Child Neuropsychol 2007. DOI:10.1080/09297040600634579.

203   Radiology Insights. May, 28. 2016. https://radiologykey.com/tissue-contrast-some-clinical-applications/.

204   Mori S, Zhang J. Principles of Diffusion Tensor Imaging and Its Applications to Basic Neuroscience Research.

Neuron. 2006; 51: 527–39.

205 Fox MD, Raichle ME. Spontaneous fluctuations in brain activity observed with functional magnetic resonance imaging. Nat Rev Neurosci 2007; 8: 700–11.

206 Heeger DJ, Ress D. What does fMRI tell us about neuronal activity? Nat. Rev. Neurosci. 2002; 3: 142–51.

207 Langeveld N, Stam H, Grootenhuis M, Last B. Quality of life in young adult survivors of childhood cancer. Support Care Cancer 2002; 10: 579–600.

208 Langeveld NE, Ubbink MC, Last BF, Grootenhuis MA, Voûte PA, De Haan RJ. Educational achievement, employment and living situation in long-term young adult survivors of childhood cancer in the Netherlands. Psychooncology 2003; 12: 213–25.

209 Anderson VA, Godber T, Smibert E, Weiskop S, Ekert H. Cognitive and academic outcome following cranial irradiation and chemotherapy in children: a longitudinal study. Br J Cancer 2000; 82: 255–62.

210 Reddick WE, Shan ZY, Glass JO, et al. Smaller white-matter volumes are associated with larger deficits in attention and learning among long-term survivors of acute lymphoblastic leukemia. Cancer 2006; 106: 941–9.

211 Peterson CC, Johnson CE, Ramirez LY, et al. A meta-analysis of the neuropsychological sequelae of chemotherapy-only treatment for pediatric acute lymphoblastic leukemia. Pediatr Blood Cancer 2008; 51: 99–104.

212 Ciesielski KT, Lesnik PG, Benzel EC, Hart BL, Sanders J a. MRI morphometry of mamillary bodies, caudate nuclei, and prefrontal cortices after chemotherapy for childhood leukemia: multivariate models of early and late developing memory subsystems. Behav Neurosci 1999; 113: 439–50.

213 Hill DE, Ciesielski KT, Sethre-Hofstad L, Duncan MH, Lorenzi M. Visual and verbal short-term memory deficits in childhood leukemia survivors after intrathecal chemotherapy. J Pediatr Psychol 1997; 22: 861–70.

214 Mennes M, Stiers P, Vandenbussche E, et al. Attention and information processing in survivors of childhood acute lymphoblastic leukemia treated with chemotherapy only. Pediatr Blood Cancer 2005; 44: 478–86.

215 Rodgers J, Marckus R, Kearns P, Windebank K. Attentional ability among survivors of leukaemia treated without cranial irradiation. Arch Dis Child 2003; 88: 147–50.

216 Buizer AI, De Sonneville LMJ, Van Den Heuvel-Eibrink MM, Veerman AJP. Chemotherapy and attentional dysfunction in survivors of childhood acute lymphoblastic leukemia: Effect of treatment intensity. Pediatr Blood Cancer 2005; 45: 281–90.

217 Kingma A, Van Dommelen RI, Mooyaart EL, Wilmink JT, Deelman BG, Kamps WA. No major cognitive impairment in young children with acute lymphoblastic leukemia using chemotherapy only: a prospective longitudinal study. J Pediatr Hematol Oncol 2002; 24: 106–14.

218 Halsey C, Buck G, Richards S, Vargha-Khadem F, Hill F, Gibson B. The impact of therapy for childhood acute lymphoblastic leukaemia on intelligence quotients; Results of the risk-stratified randomized central nervous system treatment trial MRC UKALL XI. J Hematol Oncol 2011; 4. DOI:10.1186/1756-8722-4-42.

219 Jansen NC, Kingma A, Schuitema A, et al. Post-treatment intellectual functioning in children treated for acute lymphoblastic leukaemia (ALL) with chemotherapy-only: A prospective, sibling-controlled study. Eur J Cancer 2006; 42: 2765–72.

220 Uyttebroeck A, Suciu S, Laureys G, et al. Treatment of childhood T-cell lymphoblastic lymphoma according to the strategy for acute lymphoblastic leukaemia, without radiotherapy: Long term results of the EORTC CLG 58881 trial. Eur J Cancer 2008; 44: 840–6.

221 Vilmer E, Suciu S, Ferster A, et al. Long-term results of three randomized trials (58831, 58832, 58881) in childhood acute lymphoblastic leukemia: a CLCG-EORTC report. Leukemia 2000; 14: 2257–66.

222 Turkheimer E, Haley A, Waldron M, D'Onofrio B, Gottesman II. Socioeconomic status modifies heritability of IQ in young children. Psychol Sci 2003; 14: 623–8.

223 Irwing P, Lynn R. Sex differences in means and variability on the progressive matrices in university students: A meta-analysis. Br J Psychol 2005; 96: 505–24.

224 Mody R, Li S, Dover DC, et al. Twenty-five-year follow-up among survivors of childhood acute lymphoblastic leukemia: A report from the Childhood Cancer Survivor Study. Blood 2008. DOI:10.1182/blood-2007-10-117150.

225 Anderson V, Spencer-Smith M, Wood A. Do children really recover better? Neurobehavioural plasticity after early brain insult. Brain. 2011; 134: 2197–221.

226 Chang EL, Wefel JS, Hess KR, et al. Neurocognition in patients with brain metastases treated with radiosurgery or radiosurgery plus whole-brain irradiation: a randomised controlled trial. Lancet Oncol 2009; 10: 1037–44.

227 McDuff SGR, Taich ZJ, Lawson JD, et al. Neurocognitive assessment following whole brain radiation therapy and radiosurgery for patients with cerebral metastases. J Neurol Neurosurg Psychiatry 2013; 84: 1384–91.

228 Sleurs C, Lemiere J, Vercruysse T, et al. Intellectual development of childhood ALL patients: A multicenter longitudinal study. Psychooncology 2016. DOI:10.1002/pon.4186.

229 Cheung YT, Krull KR. Neurocognitive outcomes in long-term survivors of childhood acute lymphoblastic leukemia treated on contemporary treatment protocols: A systematic review. Neurosci Biobehav Rev 2015; 53: 108–20.

230 Cheung YT, Sabin ND, Reddick WE, et al. Leukoencephalopathy and long-term neurobehavioural, neurocognitive, and brain imaging outcomes in survivors of childhood acute lymphoblastic leukaemia treated with chemotherapy: a longitudinal analysis. Lancet Haematol 2016; 3: 456–66.

231 Bhojwani D, Sabin ND, Pei D, et al. Methotrexate-induced neurotoxicity and leukoencephalopathy in childhood acute lymphoblastic leukemia. J Clin Oncol 2014; 32: 949–59.

232 Krull KR, Minoshima S, Edelmann M, et al. Regional brain glucose metabolism and neurocognitive function in adult survivors of childhood cancer treated with cranial radiation. J Nucl Med 2014; 55: 1805–10.

233 Brajnik V, Kastrup O. Differential diagnosis of stroke: Subacute leukoencephalopathy following high-dose methotrexate therapy in a young patient with osteosarcoma. Interdiscip Neurosurg 2016; 3: 15–6.

234 Szabatura AH, Cirrone F, Harris C, et al. An assessment of risk factors associated with ifosfamide-induced encephalopathy in a large academic cancer center. J Oncol Pharm Pract 2014. DOI:10.1177/1078155214527143.

235 Deprez S, Amant F, Yigit R, et al. Chemotherapy-induced structural changes in cerebral white matter and its correlation with impaired cognitive functioning in breast cancer patients. Hum Brain Mapp 2011; 32: 480–93.

236 Stouten-Kemperman MM, de Ruiter MB, Koppelmans V, Boogerd W, Reneman L, Schagen SB. Neurotoxicity in breast cancer survivors ≥10 years post-treatment is dependent on treatment type. Brain Imaging Behav 2014; : 275–84.

237 Amidi A, Agerbaek M, Wu LM, et al. Changes in cognitive functions and cerebral grey matter and their associations with inflammatory markers, endocrine markers, and APOE genotypes in testicular cancer patients undergoing treatment. Brain Imaging Behav. 2016; : 1–15.

238 Tournier J-D, Mori S, Leemans A. Diffusion tensor imaging and beyond. Magn Reson Med 2011; 65: 1532–56.

239 Menning S, de Ruiter MB, Veltman DJ, et al. Changes in brain white matter integrity after systemic treatment for breast cancer: a prospective longitudinal study. Brain Imaging Behav 2017; published online March. DOI:10.1007/s11682-017-9695-x.

240 Krull KR, Bhojwani D, Conklin HM, et al. Genetic mediators of neurocognitive outcomes in survivors of childhood acute lymphoblastic leukemia. J Clin Oncol 2013; 31: 2182–8.

241 Krull KR, Brouwers P, Jain N, et al. Folate Pathway Genetic Polymorphisms are Related to Attention Disorders in Childhood Leukemia Survivors. J Pediatr 2008; 152: 101–5.

242 Schilling S, DeStefano AL, Sachdev PS, et al. APOE genotype and MRI markers of cerebrovascular disease. Neurology. 2013; 81: 292–300.

243 Puglielli L, Tanzi RE, Kovacs DM. Alzheimer's disease: the cholesterol connection. Nat Neurosci 2003; 6: 345–51.

244 Koleck TA, Bender CM, Sereika SM, et al. Apolipoprotein E genotype and cognitive function in postmenopausal women with early-stage breast cancer. Oncol Nurs Forum 2014; 41: E313-25.

245 Correa D, DeAngelis L, Shi W, Thaler H, Lin M, Abrey L. Cognitive functions in low-grade gliomas: Disease and treatment effects. J Neurooncol 2007; 81: 175–84.

246 Correa DDD, Satagopan J, Baser R, et al. APOE polymorphisms and cognitive functions in patients with brain tumors. Neurology 2014; 83: 320–7.

247 Oberlin O, Rey A, Sanchez De Toledo J, et al. Randomized comparison of intensified six-drug versus standard three-drug chemotherapy for high-risk nonmetastatic rhabdomyosarcoma and other chemotherapy-sensitive childhood soft tissue sarcomas: Long-term results from the International Society of Pediatr. J Clin Oncol 2012; 30: 2457–65.

248 Le Deley MC, Paulussen M, Lewis I, et al. Cyclophosphamide compared with ifosfamide in consolidation treatment of standard-risk Ewing sarcoma: Results of the randomized noninferiority Euro-EWING99-R1 trial. J Clin Oncol 2014; 32: 2440–8.

249 Bielack SS, Werner M, Tunn PU, et al. Methotrexate, doxorubicin, and cisplatin (MAP) plus maintenance pegylated interferon alfa-2b versus MAP alone in patients with resectable high-grade osteosarcoma and good histologic response to preoperative MAP: First results of the EURAMOS-1 good respons. J Clin Oncol

2015; 33: 2279–87.

250 Ferrari A, de Salvo GL, Brennan B, et al. Synovial sarcoma in children and adolescents: The European Pediatric Soft Tissue Sarcoma Study Group prospective trial (EpSSG NRSTS 2005). Ann Oncol 2015; 26: 567–72.

251 Debette S, Markus HS. The clinical importance of white matter hyperintensities on brain magnetic resonance imaging: Systematic review and meta-analysis. BMJ Br Med J 2010; 341: 1–9.

252 Fazekas F, Chawluk JB, Alavi A. MR signal abnormalities at 1.5 T in Alzheimer's dementia and normal aging. Am. J. Neuroradiol. 1987; 8: 421–6.

253 Billiet T, Vandenbulcke M, Maedler B, et al. Age-related microstructural differences quantified using myelin water imaging and advanced diffusion MRI. Neurobiol Aging 2015; 36: 2107–21.

254 Hackman DA, Farah MJ. Socioeconomic status and the developing brain. Trends Cogn. Sci. 2009; 13: 65–73.

255 Hackman DA, Farah MJ, Meaney MJ. Socioeconomic status and the brain: mechanistic insights from human and animal research. Nat Rev Neurosci 2010; 11: 651–9.

256 Rock PL, Roiser JP, Riedel WJ, Blackwell AD. Cognitive impairment in depression: a systematic review and meta-analysis. Psychol Med 2014; 44: 2029–40.

257 Arrieta O, Angulo LP, Núñez-Valencia C, et al. Association of depression and anxiety on quality of life, treatment adherence, and prognosis in patients with advanced non-small cell lung cancer. Ann Surg Oncol 2013; 20: 1941–8.

258 Papp K V, Kaplan RF, Springate B, et al. Processing speed in normal aging: effects of white matter hyperintensities and hippocampal volume loss. Neuropsychol Dev Cogn B Aging Neuropsychol Cogn 2014; 21: 197–213.

259 Cheung YT, Khan RB, Liu W, et al. Association of Cerebrospinal Fluid Biomarkers of Central Nervous System Injury With Neurocognitive and Brain Imaging Outcomes in Children Receiving Chemotherapy for Acute Lymphoblastic Leukemia. JAMA Oncol 2018; 38105: 1–8.

260 Billiet T, Emsell L, Vandenbulcke M, et al. Recovery from chemotherapy-induced white matter changes in young breast cancer survivors? Brain Imaging Behav. 2017; : 1–14.

261 Wardlaw JM, Valdés Hernández MC, Muñoz-Maniega S. What are white matter hyperintensities made of? Relevance to vascular cognitive impairment. J. Am. Heart Assoc. 2015; 4: 001140.

262 Taheri S, Gasparovic C, Huisa BN, et al. Blood-brain barrier permeability abnormalities in vascular cognitive impairment. Stroke 2011; 42: 2158–63.

263 Reddick WE, Glass JO, Helton KJ, et al. Prevalence of leukoencephalopathy in children treated for Acute Lymphoblastic Leukemia with high-dose methotrexate. AJNR Am J Neuroradiol 2005; 26: 1263–9.

264 Duffner PK, Armstrong FD, Chen L, et al. Neurocognitive and neuroradiologic central nervous system late effects in children treated on Pediatric Oncology Group (POG) P9605 (standard risk) and P9201 (lesser risk) acute lymphoblastic leukemia protocols (ACCL0131): a methotrexate consequence? A rep. J Pediatr Hematol Oncol 2014; 36: 8–15.

265 Krull KR, Okcu MF, Potter B, et al. Screening for neurocognitive impairment in pediatric cancer long-term survivors. J Clin Oncol 2008; 26: 4138–43.

266 Krull KR, Brinkman TM, Li C, et al. Neurocognitive outcomes decades after treatment for childhood acute lymphoblastic leukemia: A report from the St jude lifetime cohort study. J Clin Oncol 2013; 31: 4407–15.

267 Khong P. White Matter Anisotropy in Post-Treatment Childhood Cancer Survivors: Preliminary Evidence of Association With Neurocognitive Function. J Clin Oncol 2006; 24: 884–90.

268 Schuitema I, Deprez S, Van Hecke W, et al. Accelerated aging, decreased white matter integrity and associated cognitive dysfunction 25 years after childhood acute lymphoblastic leukemia. Pediatr Blood Cancer 2012; 59: 965–1152.

269 Edelmann MN, Krull KR, Liu W, et al. Diffusion tensor imaging and neurocognition in survivors of childhood acute lymphoblastic leukaemia. Brain 2014; 137: 2973–83.

270 Kesler SR, Gugel M, Huston-Warren E, Watson C. Atypical Structural Connectome Organization and Cognitive Impairment in Young Survivors of Acute Lymphoblastic Leukemia. Brain Connect 2016; 6: 273–82.

271 Tamnes CK, Zeller B, Amlien IK, et al. Cortical surface area and thickness in adult survivors of pediatric acute lymphoblastic leukemia. Pediatr Blood Cancer 2015; 62: 1027–34.

272 Krull KR, Cheung YT, Liu W, et al. Chemotherapy Pharmacodynamics and Neuroimaging and Neurocognitive Outcomes in Long-Term Survivors of Childhood Acute Lymphoblastic Leukemia. www.jco.org June J Clin Oncol 2016; 6: 2644–53.

273 Koppelmans V, Breteler MMB, Boogerd W, Seynaeve C, Schagen SB. Late effects of adjuvant

chemotherapy for adult onset non-CNS cancer; cognitive impairment, brain structure and risk of dementia. Crit. Rev. Oncol. Hematol. 2013; 88: 87–101.

274   van der Plas E, Nieman BJ, Butcher DT, et al. Neurocognitive Late Effects of Chemotherapy in Survivors of Acute Lymphoblastic Leukemia: Focus on Methotrexate. J Can Acad Child Adolesc Psychiatry 2015; 24: 25–32.

275   Schapiro M, Hayashi R, Liu W, et al. Neurocognitive, emotional, and quality of life outcomes in long-term survivors of rhabdomyosarcoma: A report from the Childhood Cancer Survivor Study (CCSS). J. Clin. Oncol. 2015; 33: no pagination.

276   Ahles T, Li Y, McDonald B, et al. Longitudinal assessment of cognitive changes associated with adjuvant treatment for breast cancer: the impact of APOE and smoking. Psycho-oncol 2014; 23: 1382–90.

277   Madden DJ, Bennett IJ, Song AW. Cerebral white matter integrity and cognitive aging: Contributions from diffusion tensor imaging. Neuropsychol. Rev. 2009; 19: 415–35.

278   Partridge SC, Ziadloo A, Murthy R, et al. Diffusion tensor MRI: Preliminary anisotropy measures and mapping of breast tumors. J Magn Reson Imaging 2010; 31: 339–47.

279   Koppelmans V, de Groot M, de Ruiter MB, et al. Global and focal white matter integrity in breast cancer survivors 20 years after adjuvant chemotherapy. Hum Brain Mapp 2014; 35: 889–99.

280   Abraham J, Haut MW, Moran MT, Filburn S, Lemiuex S, Kuwabara H. Adjuvant chemotherapy for breast cancer: effects on cerebral white matter seen in diffusion tensor imaging. Clin Breast Cancer 2008; 8: 88–91.

281   Zhang H, Schneider T, Wheeler-Kingshott CA, Alexander DC. NODDI: Practical in vivo neurite orientation dispersion and density imaging of the human brain. Neuroimage 2012; 61: 1000–16.

282   Jeurissen B, Leemans A, Tournier JD, Jones DK, Sijbers J. Investigating the prevalence of complex fiber configurations in white matter tissue with diffusion magnetic resonance imaging. Hum Brain Mapp 2013; 34: 2747–66.

283   Raffelt DA, Tournier JD, Smith RE, et al. Investigating white matter fibre density and morphology using fixel-based analysis. Neuroimage. 2016. DOI:10.1016/j.neuroimage.2016.09.029.

284   Leemans A, Jeurissen B, Sijbers J, Jones D. ExploreDTI: a graphical toolbox for processing, analyzing, and visualizing diffusion MR data. Proc 17th Sci Meet Int Soc Magn Reson Med 2009; 17: 3537.

285   Tustison NJ, Avants BB, Cook PA, et al. N4ITK: Improved N3 bias correction. IEEE Trans Med Imaging 2010; 29: 1310–20.

286   Raffelt D, Tournier JD, Rose S, et al. Apparent Fibre Density: A novel measure for the analysis of diffusion-weighted magnetic resonance images. Neuroimage 2012; 59: 3976–94.

287   Tournier JD, Calamante F, Connelly A. MRtrix: Diffusion tractography in crossing fiber regions. Int J Imaging Syst Technol 2012; 22: 53–66.

288   Tournier JD, Calamante F, Connelly A. Determination of the appropriate b value and number of gradient directions for high-angular-resolution diffusion-weighted imaging. NMR Biomed 2013; 26: 1775–86.

289   Raffelt D, Tournier JD, Fripp J, Crozier S, Connelly A, Salvado O. Symmetric diffeomorphic registration of fibre orientation distributions. Neuroimage 2011; 56: 1171–80.

290   Raffelt DA, Smith RE, Ridgway GR, et al. Connectivity-based fixel enhancement: Whole-brain statistical analysis of diffusion MRI measures in the presence of crossing fibres. Neuroimage 2015; 117: 40–55.

291   Smith SM, Nichols TE. Threshold-free cluster enhancement: Addressing problems of smoothing, threshold dependence and localisation in cluster inference. Neuroimage 2009; 44: 83–98.

292   Simó M, Rifà-Ros X, Rodriguez-Fornells A, Bruna J. Chemobrain: A systematic review of structural and functional neuroimaging studies. Neurosci. Biobehav. Rev. 2013; 37: 1311–21.

293   Kochunov P, Williamson DE, Lancaster J, et al. Fractional anisotropy of water diffusion in cerebral white matter across the lifespan. Neurobiol Aging 2012; 33: 9–20.

294   Abbott NJ. Evidence for bulk flow of brain interstitial fluid: Significance for physiology and pathology. Neurochem. Int. 2004; 45: 545–52.

295   Concha L. A macroscopic view of microstructure: Using diffusion-weighted images to infer damage, repair, and plasticity of white matter. Neuroscience. 2014; 276: 14–28.

296   Garg N, Reddel SW, Miller DH, et al. The corpus callosum in the diagnosis of multiple sclerosis and other CNS demyelinating and inflammatory diseases. J Neurol Neurosurg Psychiatry 2015; : 1–9.

297   Smith KW, Gierski F, Andre J, et al. Altered white matter integrity in whole brain and segments of corpus callosum, in young social drinkers with binge drinking pattern. Addict Biol 2017; 22: 490–501.

298   Kapogiannis D, Kisser J, Davatzikos C, Ferrucci L, Metter J, Resnick SM. Alcohol consumption and premotor corpus callosum in older adults. Eur Neuropsychopharmacol 2012; 22: 704–10.

299   Vos SB, Jones DK, Viergever MA, Leemans A. Partial volume effect as a hidden covariate in DTI analyses.

Neuroimage 2011; 55: 1566–76.

300 Whelan JS, Bielack SS, Marina N, et al. EURAMOS-1, an international randomised study for osteosarcoma: Results from pre-randomisation treatment. Ann Oncol 2015; 26: 407–14.

301 Ferrari A, Trama A, De Paoli A, et al. Access to clinical trials for adolescents with soft tissue sarcomas: Enrollment in European pediatric Soft tissue sarcoma Study Group (EpSSG) protocols. Pediatr Blood Cancer 2017; 64. DOI:10.1002/pbc.26348.

302 Gooijers J, Swinnen SP. Interactions between brain structure and behavior: The corpus callosum and bimanual coordination. Neurosci. Biobehav. Rev. 2014; 43: 1–19.

303 Armstrong RC, Mierzwa AJ, Marion CM, Sullivan GM. White matter involvement after TBI: Clues to axon and myelin repair capacity. Exp. Neurol. 2016; 275: 328–33.

304 Armstrong RC, Mierzwa AJ, Sullivan GM, Sanchez MA. Myelin and oligodendrocyte lineage cells in white matter pathology and plasticity after traumatic brain injury. Neuropharmacology. 2016; 110: 654–9.

305 Ahles T, Saykin A. Candidate mechanisms for chemotherapy-induced cognitive changes. Nat Rev Cancer 2007; 7: 192–201.

306 Hampson JP, Zick SM, Khabir T, Wright BD, Harris RE. Altered resting brain connectivity in persistent cancer related fatigue. NeuroImage Clin 2015; 8: 305–13.

307 Duncan NW, Hayes DJ, Wiebking C, et al. Negative childhood experiences alter a prefrontal-insular-motor cortical network in healthy adults: A preliminary multimodal rsfMRI-fMRI-MRS-dMRI study. Hum Brain Mapp 2015; 36: 4622–37.

308 Yoshikawa E, Matsuoka Y, Yamasue H, et al. Prefrontal cortex and amygdala volume in first minor or major depressive episode after cancer diagnosis. Biol Psychiatry 2006; 59: 707–12.

309 Hakamata Y, Matsuoka Y, Inagaki M, et al. Structure of orbitofrontal cortex and its longitudinal course in cancer-related post-traumatic stress disorder. Neurosci Res 2007; 59: 383–9.

310 Zhang Y, Zou P, Mulhern RK, Butler RW, Laningham FH, Ogg RJ. Brain structural abnormalities in survivors of pediatric posterior fossa brain tumors: A voxel-based morphometry study using free-form deformation. Neuroimage 2008; 42: 218–29.

311 Porto L, Preibisch C, Hattingen E, et al. Voxel-based morphometry and diffusion-tensor MR imaging of the brain in long-term survivors of childhood leukemia. Eur Radiol 2008; 18: 2691–700.

312 Genschaft M, Huebner T, Plessow F, et al. Impact of chemotherapy for childhood leukemia on brain morphology and function. PLoS One 2013; 8. DOI:10.1371/journal.pone.0078599.

313 Zou L, Su L, Xu J, et al. Structural brain alteration in survivors of acute lymphoblastic leukemia with chemotherapy treatment: A voxel-based morphometry and diffusion tensor imaging study. Brain Res 2017; 1658: 68–72.

314 Inagaki M, Yoshikawa E, Matsuoka Y, et al. Smaller regional volumes of brain gray and white matter demonstrated in breast cancer survivors exposed to adjuvant chemotherapy. Cancer 2007; 109: 146–56.

315 Lepage C, Smith AM, Moreau J, et al. A prospective study of grey matter and cognitive function alterations in chemotherapy-treated breast cancer patients. Springerplus 2014; 3: 444.

316 Conroy SK, McDonald BC, Smith DJ, et al. Alterations in brain structure and function in breast cancer survivors: effect of post-chemotherapy interval and relation to oxidative DNA damage. Breast Cancer Res Treat 2013; 137: 493–502.

317 McDonald BC, Conroy SK, Ahles TA, West JD, Saykin AJ. Gray matter reduction associated with systemic chemotherapy for breast cancer: a prospective MRI study. Breast Cancer Res Treat 2010; 123: 819–28.

318 McDonald BC, Conroy SK, Smith DJ, West JD, Saykin AJ. Frontal gray matter reduction after breast cancer chemotherapy and association with executive symptoms: a replication and extension study. Brain Behav Immun 2013; 30 Suppl: S117-25.

319 Koppelmans V, De Ruiter MB, Van Der Lijn F, et al. Global and focal brain volume in long-term breast cancer survivors exposed to adjuvant chemotherapy. Breast Cancer Res Treat 2012; 132: 1099–106.

320 Correa DD, Root JC, Kryza-Lacombe M, et al. Brain structure and function in patients with ovarian cancer treated with first-line chemotherapy: a pilot study. Brain Imaging Behav 2016; : 1–12.

321 Amidi A, Agerbaek M, Wu LM, et al. Changes in cognitive functions and cerebral grey matter and their associations with inflammatory markers, endocrine markers, and APOE genotypes in testicular cancer patients undergoing treatment. Brain Imaging Behav 2017; 11: 769–83.

322 Simo M, Root JC, Vaquero L, et al. Cognitive and brain structural changes in a lung cancer population. J Thorac Oncol 2015; 10: 38–45.

323 Willard VW, Cox LE, Russell KM, et al. Cognitive and Psychosocial Functioning of Preschool-Aged Children with Cancer. J Dev Behav Pediatr 2017; 38: 638–45.

324 Lähteenmäki PM, Krause CM, Sillanmäki L, Salmi TT, Lang AH. Event-related alpha

synchronization/desynchronization in a memory-search task in adolescent survivors of childhood cancer. Clin Neurophysiol 1999; 110: 2064–73.

325 Yi J, Zebrack B, Kim MA, Cousino M. Posttraumatic Growth Outcomes and Their Correlates Among Young Adult Survivors of Childhood Cancer. J Pediatr Psychol 2015; 40: 981–91.

326 Wilson JZ, Marin D, Maxwell K, et al. Association of Posttraumatic Growth and Illness-Related Burden With Psychosocial Factors of Patient, Family, and Provider in Pediatric Cancer Survivors. J Trauma Stress 2016; 29: 448–56.

327 Frederick NN, Kenney L, Vrooman L, Recklitis CJ. Fatigue in adolescent and adult survivors of non-CNS childhood cancer: a report from project REACH. Support Care Cancer 2016; 24: 3951–9.

328 D'Agostino NM, Edelstein K, Zhang N, et al. Comorbid symptoms of emotional distress in adult survivors of childhood cancer. Cancer 2016; 122: 3215–24.

329 Friend AJ, Feltbower RG, Hughes EJ, Dye KP, Glaser AW. Mental health of long-term survivors of childhood and young adult cancer: A systematic review. Int J Cancer 2018. DOI:10.1002/ijc.31337.

330 Jenkinson M, Pechaud M, Smith S. BET2 - MR-Based Estimation of Brain , Skull and Scalp Surfaces. Elev Annu Meet Organ Hum Brain Mapp 2002; 17: 2002.

331 Gaser C, Dahnke R. CAT - A Computational Anatomy Toolbox for the Analysis of Structural MRI Data. 2016.

332 Jaworska N, Yücel K, Courtright A, Macmaster FP, Sembo M, Macqueen G. Subgenual anterior cingulate cortex and hippocampal volumes in depressed youth: The role of comorbidity and age. J. Affect. Disord. 2016; 190: 726–32.

333 Schmaal L, Hibar DP, Sämann PG, et al. Cortical abnormalities in adults and adolescents with major depression based on brain scans from 20 cohorts worldwide in the ENIGMA Major Depressive Disorder Working Group. Mol Psychiatry 2017; 22: 900–9.

334 Marusak HA, Iadipaolo AS, Harper FW, et al. Neurodevelopmental consequences of pediatric cancer and its treatment: applying an early adversity framework to understanding cognitive, behavioral, and emotional outcomes. Neuropsychol. Rev. 2017; : 1–53.

335 Andreotti C, Root JC, Ahles TA, McEwen BS, Compas BE. Cancer, coping, and cognition: a model for the role of stress reactivity in cancer-related cognitive decline. Psychooncology 2015; 24: 617–23.

336 Jenkins V, Atkins L, Fallowfield L. Does endocrine therapy for the treatment and prevention of breast cancer affect memory and cognition? Eur J Cancer 2007; 43: 1342–7.

337 Andreano JM, Waisman J, Donley L, Cahill L. Effects of breast cancer treatment on the hormonal and cognitive consequences of acute stress. Psychooncology 2012; 21: 1091–8.

338 Chao HH, Hu S, Ide JS, et al. Effects of androgen deprivation on cerebral morphometry in prostate cancer patients--an exploratory study. PLoS One 2013; 8: e72032.

339 Noble KG, Houston SM, Kan E, Sowell ER. Neural correlates of socioeconomic status in the developing human brain. Dev Sci 2012. DOI:10.1111/j.1467-7687.2012.01147.x.

340 Lawson GM, Duda JT, Avants BB, Wu J, Farah MJ. Associations between children's socioeconomic status and prefrontal cortical thickness. Dev Sci 2013. DOI:10.1111/desc.12096.

341 Avants BB, Hackman DA, Betancourt LM, Lawson GM, Hurt H, Farah MJ. Relation of childhood home environment to cortical thickness in late adolescence: Specificity of experience and timing. PLoS One 2015. DOI:10.1371/journal.pone.0138217.

342 Gennatas ED, Avants BB, Wolf DH, et al. Age-Related Effects and Sex Differences in Gray Matter Density, Volume, Mass, and Cortical Thickness from Childhood to Young Adulthood. J Neurosci 2017; 37: 5065–73.

343 Walhovd KB, Fjell AM, Giedd J, Dale AM, Brown TT. Through Thick and Thin: a Need to Reconcile Contradictory Results on Trajectories in Human Cortical Development. Cereb. Cortex. 2017; 27: 1472–81.

344 White T, Su S, Schmidt M, Kao CY, Sapiro G. The development of gyrification in childhood and adolescence. Brain Cogn. 2010; 72: 36–45.

345 Kharitonova M, Martin RE, Gabrieli JDE, Sheridan MA. Cortical gray-matter thinning is associated with age-related improvements on executive function tasks. Dev Cogn Neurosci 2013; 6: 61–71.

346 Frodl T, O'Keane V. How does the brain deal with cumulative stress? A review with focus on developmental stress, HPA axis function and hippocampal structure in humans. Neurobiol. Dis. 2013; 52: 24–37.

347 Jacobson L, Sapolsky R. The role of the hippocampus in feedback regulation of the hypothalamic-pituitary-adrenocortical axis. Endocr Rev 1991; 12: 118–34.

348 Sapolsky RM. Atrophy of the hippocampus in posttraumatic stress disorder: How and when? Hippocampus 2001; 11: 90–1.

349 Sapolsky RM, Krey LC, McEwen BS. The neuroendocrinology of stress and aging: The glucocorticoid cascade hypothesis. Endocr Rev 1986; 7: 284–301.

350 Campbell S, MacQueen G. The role of the hippocampus in the pathophysiology of major depression. J.

Psychiatry Neurosci. 2004; 29: 417–26.

351 Rothschild G, Eban E, Frank LM. A cortical-hippocampal-cortical loop of information processing during memory consolidation. Nat Neurosci 2017; 20: 251–9.

352 Aggleton JP. Multiple anatomical systems embedded within the primate medial temporal lobe: Implications for hippocampal function. Neurosci. Biobehav. Rev. 2012; 36: 1579–96.

353 DePrince AP, Weinzierl KM, Combs MD. Executive function performance and trauma exposure in a community sample of children. Child Abuse Negl 2009; 33: 353–61.

354 Kesler SR, Adams M, Packer M, et al. Disrupted brain network functional dynamics and hyper-correlation of structural and functional connectome topology in patients with breast cancer prior to treatment. Brain Behav 2017; 7: e00643.

355 Amidi A, Hosseini SMH, Leemans A, et al. Changes in Brain Structural Networks and Cognitive Functions in Testicular Cancer Patients Receiving Cisplatin-Based Chemotherapy. J Natl Cancer Inst 2017; 109. DOI:10.1093/jnci/djx085.

356 Murphy K, Fox MD. Towards a consensus regarding global signal regression for resting state functional connectivity MRI. Neuroimage 2017; 154: 169–73.

357 Mingmei L, Caeyenberghs K. Longitudinal assessment of chemotherapy-induced changes in brain and cognitive functioning: A systematic review. Neurosci Biobehav Rev 2018.

358 Krappmann P, Paulides M, Stöhr W, et al. Almost normal cognitive function in patients during therapy for childhood acute lymphoblastic leukemia without cranial irradiation according to ALL-BFM 95 and COALL 06-97 protocols: Results of an Austrian-German multicenter longitudinal study and implicat. Pediatr Hematol Oncol 2007; 24: 101–9.

359 Hockenberry M, Krull K, Moore K, Gregurich MA, Casey ME, Kaemingk K. Longitudinal evaluation of fine motor skills in children with leukemia. J Pediatr Hematol Oncol 2007; 29: 535–9.

360 Espy KA, Moore IM, Kaufmann PM, Kramer JH, Matthay K, Hutter JJ. Chemotherapeutic CNS prophylaxis and neuropsychologic change in children with acute lymphoblastic leukemia: a prospective study. J Pediatr Psychol 2001; 26: 1–9.

361 Insel K, Hockenberry M, Harris L, et al. Declines Noted in Cognitive Processes and Association With Achievement Among Children With Leukemia. Oncol Nurs Forum 2017; 44: 503–11.

362 Jacola LM, Krull KR, Pui C-H, et al. Longitudinal Assessment of Neurocognitive Outcomes in Survivors of Childhood Acute Lymphoblastic Leukemia Treated on a Contemporary Chemotherapy Protocol. J Clin Oncol 2016; 34: 1239–47.

363 Reddick WE, Glass JO, Johnson DP, Laningham FH, Pui CH. Voxel-based analysis of T2 hyperintensities in white matter during treatment of childhood leukemia. Am J Neuroradiol 2009; 30: 1947–54.

364 Reddick WE, White HA, Glass JO, et al. Developmental model relating white matter volume to neurocognitive deficits in pediatric brain tumor survivors. Cancer 2003; 97: 2512–9.

365 Nudelman KNH, Wang Y, McDonald BC, et al. Altered cerebral blood flow one month after systemic chemotherapy for breast cancer: a prospective study using pulsed arterial spin labeling MRI perfusion. PLoS One 2014; 9: e96713.

366 Jenkins V, Shilling V, Deutsch G, et al. A 3-year prospective study of the effects of adjuvant treatments on cognition in women with early stage breast cancer. Br J Cancer 2006; 94: 828–34.

367 McDonald BC, Conroy SK, Ahles TA, West JD, Saykin AJ. Alterations in brain activation during working memory processing associated with breast cancer and treatment: A prospective functional magnetic resonance imaging study. J Clin Oncol 2012; 30: 2500–8.

368 Chen X, He X, Tao L, et al. The attention network changes in breast cancer patients receiving neoadjuvant chemotherapy: Evidence from an arterial spin labeling perfusion study. Sci Rep 2017; 7. DOI:10.1038/srep42684.

369 Conroy SK, McDonald BC, Ahles TA, West JD, Saykin AJ. Chemotherapy-induced amenorrhea: a prospective study of brain activation changes and neurocognitive correlates. Brain Imaging Behav 2013; 7: 491–500.

370 Lopez Zunini RA, Scherling C, Wallis N, et al. Differences in verbal memory retrieval in breast cancer chemotherapy patients compared to healthy controls: a prospective fMRI study. Brain Imaging Behav 2013; 7: 460–77.

371 Menning S, de Ruiter MB, Veltman DJ, et al. Changes in brain activation in breast cancer patients depend on cognitive domain and treatment type. PLoS One 2017; 12: e0171724.

372 Kim HG, Shin N-Y, Bak Y, et al. Altered intrinsic brain activity after chemotherapy in patients with gastric cancer: A preliminary study. Eur Radiol 2017; 27: 2679–88.

373 Menning S, de Ruiter MB, Veltman DJ, et al. Multimodal MRI and cognitive function in patients with breast cancer prior to adjuvant treatment--the role of fatigue. NeuroImage Clin 2015; 7: 547–54.

374   Stouten-Kemperman MM, de Ruiter MB, Koppelmans V, Boogerd W, Reneman L, Schagen SB. Neurotoxicity in breast cancer survivors ≥10 years post-treatment is dependent on treatment type. Brain Imaging Behav 2015; 9: 275–84.

375   Dietrich RB, Bradley WG, Zaragoza IV EJ, et al. MR evaluation of early myelination patterns in normal and developmentally delayed infants. Am J Neuroradiol 1988. DOI:10.2214/ajr.150.4.889.

376   Murakami JW, Weinberger E, Shaw DWW. Normal myelination of the pediatric brain imaged with fluid-attenuated inversion-recovery (FLAIR) MR imaging. Am J Neuroradiol 1999.

377   Parazzini C, Baldoli C, Scotti G, Triulzi F. Terminal zones of myelination: MR evaluation of children aged 20-40 months. Am J Neuroradiol 2002.

378   Koppelmans V, Vernooij MW, Boogerd W, et al. Prevalence of cerebral small-vessel disease in long-term breast cancer survivors exposed to both adjuvant radiotherapy and chemotherapy. J Clin Oncol 2015; 33: 588–93.

379   Sleurs C, Billiet T, Peeters R, Sunaert S, Uyttebroeck A, Deprez S. Advanced MR diffusion imaging and chemotherapy-related changes in cerebral white matter microstructure of survivors of childhood bone and soft tissue sarcoma ? 2018; : 1–13.

380   Monje M, Dietrich J. Cognitive side effects of cancer therapy demonstrate a functional role for adult neurogenesis. Behav Brain Res 2012; 227: 376–9.

381   Gleichgerrcht E, Fridriksson J, Rorden C, Bonilha L. Connectome-based lesion-symptom mapping (CLSM): A novel approach to map neurological function. NeuroImage Clin. 2017; 16: 461–7.

382   Carrera E, Tononi G. Diaschisis: past, present, future. Brain 2014; 137: 2408–22.

383   Aerts H, Fias W, Caeyenberghs K, Marinazzo D. Brain networks under attack: Robustness properties and the impact of lesions. Brain. 2016; 139: 3063–83.

384   Carroll, C, Wagner A, Watson P, et al. Long-Term cognitive outcome in adult survivors of an early childhood posterior fossa brain tumour. Neuro. Oncol. 2016; 18: iii154.

385   Patay Z. Postoperative posterior fossa syndrome: unraveling the etiology and underlying pathophysiology by using magnetic resonance imaging. Child's Nerv. Syst. 2015; 31: 1853–8.

386   Marien P, De Smet HJ, Paquier PF, Verhoeven J. Cerebellocerebral diaschisis and postsurgical posterior fossa syndrome in pediatric patients. AJNR. Am. J. Neuroradiol. 2010; 31: E82; author reply E83.

387   De Smet HJ, Baillieux H, Wackenier P, et al. Long-term cognitive deficits following posterior fossa tumor resection: a neuropsychological and functional neuroimaging follow-up study. Neuropsychology 2009; 23: 694–704.

388   Sang L, Qin W, Liu Y, et al. Resting-state functional connectivity of the vermal and hemispheric subregions of the cerebellum with both the cerebral cortical networks and subcortical structures. Neuroimage 2012; 61: 1213–25.

389   Kirschen MP, Chen SHA, Desmond JE. Modality specific cerebro-cerebellar activations in verbal working memory: An fMRI study. Behav Neurol 2010; 23: 51–63.

390   Kirschen MP, Davis-Ratner MS, Milner MW, et al. Verbal memory impairments in children after cerebellar tumor resection. Behav Neurol 2008; 20: 39–53.

391   Soelva V, Hernaiz Driever P, Abbushi A, et al. Fronto-cerebellar fiber tractography in pediatric patients following posterior fossa tumor surgery. Childs Nerv Syst 2013; 29: 597–607.

392   Law N, Bouffet E, Laughlin S, et al. Cerebello–thalamo–cerebral connections in pediatric brain tumor patients: Impact on working memory. Neuroimage 2011; 56: 2238–48.

393   Makola M, Douglas Ris M, Mark Mahone E, Yeates KO, Cecil KM. Long-term effects of radiation therapy on white matter of the corpus callosum: a diffusion tensor imaging study in children. Pediatr Radiol 2017. DOI:10.1007/s00247-017-3955-1.

394   Kralik SF, Ho CY, Finke W, Buchsbaum JC, Haskins CP, Shih C-S. Radiation Necrosis in Pediatric Patients with Brain Tumors Treated with Proton Radiotherapy. AJNR Am J Neuroradiol 2015; 36: 1572–8.

395   Hanzlik E, Woodrome SE, Abdel-Baki M, Geller TJ, Elbabaa SK. A systematic review of neuropsychological outcomes following posterior fossa tumor surgery in children. Childs Nerv Syst 2015; 31: 1869–75.

396   Gudrunardottir T, Lannering B, Remke M, et al. Treatment developments and the unfolding of the quality of life discussion in childhood medulloblastoma: a review. Childs Nerv Syst 2014; 30: 979–90.

397   Stam CJ. Modern network science of neurological disorders. Nat Rev Neurosci 2014; 15: 683–95.

398   Dunn LM, Dunn DM. Peabody Picture Vocabulary Test, Fourth Edition. Work Pap 2008.

399   Patterson J. Controlled Oral Word Association Test. In: Encyclopedia of Clinical Neuropsychology. 2011: 703–6.

400   Spielberger CD. State-Trait Anxiety Inventory. Anxiety. 1987; 19: 2009.

401   Andersson JLR, Sotiropoulos SN. Non-parametric representation and prediction of single- and multi-shell

diffusion-weighted MRI data using Gaussian processes. Neuroimage 2015; 122: 166–76.

402   Veraart J, Novikov DS, Christiaens D, Ades-aron B, Sijbers J, Fieremans E. Denoising of diffusion MRI using random matrix theory. Neuroimage 2016; 142: 394–406.

403   Kellner E, Dhital B, Kiselev VG, Reisert M. Gibbs-ringing artifact removal based on local subvoxel-shifts. Magn Reson Med 2016; 76: 1574–81.

404   Jeurissen B, Tournier JD, Dhollander T, Connelly A, Sijbers J. Multi-tissue constrained spherical deconvolution for improved analysis of multi-shell diffusion MRI data. Neuroimage 2014; 103: 411–26.

405   Zhang Y, Brady M, Smith S. Segmentation of brain MR images through a hidden Markov random field model and the expectation-maximization algorithm. IEEE Trans Med Imaging 2001; 20: 45–57.

406   Fornito A, Zalesky A, Breakspear M. Graph analysis of the human connectome: Promise, progress, and pitfalls. Neuroimage 2013; 80: 426–44.

407   Tzourio-Mazoyer N, Landeau B, Papathanassiou D, et al. Automated Anatomical Labeling of Activations in SPM Using a Macroscopic Anatomical Parcellation of the MNI MRI Single-Subject Brain. Neuroimage 2002; 15: 273–89.

408   Smith RE, Tournier JD, Calamante F, Connelly A. Anatomically-constrained tractography: Improved diffusion MRI streamlines tractography through effective use of anatomical information. Neuroimage 2012; 62: 1924–38.

409   Smith RE, Tournier JD, Calamante F, Connelly A. SIFT2: Enabling dense quantitative assessment of brain white matter connectivity using streamlines tractography. Neuroimage 2015; 119: 338–51.

410   Smith RE, Tournier JD, Calamante F, Connelly A. The effects of SIFT on the reproducibility and biological accuracy of the structural connectome. Neuroimage 2015; 104: 253–65.

411   Batalle D, Hughes EJ, Zhang H, et al. Early development of structural networks and the impact of prematurity on brain connectivity. Neuroimage 2017; 149: 379–92.

412   Lanier JC, Abrams AN. Posterior fossa syndrome: Review of the behavioral and emotional aspects in pediatric cancer patients. Cancer 2017; 123: 551–9.

413   Hoang DH, Pagnier A, Guichardet K, et al. Cognitive disorders in pediatric medulloblastoma: what neuroimaging has to offer. J Neurosurg Pediatr 2014; 14: 136–44.

414   Ailion AS, Hortman K, King TZ. Childhood Brain Tumors: a Systematic Review of the Structural Neuroimaging Literature. Neuropsychol. Rev. 2017; 27: 220–44.

415   Palmer SL, Glass JO, Li Y, et al. White matter integrity is associated with cognitive processing in patients treated for a posterior fossa brain tumor. Neuro Oncol 2012; 14: 1185–93.

416   Rueckriegel SM, Driever PH, Blankenburg F, Lüdemann L, Henze G, Bruhn H. Differences in Supratentorial Damage of White Matter in Pediatric Survivors of Posterior Fossa Tumors With and Without Adjuvant Treatment as Detected by Magnetic Resonance Diffusion Tensor Imaging. Int J Radiat Oncol Biol Phys 2010; 76: 859–66.

417   Scantlebury N, Bouffet E, Laughlin S, et al. White matter and information processing speed following treatment with cranial-spinal radiation for pediatric brain tumor. Neuropsychology 2016; 30: 425–38.

418   Camara-Costa H, Resch A, Kieffer V, et al. Neuropsychological Outcome of Children Treated for Standard Risk Medulloblastoma in the PNET4 European Randomized Controlled Trial of Hyperfractionated Versus Standard Radiation Therapy and Maintenance Chemotherapy. Int J Radiat Oncol Biol Phys 2015; 92: 978–85.

419   Aukema EJ, Caan MWA, Oudhuis N, et al. White Matter Fractional Anisotropy Correlates With Speed of Processing and Motor Speed in Young Childhood Cancer Survivors. Int J Radiat Oncol Biol Phys 2009; 74: 837–43.

420   Brinkman TM, Reddick WE, Luxton J, et al. Cerebral white matter integrity and executive function in adult survivors of childhood medulloblastoma. Neuro Oncol 2012; 14 Suppl 4: iv25-36.

421   Khong PL, Kwong DLW, Chan GCF, Sham JST, Chan FL, Ooi GC. Diffusion-tensor imaging for the detection and quantification of treatment-induced white matter injury in children with medulloblastoma: a pilot study. AJNR Am J Neuroradiol 2003; 24: 734–40.

422   Law N, Greenberg M, Bouffet E, et al. Visualization and segmentation of reciprocal cerebrocerebellar pathways in the healthy and injured brain. Hum Brain Mapp 2015; 36: 2615–28.

423   Qiu D, Kwong DLW, Chan GCF, Leung LHT, Khong PL. Diffusion Tensor Magnetic Resonance Imaging Finding of Discrepant Fractional Anisotropy Between the Frontal and Parietal Lobes After Whole-Brain Irradiation in Childhood Medulloblastoma Survivors: Reflection of Regional White Matter Radiosensitivity? Int J Radiat Oncol Biol Phys 2007; 69: 846–51.

424   Saykin AJ, de Ruiter MB, McDonald BC, Deprez S, Silverman DHS. Neuroimaging biomarkers and cognitive function in non-CNS cancer and its treatment: current status and recommendations for future research.

Brain Imaging Behav. 2013; 7: 363–73.

425   Seigers R, Loos M, Van Tellingen O, Boogerd W, Smit AB, Schagen SB. Neurobiological changes by cytotoxic agents in mice. Behav Brain Res 2016; 299: 19–26.

426   Han R, Yang YM, Dietrich J, Luebke A, Mayer-Pröschel M, Noble M. Systemic 5-fluorouracil treatment causes a syndrome of delayed myelin destruction in the central nervous system. J Biol 2008; 7. DOI:10.1186/jbiol69.

427   Croteau-Chonka EC, Dean DC, Remer J, Dirks H, O'Muircheartaigh J, Deoni SCL. Examining the relationships between cortical maturation and white matter myelination throughout early childhood. Neuroimage 2016; 125: 413–21.

428   Dumas JA, Makarewicz J, Schaubhut GJ, et al. Chemotherapy altered brain functional connectivity in women with breast cancer: a pilot study. Brain Imaging Behav 2013; 7: 524–32.

429   Shen Q, Lin F, Rong X, et al. Temporal Cerebral Microbleeds Are Associated With Radiation Necrosis and Cognitive Dysfunction in Patients Treated for Nasopharyngeal Carcinoma. Int J Radiat Oncol Biol Phys 2016; 94: 1113–20.

430   D'Esposito M, Deouell LY, Gazzaley A. Alterations in the BOLD fMRI signal with ageing and disease: A challenge for neuroimaging. Nat Rev Neurosci 2003; 4: 863–72.

431   Bruno J, Hosseini SMH, Kesler S. Altered resting state functional brain network topology in chemotherapy-treated breast cancer survivors. Neurobiol Dis 2012; 48: 329–38.

432   Button KS, Ioannidis JPA, Mokrysz C, et al. Power failure: Why small sample size undermines the reliability of neuroscience. Nat Rev Neurosci 2013; 14: 365–76.

433   Greve DN, Fischl B. False positive rates in surface-based anatomical analysis. Neuroimage 2018; 171: 6–14.

434   Winkler AM, Webster MA, Brooks JC, Tracey I, Smith SM, Nichols TE. Non-parametric combination and related permutation tests for neuroimaging. Hum Brain Mapp 2016; 37: 1486–511.

435   Carandini M. From circuits to behavior: A bridge too far? Nat. Neurosci. 2012; 15: 507–9.

436   Palmeri TJ, Love BC, Turner BM. Model-based cognitive neuroscience. J Math Psychol 2017; 76: 59–64.

437   Storsve AB, Fjell AM, Tamnes CK, et al. Differential Longitudinal Changes in Cortical Thickness, Surface Area and Volume across the Adult Life Span: Regions of Accelerating and Decelerating Change. J Neurosci 2014; 34: 8488–98.

438   Jernigan TL, Brown TT, Bartsch H, Dale AM. Toward an integrative science of the developing human mind and brain: Focus on the developing cortex. Dev Cogn Neurosci 2016; 18: 2–11.

439   Makropoulos A, Robinson EC, Schuh A, et al. The developing human connectome project: A minimal processing pipeline for neonatal cortical surface reconstruction. Neuroimage 2018; 173: 88–112.

440   Thompson PM, Stein JL, Medland SE, et al. The ENIGMA Consortium: Large-scale collaborative analyses of neuroimaging and genetic data. Brain Imaging Behav 2014; 8: 153–82.

441   Williams N, Henson RN. Recent advances in functional neuroimaging analysis for cognitive neuroscience. Brain Neurosci Adv 2018; 2: 239821281775272.

442   Kam JWY, Brenner CA, Handy TC, et al. Sustained attention abnormalities in breast cancer survivors with cognitive deficits post chemotherapy: An electrophysiological study. Clin Neurophysiol 2016; 127: 369–78.

443   Deprez S, Kesler SR, Saykin AJ, Silverman DHS, de Ruiter MB, McDonald BC. International Cognition and Cancer Task Force Recommendations for Neuroimaging Methods in the Study of Cognitive Impairment in Non-CNS Cancer Patients. JNCI J Natl Cancer Inst 2018; 110.

444   Kesler SR, Watson C, Koovakkattu D, et al. Elevated prefrontal myo-inositol and choline following breast cancer chemotherapy. Brain Imaging Behav 2013; 7: 501–10.

445   Khan RB, Sadighi ZS, Zabrowski J, Gajjar A, Jeha S. Imaging Patterns and Outcome of Posterior Reversible Encephalopathy Syndrome During Childhood Cancer Treatment. Pediatr Blood Cancer 2016; 63: 523–6.

446   Moore HCF, Parsons MW, Yue GH, Rybicki LA, Siemionow W. Electroencephalogram power changes as a correlate of chemotherapy-associated fatigue and cognitive dysfunction. Support care cancer Off J Multinatl Assoc Support Care Cancer 2014; 22: 2127–31.

447   Silverman DHS, Dy CJ, Castellon SA, et al. Altered frontocortical, cerebellar, and basal ganglia activity in adjuvant-treated breast cancer survivors 5-10 years after chemotherapy. Breast Cancer Res Treat 2007; 103: 303–11.

448   Zimmer L, Luxen A. PET radiotracers for molecular imaging in the brain: Past, present and future. Neuroimage. 2012; 61: 363–70.

449   Kandula T, Park SB, Cohn RJ, Krishnan A V., Farrar MA. Pediatric chemotherapy induced peripheral neuropathy: A systematic review of current knowledge. Cancer Treat. Rev. 2016; 50: 118–28.

450   Miaskowski C, Mastick J, Paul SM, et al. Chemotherapy-Induced Neuropathy in Cancer Survivors. J Pain Symptom Manage 2017; 54: 204–218.e2.

451   Muthuraman M, Raethjen J, Koirala N, et al. Cerebello-cortical network fingerprints differ between essential, Parkinson's and mimicked tremors. Brain 2018; : 1770–81.

452   Tell D, Mathews HL, Burr RL, Witek Janusek L. During stress, heart rate variability moderates the impact of childhood adversity in women with breast cancer. Stress 2018; 21: 179–87.

453   Park H, Oh S, Noh Y, Kim JY, Kim J-H. Heart Rate Variability as a Marker of Distress and Recovery: The Effect of Brief Supportive Expressive Group Therapy With Mindfulness in Cancer Patients. Integr Cancer Ther 2018; : 153473541875619.

454   Zimmer P, Mierau A, Bloch W, et al. Post-chemotherapy cognitive impairment in patients with B-cell non-Hodgkin lymphoma: a first comprehensive approach to determine cognitive impairments after treatment with rituximab, cyclophosphamide, doxorubicin, vincristine and prednisone or rituximab a. Leuk Lymphoma 2015; 56: 347–52.

455   Jehn CF, Becker B, Flath B, et al. Neurocognitive function, brain-derived neurotrophic factor (BDNF) and IL-6 levels in cancer patients with depression. J Neuroimmunol 2015; 287: 88–92.

456   Cheung YT, Chemaitilly W, Mulrooney DA, et al. Association between dehydroepiandrosterone-sulfate and attention in long-term survivors of childhood acute lymphoblastic leukemia treated with only chemotherapy. Psychoneuroendocrinology 2017; 76: 114–8.

457   Fisher PL, McNicol K, Young B, Smith E, Salmon P. Alleviating Emotional Distress in Adolescent and Young Adult Cancer Survivors: An Open Trial of Metacognitive Therapy. J Adolesc Young Adult Oncol 2015; 4: 64–9.

458   Murphy LK, Bettis AH, Gruhn MA, Gerhardt CA, Vannatta K, Compas BE. Resilience in Adolescents with Cancer: Association of Coping with Positive and Negative Affect. J Dev Behav Pediatr 2017; 38: 646–53.

459   Vander Haegen M, Luminet O. Stress, Psychosocial Mediators, and Cognitive Mediators in Parents of Child Cancer Patients and Cancer Survivors: Attention and Working Memory Pathway Perspectives. J Psychosoc Oncol 2015; 33: 504–50.

460   Valentine AD, Meyers CA. Cognitive and mood disturbance as causes and symptoms of fatigue in cancer patients. Cancer 2001; 92: 1694–8.

461   Patel SK, Wong AL, Cuevas M, Van Horn H. Parenting stress and neurocognitive late effects in childhood cancer survivors. Psychooncology 2013; 22: 1774–82.

462   Jain N, Brouwers P, Okcu MF, Cirino PT, Krull KR. Sex-specific attention problems in long-term survivors of pediatric acute lymphoblastic leukemia. Cancer 2009; 115: 4238–45.

463   Mulhern RK, Palmer SL, Reddick WE, et al. Risks of young age for selected neurocognitive deficits in medulloblastoma are associated with white matter loss. J Clin Oncol 2001; 19: 472–9.

464   Mrakotsky CM, Silverman LB, Dahlberg SE, et al. Neurobehavioral side effects of corticosteroids during active treatment for acute lymphoblastic leukemia in children are age-dependent: Report from Dana-Farber Cancer Institute ALL Consortium Protocol 00-01. Pediatr Blood Cancer 2011; 57: 492–8.

465   Monje M, Thomason ME, Rigolo L, et al. Functional and structural differences in the hippocampus associated with memory deficits in adult survivors of acute lymphoblastic leukemia. Pediatr Blood Cancer 2013; 60: 293–300.

466   Hodgson KD, Hutchinson AD, Wilson CJ, Nettelbeck T. A meta-analysis of the effects of chemotherapy on cognition in patients with cancer. Cancer Treat Rev 2013; 39: 297–304.

467   Brouwers P. Commentary: Study of the neurobehavioral consequences of childhood cancer: Entering the genomic era? J. Pediatr. Psychol. 2005; 30: 79–84.

468   Cole PD. Does genetic susceptibility increase risk for neurocognitive decline among patients with acute lymphoblastic leukemia? Futur Oncol 2015; 11: 1855–8.

469   Correa DD, Satagopan J, Cheung K, et al. COMT, BDNF, and DTNBP1 polymorphisms and cognitive functions in patients with brain tumors. Neuro Oncol 2016; 18: 1425–33.

470   Rocha JC, Cheng C, Liu W, et al. Pharmacogenetics of outcome in children with acute lymphoblastic leukemia. Blood 2005; 105: 4752–8.

471   Brackett J, Krull KR, Scheurer ME, et al. Antioxidant enzyme polymorphisms and neuropsychological outcomes in medulloblastoma survivors: a report from the Childhood Cancer Survivor Study. Neuro Oncol 2012; 14: 1018–25.

472   Tsujimoto S ichi, Yanagimachi M, Tanoshima R, et al. Influence of ADORA2A gene polymorphism on leukoencephalopathy risk in MTX-treated pediatric patients affected by hematological malignancies. Pediatr Blood Cancer 2016; 63: 1983–9.

473   Patiño-García A, Zalacaín M, Marrodán L, San-Julián M, Sierrasesúmaga L. Methotrexate in Pediatric

Osteosarcoma: Response and Toxicity in Relation to Genetic Polymorphisms and Dihydrofolate Reductase and Reduced Folate Carrier 1 Expression. J Pediatr 2009; 154: 688–93.

474   Fjell AM, Grydeland H, Krogsrud SK, et al. Development and aging of cortical thickness correspond to genetic organization patterns. Proc Natl Acad Sci 2015; 112: 15462–7.

475   Gilbert SL, Dobyns WB, Lahn BT. Genetic links between brain development and brain evolution. Nat. Rev. Genet. 2005; 6: 581–90.

476   Dorus S, Vallender EJ, Evans PD, et al. Accelerated evolution of nervous system genes in the origin of Homo sapiens. Cell 2004; 119: 1027–40.

477   Butler RW, Copeland DR. Attentional processes and their remediation in children treated for cancer: A literature review and the development of a therapeutic approach. J Int Neuropsychol Soc 2002; 8: 115–24.

478   Patel SK, Fernandez N, Dekel N, et al. Socioeconomic status as a possible moderator of neurocognitive outcomes in children with cancer. Psychooncology. 2016; 25: 115–8.

479   Kazak AE, Brier M, Alderfer MA, et al. Screening for psychosocial risk in pediatric cancer. Pediatr Blood Cancer 2012; 59: 822–7.

480   Wenninger K, Helmes A, Bengel J, Lauten M, Völkel S, Niemeyer CM. Coping in long-term survivors of childhood cancer: Relations to psychological distress. Psychooncology 2013; 22: 854–61.

481   Kazak AE, Alderfer M a, Streisand R, et al. Treatment of posttraumatic stress symptoms in adolescent survivors of childhood cancer and their families: a randomized clinical trial. J Fam Psychol 2004; 18: 493–504.

482   Alvarez J, Meyer FL, Granoff DL, Lundy A. The effect of EEG biofeedback on reducing postcancer cognitive impairment. Integr Cancer Ther 2013; 12: 475–87.

483   Prinsloo S, Gabel S, Lyle R, Cohen L. Neuromodulation of cancer pain. Integr Cancer Ther 2014; 13: 30–7.

484   Prinsloo S, Novy D, Driver L, et al. The Long-Term Impact of Neurofeedback on Symptom Burden and Interference in Patients With Chronic Chemotherapy-Induced Neuropathy: Analysis of a Randomized Controlled Trial. J Pain Symptom Manage 2018; 55: 1276–85.

485   Lee EJ, Bhattacharya J, Sohn C, Verres R. Monochord sounds and progressive muscle relaxation reduce anxiety and improve relaxation during chemotherapy: A pilot EEG study. Complement Ther Med 2012; 20: 409–16.

486   Carlson LE, Speca M, Faris P, Patel KD. One year pre-post intervention follow-up of psychological, immune, endocrine and blood pressure outcomes of mindfulness-based stress reduction (MBSR) in breast and prostate cancer outpatients. Brain Behav Immun 2007; 21: 1038–49.

487   Van der Gucht K, Takano K, Labarque V, et al. A Mindfulness-Based Intervention for Adolescents and Young Adults After Cancer Treatment: Effects on Quality of Life, Emotional Distress, and Cognitive Vulnerability. J Adolesc Young Adult Oncol 2016. DOI:10.1089/jayao.2016.0070.

488   Wilke C, Grosshans D, Duman J, Brown P, Li J. Radiation-induced cognitive toxicity: Pathophysiology and interventions to reduce toxicity in adults. Neuro Oncol 2018; 20: 597–607.

489   Hart MG, Ypma RJF, Romero-Garcia R, Price SJ, Suckling J. Graph theory analysis of complex brain networks: new concepts in brain mapping applied to neurosurgery. J Neurosurg 2015; 124: 1–14.

490   Jackson SE, Chester JD. Personalised cancer medicine. Int. J. Cancer. 2015; 137: 262–6.

491   Davis J, Ahlberg FM, Berk M, Ashley DM, Khasraw M. Emerging pharmacotherapy for cancer patients with cognitive dysfunction. BMC Neurol 2013; 13: 153.

492   Kohli S, Fisher SG, Tra Y, et al. The effect of modafinil on cognitive function in breast cancer survivors. Cancer 2009; 115: 2605–16.

493   Blackhall L, Petroni G, Shu J, Baum L, Farace E. A pilot study evaluating the safety and efficacy of modafinal for cancer-related fatigue. J Palliat Med 2009; 12: 433–9.

494   Mar Fan HG, Clemons M, Xu W, et al. A randomised, placebo-controlled, double-blind trial of the effects of d-methylphenidate on fatigue and cognitive dysfunction in women undergoing adjuvant chemotherapy for breast cancer. Support care cancer Off J Multinatl Assoc Support Care Cancer 2008; 16: 577–83.

495   Rapp SR, Case LD, Peiffer A, et al. Donepezil for Irradiated Brain Tumor Survivors: A Phase III Randomized Placebo-Controlled Clinical Trial. J Clin Oncol 2015; 33: 1653–9.

496   Shaw EG, Rosdhal R, D'Agostino RBJ, et al. Phase II study of donepezil in irradiated brain tumor patients: effect on cognitive function, mood, and quality of life. J Clin Oncol 2006; 24: 1415–20.

497   Brown PD, Pugh S, Laack NN, et al. Memantine for the prevention of cognitive dysfunction in patients receiving whole-brain radiotherapy: a randomized, double-blind, placebo-controlled trial. Neuro Oncol 2013; 15: 1429–37.

Conflicts of interest and Personal contribution

Curriculum vitae

Personal

Name	Charlotte Sleurs
Address	Hoekstraat 47, 3900 Overpelt, Belgium
Email	charlotte.sleurs@gmail.com
Phone	+32 476 38 94 01
Date of birth	May 2nd, 1991

Education

2014 - 2018
Doctoral studies in Cognitive and Molecular neurosciences
Doctoral School Biomedical Sciences, Faculty of Medicine
Neurotoxicity and potential risk factors in childhood solid tumor patients
Promotors: Prof. Dr. Anne Uyttebroeck, Dr. Sabine Deprez, Dr. Jurgen Lemiere

2015 – 2017
Postgraduate Studies in Clinical Neuropsychology,
Magna Cum Laude, KU Leuven, Leuven, Belgium
The role of the ApoE polymorphism in brain development during childhood cancer
Promotor: Prof. dr. Rudi D'hooghe

2009 – 2014
Master of Science (MSc), Clinical and Health Psychology
Magna Cum Laude, KU Leuven
Sensitivity to non-accidental configurations of two-line configurations
Promotor: Prof. dr. Johan Wagemans

2003 – 2009
Latin-Mathematics Secondary School
Cum Laude, Sint-Hubertus College, Neerpelt, Belgium

Professional career

2014 - 2018
Phd-researcher @ KU Leuven, Dept. Oncology

2013 – 2014
Clinical Psychologist in training @ UZ Leuven
Registered Psychologist; RegNr. 912115978

2013 – 2014
Research assistent in training @ UZ Leuven
Prof. Dr. Jan Van Den Stock & Prof. Dr. Mathieu Vandenbulcke,
Emotion and cognition in Huntington's disease and Frontotemporal Dementia.

2012
Research assistent during holidays @ KU Leuven
Prof. Dr. Batja Mesquita & Dr. Canan Coskan
International research project Youth European Study (YESsurvey)

Miscellaneous

Additional courses

2017	Practical Neuroradiology course – Great Ormond St. London
2016	Human Connectome - Summer School Connectome Lab Utrecht
	Supervising Master's thesis KUL courses
2015	Lectures on MR - Resting state fMRI ESMRM course Berlin
	Medical Imaging and Analysis KUL courses B-KUL-E00D3
	Matlab coding Part I & II KUL course

Current memberships

2018	Cancer and Cognition Focus Group, Leuven Cancer Institute
2016	Scientific Psychosocial Working Group member, Cédric Hèle instituut
	Editorial Board member Tijdschrift Klinische Psychologie
	http://www.vvkp.be/tkp
2015	International Late Effects of Childhood Cancer Guideline Harmonization Group member, IGHG http://www.ighg.org/
2014	Belgian Society of Pediatric Hematology/Oncology (BSPHO)
	Belgian Association for Psychological Sciences (BAPS)
2006	Animator for youth holidays @ Akindo vzw Lommel

Reviewer of journal articles

Neuroscience & Biobehavioral Reviews
Magnetic Resonance Materials in Physics, Biology and Medicine

Guidance master's theses

2017-2019	Faculty of Psychology		
		Nollet Kathleen	*Tractography of executive and sensorimotor tracts in survivors of childhood posterior fossa tumors*
		Vertommen Julie	*Tractography of visuospatial and language tracts in survivors of childhood posterior fossa tumors*
	Faculty of Medicine		
		Janssen Kaat	*Prevalence of leukoencephalopathy and acute neurotoxicity in childhood leukemia patients*
		Meylaers Michiel	*Prevalence and follow-up of leukoencephalopathy in cancer patients: A systematic review*
		Wauters Maarten	*The association between neuroimaging and neurocognition in pediatric medulloblastoma patients*
2016-2018	Faculty of Psychology		
		Maes Lissa & Turelinckx Ellen	*Long-term neurocognitive functioning in posterior fossa tumor survivors*
	Faculty of Medicine		
		Gheysen Mathilde	*Posterior fossa tumors in children and therapy-related long term effects: A systematic review*
		Madoe Aline	*Genetic modulation of treatment-related neurocognitive impairment in pediatric cancer survivors: A systematic review*

2015-2017	Faculty of Psychology	
	Janssen Mira	*Longitudinale opvolging Quality of Life bij kinderen met solide tumoren*
	Pelkmans Floris	*Neurocognitie na chemobehandeling bij jongeren met een bottumor of tumor van de weke delen: een cross-sectionele studie*
2014-2016	Faculty of Psychology	
	Bauwens Jana	*Neurocognitie na chemobehandeling bij jongeren met een bottumor of tumor van de weke delen*

Jury member master's theses

2018	Faculty of Medicine	
	Deman Helena & Vandecruys Floor	*Structurele neuroconnectiviteit bij kinderen met ontwikkelingsstotteren - een DTI-studie van de Superieure Longitudinale Fasciculus en de Inferieure Fronto-Occipitale Fasciculus*
2017	Faculty of Medicine	
	Van Haesendonck Louise & Vanluydt Ellen	*Het taalnetwerk bij kinderen met rolandische epilepsie en ontwikkelingsdysfasie: een vergelijkende DTI studie*
2016	Faculty of Medicine	
	Rohaert Zinke	*The language connectome in typically developing left- and right-handed children*

Awards & Grants

2016	Best Poster Award SIOP
	Potential neurotoxicity of non-CNS-directed chemotherapy during childhood: A neuromaging study of brain structure and function
	Awarded by: The International Society of Paediatric Oncology (SIOP)
2017	Travel grant for 3-month-stay @ King's College University
	The application of Graph Theory in Pediatric Brain Tumors
	Dept. of Perinatal Neuroimaging, supervised by Prof. Dr. Serena Counsell, Prof. Dr. Donald Tournier, Dr. Dafnis Batalle & Dr. Daan Christiaens
	Awarded by Fonds voor Wetenschappelijk Onderzoek (FWO)

Publication list

International journal articles

1. **Sleurs C.**, Lemiere J., Christiaens D., Billiet T., Peeters R., Sunaert S., Uyttebroeck A., Deprez S. (2018). Advanced MR diffusion imaging and chemotherapy-related changes in cerebral white matter microstructure of survivors of childhood bone and soft tissue sarcoma? *Human brain mapping*. art.nr. 10.1002/hbm.24082.
2. Verly M., Gerrits R., Sleurs C., Lagae, L., Sunaert, S., Zink I., Rommel N. (2018). The mis-wired language network in children with developmental language disorder: insights from DTI tractography. *Brain, Imaging and Behavior*, art.nr. 10.1007/s11682-018-9903-3.
3. Gheysen M., **Sleurs C.,** Jacobs S., Lemiere J., Uyttebroeck A. (2018). Therapy-related long-term effects in childhood posterior fossa tumors. *Journal of Neurology and Neuroscience*, art.nr. 10.21767/2171-6625.1000252.
4. Billiet* T., Elens* I., **Sleurs* C.**, Uyttebroeck A., D'Hooge R., Lemiere J., Deprez S. (2018). Brain Connectivity and Cognitive Flexibility in Nonirradiated Adult Survivors of Childhood Leukemia. *Journal of the National Cancer Institute, 110* (8), art.nr. 10.1093/jnci/djy009.
5. Lambrecht L., **Sleurs C.**, Labarque V., Dhooge C., Laenen A., Sinnaeve F., Renard M., Uyttebroeck A. (2017). The role of the MTHFR C677T polymorphism in methotrexate-induced toxicity in pediatric osteosarcoma patients. *Pharmacogenomics, 18* (8), art.nr. 10.2217/pgs-2017-0013, 787-795.
6. *Kubilius J., **Sleurs C.**, Wagemans J.* (2017). Sensitivity to nonaccidental configurations of two-line stimuli. *i-Perception, 8* (2), 1-12.
7. ***Sleurs C.,** Lemiere J., Vercruysse T., Nolf N., Van Calster B., Deprez S., Renard M., Vandecruys E., Benoit Y., Uyttebroeck A.* (2017). Intellectual Development of Childhood ALL patients: A Multicenter Longitudinal Study. *Psycho-oncology, 26* (4), 508-514.
8. ***Sleurs C.,** Deprez S., Emsell L., Lemiere J., Uyttebroeck A.* (2016). Chemotherapy-induced Neurotoxicity in Pediatric Solid Non-CNS-tumor Patients: An Update on Current State of Research and Recommended Future Directions. *Critical Reviews in Oncology/Hematology, 103*, 37-48.

International journal articles submitted for publication

1. **Sleurs C.,** Lemiere J., Radwan A., Verly M., Elens I., Renard M., Jacobs S., Sunaert S., Deprez S., Uyttebroeck A. (2018). Long-term leukoencephalopathy, neurocognitive functioning and potential risk factors in childhood bone and soft tissue sarcoma survivors. *Journal of Cancer Survivorship*, 2018 (submitted).
2. Madoe A.*, **Sleurs C.***, Lagae L., Jacobs S., Deprez S., Lemiere J., Uyttebroeck, A. Genetic modulation of neurocognitive impairment in cancer patients and the importance in pediatrics: A systematic review. *Neuropsychology Reviews*, 2018 (resubmitted after major revision).

National journal articles

1. Sleurs C. (2017). Het creatieve brein van Dick Swaab. *Tijdschrift Klinische Psychologie, 47* (3), 73-75.
2. Sleurs C. (2016). Op de grens van het subcorticale: Een zoektocht naar de balans tussen romantiek en cognitie in het brein, in het zijn. Een hommage aan Oliver Sacks. *Tijdschrift Klinische Psychologie, 46* (3), 185-188.

Conference abstracts

1. **Sleurs C.**, Batalle D., Lemiere J., Christiaens D., Tournier J., Sunaert S., Uyttebroeck A., Jacobs S., Counsell S., Deprez S. (2018). Supratentorial reorganization after treatment for childhood infratentorial tumors from a graph theoretical perspective. ISMRM. Paris, 16-21 June 2018.
2. **Sleurs C.**, Deprez S., Uyttebroeck A., Lemiere J., Jacobs S. (2018). Supra- and infratentorial tractogram changes in childhood posterior fossa tumor survivors. ISPNO. Denver, 29 June - 3 July 2018.
3. **Sleurs C.**, Turelinckx E., Maes L., Deprez S., Uyttebroeck A., Jacobs S., Lemiere J. (2018). Long-term cognitive functioning and treatment-related risk factors in childhood posterior fossa tumor survivors. ISPNO. Denver, 29 June - 3 July 2018.
4. **Sleurs C.**, Lemiere J., Christiaens D., Billiet T., Verly M., Blommaert J., Peeters R., Sunaert S., Uyttebroeck A., Deprez S. (2017). White matter density in solid tumor survivors using advanced diffusion models. OHBM. Vancouver, 25-29 June 2017.
5. Verly M., Gerrits R., **Sleurs C.**, Peeters R., Lagae L., Sunaert S., Zink I., Rommel N. (2017). The mis-wired language network in rolandic epilepsy: role of the cerebellum. ECMRN. Tübingen, 8-10 June 2017.
6. Van den Wyngaert L., Vercruysse T., Vandenabeele K., Haers M., **Sleurs C.**, Uyttebroeck A., Jacobs S., Lemiere J. (2017). The Link Between Neurocognitive Functioning and Health-related Quality of Life in Pediatric Brain Tumors. Pediatric Blood & Cancer: vol. 64. SIOP. Washington DC, 12-15 October, S317-S317.
7. **Sleurs C.**, Lemiere J., Vercuysse T., Van den Wyngaert L., Labarque V., Jacobs S., Sunaert S., Deprez S., Uyttebroeck A. (2017). The ApoE genotype and White Matter lesions in childhood non-CNS tumor survivors. SIOP. Washington DC, 12-15 October.
8. Ceccarini J., Leurquin-Sterk G., **Sleurs C.**, Devrome M., Deprez S., Sunaert S., Van Laere K. (2017). Structural Changes in White Matter in Relation to Lifetime Alcohol Exposure in Alcoholic Patients. OHBM. Vancouver, 25-29 June 2017.
9. **Sleurs C.**, Lemiere J., Christiaens D., Billiet T., Verly M., Peeters R., Sunaert S., Uyttebroeck A., Deprez S. (2017). Measuring white matter structure in solid tumor survivors: a fixel-based versus voxel-based approach. ISMRM. Honolulu, 22-27 April 2017.
10. Blommaert J., Amant F., Peeters R., Radwan A., Smeets A., **Sleurs C.**, Sunaert S., Vandenbulcke M., Deprez S. (2017). Longitudinal assessment of morphometric brain changes after chemotherapy in pre- and post-menopausal breast cancer patients. Magnetic Resonance Materials in Biology, Physics and Medicine: vol. 30 (Suppl 1). ESMRMB. Barcelona, 18-21 October 2017, 432-433.
11. **Sleurs C.**, Lemiere J., Renard M., Sunaert S., Deprez S., Uyttebroeck A. (2017). How to predict and interpret White Matter hyperintensities on FLAIR MR images in childhood non-CNS tumor patients and survivors?. ECMRN. Tübingen, 8-10 June 2017.

12. Verly M., Lagae L., **Sleurs C.**, Deprez S., Sunaert S., Peeters R., Zink I., Rommel N. (2017). Cortico-cerebellar underconnectivity of the language network in children with rolandic epilepsy. OHBM. Vancouver, 26-29 June 2017.

13. Verly M., Lagae L., Sunaert S., **Sleurs C.**, Peeters R., Zink I., Rommel N. (2017). Aberrant intrinsic functional connectivity of the language network in rolandic epilepsy. ISMRM Benelux. Tilburg, 20 January 2017.

14. **Sleurs C.**, Deprez S., Vercruysse G., Elens I., Peeters R., Sunaert S., Segers H., Labarque V., Renard M., Lemiere J., Uyttebroeck A. (2016). Potential Neurotoxicity of Non-CNS-Directed Chemotherapy During Childhood: A Neuroimaging Study of Brain Structure and Function. SIOP. Dublin, 19-22 October 2016.

15. Vercruysse D., Billiet T., **Sleurs C.**, Sunaert S., Vandenbulcke M., Peeters R., Smeets A., Dupont P., Amant F., Deprez S. (2016). Longitudinal changes in DMN Connectivity following chemotherapy in Breast Cancer. ICCTF congress. Amsterdam, 14-16 March 2016.

16. **Sleurs C.**, Bauwens J., Lemiere J., Elens I., Van Broeck N., Vercruysse G., Deprez S., Renard M., Uyttebroeck A. (2016). Is neurocognitive functioning altered in childhood solid non-CNS tumor survivors? A multivariate exploration. BAPS Annual Meeting. Antwerp, 24th of May 2016.

17. Elens I., Lemiere J., Bossuyt E., Van Soest C., Vanderstichele H., Deprez S., Billiet T., **Sleurs C.**, Uyttebroeck A., Labarque V., Bijttebier P., Danckaerts M., D'Hooge R., Van Gool S. (2016). In search of predictors of the long term cognitive impact of chemotherapeutics in childhood leukemia survivors. ICCTF congress. Amsterdam, 14-16 March 2016.

18. **Sleurs C.**, Elens I., Lemiere J., Billiet T., Vercruysse D., Bijttebier P., Danckaerts M., D'Hooge R., Sunaert S., Uyttebroeck A., Van Gool S., Deprez S. (2016). Functional connectivity changes in attention-related networks of childhood leukemia survivors. ICCTF congress. Amsterdam, 14-16 March 2016, Abstract No. 44.

19. Nicolini M., Jastorff J., **Sleurs C.**, Sunaert S., Vandenbulcke M., Van den Stock J. (2016). Effects of emotion, object category, and encoding-recognition delay on non-verbal memory. OHBM. Geneva, 26-30 June 2016.

20. **Sleurs C.**, Deprez S., Lemiere J., Billiet T., Vercruysse D., Peeters R., Sunaert S., Renard M., Uyttebroeck A. (2016). Dual regression analysis of attention-related networks of childhood solid non-CNS tumor survivors. OHBM. Geneva, 26-30 June 2016.

21. **Sleurs C.**, Deprez S., Peeters R., Sunaert S., Elens I., Vercruysse G., Labarque V., Renard M., Lemiere J., Uyttebroeck A. (2016). Could non-CNS-directed chemotherapy induce longterm neurotoxicity in childhood cancer patients?. ESLCCC. Copenhagen, 22-23 September 2016.

22. Vercruysse D., Billiet T., **Sleurs C.**, Sunaert S., Vandenbulcke M., Peeters R., Smeets A., Dupont P., Amant F., Deprez S. (2016). Chemotherapy-Induced Functional Connectivity Changes in Breast Cancer Patients. OHBM. Geneva, 26-30 June 2016.

23. Lemiere J., Thijs L., Vandenwyngaert L., Vercruysse G., **Sleurs C.**, Haers M., Vandenabeele K., Jacobs S. (2016). A two-year follow-up study of neurocognition in children treated for a brain tumor. International Symposium on Neuro-Oncology. Liverpool, 12-15 June 2016.

24. **Sleurs C.**, Lemiere J., Vercruysse T., Nolf N., Van Calster B., Deprez S., Renard M., Vandecruys E., Benoit Y., Uyttebroeck A. (2015). No evidence for longterm chemotherapy-induced neurotoxicity for pediatric ALL patients: A prospective study. Pancare Meeting. Vienna, 23-25 September 2015.

25. Wagemans J., **Sleurs C.**, Kubilius J. (2014). Sensitivity to nonaccidental properties in two-line configurations. Psychonomic Society's Annual Meeting. Long Beach, California, USA, 20-23 November 2014.

26. **Sleurs C.**, Kubilius J., Wagemans J., Op de Beeck H. (2013). Sensitivity to non-accidental configurations of two-line stimuli. Applied Vision Association. Leuven, Belgium, 19-20 December 2013.

Dankwoord

Geachte juryleden, beste promotoren,
Beste familieleden en vrienden,

Hoogstwaarschijnlijk zijn dit de eerste (en mogelijk laatste) woorden die u leest. Een goede keuze, want het zijn wellicht de meest voorname woorden van dit proefschrift.

Eerst en vooral, had ik het voorrecht om te werken voor een lofwaardig promotor team. Anne, Sabine en Jurgen, jullie waren een promotor team voor wie het woord "U" tekort schiet. Jullie warmte, interesse, kennis en tijd waren van onbeschrijflijke waarde voor dit doctoraat. Een 4-tal jaren geleden namen jullie het risico een blonde psychologe aan te nemen voor een neuroimaging project voor de dienst kinderoncologie. Ik werkte met hart en ziel, in de hoop om samen met jullie een steen, of grindkorrel, te verleggen.

Anne, je bent niet enkel een ervaren, gepassioneerd, gerenommeerd kliniekhoofd. Je bent een fantastische promotor, een persoon naar mijn hart. Ondanks jouw extreme agenda, kon ik op eender welk moment bij jou terecht voor een vraag, telefoontje, of persoonlijk gesprek als ik daar nood aan had. Ik herinner me het gevoel na mijn sollicitatiegesprek 'Dit kan ik met 100% zekerheid vergeten.' Gelukkig ging ik daar als psycholoog even de mist in. Bedankt voor alles wat je voor me deed, alles wat je me bijbracht, je oprechte aandacht, geduld en bijstand ondanks de continue drukte.

Sabine, wij hebben op drie jaar tijd naast elkaar aan het eiland, elkaar op zoveel vlakken leren kennen. Jij ging een ambitieuze onderneming aan mij te bekeren tot een halve ingenieur. Als ingenieur leerde je me de technische aspecten van MRI-beeldvorming, met een onwaarschijnlijke hoeveelheid geduld en tijd. Maar nog veel belangrijker, als mens leerde jij me als geen ander, tussen de drukte door, het meest relativeren. Je staat steeds paraat voor jan en alleman. Bedankt voor je kennis, je tijd en voor je respectabel voorbeeld aan kracht en relativeringsvermogen.

Jurgen, als man in mijn promotor team hield jij de gender-equality in stand. Eind augustus 2014 ontving ik volgend bericht: *"U bent weerhouden voor de laatste ronde voor deze kandidatuur. Eén van de medewerkers had u nog graag voor een laatste gesprek uitgenodigd op **maandag 25/08/2014 om 16u**."* Ik herinner me jouw telefoontje die avond na ons gesprek, alsof het gisteren was: "Goedenavond Charlotte, ik denk dat ik goed nieuws heb voor jou…", "Echt waar?! Dank u, dank u, dank u. U maakt van mij een gelukkig mens!". En zo geschiedde… Je bood me steeds de nuchtere en psychologische kijk op de zaak. Jij legde voor mij de link met de kinderpsychologen, de neuropsychologen, en de Faculteit Psychologie. Je motiveerde mij ook de postgraduaat studies aan te gaan, en grondig na te denken over de dagelijkse uitkomst voor de kankerpatiëntjes. Het was oprecht een grote eer, een waar genoegen, om voor jullie

te mogen werken. Ik zal jullie steeds dankbaar zijn voor jullie warmte, ondersteuning en vertrouwen! Eindelijk kunnen we vandaag de langverwachte cava-flessen samen kraken!

Secondly, I would like to thank my jury members for their review of this manuscript, their valuable feedback and their time and all efforts to travel to this PhD defense.

Professor Lieven Lagae, ik herinner me mijn eerste bezoek bij u na mijn tweede jaar van mijn PhD. U gaf onmiddellijk zeer waardevolle feedback, en uw interesse leek snel uit te gaan naar de fossa posterior studie. Ik ben u dan ook zeer dankbaar voor het delen van uw tijd en uw neurologische kennis, ook bij het schrijven van onze recente genetica paper. Hopelijk kon die paper doen smaken naar meer gelijkaardige samenwerking in de toekomst.

Professor Hans Op de Beeck, als masterstudent had ik de eer om heel even mijn statistiek met met u en mijn toenmalige begeleider Jonas Kubilius en professor Wagemans te bespreken. Een gelijkaardig evaluatiemoment herhaalt zich vandaag, in een ietwat groter formaat. Graag wil ik u bedanken voor uw neuroimaging kennis en uw kritische blik op de methodieken tijdens ieder feedback moment.

Binnen beperkte tijdsspanne boden jullie mij beiden constructieve inzichten en appreciatie, hetgeen de spanning steeds snel reduceerde. Dank jullie wel.

Professor Peet, I am very happy to have met you at the Otto Wolff symposium in GOSH, and I feel honored to have you as a jury member. I will never forget your memorable sentence "Life is too short to collaborate with people you do not like.", which made me appreciate my lab colleagues even more and enjoy my workplace. Thank you very much for attending this PhD defense and sharing your specialized knowledge about MRI and biochemical mechanisms.

Professor Demeyere, ik ben blij u vandaag opnieuw te mogen ontmoeten, na onze eerste ontmoeting op de Leuven Neuropsychology Workshop 2015 (in de vroege fase van mijn doctoraat). Graag wil ik u hartelijk danken voor uw tijd en interesse, en voor uw nauwkeurige en uitgebreide feedback op de PhD thesis. Ik hoop dat we het idee over cognitieve screening bij kinderen samen verder kunnen uitvoeren in de praktijk.

Tot slot bedank ik bij deze ook graag chairman Professor Michel Delforge en juryvoorzitter Professor Johan Swinnen voor hun tijd om zowel de schriftelijke evaluatie als de mondelinge doctoraatsverdediging in goede banen te leiden.

Dan ga ik graag even terug in de tijd om enkele supervisoren tijdens mijn studies te bedanken. Jonas and Professor Johan Wagemans, thank you very much for sharing your impressive passion for science a few years ago! Jonas, thank you for sharing your doubts about an academic career and its difficulties. The fact that we both prefer to stay, probably reflects passion, addiction, or stubbornness, you name it. Prof. Dr. Jan Vandenstock en Prof. Dr. Mathieu Vandenbulcke, bedankt voor jullie hulp en vertrouwen tijdens mijn onderzoeksstage. Ondanks de teleurstelling van onze toenmalige FWO-aanvraag, ben ik blij dat onze paden blijven kruisen zij het op publicaties, zij het op HBM of in Gasthuisberg. Tot slot, Professor Christophe Lafosse, dank u wel voor de geslaagde coördinatie van de gemoedelijke postgraduaat opleiding Klinische Neuropsychologie, die tijdig de nodige ontspanning bracht.

samen met jullie studies (of toch alvast financieringsaanvragen) aan te gaan in het kader van de bestralingseffecten. Om het met Sandra haar memorabele woorden te stellen: "We staan voor een boeiend tijdperk ;-) Ik kijk er naar uit!". Wel, ik ook!

Verder bedank ik graag de kinderartsen Lien De Somer, Liesbeth De Waele, Peter Witters en Mieke Boon, voor mijn eerste bureauplaats in jullie kantoor. Als jonge psychologe hoorde ik al snel een massa aan medisch vakjargon in jullie (telefoon-)gesprekken, hetgeen veel spontaan opzoekingswerk heeft teweeggebracht.

Loes, ik ben ook blij dat ik jou mocht leren kennen tijdens de uitdagende fase van je thesis. Je blijkt een uitstekende kinderarts. Dank je wel om steeds je vrolijke zelf te zijn. Onze sushi dates zijn wat mij betreft dan ook voor vele herhalingen vatbaar.

To colleagues of the MIRC, sincerely thank you to help me find and share our mental 'out-of-office'-status during the (many) coffee breaks. Catarina, thank you very much for introducing me to the ESAT team. Only from that moment onwards, Dorothee and me had the courage to start socializing with all of the other people in the Louvre ☺!

From the ESAT team: Jeroen, David, Philippe, Daan, Tom, Anke, Ine, Jasmien, Markus, Stijn, Jonatan, Janaki, Dzemilla, Wouter, Charlotte, Simon, thank you all for our relaxing, but always ridiculously informative, 4 o'clock fruit-times, as well as the great bbq-PhDdefense-swimming-oldmarket-times! Babs en Walter, dank jullie wel om steeds jullie schitterende zelve te zijn! Jullie luisterend oor en het bijbrengen van levenswijsheid doen me steeds veel deugd! Dominique, dank je wel om steeds voor ons allen klaar te staan voor eender welk IT-probleem!

From the cardiovascular team: Bidisha, Hanan, Natalya, Natasha, Adriyana, Brecht, Vanjush, Anna, Ahmed, Mahvish, Mehdi, Joao, Pedro, Jürgen, thank you very much for our fun talks in the kitchen, as well as the nice informal dinners including food from all over the world.

Finally, thanks to the nuclear medicine (or interdepartmental) people: June, Joke, Igor, Georg, Stefanie, Donatienne, Michel, for the warm interactions and (in)formal monthly interdepartmental meetings, which are now extended to the interdepartmental "borrels". Martijn and Jenny, thank you also for our great shared Vancouver experience at HBM. Martijn, as my new neighbor, you are not doing too bad, neither as a new psychologist ;).

Professor Patrick Dupont, dank je wel voor de jaarlijkse coordinatie van onze journal clubs. Dank je wel ook aan jou en aan Koen C. voor de kalmerende Limburgse babbels (op radiologie, het HBM congres of in het MIRC). Jolien, fitness is duidelijk niet aan ons weggelegd. Neurowetenschappelijke nerdtaal ligt ons duidelijk beter. Dank je wel om een evenwaardige nerd te zijn, en onze vrije tijd even leuk te vinden met babbels over neurotransmitters. Matthijs en Jeroen, dank jullie wel voor de (langverwachte maar) smakelijke pizza. Volgende keer is het onze tour. Danielle, Tarik, Thanh, Sylvie, Laura, Marie, thank you all for our journal club times together. By creating a positive atmosphere, our time seemed to fly a bit faster.

Bedankt ook aan alle collega's van de dienst (neuro-)radiologie.

Katrijn en Thibo, jullie waren de PhD eilandbewoners bij de start van mijn doctoraat. Dankzij jouw droge humor Thibo en jouw stralende glimlach Katrijn, was het steeds een plezier

om naar het MIRC te komen. Hoewel het moeilijk was jullie te zien vertrekken, hoop ik dat jullie nieuwe uitdaging en inmiddels uitgebreid gezinsleven jullie veel geluk mogen brengen! Katja, jou leerde ik voornamelijk in mijn laatste jaar kennen, aan het eiland, maar vooral op onze vele etentjes in Londen. Je hielp Londen meer vertrouwd doen voelen, ook dankzij jullie gastvrijheid in jullie warm gezin. Dank je wel voor die fijne periode. Voor herhaling vatbaar! Vincent, dank je wel om steeds je aanstekelijke lach boven te halen aan het eiland, in het koffiekot, of de wandelgang, die de eilandbewoners steeds een plezier geeft.

Marjolein, jij was een continu figuur doorheen mijn doctraat. Met je positieve instelling en hard werken, ben je voor mij een schitterend voorbeeld geweest, en nog steeds. Naast het harde werken, zagen we ook een lach en een traan van elkaar, in binnen- en buitenland, op en na het werk. Ik ben dan ook heel blij dat wij elkaar ook buiten de werkuurtjes kunnen vinden! Ook je vroegere student Robin bedank ik graag voor zijn harde werk en sympathie. Robin, je werd voor korte tijd deel van het team. Ik ben heel blij jou in die periode te hebben ontmoet!

Ahmed, the day you came in, everyone was surprised… Not only by the fact that Egypt has more to offer than pyramids ;) also by the fact that we actually gained a strong new force. Your smile and radiological knowledge really multiplied the value of the neuroradiology team at that point with a great value. Thanks for all geeky talks and dinners. Gwen, ik herken mezelf in je (initiële) gedrevenheid. Je bent een ambitieuze, en steelds positief gestemde bij. Wacht tot een over een paar jaar ;) nee nee, ik ben er 100% van overtuigd dat je met glans zal slagen voor je PhD, en zeker na onze succesvolle top-ervaringen op PKP! Soumaya, jij kwam een dik half jaartje geleden als nieuweling binnen. In het begin was het de weg wat zoeken binnen deze 'bende', en nam je (zeer diplomatisch!) een voorzichtige houding aan. Intussen maak je ook een 'babbelend' deel uit van het geheel, en zijn we blij met zo'n sympathieke nieuwe aanwinst!

Jeroen, gast. De eerste dag jij ons team vervoegde, dacht ik 'Allez, 't is weer nen ingenieur'. Normaal gezien heb ik snel een psycho-analyse op punt, maar jouw analyse werd doorheen de tijd wat gewijzigd ;). Jeroen, ik wil je bedanken, niet enkel voor je spoedig programmeren, maar ook voor het steeds kleuren van onze dag. Je bent oprecht en recht voor de raap. Dat siert je, en apprecieer ik enorm.

Sil, als 2 collega's van Noord-Limburg hebben we onze roots een hele tijd goed vertegenwoordigd aan het eiland! Bedankt voor je hulp bij onze PhD opstart, moeilijkheden aan de scanner, en het helpen plannen van onze scans, ook toen we nauwer samenwerkten voor Sabine haar studie. Als je nog hulp kan gebruiken bij hek -of schilderwerken, weet je me steeds dichtbij te vinden ☺. Ilse, bedankt voor de steeds acute hulp bij het aanvaarden van de MRI bonnen ;) maar vooral voor je dagelijkse goedgezindheid, je lach en je babbel tijdens de lunch en aan ons eiland! We hebben tijdens je verlof gemerkt hoe ontzettend waardevol dit voor ons is! Ook aan Soumia een warm dank je wel voor de geslaagde tijdelijke vervanging van Ilse. Aan de verpleging radiologie, dank jullie wel voor het delen van de lekkere koffie!

Louise, thank you for our nice time and chats at the ISMRM conference. Although we don't often have the chance anymore to see you in the Louvre, we are happy when seeing you every time at the teambuildings and meetings! Stefan, jij introduceerde mij en Dorothée in verschillende neuroimaging technieken, en leerde ons steeds kritisch te blijven nadenken over

gekozen settings van acquisitie en analyses. Dank je wel voor alle bijstand en je kennis, alsook voor de aangename ervaringen op ISMRM 2018 en onze geslaagde jaarlijkse teambuildings.

Ron, enorm, nee, ENORM bedankt voor je continue en onmiddellijke bijstand bij de MRI scanners, maar ook voor de hoogstaande humor! Great minds... ;) als we het zelf zeggen... Ook voor de periode dat jij, Stefan, Kris en Guido me adopteerden bij plaatsgebrek in het MIRC. Het was me een genoegen jullie dagelijkse humor en aanstekelijke lach te mogen ervaren. Nathalie, ik weiger je bij nucleaire te schrijven, gezien ik je op radiologie leerde kennen, en je daar ook blijf tegenkomen. Hoewel onze taal zodanig verschilt, ben ik blij dat we elkaar toch steeds kunnen vinden in humor, in de wandelgangen en op de interdepartmental meetings voor een poging tot een babbel ;).

Tom, Frederik, Stefan, Guido, Kris, jullie zijn van harte bedankt voor de hoogstaande gesprekken tijdens de vele gedeelde middagpauzes. Dankzij jullie werd ik steeds gemotiveerd voor de tweede helft van de dag, voor doorzettings- en lachvermogen tot in de late uurtjes. Frederik, onze race voor het PhD certificaat en potentieel gedeelde receptie bleef tot vandaag de dag nog heel spannend, maar u was een waardige tegenstander ;).

Tot slot, Dorothée, maatje. Wij begonnen samen aan ons doctoraat onder co-promotorschap van Sabine. Je beschouwde me steeds als de Limburgse strever, en ik moet toegeven... Sinds jouw vertrek (na 2 jaar intens met elkaar te delen), toonde mijn resultatencurve een behoorlijk steile toename ☺. Echter, wat heb ik onze slappe lach, falende relatieverhalen, roddels, kortom vriendschap, op de bureau enorm gemist. Ik ben heel blij dat ik je heb mogen leren kennen, en nog blijer dat we die vriendschap in stijl en in stand blijven houden.

I also wish to thank all colleagues who collaborated in the work of this PhD project, including UZ Ghent colleagues Geertrui, Nathalie, Hanne, Professor Catarina Dhooge, and UCL Saint-Luc colleagues Mélodie, (each) Sophie, Professor An Van Damme, for all their efforts during patient recruitment and data assessments of current patients in their hospitals. Perrine and Professor Thierry Duprez, thank you for the great coordination of MRI scans and your regular updates. Daarnaast bedank ik graag Iris, Bea, professoren Céline Gillebert en Rudi D'hooghe vanuit de Faculteit Psychologie voor onze aangename interacties en vlotte interfacultaire samenwerking te bevorderen. Ook statistici Ben en Annouschka, dank jullie wel voor jullie hulp bij de minder voor de hand liggende statistieken. Colleagues in King's College, Serena, Dafnis, Daan and Donald, thank you very much for your great assistance in the application of graph theory and diffusion analyses of our challenging datasets. Arian, Nuno, Rui, Samy, Tom, Johnny, Jana, Vasiliki, Ana, Prachi, thank you guys for shortening my experienced time of staying. I am really convinced that all of you will become famous one day.

Verder een warm dank je wel aan studenten psychologie Inez, Jana, Floris, Mira, Ellen, Lissa, Kathleen, Julie voor jullie indrukwekkende inspanningen en flexibiliteit voor testafnames en data invoer. Studenten geneeskunde Aline, Mathilde, Kaat, Maarten en Michiel, dank jullie wel voor de boeiende literatuurstudies en uitgebreide checks van medische rapporten! Dankzij jullie hebben we veel kennis kunnen verwerven en hypothesen kunnen genereren!

Ik wil ook heel graag de jonge en oudere helden die deelnamen aan de beschreven studies bedanken, voor hun indrukwekkende inzet: een aantal MRI scans, en zo maar even een neuropsychologisch onderzoek van drie uur, en dit in een behoorlijk zware periode. Deelname leek voor velen misschien vanzelfsprekend, maar de resultaten van de beschreven studies waren er nooit geweest zonder die indrukwekkende inspanningen. Bovendien hebben alle persoonlijke verhalen, de geziene veerkracht en doorzettingsvermogen mij ontzettend doen leren relativeren, en genieten van de dagelijkse, kleine dingen. Dank jullie wel hiervoor.

Daarnaast wil ik graag mijn vrienden en mijn familie bedanken voor de (nodige) humor, hun geduld en hun steun.

Glenn, na onze jaren van streven in de opleiding psychologie, besloten we de sprong naar de academische wereld te maken. Na het wederkerend delen van ons geklaag en gezaag, vormen we steeds toch maar weer dezelfde conclusie: 'Och, op zich hebben we het toch zo slecht nog niet'. Dank je wel aan jou en aan prachtige Tessa voor de fijne vriendschap.

Dan een warm dank je wel aan mijn trouwe Noord-Limburgse vrienden en vriendinnen, voor onze ontspannende tijden samen op mooie huwelijksfeesten, citytrips, vakanties, in het Vlaamsch, op de festivalweides, op oudejaarsnacht, ... Zoals Bert het zou zeggen: "Alle wegen leiden naar Hamont-Achel". Roots blijven roots ☺.

Elita, Dorien, Carmen, Manon, dank jullie zo wel voor jullie memorabel bezoekje in Londen ☺. Dankzij jullie voelde de grootstad even aan zoals onze hometown Neerpelt, zij het niet in het *Vlaamsch Huis*, zij het in *The Elephant Head*. Hopelijk blijven de citytrips en weekendjes Ardennen met de meisjes, voor vele herhalinging vatbaar.

Tot slot, mama en papa. Ik moet toegeven, inhoudelijk hadden jullie bij dit boekje weinig suggesties of commentaar, maar wat in hemelsnaam kan ik zeggen, geven of doen, om uit te drukken wat jullie voor me betekenen? Mama, bedankt voor de was, de strijk, de poets, maar vooral je eeuwig luisterend oor, en je extreem hoge emotionele begaafdheid! Dankzij jou keek ik op jonge leeftijd in de richting van de Klinische Psychologie, en hielp je me steeds realistisch te blijven. Papa, bedankt voor je onuitputtelijke wetenschappelijke interesse, en je pogingen tot inhaalmanoeuvres in de neurowetenschappen. Jouw motivatie om levenslang leergierig te blijven, motiveerde mij om de academische wereld te exploreren.
Mama, papa, bij deze. Bedankt voor alles! De liefde is wederzijds.

Het is wat het is, omdat het zo geworden is.

Charlotte

BEDANKT